Novel Tocopherol Based Cationic Lipids for Non-Viral Gene delivery: Design, Synthesis and Evaluation

THESIS SUBMITTED
TO
NATIONAL INSTITUTE OF TECHNOLOGY
WARANGAL

FOR THE DEGREE OF
DOCTOR OF PHILOSOPHY
(IN CHEMISTRY)

BY

VENKANNA MURIPITI

DEPARTMENT OF CHEMISTRY
NATIONAL INSTITUTE OF TECHNOLOGY
WARANGAL-506004, INDIA

MAY 2018

DECLARATION

I hereby declare that the matter embodies in this thesis entitled "**Novel Tocopherol Based Cationic Lipids for Non-Viral Gene delivery: Design, Synthesis and Evaluation**" is based entirely on the results of the investigations and research work carried out by me under the supervision of **Prof. P.V. Srilakshmi**, Department of Chemistry, National institute of Technology, Warangal. I declare that this work is original and has not been submitted in part or full, for any degree or diploma to this or any other University.

Date: **MURIPITI VENKANNA**

Place: Warangal

Prof. P.V.Srilakshmi

E. mail: patrisrilakshmi@nitw.ac.in

Department of Chemistry
National Institute of Technology
Warangal-506 004, T.S, India.

CERTIFICATE

I certify that **Mr. VENKANNA MURIPITI** a bonafide student of Ph. D degree in National Institute of Technology, Warangal, has carried out research work under my direct supervision. The investigations, observations and the conclusions reported by him in this thesis entitled "**Novel Tocopherol Based Cationic Lipids for Non-Viral Gene delivery: Design, Synthesis and Evaluation**" being submitted for the award of Ph. D degree in Chemistry are his original contributions to the Chemical Sciences. It is also certified that he has not submitted the same in part or in full to this or any other University for the award of a degree or diploma.

Date: **(Prof. P.V. Srilakshmi)**

CONTENTS

CHAPTER 3

Hepatocellular targeted α-tocopherol based pH sensitive galactosylated lipid: design, synthesis and transfection Studies

3.1 Introduction

3.2 Results and Discussion

3.3 Conclusion

3.4 Experimental Section

3.5 References

Spectra

CHAPTER 4

A novel amphiphilic of azasugar head group based cationic lipids: Design, synthesis and transfection studies.

4.1 Introduction

4.2 Results and Discussion

4.3 Conclusion

4.4 Experimental Section

4.5 References

Spectra

CHAPTER 5

Structure –activity analysis of serotonin modified tocopherol based lipids: Design, synthesis and transfection biology

5.1 Introduction

5.2 Results and Discussion

Acknowledgements

My soul feels elevated with gratification, heart feels happy with emotions, and mind feels light with revelation of truth to thank all those who helped me to sail through this long journey to achieve the most cherished dream of my life. The journey would not have been completed without the efforts & help from my co-workers, friends and well-wishers who have been an integral part of this saga. I would like to thank every person whom I have encountered in my life whose dreams have been part of my dreams and whose advice, respect, love and appreciation have been an important motivation in my career.

At this moment of accomplishment, first and the foremost, I would like to express my deep sense of gratitude and thanks to ***Prof. P.V. Srilakshmi*** *(Thesis supervisor) for h guidance, scientific or otherwise, throughout the different stages of my doctoral investigation. I will always be indebted to him for his valuable guidance and constant encouragement. He has been source of inspiration by his dedication and commitment to the research.*

I would like to express my profound sense of gratitude and thanks to all my teachers who shaped my career right from school days to college, in particular ***Laxmipathi****,* ***karim****,* ***Pramila****,* ***Neeraja****,* ***Nageswar Rao****,* ***Anjaiah*** *and* ***Dr. Basavoju Chandramouli*** *for their value added education, inspiring support, encouragement and invaluable guidance.*

I feel deeply grateful and privileged to have a teacher like friend, ***Dr. Basavoju Chandramouli*** *who has always been a constant source of encouragement, not only because of her timely guidance, but also because of his kindness, moral and intellectual honesty with which he taught me to handle challenges and problems of any kind.*

I want to thank ***Dr. Srujan Kumar*** *and* ***Dr.Chandrasekhar*** *for their inspiring support and invaluable scientific suggestions from time to time. Their always extended their helpful hands towards me whenever I needed them.*

I thank to ***Dr. Rajkumar Benarjee****,* ***Arabinda Chaudhuri*** *and,* ***Dr.Sitharanjan patra****, IICT Hyderabad, Lipid science technology, for their support and other members of the division for their valuable assistance and help during my research tenure.*

I do not have words to express my indebtedness to my friend ***Gondru Ramesh****,* ***Brijesh*** *and* ***Rachamalla Hari Krishna Reddy****, who has always helped me during my research work and without his contribution completion of my projects, was impossible. I have special words of thanks for* ***Kathyani****,* ***Sahithi****,* ***Priya****,* ***Rakesh****,* ***Anirban Gangoli****,* ***Rama Rao****,* ***Sushilkumar, Vishnu****,* ***Sudhakar****,* ***Shekar****,* ***Ayan****,* ***Sudheepmukarge*** *and* ***Gopikrishna*** *for their timely help during my research work. I also gratefully acknowledge the unstinted support of my past & present lab members* ***Bhavani Kedika****,* ***Amarnath****,* ***Venkatesh****,* ***Krishnaiah****,* ***Bharat****,* ***Vinay, Bhargav, Shirisha, Saikumar, Shivaparvathi, Chandra mohan, Ramaiah, Vijendar, Babji, Sanjay, Naveen, G. Srinivas, Raju, Varun, Sujatha, Sathyanarayana, Soumya, Sunil, Mayuri, Dhanjay, Suman, and Ramesh*** *during the different phases of my doctoral research work.*

I also thank Dr. Aravinda Rathod (I & PC Division) for their help in HPLC and Mass experiments. I would like to thank everybody who was important to the successful realization of thesis, as well as expressing my apology that I could not mention personally one by one. Very very special thanks to my childhood friends Bala Krishna, Durgaiah and Narasimha Rao for their constant moral support. My heartfelt thanks are due to my friends ***Bhavani Shankar****,* ***Ganesh****,* ***Venkateswarlu****,* ***Venkata Narayana****, and* ***Srilaxmi*** *for their kind affection and love. I express special thanks to* ***Dr. B.Srinivas, Prof. Gobi, Head****, Dept. of Chemistry,* ***Prof. Rajeswar Rao****,* ***Prof. Ramachandraiah****,* ***Prof. Laxma Reddy****,* ***Prof. Nageswar Rao****,* ***Dr. Hari Prasad, Dr.***

Kashinath, Dr. Vishnu Shankar, Dr. Venkatadri, Prof. Rajitha, Prof. Chandramouli *for their kind support. Financial assistance from CSIR (in the form of a doctoral fellowship) is gratefully acknowledged.*

I thank Director, NITW for extending the research facilities and IICT Hyderabad for allowing me to do the biological work.

I express my thanks to Prof.Y.Pydisetty, Department of Chemical Engineering, National Institute of Technology, Warangal for his support.

My sincere thanks to all ***the members of my family*** *for their constant support, cooperation, love and affection.*

(VENKANNA MURIPITI)

ABBREVIATIONS

Aq	:	Aqueous
BGTC	:	bis-guanidinium-tren-cholesterol
Boc	:	di-tert-butyl-pyrocarbonate
DMF	:	Dimethylformamide
DMSO	:	dimethyl sulfoxide
DCM	:	Dichloromethane
DMEM	:	Dulbecco's modified Eagles medium
DMRIE	:	1,2-Dimyristyloxypropyl-3-dimethyl-hydroxyethyl ammonium bromide
DORIE	:	1,2-Dioleyloxypropyl-3-dimethyl-hydroxyethyl ammonium bromide
DOSPA	:	2,3-dioleyloxy-N-[2(sperminecarboxamidolethyl]-N,N-di-methyl-l-propanaminium trifluoroacetate
DOTMA	:	*N*-[1-(2,3-Dioleyloxy)propyl]-*N*,*N*,*N*-trimethyl ammonium chloride
DOTIM	:	1-[2-(9-(Z)-octadecenoyloxy)ethyl]-2-(8-(Z)-heptadecenyl)-3-(hydroxyethyl)imidazolinium chloride

DDAB	:	Dimethyldioctadecylammonium bromide
DOTAP	:	1,2-Dioleoyloxy-3-(trimethylammonio)propane
DC-Chol	:	3□-[*N*-(*N',N'*-dimethylaminomethane) carbamoyl] cholesterol
DOPE	:	1,2-dioleoyl-*sn*- glycero-3-phosphoethanolamine
DOPC	:	1,2-dioleoyl-*sn*- glycero-sn-3-phosphatidylcholine
DMDHP	:	(±)-*N*,*N*-[Bis(2-hydroxyethyl)]-*N*-[2,3-bis (tetradecano yloxy) propyl] ammonium chloride
Et	:	Ethyl
EDTA	:	Ethylenediaminetetraacetic acid
EDCI	:	1-(3-dimethylaminopropyl)-3-ethyl carbodi imide
FBS	:	Fetal bovine serum
ESIMS	:	Electrospray Ionisation Mass Spectroscopy
ONPG	:	*o*-nitrophenyl-□-D-galactopyranoside
Lipofect	:	LipofectAmine-2000
OD	:	optical density
PBS	:	Phosphate buffered saline
Pr	:	Propyl
r.t	:	room temperature

SAINT	:	1-methyl-4(dioleoyl)methyl-pyrimidinium chloride
TFA	:	Trifluorocetic acid
TMS	:	Trimethylsilyl
THF	:	Tetrahydrofuran
TLC	:	Thin Layer Chromatography
UV	:	Ultra Violet

CHAPTER 1
INTRODUCTION

Introduction

1.1 The concept of Gene therapy

The objective of gene therapy involves the introduction of the functional genetic material of a malfunctioning gene into cells to treat genetic diseases. An essential prerequisite is necessary for the success of gene therapy, with respect to safe and efficient gene delivery vectors. Even though, these veral principles and objectives of gene therapy had been well-defined several decades back[1] its function as an adaptable. The therapeutically successful approach of the gene delivery has not reached expectations. Nowadays, the gene therapy is not limited to replace the deficient gene but extended to include the genetic defects beyond inherited disorders, because the modulated regulation of gene expression was involved in the of the numerous acquired diseases.[2]. The potential of gene therapy for therapeutic applications thereby grew with the comprehension of mechanisms of diseases and the implication of genes in these events.

1.1.2 The Role of Gene Therapy in Medicine

Gene therapy is predictable to have a great enthusiasm impact on the field of medicine, due to a large number of diseases amenable to it and relative ineffectiveness of many current inventions. In principle, any disease with a causative genetic component may be a candidate for gene therapy. However certain genetic disorders are presently more amenable to gene therapy than others. Moving beyond genetic diseases, gene therapy idea has also been utilized in the field of immunology[3]. pDNA vaccines have the chance to address a number of limitations of conventional vaccine formulations.

Highest of human diseases are potential targets of gene therapy as the root causes of nearly all the diseases are either monogenic disorder or multiple gene defects. Simple, single gene disorders like Adenosine deaminase (ADA) deficiency, cystic fibrosis, hemophilia, familial hypercholesterolemia, Gaucher's disease, alpha-1-antitrypsin deficiency etc. are the most appropriate and attractive candidates for gene therapy treatment[4]. The maximum of diseases are

known to be caused by various gene defects (coupled with other environmental factors) and these are also the subjects of gene therapy treatments. These include diabetes, coronary vascular disease, AIDS, arteriosclerosis and many forms of cancer including breast, colon, ovarian, prostate, renal, leukemia, myeloma etc.[5]. With the current completion of working draft of the human genome[6], identifying disease targets for gene therapy are likely to dominate the field of medicine in the coming future.

1.1.3 Gene Delivery Vectors: Key to success in Gene therapy

Putting a new gene into a cell is not an easy job. Double-stranded DNA, the material that makes up genes, cannot be easy swallowed like a pill or even injected into the blood, as the unprotected Double-stranded DNA in the body is likely to be broken down, and any surviving Double-stranded DNA may not effectively recognize or enter the target cells for adsorption. pDNA, being a polyanionic macromolecule, is not probable to spontaneously enter into our body cells as biological cell surfaces are negatively charged. Double-stranded DNA delivery vector needs to meet 3 criteria: [i] it should defend the transgene against degradation by nucleases in intercellular matrices, [ii] it should carry the transgene across the plasma membrane and into the nucleus of target cells, and [iii] it should have no harmful effects. Thus, efficient delivery of genes into body cells (a process biologists call "transfection") is always easier said than done. In other words, the troubles of developing clinically viable gene therapeutic approach and designing safe & efficient gene delivery reagents are undividable from each other shortcomings as one is going to negatively affect the success of the other. Hence the understanding of the full potential of gene therapy will depend, in a major way, on the future development of safe and efficient gene delivery reagents[7]. Currently, there are three major types of nucleic acid delivery methods commonly in use: viral vectors, non-viral vectors, and physical methods.

Depending on the vectors used for nucleic acid transfer, gene delivery reagents remain divided into 2 main categories: viral and non-viral.

1.1.4 Viral gene delivery

Viruses, nature's own infecting vehicles, have evolved exquisite mechanisms through the course of evolution to deliver their genetic material into host cells. Thus, owing to their natural ability to infect cells, viruses have been used as vectors in gene therapy through substitute the genes essential for the replication phase of virus life cycles with the therapeutic genes of interest. Maximum of the clinical trials at present underway is based on the use of mostly five categories of viruses including retrovirus, adenovirus, adeno-associated virus, lentiviruses, and herpes simplex virus. Sustained transgene expression has been achieved by delivering therapeutic genes with retroviral vectors (such as murine leukemia virus, MLV) which integrate their double-stranded DNA into the host genome. Though the viral vectors are amazingly efficient in transfecting our body cells, they are potentially able to generate replication-competent virus through various recombination events with the host genome, inducing inflammatory and adverse immunogenic responses, and producing inspectional mutagenesis through unsystematic integration into the host genome. For example, the first fatality in gene therapy clinical trial involving the use of viral transfection vector was imputed to an inflammatory reaction to an adenovirus vector. Ectopic chromosomal integration of viral DNA has been demonstrated to either disrupt expression of a tumor-suppressor gene or to activate an oncogene, leading to the malignant transformation of cells[8]. Recently, it has been reported that retrovirus vector insertion near the promoter of the proto-oncogene LMO2 in two human patients with X-linked severe combined immunodeficiency (SCID-XI) is proficient of triggering de-regulated pre-malignant cell proliferation with unexpected frequency[9].

All the above-mentioned alarming concerns linked to the use of viral vectors are increasingly making non-viral vectors as transfection vectors of choice in gene delivery.

1.2.1 Non-Viral Gene Delivery

1.2.2 Non-viral Gene Delivery Vectors can be broadly classified into the following classes:

(a) Naked DNA: The simplest approach to non-viral gene delivery system is straight gene transfer using naked plasmid DNA. While naked DNA gives virtually no transfection under normal conditions, unexpectedly, efficient transfer of naked gene is probable following local injection, notably in muscle and skin[10].

(b) Synthetic Gene Delivery systems: Synthetic gene delivery systems encapsulate or complex the pDNA to protect it and modulate its interaction with the biological system. The maximum of these systems is based on the use of cationic lipids or cationic polymers (or combinations thereof) which show electrostatic interaction with the anionic double-stranded DNA. Due to this strong favorable interaction, the DNA is condensed and becomes part of the carrier system.

Cationic Lipids: The positively charged cationic delivery vectors that are amphiphilic molecules which self–assemble into molecular aggregates such as vesicles. Since the first explanation of successful in vitro transfection using cationic lipids by Felgner et al. in 1987, substantial progress in cationic lipid-mediated gene delivery has been witnessed[11].

Polyplexes (molecular conjugate): One more class of synthetic vectors widely used as non-viral gene delivery vectors are cationic polymers[12]. Several different types of polymers have been used as gene delivery systems of which PEI (polyethyleneimine) is the most potential[11a, 13].

However non-viral gene delivery vectors are widely used, they have their intrinsic drawback too. The main drawbacks in the evolution of non-viral vectors have been that they are less efficient than their viral counterparts especially *in vivo* and need to be delivered to the target cells in high concentration. They are quickly removed from circulation by white blood cells and the reticuloendothelial system and deposits in the large capillary bed of the lungs.

1.2.3.The Ideal vector: The good gene transfer vector would be: [a] able of efficiently delivering an appearance cassette carrying one or more genes of the size appropriate for clinical application; [b] exact for its target; [c] not documented by the immune system; [d] stable & easily reproducible; [e] purifiable in large quantities at high concentrations; [f] not inducing inflammation; and [g] safe for the recipient & the environment. Finally, it should express the gene (or genes) it carries for as long as required in a suitably regulated fashion. Moreover, incorporating all these desired characteristics into a single delivery system sounds like designing a "magic bullet", the clinicalapplication of gene therapy almost certainly relays on accomplishing this truly up-hill and task.

Among the arsenal of the above-explained non-viral gene reagents, cationic gene transfecting lipids and cationic polymers have been demonstrated to be predominantly efficacious in delivering therapeutic genes into body cells[14]. The distinct advantages connected with the use of cationic lipids as non- viral gene delivery vectors include there: [a] robust manufacture; [b] simplicity in handling & preparation techniques; [c] ability to inject large lipoplexes and [d] less immunogenic response[15].

In contrast to viral particles, they are not limited to the delivery of only polynucleic acids but can accommodate a greater diversity of cargo, including antisense siRNAs ODNs, and entire genetic material[16]. To conclude, non-viral gene vectors are easier to synthesize and better amenable to structurally design for the purpose of effectuating therapeutic applicable. Though, the main drawback of non-viral vectors is minimum transfection efficiency in gene delivery system, particularly *in vivo*, that hinders their use for in vivo therapeutic applications. Therefore, an improved knowledge of the pathway of transfection mediated by non-viral vectors will permit the development of highly efficient non-viral vectors for gene therapy uses.

1.2.4 Liposomes:"The Artificial Fat Bubbles"

Many cationic amphiphilic molecules containing two hydrophobic chains and polar head-groups, when dissolved in water spontaneously form multilamellar vesicular structures (MLV) called liposomes above a certain critical vesicular concentration (CVC). On sonication through various pore size membranes, the multilamellar liposome (MLV) assumes the size of the small unilamellar vesicle (SUV, 20-100 nm) or large unilamellar vesicle (LUV, 150-250 nm) respectively (**Figure 1**). Though initially urbanized as model biomembranes (30), liposomes have been broadly used in the area of targeted and controlled drug delivery. Liposomes offer the essential advantage of targeting the drug to selected tissues *via* apt modifications by either passive or active mechanisms with negligible adverse effects to normal tissues[17]. In early 1980, as a natural extension of their drug delivery properties, liposomes made by phospholipids were used for the first time, to deliver genes to cultured cells[18]. Unilamellar phospholipids vesicles (liposomes) were loaded with supercoiled DNA and the resulting vesicular solution with the encapsulated DNA was then incubated with cultured cells. This approach relied on the fusion of the negative charged DNA-containing vesicles with the plasma membrane of the recipient cells.

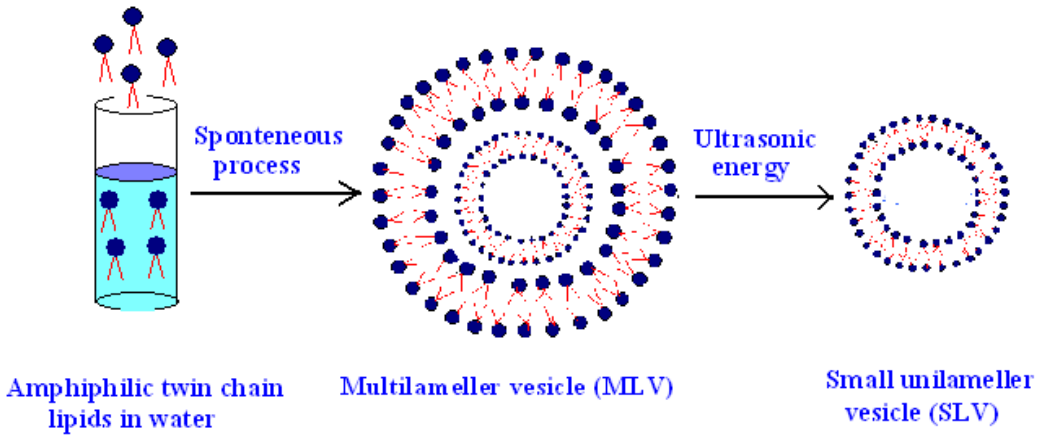

Figure 1. Formation of Liposomes.

1.2.5 Cationic liposomes in gene delivery reagents

The positivelycharged liposomes, microscopic bubbles of fatty lipids surrounding a watery interior, have long been viewed as able biocompatible drug transfer systemsbecause of their

similarity to cell membranes. Depending on the molecular make-up of the polar head-groups, the liposomes can be anionic-, cationic-, zwitterionic- or non-ionic. Cationic liposomes are prepared from cationic delivery vehicles containing two hydrophobic aliphatic long chains and positively charged functionalities in their polar head-group region (**Figure 2**).

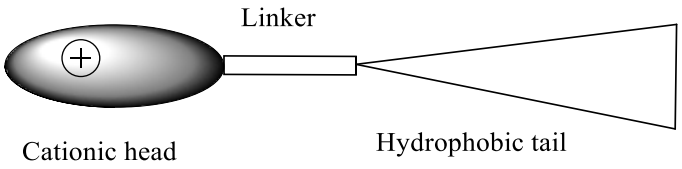

Figure 2. The general structure of Cationic lipid

Cationic liposomes are usually formulated using co cationic delivery amphiphiles in mixed with fusogenic neutral lipids like DOPE or cholesterol for use as gene transfer vectors. Because of their opposite charge of the surface, cationic liposomes can form an electrostatic complex with negatively charged double-stranded DNA molecule. The resulting charged lipid- double-stranded DNA complexes do not experience the electrostatic barrier faced by the naked pDNA in entering biological cells and get endocytosed by the cell plasma membrane. In addition, cationic liposomes also protect double-stranded DNA from attack by the en-route DNases. Generally, cationic lipids are designed to protect double-stranded DNA so that favorable interactions with plasma membrane can occur and thus leading to efficient endocytosis and subsequent destabilization of endosomes. In 1987, Felgner et.al, initially used chemically designed and synthesized cationic vectors in transfecting cultured cells with supercoiled pDNA[19]. Since then, a maximum number of efficient cationic lipids having different molecular architectures have been reported till date[20]. The main benefit associated with the use of cationic transfection lipids include the factors: [a] robust manufacture; [b] ease in handling & preparation techniques; [c] ability to inject large lipid: DNA complexes and [d] low immunogenic response.

1.2.6 Commonly used Cationic Transfection Lipids

Cationic transfecting amphiphiles could be classified into a different of groups and subgroups depending on the nature of the head group, hydrocarbon anchor or the linker bonds. Illustrative examples are shown in (**Figure 3)**.

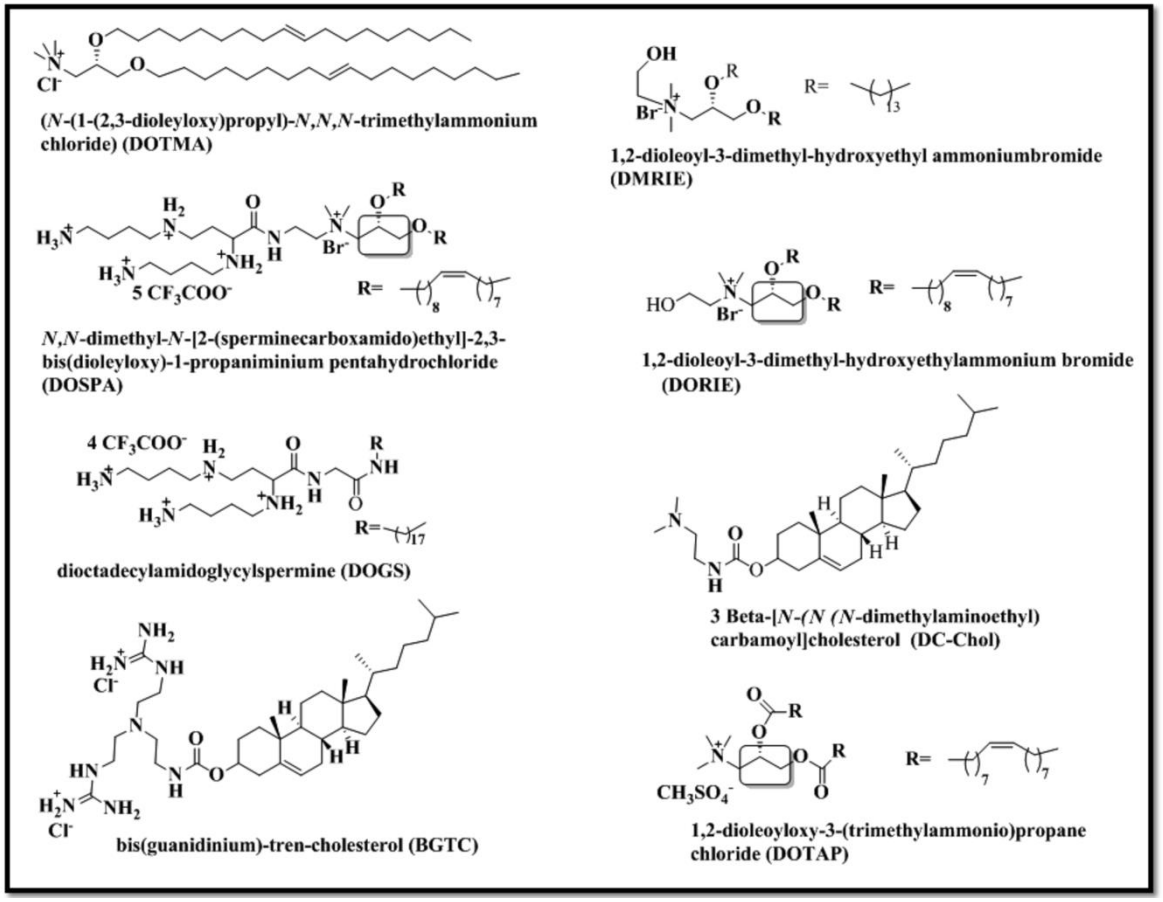

Figure 3. Some of the commonly used cationic transfection lipids

(a) Glycerol-based Cationic Lipids: In this class, the cationic head-group is linked to the hydrophobic tail *via* a glycerol-backbone. Noteworthy examples include DOTAP, DMRIE, DOSPA, GAP-DLRIE etc. [21].

(b) Non-Glycerol based Cationic reagents: This class comprises a wide variety of lipids having different linkers (carbamates, amides, esters, and carbonates), head-groups directly hybrid with the hydrophobic tail. Some important examples are DOGS, di-C14-amidine, DMDHP, DOTIM, SAINT etc. [20-21].

(c) Cholesterol based Cationic Lipids: A number of cationic transfected vehicles contain cholesterol skeleton as the hydrophobic tail and biodegradable linker's e.g, carbamates functionality. Important examples include DC-Chol, BGTC, CTAP, etc[22].

1.2.5 Cationic Lipids: Influence of Structural Variations

The molecular architecture of cationic delivery vehicles consists of a hydrophobic domain, linker functionality and a cationic head-group (**Figure 2**).

1. Hydrophobic Domain:

The hydrophobic part of the cationic delivery vehicle is mainly derived from either steroid or aliphatic hydrocarbon chains.

A. Steroid hydrophobic domain: DC-Chol and BGTC are examples of two frequently used cationic delivery vehicles based on cholesterol as the hydrophobic domain. Other steroid compounds used as hydrophobic moieties for cationic transfection lipids include vitamin D, bile acids, cholestane and lithocholic acid [23].

B. Aliphatic hydrocarbon chains

***(i) Varying Chain lengths*:** Completely structure-activity relationship studies have revealed that the gene transfer efficacies of cationic lipids depend on the length of their hydrophobic chain. In general, lipids consist of one part hydrocarbon chain tend to form micelles, transfect poorly and are more toxic [24]whereas, the lipids consist of 3 aliphatic chains tend to be poorly transfecting than the ones with two hydrocarbon chains [25]. The most used aliphatic chains include lauryl (C12:0), myristyl (C14:0), palmityl (C16:0), stearyl (C18:0), and oleyl (C18:1). Detailed structure-activity investigations reported by various groups that lipids comprising lauryl, myristyl, and palmityl chains exhibit maximum in vitro transfection efficacies while stearyl chains are optimal for in vivo transfection[19c].

***(ii). Aliphatic Vs Olefinic chains*:** Transfection is related with the increase of chain unsaturation. The Unsaturation in the chain exhibit extensive phase coexistence and hetero geneity, there by facilitating super coiled pDNA release and leading to excellent transfection efficiency. In 2006, in a thought infuriating structure-activity study, Koynova et al. clearly demonstrated dramatically superior (about 50 fold) in vitro gene transfer efficiency of cationic lipids with asymmetric hydrocarbon chains, namely oleoyl-decanoyl-ethyl phosphatidycholine (DOPE) (C18:1/C10-EPC) to that of its structurally very similar saturated asymmetric counterpart stearoyl-decanoyl-ethylphosphatidylcholine (C18:0/C10-EPC).

1. 2.7 Head-group regions:

The head group in a cationic lipid may be a quaternary ammonium group (DOTAP, DOTMA, and DORIE), polyamine moieties (DOSPA and DOGS), amidinium& guanidinium salts (BGTC), a heterocyclic moiety (pyridinium, imidazole, and piperazine) or amino acid head-groups (lysine, arginine, ornithine and tryptophan). Many cationic transfected amphiphiles contain hydroxyl functionality in their polar head group region in addition to the quaternized

nitrogen atom. Structure-activity studies have revealed that distance of (-OHs) hydroxyl functionality from the quaternized nitrogen center critically control supercoiled pDNA binding and *in vitro* gene delivery efficacies of cationic lipids with hydrophilic alkyl head groups[16a].

1.2.8. Linker functionality:

The water-hating (hydrophobic) and water-loving species (hydrophilic) of positively charged cationic lipids are commonly connected using amide carbonate, ether, and orthoester bonds. The connecting bond mediates the stability of the cationic amphiphiles which in turn dictates their half-life, in the cell. Although no particular linker has emerged as consistently optimal, linker functionalities can be generally classified into following subgroups.

***(i)* pH-*Sensitive linkers*:** The comparatively minimum transfection efficiency of non-viral gene delivery reagent is at least imparted, due to inefficiency in escaping from the early endosomes. Really, the endosomal pH, which is first that of the extracellular medium (pH 7.2-7.4), is progressively lowered to approximately 5.0 by ATP-dependent proton pumps located in the endosomal membrane[16a]. Covalent grafting of endosomal linker sensitive in the molecular architecture of cationic lipids then likely to induce dissociation of the hydrophilic and hydrophobic region thereby imparting instability to the lipoplex structure. Thus, if the resulting supercoiled pDNA decomplexation would be concomitant with endosomal membrane destabilization, free of the supercoiled pDNA (**Figure 4**) into the cytosol should be enhanced and consequently, the level of gene transfection may be increased[16c, 26].

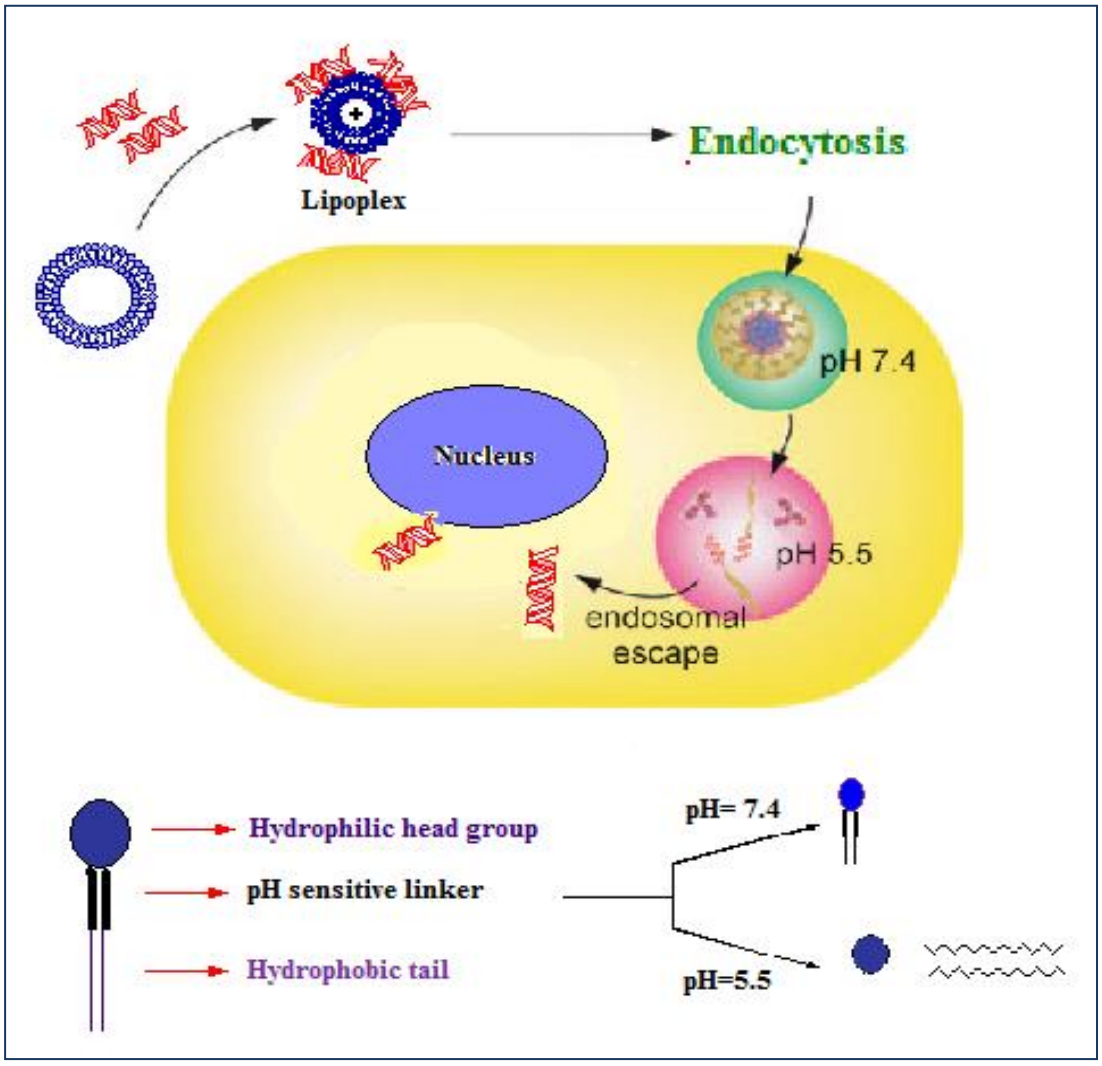

Figure 4. The release of DNA from lipoplex in acidic milieu.

***(ii). Redox-sensitive linkers*:** Redox potential-sensitive positively charge lipids constitute another family of triggerable vectors. Here, the underlying biological rationale is that once internalized into the cell, the lipoplexes presented with relatively more concentrations of reductive substances (for example, 10 mM glutathione and the enzymes thioredoxin and glutaredoxin. Incorporation of redox-sensitive disulfide bonds into the linker bond structure will consequently lead to cleavage of the group, destabilizing the complex and leading to DNA release.

1.2.9. Linker orientation:

The supercoiled pDNA-binding & gene transfection efficacies of cationic amphiphiles crucially rely on the nature of the linker-orientation used in tethering the polar head-group & hydrophobic tails. Structure-activity findings from our [27] laboratory demonstrated that even as minor structural

difference as only linker orientation reversal in cationic amphiphiles can deeply influence DNA-binding characteristics, membrane inflexibility, membrane fusibility, cellular uptake, and consequently gene delivery efficacies of cationic liposomes.

1.3. Mechanism of lipoplex-mediated transfection

Lipofection Pathways: "The Cellular Roadblocks"

The transfer of DNA (encoding the therapeutic protein of interest) into a cell with the subsequent expression of the encoded protein is called transfection (**Figure 5**). In liposomal gene delivery, cationic liposomes are mixed with DNA and the resultant lipid-DNA complexes are simply incubated with cells (*in vitro*) or injected in animals (*in vivo*). If the lipid-DNA complex containing the gene of interest is taken up by cells and eventually reaches the nucleus, the gene coding the protein of interest is expressed through transcription and translation. A quantitative test of the protein indicates the success and efficiency of the method.

At present believed lipofection pathways [28] involve: [a] formation of lipoplexes; [b] first binding of the lipid-DNA complexes to the cell surface; [c] endocytotic internalization of the liposome-pDNA complexes; [d] trafficking in the endosome/lysosome compartment and escape of lipoplex from the endosome/lysosome compartment to the cytosol; [e] convey of the endosomally released DNA to the nucleus followed by its transgene expression (**Figure 5**).

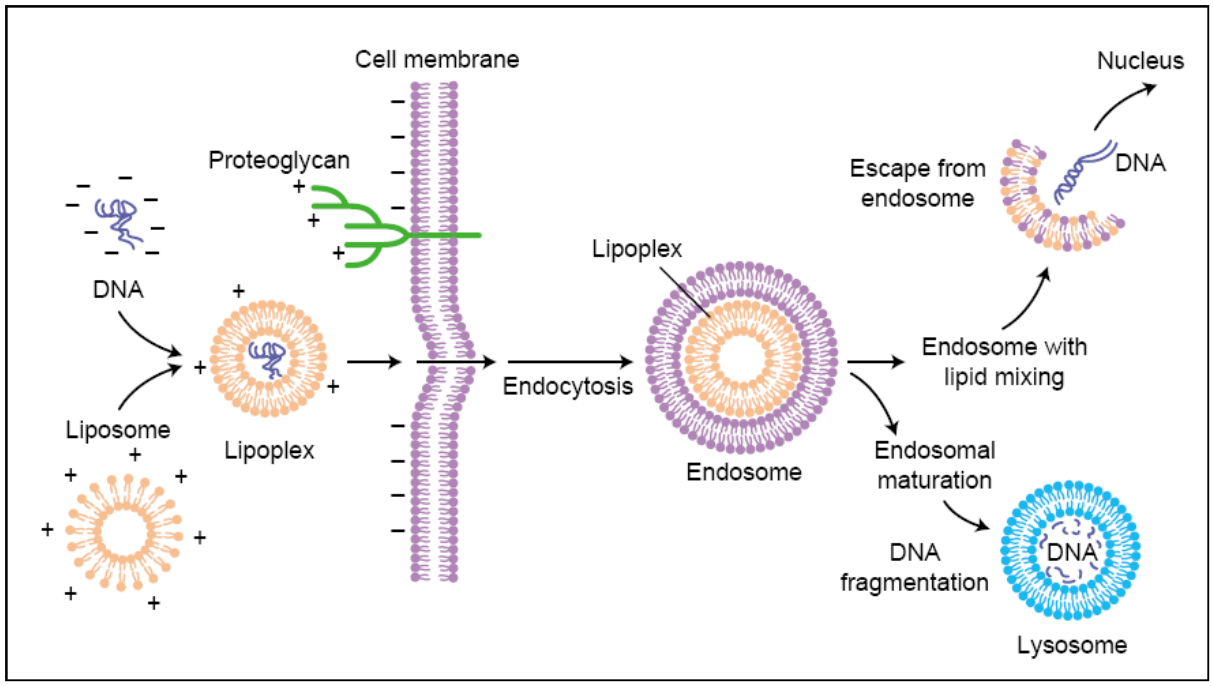

Figure 5.Lipofection Pathways

Step (a). Formation of Lipoplex assembly:

The structures of electrostatic lipoplex complexes have been characterized using techniques like freeze-fracture electron microscopy, cryo-transmission electron microscopy, small-angle X-ray scattering experiments[29] etc. and such investigations have revealed diverse structures including spaghetti and meatball structures, entrapped DNA into aggregated multilamellar structures, multilamellar structure with nucleic acid intercalating within the lipid bilayers etc. for different cationic lipid formulations[30].

Step (b). Endocytosis of lipoplexes:

The cell membrane is (-) negatively charged has it's more content of glycoproteins and glycolipids containing negatively charged sialic acid residues. In the absence of a receptor specific targeting ligands, the driving force for the binding of the lipoplex complexes to the cell membrane mainly depends on electrostatic. Electron microscopic studies [31] have revealed that internalization of the lipoplexes occurs mostly through endocytosis. The lipoplexes are engulfed into lower pH compartment called “early endosomes” in the peri-membranous region.

Step (c). The release of liposome-pDNA complex cargo from endosomes:

Once in the endocytic mechanism, the plasmid may become corrupted after reaching the lysosomes. Accordingly, for productive transfection, the nucleic acid needs to acquire cytosolic way in at an earlier stage, presumably by escape from (early) endosome prior to the endosomes-lysosomes fusion event takes. Fusogenic lipids similar to DOPE are often used as helper lipid in facilitating endosomal disruption which, in turn, leads to the efficient release of DNA to the cytoplasm. As mentioned above endosome pH-sensitive cationic transfecting lipids have been used to facilitate endosome disruption leading to the capable release of endosomally trapped lipoplex and subsequently enhanced transfection efficiency.

Step (d). Transport of DNA to the Nucleus:

The entry of supercoiled pDNA into the cell nucleus after its endosomal release into the cytosol is a prerequisite for gene expression. The precise pathway of nuclear entry of the endosomally released supercoiled pDNA still remains elusive but is believed to be an inefficient process. The presence of a single nuclear localization signal peptide (NLS) linked to one end of a supercoiled pDNA has been reported to increase the in vitro transfection efficacies by 1000-fold compared to DNA lacking the NLS sequence. Some studies have reported the link between mitotic activity and transfection by cationic lipoplex complex. While the accurate mechanism of enhancement in gene transfer has not been elucidated, it is thought that the breakdown of the nuclear membrane during mitosis could facilitate entry of nucleic acid into the nucleus [32].

1. The inspiration for the design of α-tocopherol cationic lipids

Tocopherol (vitamin E), is a natural amphiphilic molecule and it refers to a group of eight naturally occurring tocochromanols, α-, β-, γ- and delta-tocopherol and the corresponding tocotrienols. The tocopherol consists of a C_{16}-phytyl side chain; tocotrienols possess the corresponding three-fold unsaturated side chain and it was described initially as essential micronutrients for normal fertility in rats. Natural RRR-tocopherol stereoisomer owing to three

asymmetric centers in the side chain and especially the 2R, 4R, 8R tocopherol stereoisomer form is the most biologically active form[33]. Besides tocopherol, well defense role against lipid peroxidation of its radical quenching ability and prevents the cell membrane from free radical attack. α-Tocopherol can also modulate directly cellular signaling pathways, viz., protein kinase C, leading to diverse biological responses in different cell types. The antioxidative properties of α- tocopherol which is due to its hydroxyl group and also it is acting as a hydrogen donor to stabilize free radicals. In the present thesis work, the α-tocopherol is introduced as a hydrophobic chain in the cationic lipid backbone and its transfection efficacy is assessed. It is confirmed that some of these tocopherol based lipids exhibit higher transfection efficiency and low cytotoxicities[34]. Such "α-*tocopherol* S*mart Biomaterials*" can be used as carriers for delivering nucleic acid to cure the diseases without showing toxic side-effects. Effective and harmless gene therapy requires an engineering of synthetic vectors like α-tocopherol lipids which are maximum bio-compatible and target specifically in nature. Several biologically active molecules of either plant or animal origin are used directly or indirectly as polar head groups or hydrophobic domains. Koynova et al. demonstrate that natural polar lipid extract from bovine liver efficiently releases the nucleic acid from lipoplexes by forming nonlamellar phases over the other synthetic membrane mimicking lipid compositions[33-35]. Liposomes prepared from such isolated phospholipids showed minimum cytotoxic nature and may have future applications in gene delivery. Phospholipids, archaeal lipids, amino-glycosides, ceramides, fatty acids, and sphingolipids are the few examples which are widely used in the synthesis of lipids as liposomal gene delivery systems (76). Most of the currently available commercially transfection reagents are also either derived from natural sources or synthesized by principles adopted from biomaterials.

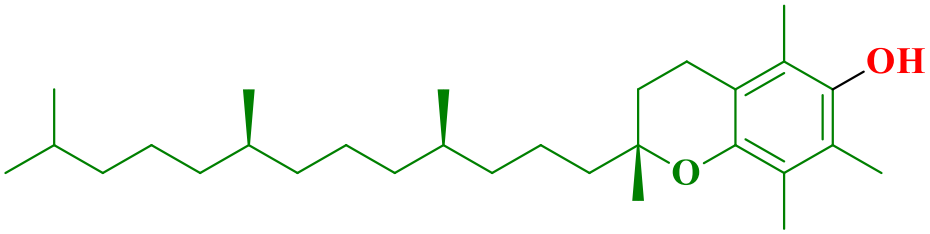

Figure. 6 α-Tocopherol

2. Receptor-targeted and Ligand-mediated gene therapy

Receptor-mediated gene delivery methods have major advantages over other methods of gene transfer currently used for gene therapy. First, it is potential to customize the gene delivery vehicle for a specific target receptor. Receptor-targeted gene transfer takes benefit of specific types of receptors present on the surface of a variety of differentiated cells to efficiently bind and then internalize a ligand through endocytosis and then form an endosome. The components used in receptor-mediated gene delivery systems include the DNA/siRNAs of interest, a protein containing the receptor targeting ligand, and a linking polycation. So far it has been hard to elucidate which are the preferred routes for the internalization of DNA-ligand complexes. However, many ligands have been exploited to date for efficient internalization of nucleic acid /DNA-ligand complexes. Ligands such as carbohydrates and particularly galactose recognizing asialoglycoprotein receptors (ASGPr) on hepatocytes cells (**Figure 8**) whereas, 5HT receptors (**Figure 9**) are abundantly and selectively more expressed on TCHO cells. Hence ASGPr and serotonin are considered as a promising candidate target for drug and gene delivery into hepatocytes and TCHO cells. D-galactose also has been exploited in targeting ASGPr and serotonin are used as ligands for targeting several pattern recognition receptors expressed in antigen presenting cells.

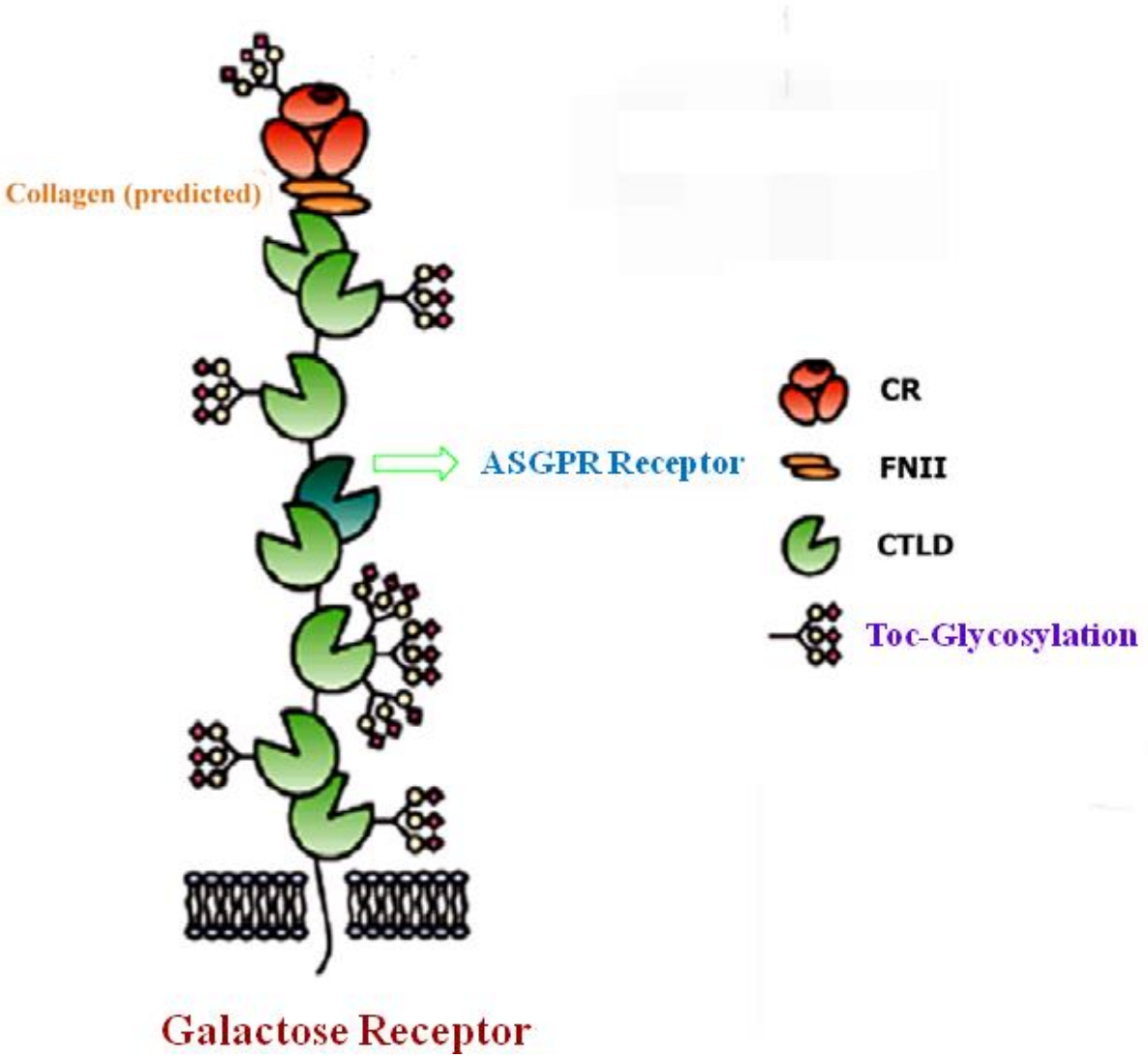

Figure 8. A schematic structure of the **ASGPR** Receptor.

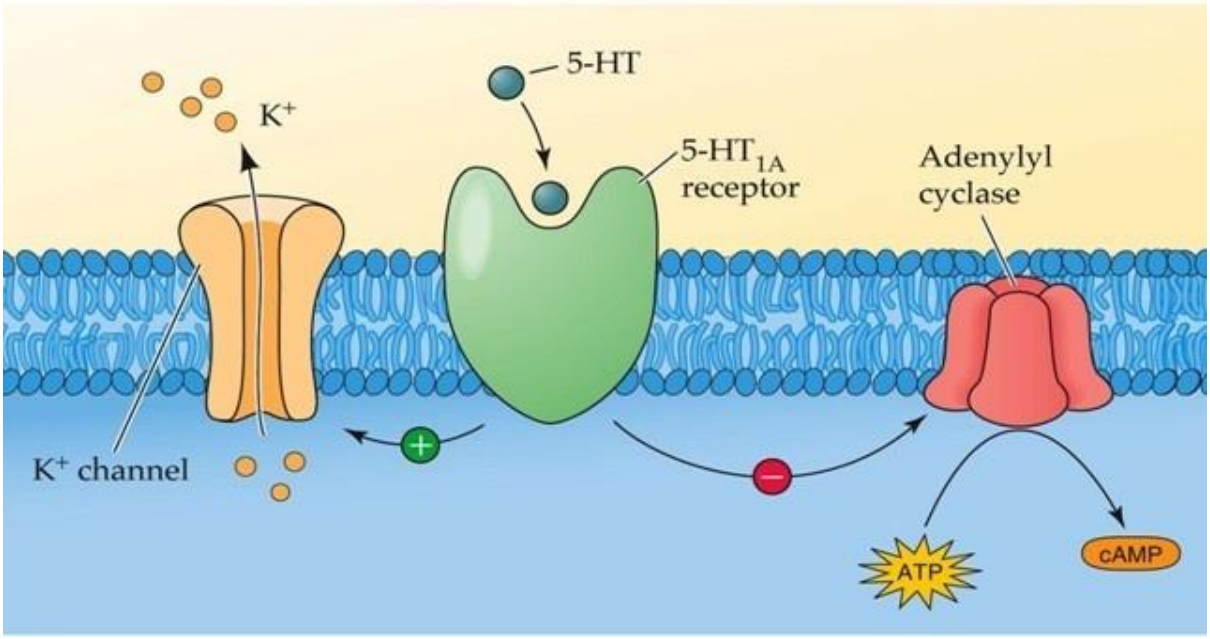

Figure 9. A schematic structure of the **5-HT 1A** Receptor.

1.4 Present Thesis

The crucial steps involved in cationic liposome-mediated gene delivery include: (a) formation of electrostatic complexes (popularly known as "lipoplexes") between polyanionic macromolecular DNA (genes) and the positively charged lipids; (b) endocytotic internalization of the resulting lipoplexes; (c) escape of DNA from the endosomal compartment to the cell cytoplasm and (d) nuclear trafficking of the endosomally released DNA to access the nuclear transcription apparatus before the final transgene expression in cytosol. Thus, gene delivery efficacies of cationic lipids depend on their ability to electrostatically compact naked DNA such that the endocytotic cellular uptake of the resulting compacted DNA (liposome: nucleic acid complex) is ensured. An obvious way of enhancing electrostatic interactions between cationic lipid and DNA is to use cationic lipids with more number of hydroxyl groups such as ascorbic acid functional groups in their head-group regions. However, the transfection efficiencies of a number of nano-cationic lipids including those reported by our own group have been demonstrated to be superior to that of Lipofect2000. However, investigations delineating transfection efficiencies of the ascorbic acid-tocopherol hydride cationic lipid have been reported. Towards this end, in **Chapter**

2, towards probing the influence of ascorbic acid as a head group of tocopherol based cationic lipid. We have designed and synthesized two novel cationic lipids (**Toc-As** and **N14-As**) and control lipid **Toc-NOH** with the same diethyl ether linker. The synthesis, *in-vitro* gene delivery efficacies and physiochemical characterization of these novel cationic lipids are described in **Chapter 2**.

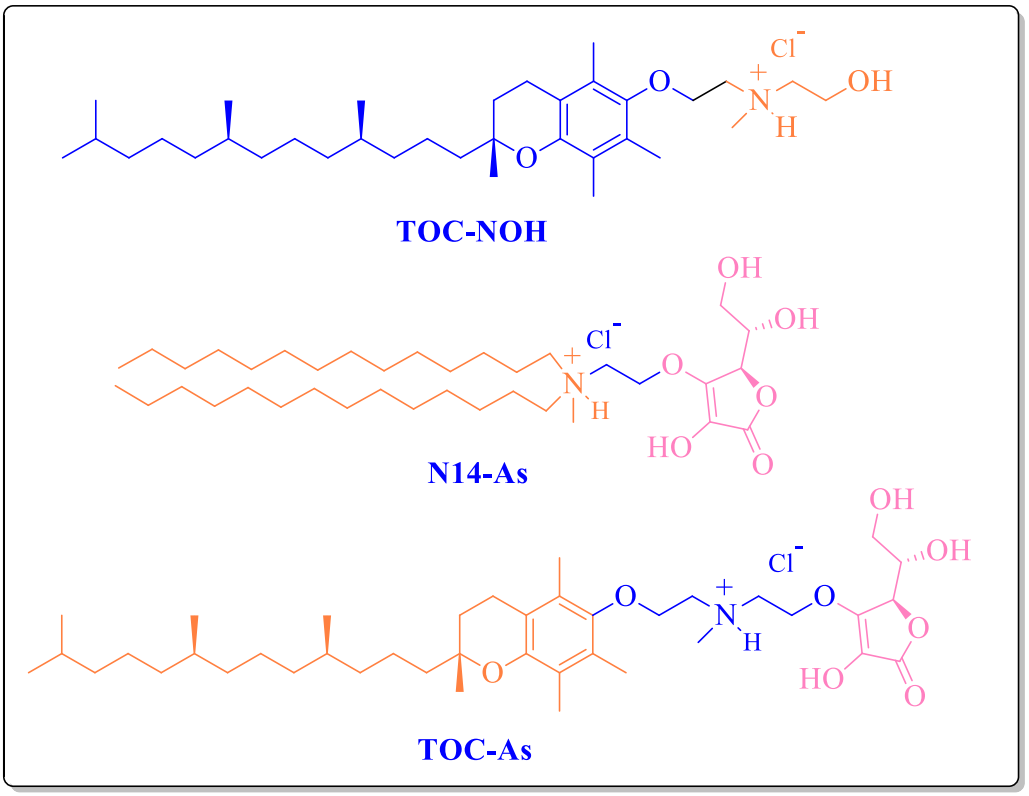

Figure10. Structure of cationic transfecting lipids.

Cationic liposomes can deliver a therapeutic payload to specific body cells by tethering receptor-specific ligands in a target-guided manner with enhanced efficacies. Liver-targeted gene therapy can make a maximum impact in the treatment of genetic disorders such as hemophilia, hereditary tyrosinemia type I (HTI). Prior findings demonstrated that galactosylated cationic lipids could effectively deliver a therapeutic payload to the liver through asialoglycoprotein receptors (ASGPRs). However, cationic liposomes exhibit necroptosis due to the high density of positive charges at the surface of liposomes which depolarize the negatively charged cell surface, leading to trigger up-regulation of intracellular reactive oxygen species (ROS) in turn leading to

necroptosis mechanism. In **Chapter 3** we developed α-tocopherol based ASGPR targeted liposomal delivery system by conjugating galactose ligand to tocopherol through a triazole linker for efficient delivery of nucleic acids into hepatocytes. In addition, we synthesized a control non-targeting lipid, Toc-OH similar to Toc-Gal lipid except ASGPR targeting ligand (D-Galactose). We characterized the biophysical properties such as size, potentials and DNA binding studies with liposomes of **Toc-Gal** and **Toc-OH** lipids. Cell viabilities, Transfection efficacies, and ASGPR receptor specific targeting property were evaluated in ASGPR receptor positive and negative cell lines (HepG2 and SK-HEP-1) using reporter gene assays and receptor saturation studies

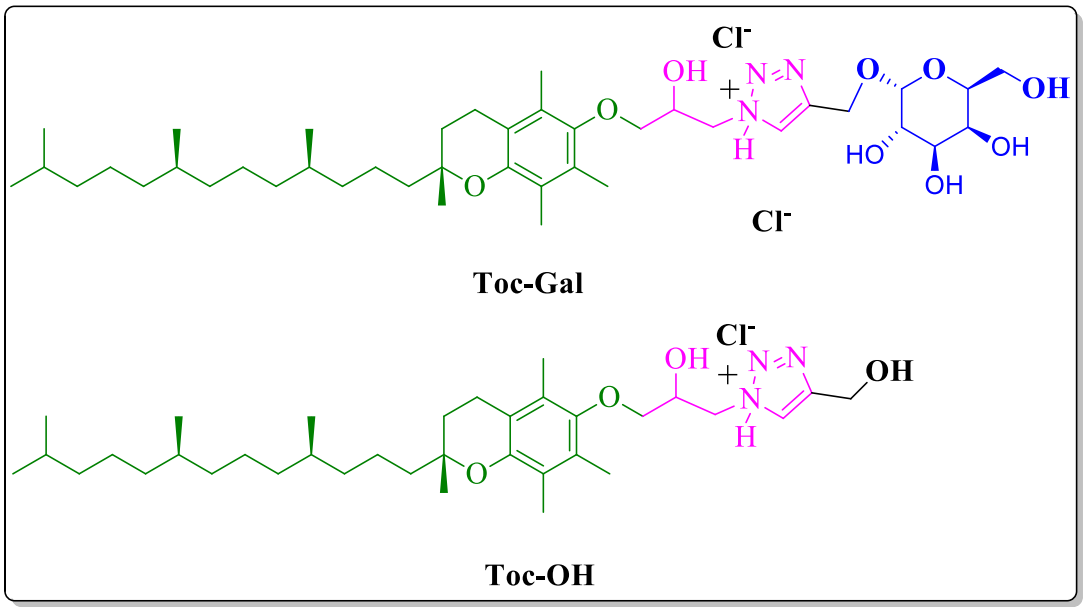

Figure 11. Structure of cationic transfecting lipids

Gene therapy appears to be a very promising technique in modern medicine that grasps a profound assurance for the treatment of a wide range of both genetic and sporadic diseases [36]. The treatments of genetic diseases have been carried out by using viral and non-viral vectors[37]. The high transfection efficiency and long-term gene expression are less achieved by viral vectors vis-à-vis non-viral vectors because of the restricted DNA packaging capacity of viral vectors to transport larger genes into the cells[38]. But, non-viral vectors are gaining attention because of their relatively safe, less toxic nature, ability to transfer larger sized genes, and potential for up-scaling

attributes[39]. In **Chapter 4** we developed α-tocopherol- azasugarhybrid liposomal delivery system through ether linker for efficient delivery of nucleic acids into multiple cell lines (HepG2, CHO, and HEK-293). These approaches often demonstrated better biocompatibility and serum-stability. Generally the maximum -OH groups on the gene transfecting vectors might help reduce their cytotoxicity as well as the gene delivery efficiency and serum-tolerance ability. In this study, we coupled the azasugar (possessed OH groups) and pyrrolidine (without OH) head group with tocopherol (**Toc-aza** and **Toc-pyr)** to form a new head group based lipids, which were expected to increase the biocompatibility of the lipids. We characterized the biophysical properties such as size, potentials and DNA binding studies with liposomes of **Toc-Aza** and **Toc-Pyr** lipids. Physicochemical characterization, cell viabilities, transfection efficacies and serum stability was carried out in **Chapter 4**.

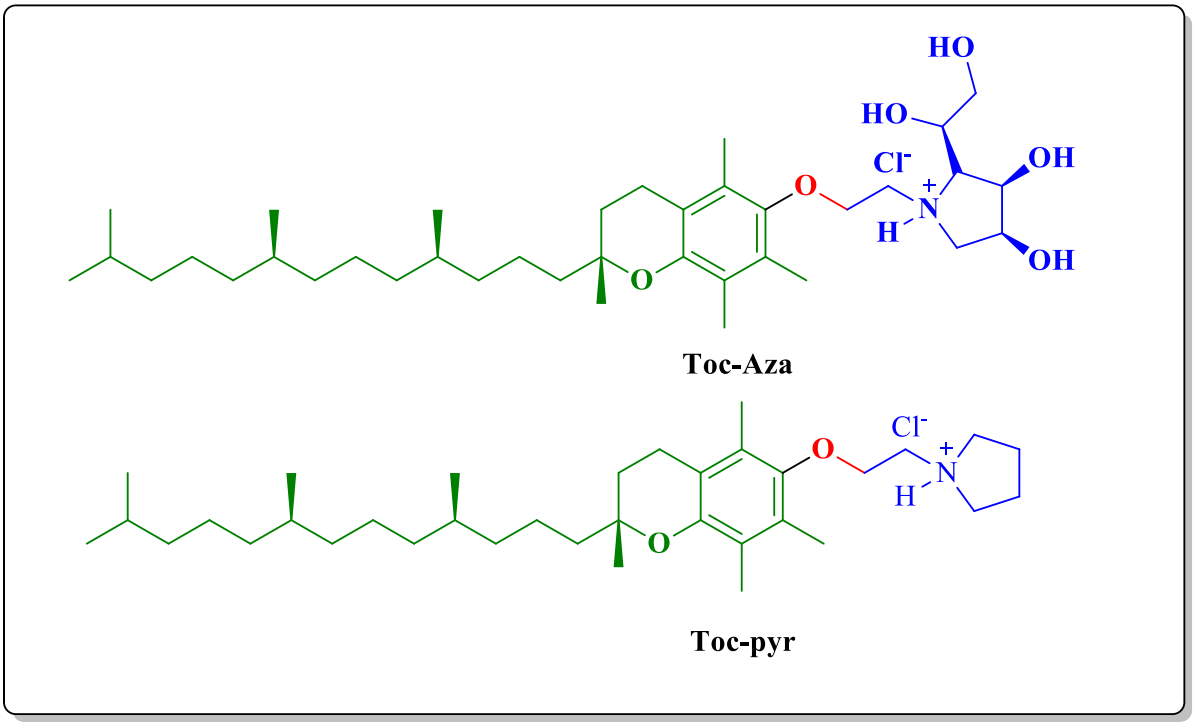

Figure 12. Structure of cationic transfecting lipids

Serotonin is an important member of the GPCR (G-protein coupled receptors) superfamily and is involved in the etiology of a large number of neurodegenerative diseases. Receptors of 5-HT are abundant in the central and peripheral nervous systems as well as in non-neural tissues such as

gut, blood, and cardiovascular system. Dizeyi et al have confirmed the overexpression of 5-HT receptors in prostate cancer tissues through ligand binding assays[40]. The work demonstrates the function of serotonin in tumor progression primarily in androgen-independent states and states the contribution of biogenic amines such as serotonin in the proliferation of prostate cancer. In chapter 5reported the design and synthesis of 5-HT functionalized lipids by tethering 5-hydroxytryptamine (5-HT), a small molecule ligand as the head group to α-tocopherol. In order to preserve the molecular recognition of 5-HT to serotonin receptors, a hydroxyl versus amine approach was adopted in the conjugation process**.** Following conjugation, the corresponding liposomes designated as **Lipid A** (-NH_2) and **Lipid B** (-OH), wherein 5-HT was conjugated to α-tocopherol *via* carbonate and β-hydroxy ether linkers respectively. Synthesis, *in vitro* gene delivery efficacies in multiple cultured cells including CHO, TCHO, HepG2, HEK-293T and Neuro-2a and physiochemical properties of these novel cationic lipids A and B is described in **chapter 5**.

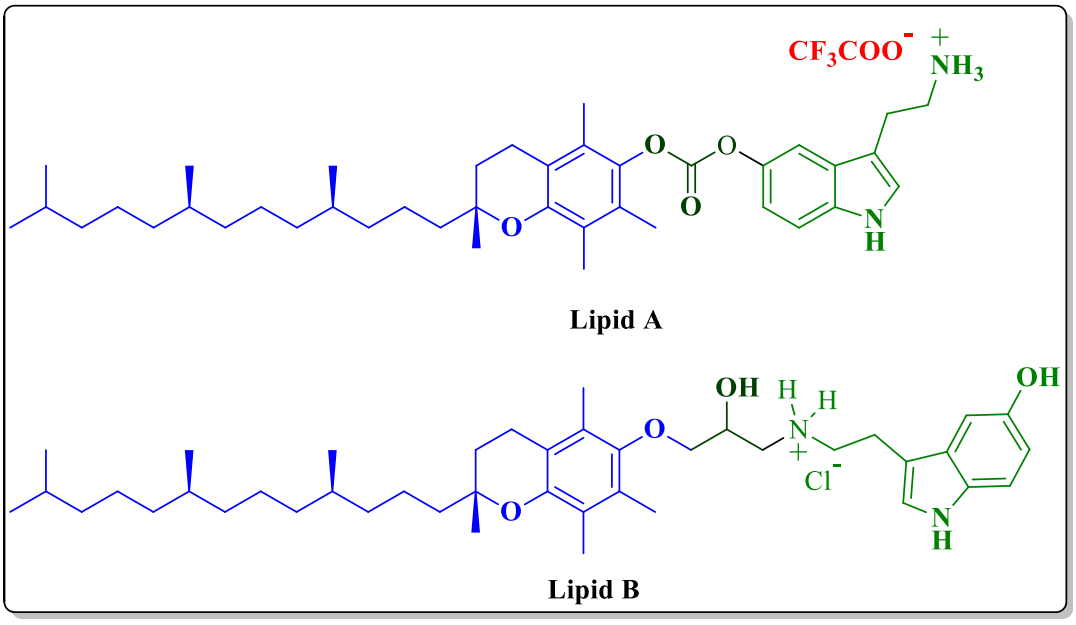

Figure 13. Chemical structures of targeted Cationic Lipids

Gene delivery is a route of inserting a genetic material into host cells, which mainly depends on developing efficient and safe vectors for delivering genes. Till date, numerous viral and non-viral

vectors have been adopted to introduce naked DNA into the cells [41]. Non-viral or synthetic vectors as promising delivery agents became the primary area of research owing to their several significant factors, *viz*., greater carrier capacity, simple structure, safety, ease of large-scale preparation, stability, potential to incorporate targeting ligands and unlimited vector size[42]. Among non-viral vectors, cationic liposomes and polymer-based vectors have gained increasing interest due to their high transfection efficacy and ideal characteristics. In **Chapter 6** we demonstrate the importance of the hybrid linker i.e. ether-β-hydroxy-triazole. In this chapter described the synthesis of three lipids **Lp1**-**Lp3**. The lipid **Lp1** consists of only 'ether-β-hydroxy' linker connecting tocopherol moiety and tris(2- hydroxyl ethyl) ammonium head group. Whereas lipid **Lp2** consists of the hybrid linker 'ether-β hydroxyl-triazole' between tocopherol moiety and tris(2-hydroxyethyl) ammonium head group. Lipid **Lp3** has the same hybrid linker and anchoring group as **Lp2** only difference is instead of tris(2-hydroxyethyl) ammonium, tris(ethyl) ammonium as the head group. Our findings demonstrate that the relative *in vitro* gene transfer efficacies of the presently described novel hybrid linker cationic amphiphiles are remarkably pH sensitive to the nature preparing lipoplexes,; *in vitro* gene delivery efficacies in B16F10, HepG2, and HEK-293 and T3T cell lines physiochemical properties of these novel cationic lipids **Lp1-Lp3** are described in **chapter 6.**

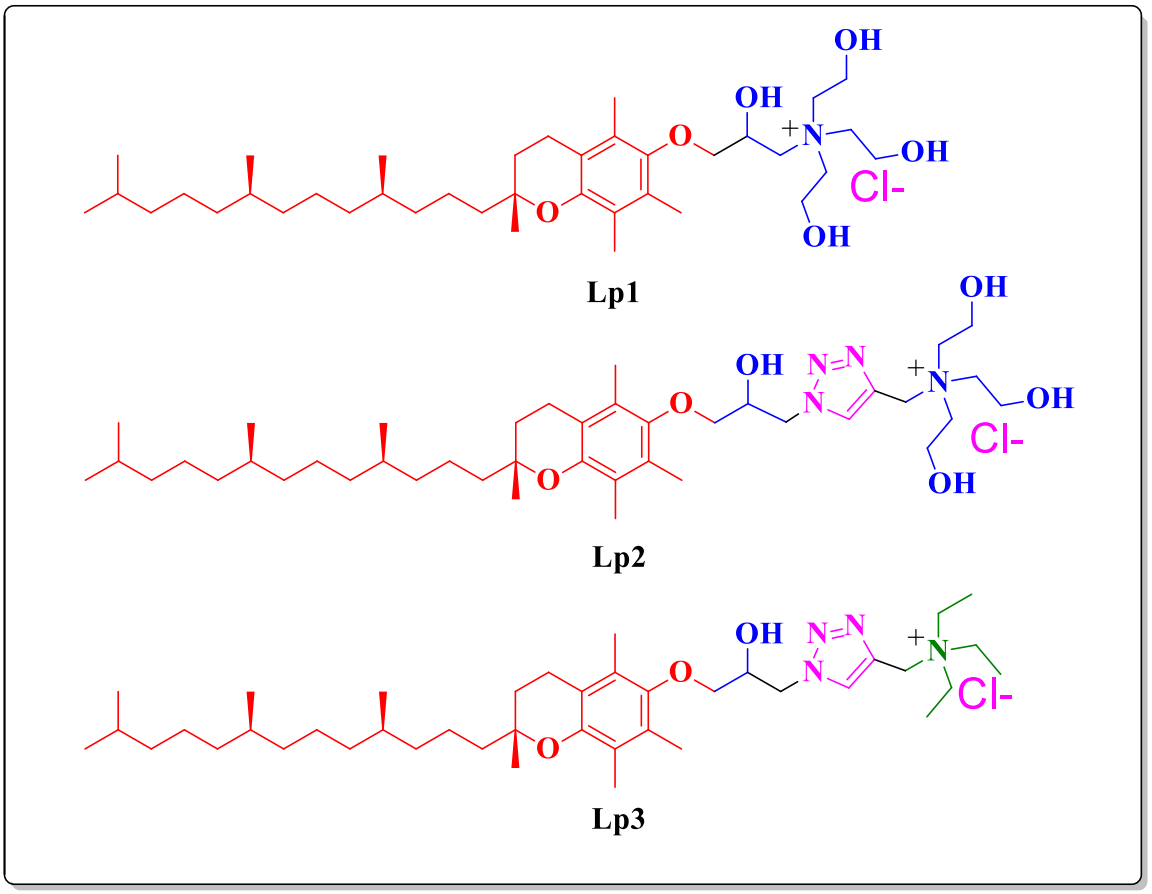

Figure 14. Chemical structures of targeted Cationic Lipids

1.5 References:

1. (a) Davis, B. D., Prospects for genetic intervention in man. *Science* **1970,***170* (3964), 1279-83;(b) Sleeper, M. M.; Bish, L. T.; Sweeney, H. L., Gene therapy in large animal models of human cardiovascular genetic disease. *ILAR journal* **2009,***50* (2), 199-205;(c) Atkinson, J.; Martin, R., Mutations to nonsense codons in human genetic disease: implications for gene therapy by nonsense suppressor tRNAs. *Nucleic acids research* **1994,***22* (8), 1327-34;(d) Gene therapy for human genetic disease? *Science* **1972,***178*(4061), 648-9;(e) Friedmann, T.; Roblin, R., Gene therapy for human genetic disease? *Science* **1972,***175* (4025), 949-55.
2. (a) Kumamoto, T.; Huang, E. K.; Paek, H. J.; Morita, A.; Matsue, H.; Valentini, R. F.; Takashima, A., Induction of tumor-specific protective immunity by in situ Langerhans cell vaccine. *Nature biotechnology* **2002,***20* (1), 64-9;(b) Cornetta, K.; Wieder, R.; Anderson, W. F., Gene transfer into primates and prospects for gene therapy in humans. *Progress in nucleic acid research and molecular biology* **1989,***36*, 311-22;(c) Morrow, J. F., The prospects for gene therapy in humans. *Annals of the New York Academy of Sciences* **1976,***265*, 13-21.
3. (a) Grossmann, M.; Leitolf, H.; Weintraub, B. D.; Szkudlinski, M. W., A rational design strategy for protein hormone superagonists. *Nature biotechnology* **1998,***16* (9), 871-5;(b) Miller, N.; Whelan, J., Progress in transcriptionally targeted and regulatable vectors for genetic therapy. *Human gene therapy* **1997,***8* (7), 803-15.
4. Yang, Y.; Nunes, F. A.; Berencsi, K.; Furth, E. E.; Gonczol, E.; Wilson, J. M., Cellular immunity to viral antigens limits E1-deleted adenoviruses for gene therapy. *Proceedings of the National Academy of Sciences of the United States of America* **1994,***91* (10), 4407-11.
5. (a) Knowles, M. R.; Hohneker, K. W.; Zhou, Z.; Olsen, J. C.; Noah, T. L.; Hu, P. C.; Leigh, M. W.; Engelhardt, J. F.; Edwards, L. J.; Jones, K. R.; et al., A controlled study of adenoviral-vector-mediated gene transfer in the nasal epithelium of patients with cystic fibrosis. *The New England journal of medicine* **1995,***333* (13), 823-31;(b) Hacein-Bey-

Abina, S.; Le Deist, F.; Carlier, F.; Bouneaud, C.; Hue, C.; De Villartay, J. P.; Thrasher, A. J.; Wulffraat, N.; Sorensen, R.; Dupuis-Girod, S.; Fischer, A.; Davies, E. G.; Kuis, W.; Leiva, L.; Cavazzana-Calvo, M., Sustained correction of X-linked severe combined immunodeficiency by ex vivo gene therapy. *The New England journal of medicine* **2002,***346* (16), 1185-93;(c) Liu, F.; Shollenberger, L. M.; Conwell, C. C.; Yuan, X.; Huang, L., Mechanism of naked DNA clearance after intravenous injection. *The journal of gene medicine* **2007,***9* (7), 613-9.

6. Felgner, P. L.; Gadek, T. R.; Holm, M.; Roman, R.; Chan, H. W.; Wenz, M.; Northrop, J. P.; Ringold, G. M.; Danielsen, M., Lipofection: a highly efficient, lipid-mediated DNA-transfection procedure. *Proceedings of the National Academy of Sciences of the United States of America* **1987,***84* (21), 7413-7.
7. (a) Jose, A.; Labala, S.; Venuganti, V. V., Co-delivery of curcumin and STAT3 siRNA using deformable cationic liposomes to treat skin cancer. *Journal of drug targeting* **2017,***25* (4), 330-341;(b) Matos, A. L. L.; Pereira, G.; Cabral Filho, P. E.; Santos, B. S.; Fontes, A., Delivery of cationic quantum dots using fusogenic liposomes in living cells. *Journal of photochemistry and photobiology. B, Biology* **2017,***171*, 43-49;(c) Bender, H. R.; Kane, S.; Zabel, M. D., Delivery of Therapeutic siRNA to the CNS Using Cationic and Anionic Liposomes. *Journal of visualized experiments: JoVE* **2016,** (113).
8. (a) Inoh, Y.; Nagai, M.; Matsushita, K.; Nakanishi, M.; Furuno, T., Gene transfection efficiency into dendritic cells is influenced by the size of cationic liposomes/DNA complexes. *European journal of pharmaceutical sciences : official journal of the European Federation for Pharmaceutical Sciences* **2017,***102*, 230-236;(b) Gai, X.; Cheng, L.; Li, T.; Liu, D.; Wang, Y.; Wang, T.; Pan, W.; Yang, X., In vitro and In vivo Studies on a Novel Bioadhesive Colloidal System: Cationic Liposomes of Ibuprofen. *AAPS PharmSciTech* **2018,***19* (2), 700-709;(c) Roursgaard, M.; Knudsen, K. B.; Northeved, H.; Persson, M.; Christensen, T.; Kumar, P. E. K.; Perrin, A.; Andresen, T. L.; Getting, T.; Lykkesfeldt, J.;

Vesterdal, L. K.; Loft, S.; Moller, P., In vitro toxicity of cationic micelles and liposomes in cultured human hepatocyte (HepG2) and lung epithelial (A549) cell lines. *Toxicology in vitro: an international journal published in association with BIBRA* **2016,***36*, 164-171.

9. (a) Mamusa, M.; Barbero, F.; Montis, C.; Cutillo, L.; Gonzalez-Paredes, A.; Berti, D., Inclusion of oligonucleotide antimicrobials in biocompatible cationic liposomes: A structural study. *Journal of colloid and interface science* **2017,***508*, 476-487;(b) Falsini, S.; Ristori, S., Lipoplexes from Non-viral Cationic Vectors: DOTAP-DOPE Liposomes and Gemini Micelles. *Methods Mol Biol* **2016,***1445*, 33-43;(c) Wang, C.; Liu, P.; Zhuang, Y.; Li, P.; Jiang, B.; Pan, H.; Liu, L.; Cai, L.; Ma, Y., Lymphatic-targeted cationic liposomes: A robust vaccine adjuvant for promoting long-term immunological memory. *Journal of controlled release : official journal of the Controlled Release Society* **2015,***213*, e16.
10. (a) Li, T.; He, J.; Horvath, G.; Prochnicki, T.; Latz, E.; Takeoka, S., Lysine-containing cationic liposomes activate the NLRP3 inflammasome: Effect of a spacer between the head group and the hydrophobic moieties of the lipids. *Nanomedicine : nanotechnology, biology, and medicine* **2018,***14* (2), 279-288;(b) De, M.; Ghosh, S.; Sen, T.; Shadab, M.; Banerjee, I.; Basu, S.; Ali, N., A Novel Therapeutic Strategy for Cancer Using Phosphatidylserine Targeting Stearylamine-Bearing Cationic Liposomes. *Molecular therapy. Nucleic acids* **2018,***10*, 9-27.
11. (a) Naseri, H.; Eskandari, F.; Jaafari, M. R.; Khamesipour, A.; Abbasi, A.; Badiee, A., PEGylation of cationic liposomes encapsulating soluble Leishmania antigens reduces the adjuvant efficacy of liposomes in murine model. *Parasite immunology* **2017,***39* (11);(b) Monpara, J.; Kanthou, C.; Tozer, G. M.; Vavia, P. R., Rational Design of Cholesterol Derivative for Improved Stability of Paclitaxel Cationic Liposomes. *Pharmaceutical research* **2018,***35* (4), 90.
12. (a) Hattori, Y.; Machida, Y.; Honda, M.; Takeuchi, N.; Yoshiike, Y.; Ohno, H.; Onishi, H., Small interfering RNA delivery into the liver by cationic cholesterol derivative-based

liposomes. *Journal of liposome research* **2017,***27* (4), 264-273;(b) Petaccia, M.; Giansanti, L.; Leonelli, F.; Bella, A.; Gradella Villalva, D.; Mancini, G., Synthesis, characterization and inclusion into liposomes of a new cationic pyrenyl amphiphile. *Chemistry and physics of lipids* **2016,***200*, 83-93.

13. Luo, D.; Geng, J.; Li, N.; Carter, K. A.; Shao, S.; Atilla-Gokcumen, G. E.; Lovell, J. F., Vessel-Targeted Chemophototherapy with Cationic Porphyrin-Phospholipid Liposomes. *Molecular cancer therapeutics* **2017,***16* (11), 2452-2461.

14. (a) Varypataki, E. M.; Silva, A. L.; Barnier-Quer, C.; Collin, N.; Ossendorp, F.; Jiskoot, W., Synthetic long peptide-based vaccine formulations for induction of cell mediated immunity: A comparative study of cationic liposomes and PLGA nanoparticles. *Journal of controlled release : official journal of the Controlled Release Society* **2016,***226*, 98-106;(b) Qiao, C.; Liu, J.; Yang, J.; Li, Y.; Weng, J.; Shao, Y.; Zhang, X., Enhanced non-inflammasome mediated immune responses by mannosylated zwitterionic-based cationic liposomes for HIV DNA vaccines. *Biomaterials* **2016,***85*, 1-17;(c) Doddapaneni, R.; Patel, K.; Owaid, I. H.; Singh, M., Tumor neovasculature-targeted cationic PEGylated liposomes of gambogic acid for the treatment of triple-negative breast cancer. *Drug delivery* **2016,***23* (4), 1232-41.

15. (a) Yao, Y.; Su, Z.; Liang, Y.; Zhang, N., pH-Sensitive carboxymethyl chitosan-modified cationic liposomes for sorafenib and siRNA co-delivery. *International journal of nanomedicine* **2015,***10*, 6185-97;(b) Kim, B. K.; Seu, Y. B.; Choi, J. S.; Park, J. W.; Doh, K. O., Synthesis and validation of novel cholesterol-based fluorescent lipids designed to observe the cellular trafficking of cationic liposomes. *Bioorganic & medicinal chemistry letters* **2015,***25* (18), 3893-6;(c) Sugano, M.; Morisaki, H.; Negishi, Y.; Endo-Takahashi, Y.; Kuwata, H.; Miyazaki, T.; Yamamoto, M., Potential effect of cationic liposomes on interactions with oral bacterial cells and biofilms. *Journal of liposome research* **2016,***26* (2), 156-62.

16. (a) Somiya, M.; Yamaguchi, K.; Liu, Q.; Niimi, T.; Maturana, A. D.; Iijima, M.; Yoshimoto, N.; Kuroda, S., One-step scalable preparation method for non-cationic liposomes with high siRNA content. *International journal of pharmaceutics* **2015,***490* (1-2), 316-23;(b) Hwang, T. L.; Hsu, C. Y.; Aljuffali, I. A.; Chen, C. H.; Chang, Y. T.; Fang, J. Y., Cationic liposomes evoke proinflammatory mediator release and neutrophil extracellular traps (NETs) toward human neutrophils. *Colloids and surfaces. B, Biointerfaces* **2015,***128*, 119-26;(c) Gasperini, A. A.; Puentes-Martinez, X. E.; Balbino, T. A.; Rigoletto Tde, P.; Correa Gde, S.; Cassago, A.; Portugal, R. V.; de La Torre, L. G.; Cavalcanti, L. P., Association between cationic liposomes and low molecular weight hyaluronic acid. *Langmuir : the ACS journal of surfaces and colloids* **2015,***31* (11), 3308-17.

17. Wang, T.; Zhen, Y.; Ma, X.; Wei, B.; Li, S.; Wang, N., Mannosylated and lipid A-incorporating cationic liposomes constituting microneedle arrays as an effective oral mucosal HBV vaccine applicable in the controlled temperature chain. *Colloids and surfaces. B, Biointerfaces* **2015,***126*, 520-30.

18. Ran, R.; Liu, Y.; Gao, H.; Kuang, Q.; Zhang, Q.; Tang, J.; Huang, K.; Chen, X.; Zhang, Z.; He, Q., Enhanced gene delivery efficiency of cationic liposomes coated with PEGylated hyaluronic acid for anti P-glycoprotein siRNA: a potential candidate for overcoming multi-drug resistance. *International journal of pharmaceutics* **2014,***477* (1-2), 590-600.

19. (a) Li, X. T.; Zhou, Z. Y.; Jiang, Y.; He, M. L.; Jia, L. Q.; Zhao, L.; Cheng, L.; Jia, T. Z., PEGylated VRB plus quinacrine cationic liposomes for treating non-small cell lung cancer. *Journal of drug targeting* **2015,***23* (3), 232-43;(b) Varypataki, E. M.; van der Maaden, K.; Bouwstra, J.; Ossendorp, F.; Jiskoot, W., Cationic liposomes loaded with a synthetic long peptide and poly(I:C): a defined adjuvanted vaccine for induction of antigen-specific T cell cytotoxicity. *The AAPS journal* **2015,***17* (1), 216-26;(c) Ma, C. C.; He, Z. Y.; Xia, S.; Ren, K.; Hui, L. W.; Qin, H. X.; Tang, M. H.; Zeng, J.; Song, X. R., alpha, omega-Cholesterol-

functionalized low molecular weight polyethylene glycol as a novel modifier of cationic liposomes for gene delivery. *International journal of molecular sciences* **2014,***15* (11), 20339-54;(d) Weecharangsan, W.; Opanasopit, P.; Yingyongnarongkul, B. E.; Kewsuwan, P.; Lee, R. J., Co-delivery of plasmid DNA and antisense oligodeoxyribonucleotide into human carcinoma cells by cationic liposomes. *Current pharmaceutical biotechnology* **2014,***15* (9), 790-9.

20. (a) Dicheva, B. M.; ten Hagen, T. L.; Schipper, D.; Seynhaeve, A. L.; van Rhoon, G. C.; Eggermont, A. M.; Koning, G. A., Targeted and heat-triggered doxorubicin delivery to tumors by dual targeted cationic thermosensitive liposomes. *Journal of controlled release : official journal of the Controlled Release Society* **2014,***195*, 37-48;(b) Knudsen, K. B.; Northeved, H.; Kumar, P. E.; Permin, A.; Gjetting, T.; Andresen, T. L.; Larsen, S.; Wegener, K. M.; Lykkesfeldt, J.; Jantzen, K.; Loft, S.; Moller, P.; Roursgaard, M., In vivo toxicity of cationic micelles and liposomes. *Nanomedicine : nanotechnology, biology, and medicine* **2015,***11* (2), 467-77.

21. (a) Naicker, K.; Ariatti, M.; Singh, M., PEGylated galactosylated cationic liposomes for hepatocytic gene delivery. *Colloids and surfaces. B, Biointerfaces* **2014,***122*, 482-490;(b) Mansourian, M.; Badiee, A.; Jalali, S. A.; Shariat, S.; Yazdani, M.; Amin, M.; Jaafari, M. R., Effective induction of anti-tumor immunity using p5 HER-2/neu derived peptide encapsulated in fusogenic DOTAP cationic liposomes co-administrated with CpG-ODN. *Immunology letters* **2014,***162* (1 Pt A), 87-93.

22. (a) Stefanutti, E.; Papacci, F.; Sennato, S.; Bombelli, C.; Viola, I.; Bonincontro, A.; Bordi, F.; Mancini, G.; Gigli, G.; Risuleo, G., Cationic liposomes formulated with DMPC and a gemini surfactant traverse the cell membrane without causing a significant bio-damage. *Biochimica et biophysica acta* **2014,***1838* (10), 2646-55;(b) Yoshizaki, Y.; Yuba, E.; Sakaguchi, N.; Koiwai, K.; Harada, A.; Kono, K., Potentiation of pH-sensitive polymer-modified liposomes with cationic lipid inclusion as antigen delivery carriers for cancer

immunotherapy. *Biomaterials* **2014,***35* (28), 8186-96;(c) Apiratikul, N.; Penglong, T.; Suksen, K.; Svasti, S.; Chairoungdua, A.; Yingyongnarongkula, B., In vitro delivery of curcumin with cholesterol-based cationic liposomes. *Bioorganicheskaia khimiia* **2013,***39* (4), 497-503.

23. Ichihara, H.; Hino, M.; Ueoka, R.; Matsumoto, Y., Therapeutic effects of cationic hybrid liposomes on the hepatic metastasis of colon carcinoma along with apoptosis in vivo. *Biological & pharmaceutical bulletin* **2014,***37* (3), 498-503.
24. Lv, H.; Zhang, S.; Wang, B.; Cui, S.; Yan, J., Toxicity of cationic lipids and cationic polymers in gene delivery. *Journal of controlled release : official journal of the Controlled Release Society* **2006,***114* (1), 100-9.
25. (a) Myint, M.; Bucki, R.; Janmey, P. A.; Diamond, S. L., Synthesis and structure-activity relationships of novel cationic lipids with anti-inflammatory and antimicrobial activities. *Bioorganic & medicinal chemistry letters* **2015,***25* (14), 2837-43;(b) Bajaj, A.; Kondiah, P.; Bhattacharya, S., Design, synthesis, and in vitro gene delivery efficacies of novel cholesterol-based gemini cationic lipids and their serum compatibility: a structure-activity investigation. *Journal of medicinal chemistry* **2007,***50* (10), 2432-42;(c) Byk, G.; Dubertret, C.; Escriou, V.; Frederic, M.; Jaslin, G.; Rangara, R.; Pitard, B.; Crouzet, J.; Wils, P.; Schwartz, B.; Scherman, D., Synthesis, activity, and structure--activity relationship studies of novel cationic lipids for DNA transfer. *Journal of medicinal chemistry* **1998,***41* (2), 229-35.
26. Audouy, S. A.; de Leij, L. F.; Hoekstra, D.; Molema, G., In vivo characteristics of cationic liposomes as delivery vectors for gene therapy. *Pharmaceutical research* **2002,***19* (11), 1599-605.
27. Kedika, B.; Patri, S. V., Influence of minor backbone structural variations in modulating the in vitro gene transfer efficacies of alpha-tocopherol based cationic transfection lipids. *Bioconjugate chemistry* **2011,***22* (12), 2581-92.

28. Aoshima, Y.; Hokama, R.; Sou, K.; Sarker, S. R.; Iida, K.; Nakamura, H.; Inoue, T.; Takeoka, S., Cationic amino acid based lipids as effective nonviral gene delivery vectors for primary cultured neurons. *ACS chemical neuroscience* **2013,***4* (12), 1514-9.

29. Liu, Q.; Yi, W. J.; Zhang, Y. M.; Zhang, J.; Guo, L.; Yu, X. Q., Biotinylated cyclen-contained cationic lipids as non-viral gene delivery vectors. *Chemical biology & drug design* **2013,***82* (4), 376-83.

30. Kearns, M. D.; Patel, Y. N.; Savva, M., Physicochemical characteristics associated with transfection of cationic cholesterol-based gene delivery vectors in the presence of DOPE. *Chemistry and physics of lipids* **2010,***163* (8), 755-64.

31. Wang, L.; Yang, L.; Wu, Y. K.; Zhao, X.; Wei, Y. Q.; Li, W.; Tian, Q., [Intravenous delivery of cationic liposomes conjugation to recombinant adenoviral vectors containing human endostatin gene inhibits ovarian cancer growth in nude mice]. *Sichuan da xue xue bao. Yi xue ban = Journal of Sichuan University. Medical science edition* **2009,***40* (2), 190-4.

32. Zuidam, N. J.; Barenholz, Y., Electrostatic and structural properties of complexes involving plasmid DNA and cationic lipids commonly used for gene delivery. *Biochimica et biophysica acta* **1998,***1368* (1), 115-28.

33. Klaczkow, G.; Anuszewska, E. L., Determination of the stereoisomers of racemic alpha-tocopherol in pharmaceutical preparations by high-performance liquid chromatography and gas chromatography. *Acta poloniae pharmaceutica* **2008,***65* (6), 715-21.

34. Yilmaz, B.; Ozturk, M.; Kadioglu, Y. Y., Comparison of two derivative spectrophotometric methods for the determination of alpha-tocopherol in pharmaceutical preparations. *Farmaco* **2004,***59* (9), 723-7.

35. (a) Klaczkow, G.; Jakoniuk, D.; Anuszewska, E. L., Determination of d-alpha-tocopherol and its impurity by chiral high performance liquid chromatography in pharmaceutical preparations. *Acta poloniae pharmaceutica* **2004,***61* (3), 181-4;(b) Dahot, M. U.; Memon,

M. A., UV-spectrophotometric determination of alpha-tocopherol acetate in pharmaceutical preparations. *Pakistan journal of pharmaceutical sciences* **1990,***3* (1), 53-9.

36. (a) Wu, P.; Chen, H.; Jin, R.; Weng, T.; Ho, J. K.; You, C.; Zhang, L.; Wang, X.; Han, C., Non-viral gene delivery systems for tissue repair and regeneration. *Journal of translational medicine* **2018,***16* (1), 29;(b) Sun, D.; Schur, R. M.; Lu, Z. R., A novel nonviral gene delivery system for treating Leber's congenital amaurosis. *Therapeutic delivery* **2017,***8* (10), 823-826;(c) Fernandez-Pineiro, I.; Pensado, A.; Badiola, I.; Sanchez, A., Development and characterisation of chondroitin sulfate- and hyaluronic acid-incorporated sorbitan ester nanoparticles as gene delivery systems. *European journal of pharmaceutics and biopharmaceutics : official journal of Arbeitsgemeinschaft fur Pharmazeutische Verfahrenstechnik e.V* **2018,***125*, 85-94;(d) McMillan, A.; Nguyen, M. K.; Gonzalez-Fernandez, T.; Ge, P.; Yu, X.; Murphy, W. L.; Kelly, D. J.; Alsberg, E., Dual non-viral gene delivery from microparticles within 3D high-density stem cell constructs for enhanced bone tissue engineering. *Biomaterials* **2018,***161*, 240-255;(e) Holstein, M.; Mesa-Nunez, C.; Miskey, C.; Almarza, E.; Poletti, V.; Schmeer, M.; Grueso, E.; Ordonez Flores, J. C.; Kobelt, D.; Walther, W.; Aneja, M. K.; Geiger, J.; Bonig, H. B.; Izsvak, Z.; Schleef, M.; Rudolph, C.; Mavilio, F.; Bueren, J. A.; Guenechea, G.; Ivics, Z., Efficient Non-viral Gene Delivery into Human Hematopoietic Stem Cells by Minicircle Sleeping Beauty Transposon Vectors. *Molecular therapy : the journal of the American Society of Gene Therapy* **2018**.

37. (a) Badamchi-Zadeh, A.; Tartaglia, L. J.; Abbink, P.; Bricault, C. A.; Liu, P. T.; Boyd, M.; Kirilova, M.; Mercado, N. B.; Nanayakkara, O. S.; Vrbanac, V. D.; Tager, A. M.; Larocca, R. A.; Seaman, M. S.; Barouch, D. H., Therapeutic Efficacy of Vectored PGT121 Gene Delivery in HIV-1-Infected Humanized Mice. *Journal of virology* **2018,***92* (7);(b) Kodama, Y.; Hanamura, H.; Muro, T.; Nakagawa, H.; Kurosaki, T.; Nakamura, T.; Kitahara, T.; Kawakami, S.; Nakashima, M.; Sasaki, H., Gene delivery system of pDNA using the blood

glycoprotein fetuin. *Journal of drug targeting* **2017**, 1-6;(c) Jeong, G. W.; Nah, J. W., Evaluation of disulfide bond-conjugated LMWSC-g-bPEI as non-viral vector for low cytotoxicity and efficient gene delivery. *Carbohydrate polymers* **2017,***178*, 322-330.

38. (a) Caroline Diana, S. M.; Rekha, M. R., Efficacy of vinyl imidazole grafted cationized pullulan and dextran as gene delivery vectors: A comparative study. *International journal of biological macromolecules* **2017,***105* (Pt 1), 947-955;(b) Nakatsuji, H.; Kawabata Galbraith, K.; Kurisu, J.; Imahori, H.; Murakami, T.; Kengaku, M., Surface chemistry for cytosolic gene delivery and photothermal transgene expression by gold nanorods. *Scientific reports* **2017,***7* (1), 4694;(c) Pacheco-Lugo, L.; Diaz-Olmos, Y.; Saenz-Garcia, J.; Probst, C. M.; DaRocha, W. D., Effective gene delivery to Trypanosoma cruzi epimastigotes through nucleofection. *Parasitology international* **2017,***66* (3), 236-239;(d) Zhang, T. Y.; Wu, J. H.; Xu, Q. H.; Wang, X. R.; Lu, J.; Hu, Y.; Jo, J. I.; Yamamoto, M.; Ling, D.; Tabata, Y.; Gao, J. Q., Design of magnetic gene complexes as effective and serum resistant gene delivery systems for mesenchymal stem cells. *International journal of pharmaceutics* **2017,***520* (1-2), 1-13.

39. (a) Ohta, T.; Hashida, Y.; Higuchi, Y.; Yamashita, F.; Hashida, M., In Vitro Cellular Gene Delivery Employing a Novel Composite Material of Single-Walled Carbon Nanotubes Associated With Designed Peptides With Pegylation. *Journal of pharmaceutical sciences* **2017,***106* (3), 792-802;(b) Miller, J. B.; Zhang, S.; Kos, P.; Xiong, H.; Zhou, K.; Perelman, S. S.; Zhu, H.; Siegwart, D. J., Non-Viral CRISPR/Cas Gene Editing In Vitro and In Vivo Enabled by Synthetic Nanoparticle Co-Delivery of Cas9 mRNA and sgRNA. *Angew Chem Int Ed Engl* **2017,***56* (4), 1059-1063;(c) Zhang, B.; Zhang, Y.; Yu, D., Lung cancer gene therapy: Transferrin and hyaluronic acid dual ligand-decorated novel lipid carriers for targeted gene delivery. *Oncology reports* **2017,***37* (2), 937-944.

40. (a) Gurbuz, N.; Ashour, A. A.; Alpay, S. N.; Ozpolat, B., Down-regulation of 5-HT1B and 5-HT1D receptors inhibits proliferation, clonogenicity and invasion of human pancreatic

cancer cells. *PloS one* **2014,***9* (9), e110067;(b) Dizeyi, N.; Bjartell, A.; Nilsson, E.; Hansson, J.; Gadaleanu, V.; Cross, N.; Abrahamsson, P. A., Expression of serotonin receptors and role of serotonin in human prostate cancer tissue and cell lines. *The Prostate* **2004,***59* (3), 328-36.

41. (a) Luo, D.; Saltzman, W. M., Synthetic DNA delivery systems. *Nature biotechnology* **2000,***18* (1), 33-7;(b) Oupicky, D.; Konak, C.; Ulbrich, K.; Wolfert, M. A.; Seymour, L. W., DNA delivery systems based on complexes of DNA with synthetic polycations and their copolymers. *Journal of controlled release : official journal of the Controlled Release Society* **2000,***65* (1-2), 149-71;(c) Soto, J.; Bessodes, M.; Pitard, B.; Mailhe, P.; Scherman, D.; Byk, G., Non-electrostatic complexes with DNA: towards novel synthetic gene delivery systems. *Bioorganic & medicinal chemistry letters* **2000,***10* (9), 911-4.

42. (a) Martin, B.; Sainlos, M.; Aissaoui, A.; Oudrhiri, N.; Hauchecorne, M.; Vigneron, J. P.; Lehn, J. M.; Lehn, P., The design of cationic lipids for gene delivery. *Current pharmaceutical design* **2005,***11* (3), 375-94;(b) Bhattacharya, S.; Bajaj, A., Advances in gene delivery through molecular design of cationic lipids. *Chem Commun (Camb)* **2009,** (31), 4632-56.

CHAPTER 2

α-Tocopherol-ascorbic acid hybrid antioxidant based cationic amphiphile for gene delivery: design, synthesis, and transfection

2.1 Introduction

Basically, gene therapy is a potential strategy to deliver foreign DNA into a target cell nucleus, resulting in the modulation of hosts malfunctioning gene thereby helpsin disease treatment[1]. Gene therapy plays a vital role in the cure of acquired diseases, such as cardiovascular diseases, cancer, AIDS, etc[2,3,4]. But, the ideal gene-vectors are needed to deliver and protect the genetic functional material that has to be entered into the host cell, against to the enzymatic degradation inside the cell milieu[5, 6,7]. Though the viral carriers are one of the widely using pDNA-carriers, they are proven to be imperfect in the past decades due to their less efficiency in gene transfer due to the existence of highest immunogenicity, mutagenicity, and sometimes fatal toxicity[8,9]. However, synthetic DNA-delivering vehicles (non-viral vectors) were emerged as promising alternatives, because of their extensive characterization, structural and synthetic simplicity, as well as synthetic ease of modification of their size, functionality[10]. Synthetic cationic reagents (lipids) were having been in use since 1987 for gene delivery. In general, non-viral vectors are categorized into cationic lipids, polymers, and peptides. The cationic lipids are considered to be one of the most efficient non-viral over viral approaches and it already has been using for *in vitro* transfection of a mammalian cell[11]. The cationic lipid-DNA complexes (lipoplexes) are one of the highly efficient systems for easy trafficking of the gene of interest into host nucleus *via* an endocytosis pathway[12]. The transfection efficiency of cationic liposomes depends upon the formulation/mixing of cationic lipids and the architecture of the gene-expression system.[13,14]. Some of the synthetic delivery systems possess radical scavenging ability along with transfection potency, which is helpful in treating ROS (reactive oxygen species) related diseases such as brain stroke/ischemia and malignancy[15], etc. Though, toxicity is one of the barriers limiting the clinical applications of cationic liposomes[16,17]. Hence, regulating this cytotoxicity should facilitate the development of safe cationic liposomes for use as non-viral vectors and thereby clarifying the mechanism of cytotoxicity of cationic liposomes[18]. Recently it is demonstrated that the

cytotoxicity of cationic liposomes is a result of apoptosis [19,20], and that cationic liposome-induced apoptosis exhibited due to the following features: generation of reactive oxygen species (ROS)[21,22]; the activation of p38 mitogen-activated protein kinase (MAPK)[23,24]; the activation of caspase-8[20, 23,24] the cleavage of Bid and its translocation to the mitochondria and the release of cytochrome c [23, 24]; and the activation of caspase-3[25]. However, it remains unclear how cationic liposomes lead to ROS generation. Particularly neurons are vulnerable to increases in ROS levels[22a,26] because these cells have a reduced capacity to detoxify ROS[24,27]. Hence, the delivery systems possessing radical scavenging ability along with transfection potency may be helpful in treating ROS (reactive oxygen species)[28] related diseases such as brain stroke/ischemia and malignancy. Antioxidant cationic lipids display their obvious role as transporters of foreign DNA into the nucleolus of the host cell, without showing any toxicity[29,30,31,32]. Herein, we designed and synthesized a new cationic lipid hybrid (**Toc-As**) by conjugating α-tocopherol and ascorbic acid together with ammonium di-ether linker and allowed it to form the self-assembled amphiphilic molecule. The rationale for the design of this conjugated lipid is that these two vitamins (E and C) are potent natural antioxidants and can form an amphiphilic surfactant when conjugated. The main role of α-tocopherol as an antioxidant is quenching of peroxyl radicals and per hydroxyl radicals and produce "tocopheroxyl radicals". Ascorbic acid (vitamin C) scavenges oxygen radicals in the aqueous phase and it converts tocopheroxyl radical into α- tocopherol, thereby permitting α-tocopherol to act as a free radical chain-breaking antioxidant and maintain biological systems. It is now apparent that ascorbic acid and tocopherol function together can protect membrane lipids from oxidative damage. To study the individual role of each antioxidant in transfection, we have developed two control lipids one is with ascorbic acid moiety without tocopherol moiety (**N14-As**) and another is with tocopherol moiety without ascorbic acid moiety (**Toc-NOH**).

The nanostructure of individual **Toc-As, Toc-NOH** and **N14-As** cationic lipids characterized in terms of size, antioxidant activity, stability, and morphology. The lipoplexes of **Toc-As**, **N14-As,** and **Toc-NOH** were evaluated for their *in vitro* activities in multiple cell lines. The cytotoxicity of the lipids is also studied using MTT assay in multiple cell lines.

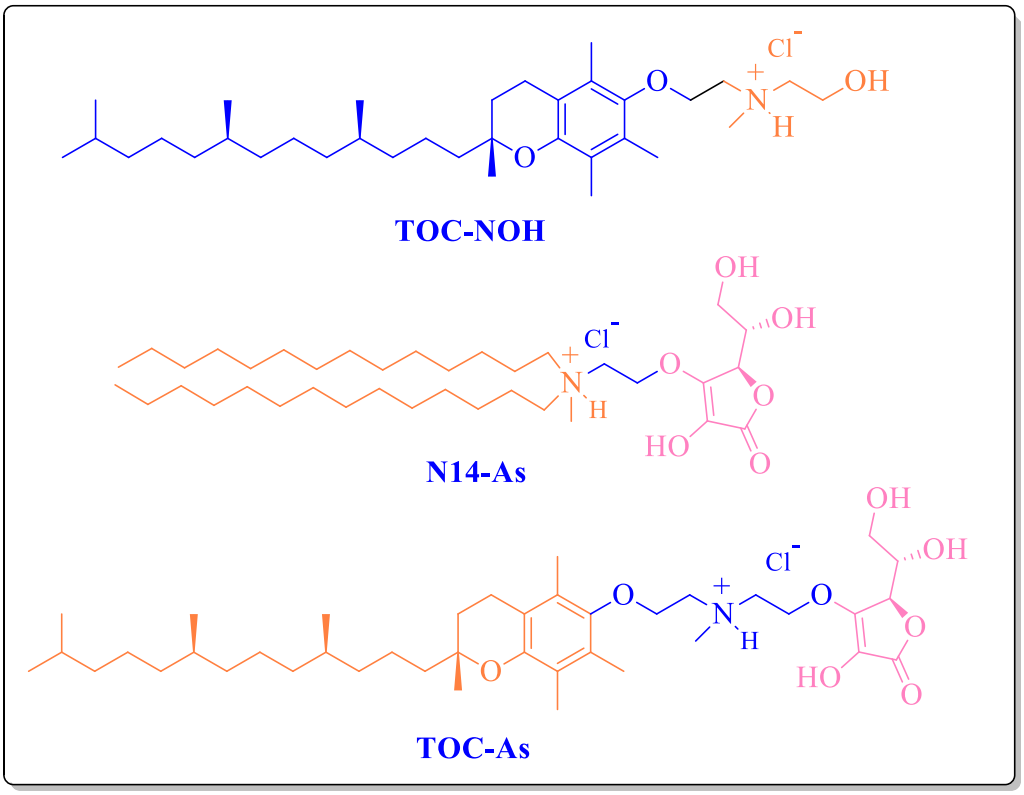

Figure.1. Chemical structures of Cationic Lipids

2.2 RESULTS AND DISCUSSION

2.2.1 Chemistry

The targeted cationic lipids**Toc-As, N14-As and Toc-NOH** were synthesized as described in the Schemes **1, 2** and **3**. The cationic lipid **Toc-As** possess α-tocopherol as the hydrophobic group and ascorbic acid as a hydrophilic group linked through *N*,*N*-diethyl ether ammonium linker, whereas **N14-As** lipid contains *N*,*N* dialkyl chain as a hydrophobic group and ascorbic acid as a hydrophilic group linked through ethyl ether linker. The lipids **Toc-NOH** possess α-tocopherol

as the hydrophobic and hydroxyethyl group as hydrophilic moiety linked via ethylether linker. The precursor intermediate *O*-aminoethyl-[*N*-hydroxy ethyl, *N*-methyl]-α-tocopherol (**1D**, **Scheme 1**) in the synthesis of both the final lipids **Toc-NOH** and **Toc-As** is prepared conventionally as shown in the **Scheme 1**. Briefly, *O*-alkylation of α-tocopherol using ethylbromoacetate in presence of 50% potassium hydroxide gave *O*-aceticacid-α-tocopherol, **1A** which upon reduction with lithium aluminum hydride gave intermediate-hydroxyethyl-α – tocopherol, **1B** (**Scheme 1**). The intermediate **1D** was obtained by *O*-tosylation of intermediate **1B** followed by *N*-alkylation of intermediate **1C.** Subsequently, the lipid **Toc-NOH** is obtained by the quaternization of **1D** using 1N HCl in methanol. **Toc-As** is obtained by treating the intermediate **1D** with5,6 isopropylidene ascorbic acid in DCM in presence of *N,N* dimethylamine followed by deprotection of acetonide group using dry hydrochloric acid in methanol (**Scheme 3**). The intermediate *N*-(2-chloroethyl)-*N*-tetradecyl tetradecane-1-amine, **2C** for the synthesis of **N14-As** lipid is prepared conventionally as mentioned in the **Scheme 2**. The intermediate **2C** upon treatment with 5,6isopropylidene ascorbic acid as described above for **Toc-As,** followed by the deprotection using dry hydrochloric acid gave lipid **N14-As** (**Scheme 2**). Chemical structures of all the synthetic intermediates lipids were confirmed by ^{1}H-NMR, ESI-MASS and final lipids shown in **Schemes 1-3** are confirmed by ^{1}H NMR,^{13}C NMR and molecular ion peaks in their ESI–HRMS mass spectra. The purity of the title lipids was characterized by using RP-HPLC, as described in the Experimental Section.

Scheme 1

Synthesis of Toc-NOH lipid

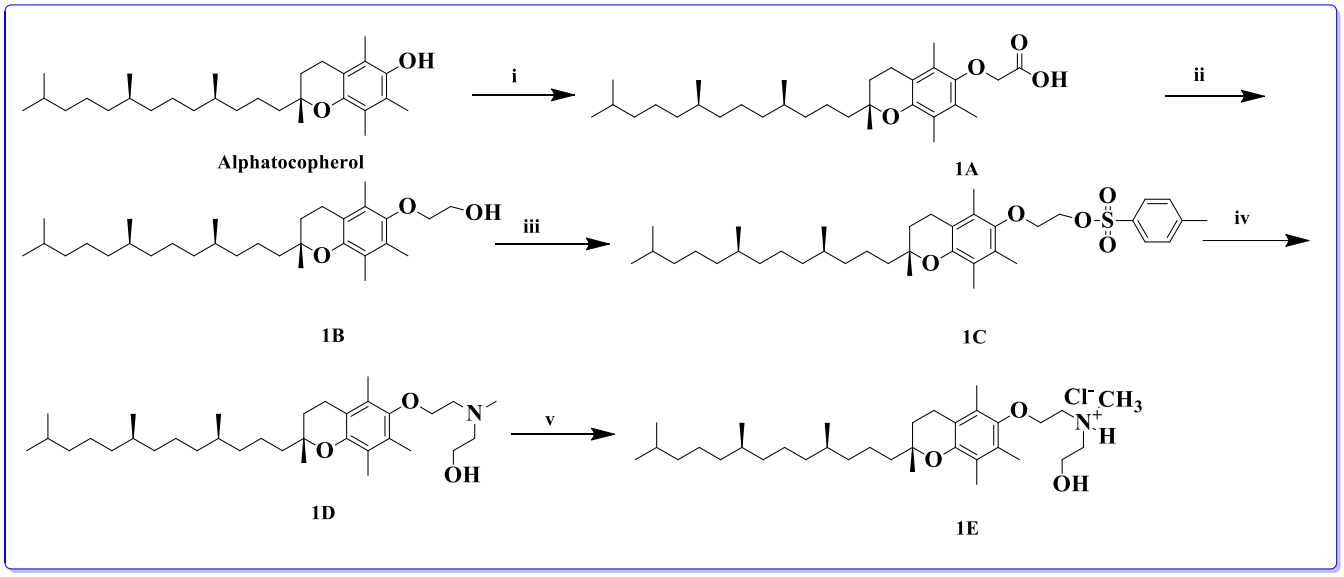

Reagents and condition: i) Ethyl bromoacetate, Dry DMF, 50% KOH solution, 12 h RT 85% ii) Dry THF, $LiAlH_4$, 6 h RT, 0-5 ˚C 92% iii) *p*-toluenesulfonyl chloride, DMAP, Dry DCM 85.10% iv) *N*-methyl ethanolamine, Methanol 63.15% v) 1N HCl in Methanol, 12 h RT 89%

Scheme 2

Synthesis of N14-As lipid

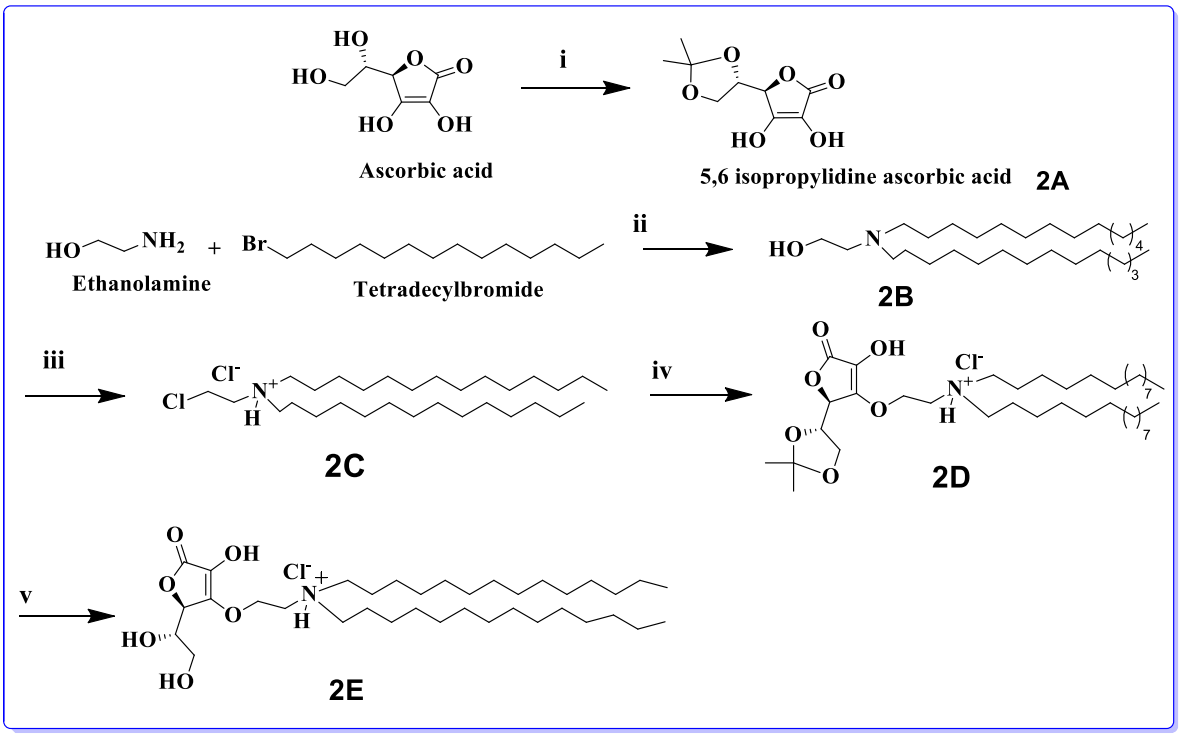

Reagents and conditions: i) Dry acetone, 2,2 Dimethoxy propane, $Sncl_2$, 82% ii) Anhydrous K_2CO_3, ethyl acetate, 48 h reflux 90% iii) $SOCl_2$, dry chloroform, 6 h reflux 91% iii) 5,6

isopropylidene ascorbic acid, dry DMSO, anhydrous K_2CO_3 89% iv) *N*-(2-chloroethyl)-*N*-tetradecyltetradecan-1-aminium, refluxed for 18 h v) 6N HCl in Methanol, 6 h RT. 75.3%

Scheme 3

Synthesis of Toc-As lipid

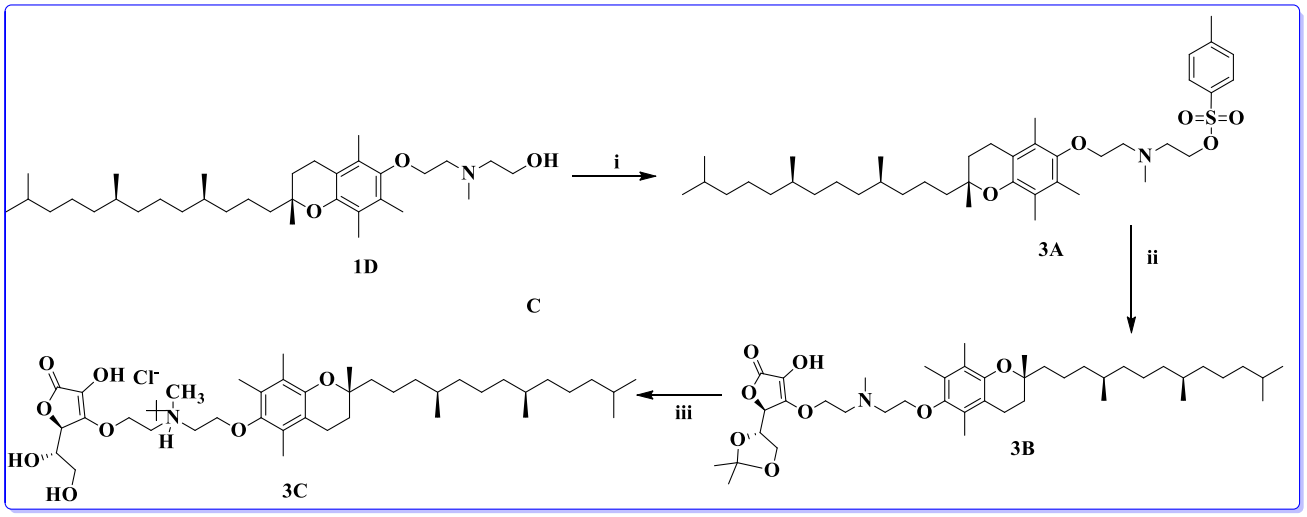

Reagents and conditions: i) p-toluenesulfonyl chloride, Triethylamine, DMAP, dry DCM, 63.15%, ii) Diethylisopropylethylamine, 5,6-isopropylidene ascorbic acid, DMAP, dry DCM 65.4 %, iii) 1N HCl in methanol, 12 h RT 85.5 %.

2.2.2Size and charge of liposomes and lipoplexes

Physicochemical characteristics viz., particle size and the surface potential of liposomes and lipoplexes of cationic lipids (**Toc-As**, **N14-As,** and **Toc-NOH**) and DOPE as co-lipid were examined using DLS technique (**Figure 2**). These measurements were made on the (+) lipid: (-) DNA charge ratios 1:1 to 8:1 in presence of free bicarbonate Dulbecco's Modified Eagle's Medium (DMEM). It is observed that the particle size of liposomes of **Toc-As** and **N14-As** are found to be 350 nm 398 nm respectively and slightly increased upon complexation with pDNA at 1:1. As we increase the charge ratio up to 4:1 the particle size observed to be decreased upto 180 nm and 220 nm respectively and a further increase in the charge ratio i.e. at 8:1 the particle size

is increased i.e. 380 nm and 350 nm respectively. The surface potential of liposomes **Toc-As** and **N14-As** (+12 mV and +9.5 mV respectively) also observed to be decreasing with increasing charge ratio upto 2:1 (+6 mV and +3.6 mV respectively) and started increasing at higher charge ratio's 4:1 and 8:1 upto +16 mV and +20 mV respectively. The least size and optimal zeta potential of lipoplexes of **Toc-As** and **N14-As** at 4:1 charge ratio is may be responsible for their greater transfection potentials at this charge ratio. It clearly indicates that when the resulting DNA-liposome complexes exhibit more charge positive or negative charge, electrostatic repulsive forces prevent extensive aggregation and/or fusion, thus leading to the formation of smaller complexes. It might also be the size of the nano-particle can be seen as a vital factor in evaluating lipoplexes suitability for gene delivery, given the size plays a role in lipoplexes endocytosis and transfection activity[33, 34,35,] Moreover, the minimal global charge of lipoplexes benefit the reduction of cytotoxicity and improve serum stability[36]. Whereas the sizes of lipoplexes of **Toc-NOH** observed to be increasing with increase in charge ratio 1:1 to 8:1 from 250 nm to 490 nm and similarly the surface charge also increases with increase in charge ratios 1:1 to 8:1from + 7.2 mV to 13.7 mV (**Figure 2**). This may be because of the aggregation of lipoplexes in presence of DMEM. Such increase in the sizes of the lipoplexes in presence of DMEM is reported previously[37]. The same reason may be considered for the increase in the sizes of lipoplexes of **Toc-As** and **N14-As** at 8:1 charge ratio.

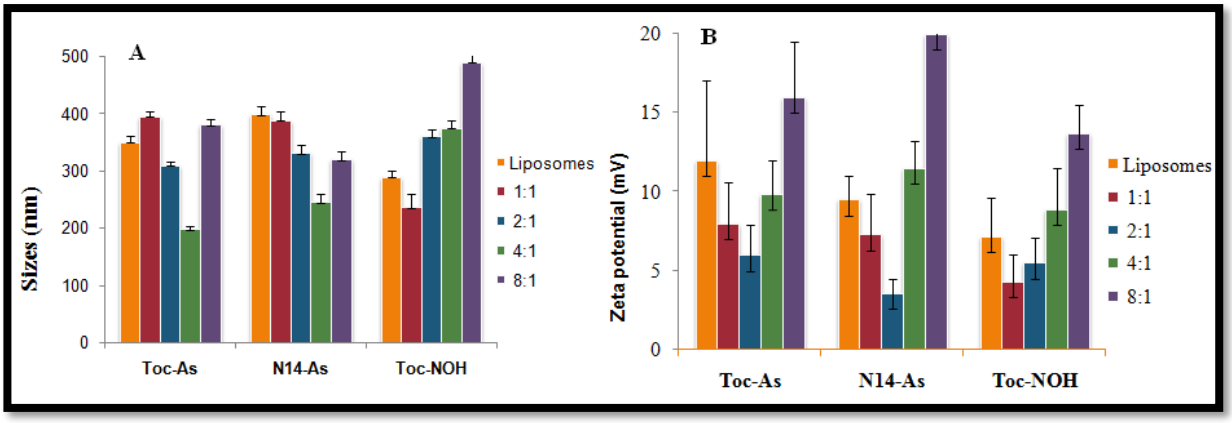

Figure.2. Physicochemical Characterization of liposomes and Lipoplexes (DLS at room temperature): Particle sizes (A) and zeta-potentials (B) of liposome of lipids **Toc-As**, **N14-As**

and **Toc-NOH** and pDNA complexes at various N/P ratios 1:1 to 1:8.Data represent mean ± SD (n = 3).

2.2.3 Liposome-DNA binding and Heparin displacement

The electrostatic binding interactions between the cationic liposome and pDNA were studied using conventional agarose gel retardation assay and heparin displacement assay across 1:1-8:1 charge ratios. The corresponding gel images reveal that all the three cationic lipids have similar capabilities in inhibiting the mobility of pDNA (**Figure 3A**). All the three lipids are capable of inhibiting 90% of pDNA mobility even at lower charge ratio's such that 2:1 (**Figure 3A**). Further, heparin displacement assay is carried out to observe the DNA binding strengths of these liposomal formulations. The results of heparin displacement assay showed a significant difference in the binding strengths of the three liposomal formulations. Liposomal formulation with **Toc-As** liposomal formulation completely resisted displacement of DNA with heparin across the lipid: DNA charge ratio 8:1-1:1 (**Figure 3B**). While **N14-As** liposomal formulation could survive pDNA displacement by heparin only at higher charge ratios i.e. 4:1 and above. (**Figure 3B**). Whereas, liposomal formulations of **Toc-NOH** could not resist much even at charge ratio 4:1 and could survive heparin displace only at higher charge ratio 8:1. It, therefore, appears that **Toc-As** and **N14-As** lipids having an ascorbic acid moiety in the head group region are capable of binding pDNA strongly and it may show any crucial role in the transfection biology. These observations are well in agreement with the size and surface potential data. The CD spectrum data also supports the binding abilities of the lipids having ascorbic acid moiety with pDNA.

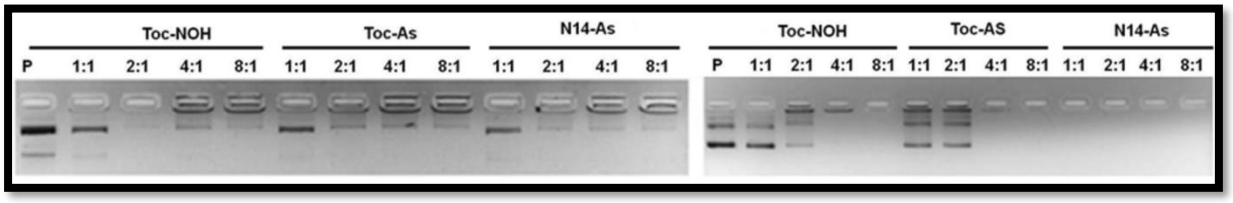

Figure.3(A) Electrophoretic gel patterns for (+) liposome/(-)DNA in gel retardation assay, (B) Electrophoretic gel patterns for liposome-pDNA complexes in Heparin displacement assay for lipids **Toc-NOH**, **N14-As,** and **Toc-As**. The liposome: pDNA charge ratios are indicated at the top of each lane. The details of the treatment are as described in the text.

2.2.4 CD Spectra of pDNA in Lipoplexes

To observe the change in the morphology of pDNA when complexed with the liposomes of the present lipids, circular dichroism (CD) measurements were carried out. Surprisingly, the formulations of **Toc-As** and **N14-As** lipids perturbed the double helix structure of DNA (**Figure 4**). Such transformed mode of compaction of pDNA by **Toc-As** and **N14-As** might be responsible for their relatively higher transfection activity, though this may be further corroborated by other physical methods to provide a comprehensive model and to prove the role of the ascorbic acid derivative of the lipids in gene transfection activity. As ascorbic acid is generally negatively charged, it cannot neutralize the charges on the negative phosphate groups of DNA. **Toc-As** and **N14-As** lipids having an ascorbic acid head group may interact with the bases inside the double-helix structure of pDNA and causes distortion in the double-helix structure. Neault et al[38] carried out an infrared and Raman spectroscopic studies on the effect of ascorbic acid on DNA[39]. They found that the OH and C-O groups of ascorbic acid interact directly with DNA bases[38, 40]. **Figure 4** demonstrates that **Toc-As** and **N14-As** lipoplexes showed linear conformation changes when compared to **Toc-NOH** lipoplex and this indicates that morphology change of lipoplexes induced by ascorbic acid head group contained lipids. These results suggest that torsional stress is generated along the double-helix DNA in ascorbic acid based lipids and this may be useful for the gene delivery. To the best of our knowledge, gene delivery efficiency of ascorbic acid head group (**Toc-As** and **N14-As**) lipids has not previously reported. In this study, it has become clear that ascorbic acid head group lipids have a dramatic effect on the confirmation of giant DNA molecules.

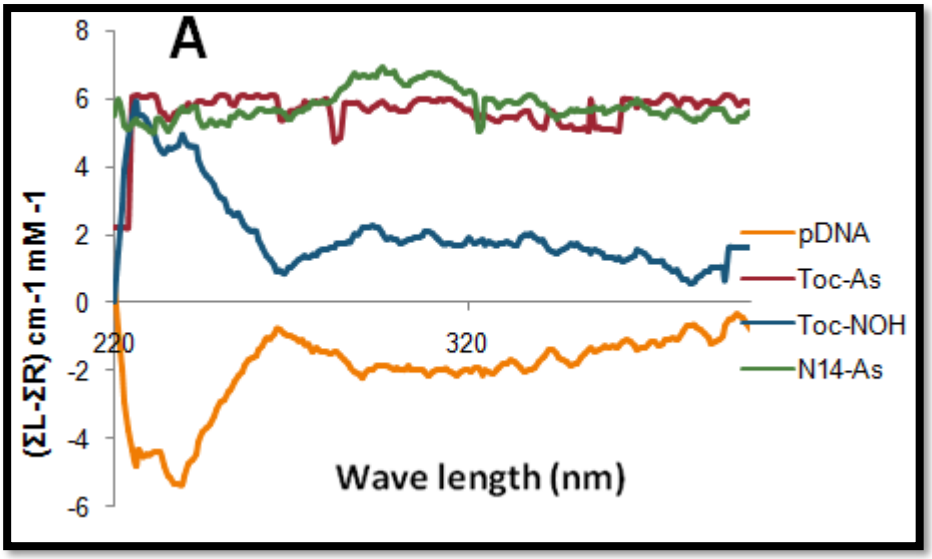

Figure 4. The lipoplexes were studied by Circular dichroism (CD) spectra. Positively charged liposomes were prepared at 1/1 molar ratio of **Toc-As**, **N14-As,** and **Toc-NOH** as cationic lipids DOPE taken as a co-lipid. Complexes were prepared at 4:1 charge ratio of the positively charged liposome-double helix structure of DNA, and CD was recorded at a pDNA concentration of 50μg/mL. The CD spectra have been compared to the profile for pDNA alone. Spectral profiles of liposomes with dextrose or of dextrose alone were subtracted as blank.

2.2.5 Antioxidant Activity

As the cytotoxicity of cationic liposomes is major because of apoptosis exhibited due to the generation of reactive oxygen species (ROS) during transfection[41],[16a]. Hence, the cationic lipids having radical scavenging ability along with transfection potency may be helpful in treating ROS (reactive oxygen species) induced toxicity[16a]. So, it is necessary to study the antioxidant efficiencies of the designed anti-oxidant cationic lipid **Toc-As** along with the control lipids **N14-As** and **Toc-NOH.** The radical scavenger ability of the synthesized lipids was evaluated calorimetrically by using 2,2-diphenyl-1-picrylhydrazyl (DPPH) radicals. The DPPH radicals show a deep-violet color in an aqueous solution of ethanol giving a strong absorption in the visible region (460–560 nm), the increase in the intensity of DPPH solution is directly proportional to the concentration of radicals and hence used as a measure of the radical-scavenging ability of **Toc-As**, **N14-As** and **NOH.** The antioxidant efficiencies of the cationic

lipids **Toc-As**, **N14-As** and **Toc-NOH** were calculated with respect to the control samples that contain only DPPH. The cationic lipids at different concentrations (0 –50 μM) were incubated in aqueous ethanol solutions of DPPH (100 μM) at room temperature in the dark. The difference in the concentration of DPPH radicals upon treatment with different cationic lipids was calculated by measuring the colorimetric intensity of the samples at 490 nm using a microplate reader after 30, 60, 90, and 120 min of incubation (**Figure 5**). The untreated DPPH sample at every time point used as controls and the anti-oxidant efficiencies observed was time and concentration dependent. After 30 min of incubation, low concentrations of the cationic lipids (<5 μM) did not show significant antioxidant activity (**Figure 5**). However, the cationic lipids, **Toc-As, Toc-NOH** and **N14-As** showed antioxidant activity at concentrations that are above 10 μM. **Toc-As** showed higher radical scavenger abilities compared to control lipids **Toc-NOH** and **N14-As**. Moreover, the antioxidant activity of **Toc-As** was found to be 2 fold higher than the natural antioxidant ascorbic acid which is used as a positive control (**Figure 2**). The cationic lipid **Toc-NOH** did not show any appreciable antioxidant activity even at higher concentrations (**Figure 5**). However, **N14-As** lipids molecules having ascorbic acid moiety as a head group showed some radical-scavenging effect after 30 min of incubation. The experimentally found superior radical-scavenging activity of **Toc-As** is attributed to the ability of the natural antioxidant properties and neutralization of the DPPH radicals.

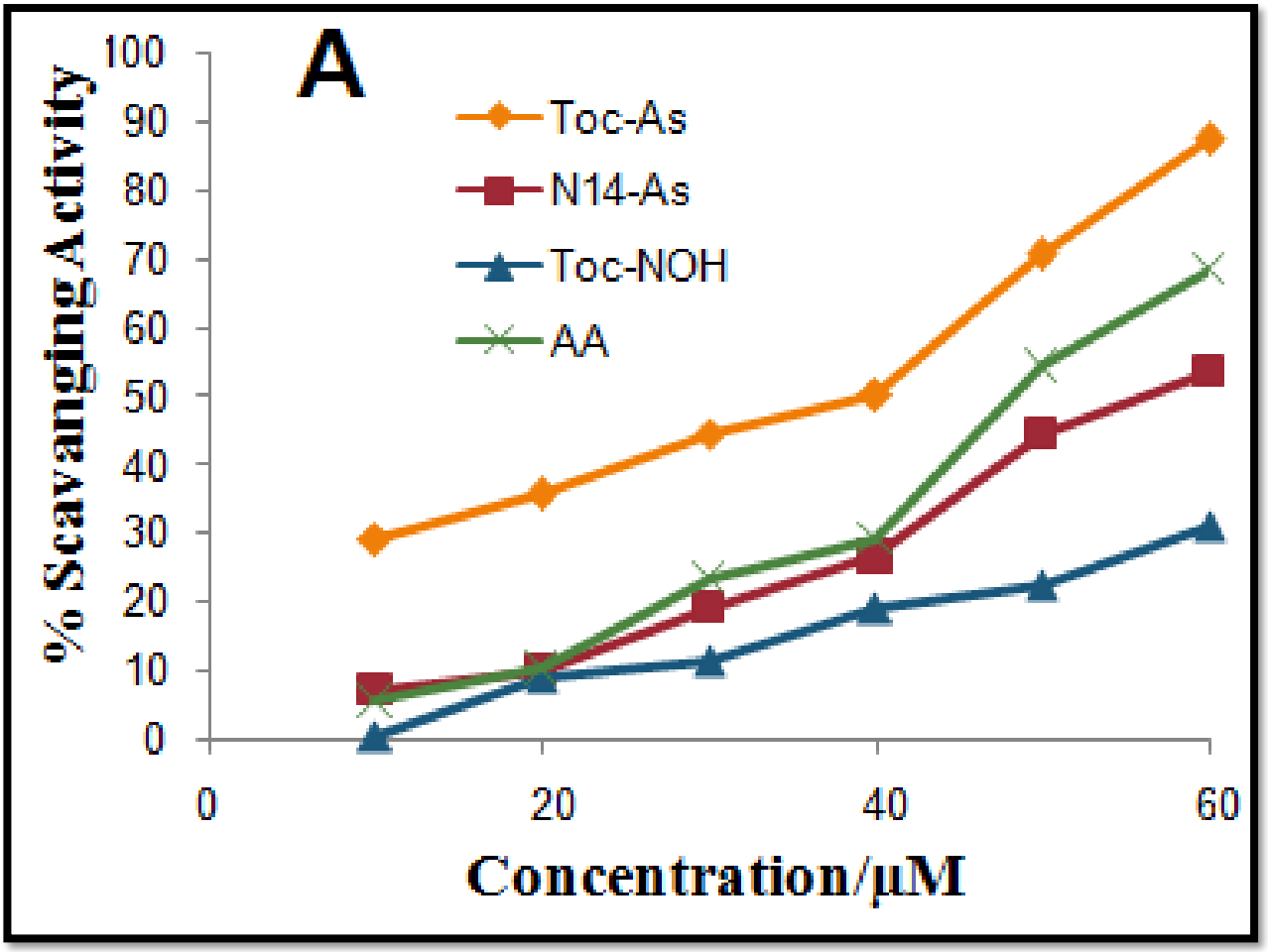

Figure.5. (A) Antioxidant assay of cationic lipids. The concentration-dependent radical-scavenging ability of **Toc-As**, **N14-As** and **Toc-NOH** cationic lipids against DPPH free radicals after 30 min of incubation at room temperature in the dark. The absorbance was measured at 490 nm. The values shown are mean ± SEM of three independent experiments carried out in three to five replicates. DPPH = 2, 2-diphenyl-1-picrylhydrazyl radicals, AA = ascorbic acid.

2.2.6 Cationic liposome preparation

Toc-As/DOPE, **N14-As** /DOPE, and-**NOH**/DOPE liposomes were prepared at 1:1 mol ratio with 1.4×10^{-2} M total lipid concentration, as a stock solution. The mixture was dissolved in chloroform (1.5 mL) in an autoclaved glass vial. The solvent was evaporated and dried under a thin flow of nitrogen gas. The resulting thin film is dried farther under high vacuum for 4h. The dried film was hydrated by the addition of 1 mL of deionized water. The mixture was allowed to swell overnight. The liposomes were vortexed for 1-2 min to remove any adhering lipid film and

then sonicated in a bath sonicator for 5 min at room temperature to obtained multilamellar vesicles. The vesicles were then sonicated in an ice bath using a probe sonifier to afford the cationic liposomes. All the liposomes formed were stable and uniform. Liposomes were stored at 4 ˚C and it was observed that no precipitation even after 3 months.

2.2.7 Transfection Biology: *In vitro* transfection studies

The relative transfection potentials of lipoplexes of lipids **Toc-As**, **Toc-NOH** and **N14-As**wereestablished against multiple cell lines viz., HepG2, HEK-293T, CHO and neuro-2a across charge ratio 1:1 to 8:1 *p*CMV-SPORT-β-gal plasmidDNA was used as a reporter gene and is complexed with cationic liposomes across1:1 to 8:1 lipid:DNA charge ratios. The transfection efficacies of **Toc-As**, **Toc-NOH,** and **N14-As** lipids were compared with that of commercial formulation, lipofectamine 2000 and the results are summarized in **Figure 6**. All the cationic lipids showed their maximum transfection efficacies at the charge ratio 4:1 irrespective of the cell lines. This may be due to the optimal particle sizes and zeta potentials of the lipoplexes at this charge ratio, which in turn affect the cellular uptake (**Figure 6**). The lipoplexes of lipids **Toc-As** and **N14-As** showed similar transfection profile in HEK-293T and CHO cells at charge ratios 2:1 and 4:1 and nearly two folds higher efficient than Lipofectamine 2000 in HEK-293T cell lines at 4:1 charge ratio. Whereas in Neuro-2a cell lines **Toc-As** is slightly better active than **N14-As** at 4:1 charge ratio and comparable to that of lipofectamine 2000.The lipoplexes of **Toc-As,** i.e. lipid having both tocopherol and ascorbic acid moieties, exhibited much superior transfection efficacy among three lipids and two and a half fold higher transfection than Lipofectamine 2000against HepG2 cell linesat 4:1 charge ratio (**Figure 6**). It is apparent, due to the better uptake of tocopherol lipids through cellular transport pathways mechanism involving cell surface receptors (tocopherol-transfer protein) present on HepG2 cell lines[42]. At the same time, the superior activity of **Toc-As** may be attributed because of the least cytotoxicity of the lipid due to its maximum anti-oxidant activity. In contrast, the lipoplexes derived from **Toc-**

NOH showed the least transfection against all the tested cell lines, indicating that the ascorbic acid in the head group region in others played a crucial role in transfection. The higher transfection efficiencies of **Toc-As** and **N14-As** compared to **Toc-NOH** may also be due to the presence of more number of hydroxyl groups present in the head group region as reported earlier[37] which are also confirmed by CD spectral data. The superior activity of **Toc-As** cationic liposomes also can be attributed because of the diethyl ether ammonium linker, which might have greatly influenced the process of liposomes formation and lipoplex-membrane fusion than **N14-As** liposomes. In detail, the lipid **Toc-As** possessed α-tocopherol and chiral ascorbic acid may show some degree of lateral freedoms to each other because of the diethyl etherlike and it might contribute to the maximum release of DNA from lipoplexes into cytosol and also the flexibility in the lipid favours the multiple H-bonding interactions of ascorbic acid moiety of the lipid with negatively charged surface of double helix plasmid DNA to significantly enlarge the overall strength of interaction between the cationic lipid and the supercoiled DNA. In summary**,** **Toc-As** lipid is capable of transfecting multiple cell lines effectively along with its higher radical scavenging ability and low cytotoxicity may be helpful in treating ROS (reactive oxygen species) related diseases such as brain stroke/ischemia and malignancy.

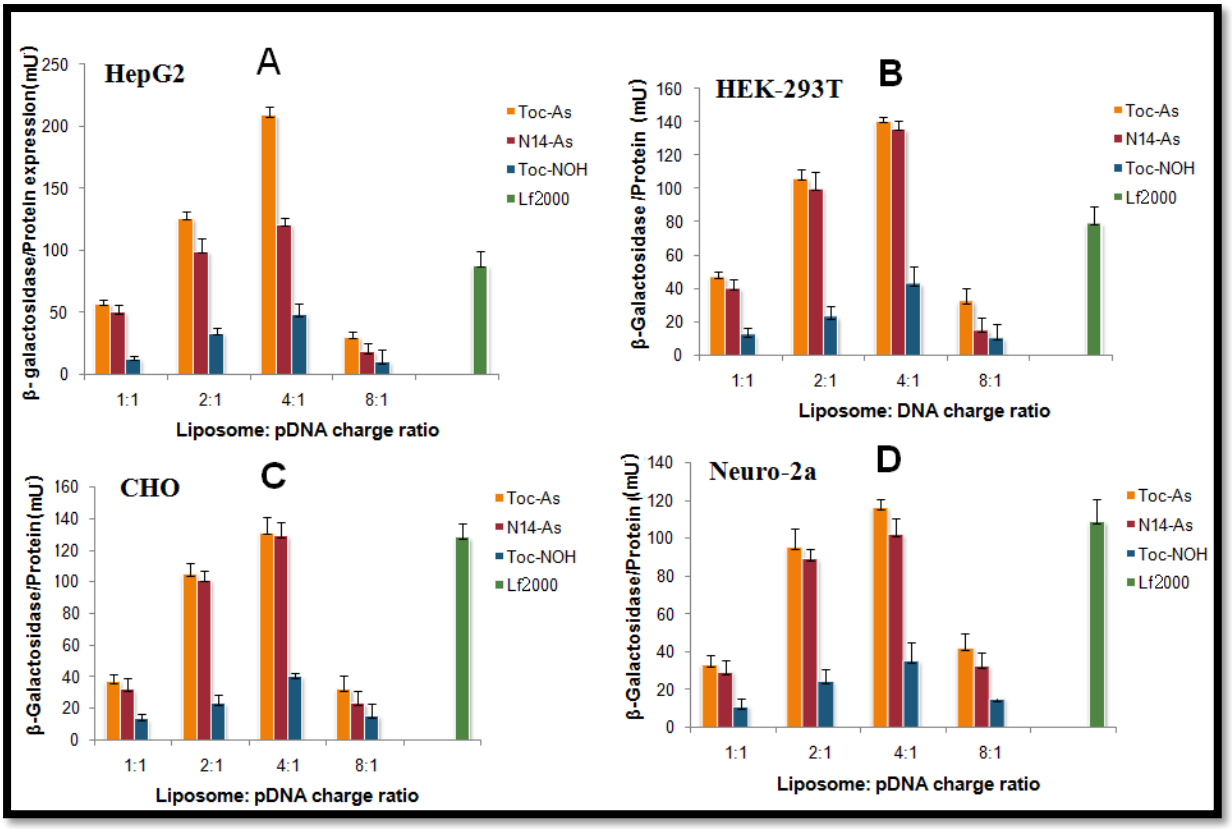

Figure 9. Transient transfection in vitro: HepG2, CHO, Neuro-2a and HEK-293T cells were treated with **Toc-As, N14-As** and **Toc-NOH** formulated with DOPE using pCMVβ-Gal in the absence of serum.

2.2.8 EGFP expression

The transfection results revealed that the present lipids **Toc-As, N14-As** and **Toc-NOH** showed their maximum transfection ability at 2:1 & 4:1, which was further supported by the qualitative examination using eGFP plasmid under epifluorescence microscopy. Towards this end, lipoplexes were prepared using eGFP plasmid at transfection efficient charge ratios 2:1 and 4:1. The formulations were incubated with HEK-293T and HepG2 cell lines in DMEM + 10% FBS for 4 hrs. The green fluorescent images were visually observed under an epi-fluorescent microscope and evaluated in terms of % GFP positive transfected cells (**Figure 7 & 8)** and geometric mean fluorescence intensities (GMFI) (**Figure7C & 8C**). The representative fluorescent images (**Figure 7A & 8A**) show that the relative fluorescent gene expression obtained from HepG2 was relatively higher than that obtained from HEK-293T cell lines. The

results represent that maximum GFP expression was observed at 4:1 charge ratio irrespective of the cell lines for all the three lipid formulations. It is also observed that **Toc-As** lipoplex showed maximum GFP expression when compared to **N14-As** and **Toc-NOH** lipoplexes at both the charge ratios in both the cell lines studied (**Figure 7 & 8**). These results were reliable with the transfection results and it reemphasizes that tocopherol-ascorbic acid hydride cationic lipid has superior transfection profile. The lipoplexes of **Toc-NOH** showed the least expression of eGFP among the three lipids studied (**Figure 7 & 8**). The order of cationic lipids according to their intensity of fluorescent expression observed in **Figure 7 & 8** can be given as **Toc-As**>**N14-As**>**Toc-NOH.**

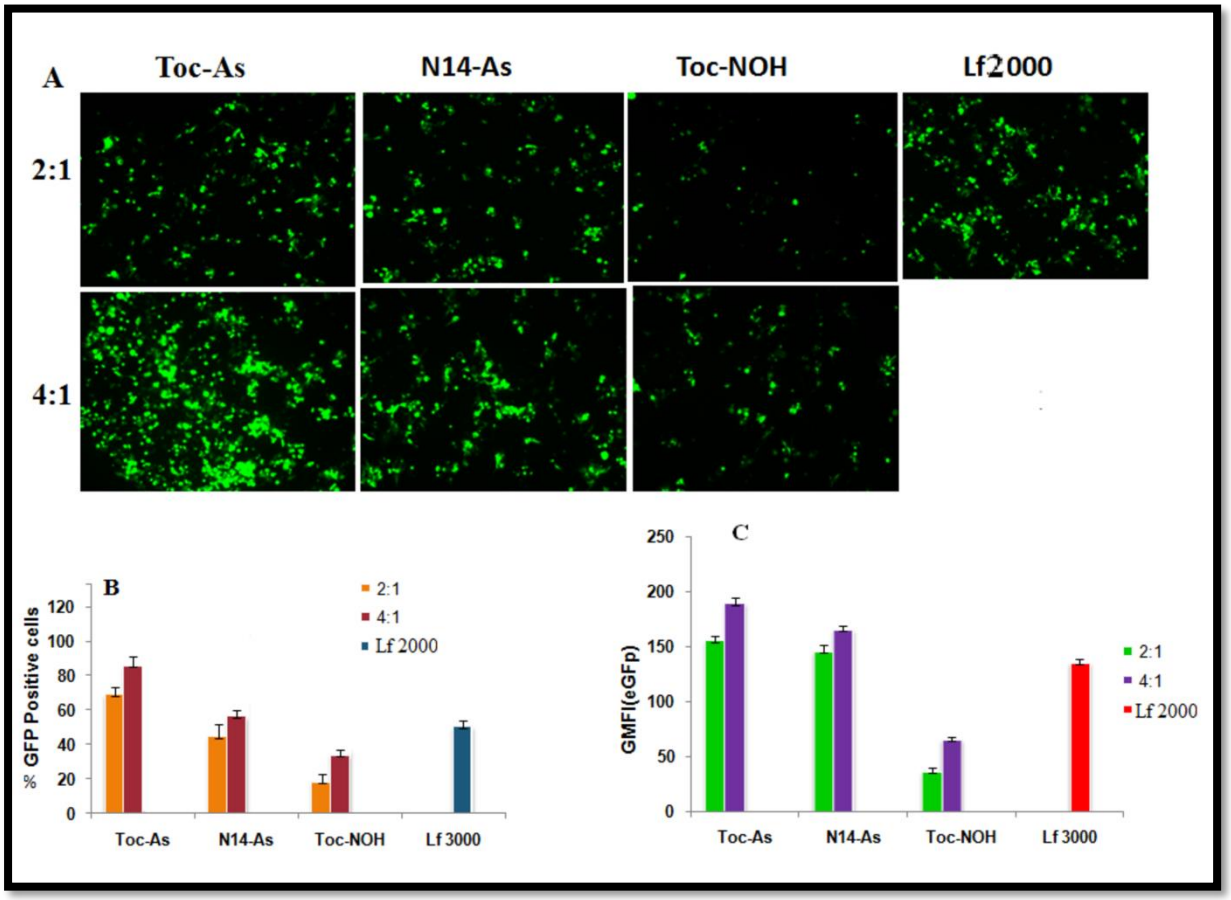

Figure 7.Transient transfection using the reporter gene, eGFP in HEK 293 cells: A) Representative fluorescence images of eGFP expression at the indicated charge ratios. Liposomes of all cationic lipids formulated with co-lipid DOPE (1:1) lipid and were complexes with negatively charged eGFP in the optimized charge ratios 2:1 and 4:1 were used. The liposome-DNA complexes were incubated for 4 h in presence of 10% serum. Images were

acquired 48 h post transfection. B) The representative graph depicts the transfection efficiencies in terms of percentage GFP positive cells. C) The graph indicating geometric mean fluorescent intensity (GMFI) of transfected cells using eGFP as the reporter gene. The data shown are the mean and standard deviation of three different experiments.

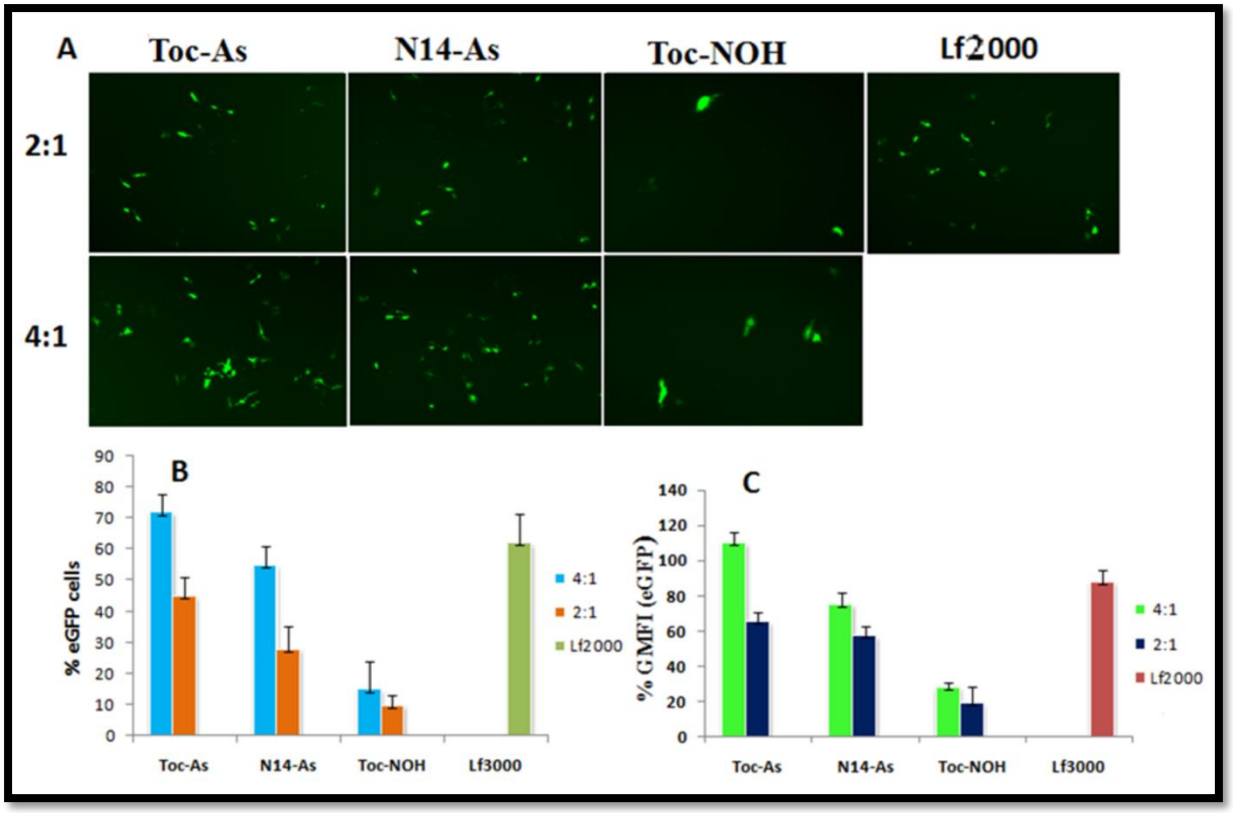

Figure 8.Transient transfection using the reporter gene, eGFP in HepG2 cells: (A) Representative fluorescence images of eGFP expression at the represent charge ratios. Liposomes of all cationic lipids formulated with co-lipid DOPE (1:1) lipid and were complexes with negatively charged eGFP in the optimized charge ratios 2:1 and 4:1 were used. The liposome-DNA complexes were incubated for 4 h in presence of 10% serum. Images were acquired 48 h post transfection. B) The representative graph depicts the transfection efficiencies in terms of percentage GFP positive cells. C) The graph indicating geometric mean fluorescent intensity (GMFI) of transfected cells using eGFP as the reporter gene. The data shown are the mean and standard deviation of three different experiments.

2.2.9. Effect of serum on transfection efficiency

Generally, the gene transfer efficacies of cationic lipids are studied either in the absolute absence of added bicarbonate-free serum or in the presence of only 10% (v/v) serum as reported in many prior investigations[37,43,44]. Still, the serum-incompatibility is one of the major setbacks regarding the clinical achievement of cationic transfection lipids. The high *in vitro* transfections of many cationic amphiphiles are often found to be adversely affected by the presence of serum. The cationic lipids show their serum incompatibility due to adsorption of (-) charged serum proteins onto the (+) charged a cationic liposome surface which in turn prevents their efficient interaction with the cell surface and/or internalization[67-69]. Hence, evaluation of gene transfer efficacies across a range of cationic lipid: pDNA charge ratios in multiple cultured cells in presence of increasing concentrations of added serum is needed for obtaining the meaningful systemic potential of any *in vitro* efficient cationic transfection lipid. In order to know the effect of serum on the transfection efficiencies of the present lipids, transfection experiment was performed by complexing with eGFP plasmid at transfection efficient charge ratio 4:1 in HEK-293T and CHO cell lines with increasing added serum concentrations from 10-50%. The *in vitro* transfection studied with increasing concentrations of added serum results show that all the three lipids**Toc-As**, **N14-As** and **Toc-NOH** lipids were unaffected even in the presence of high concentration of serum up to50% of added serum (**Figure 9**). The results demonstrate that **Toc-As** lipid showed a slight increase in the transfection with an increase in the concentration of added serum. **Toc-As** and **N14-As**exhibited higher transfection potentials even at a higher concentration of added serum compared to **Toc-NOH,** which is found to be the least. It clearly indicates that lipoplexes having zeta potential values <10 mV,which greatly benefit the serum stability of lipoplexes and decrease the cytotoxicity, exhibited serum compatibility. The maximum serum compatibility of lipids **Toc-As** and **N14-As**expected to be due to enhanced surface charge shielding of the liposome-DNA complexes induced by hydroxyl functionalities of ascorbic acid in the head group region.

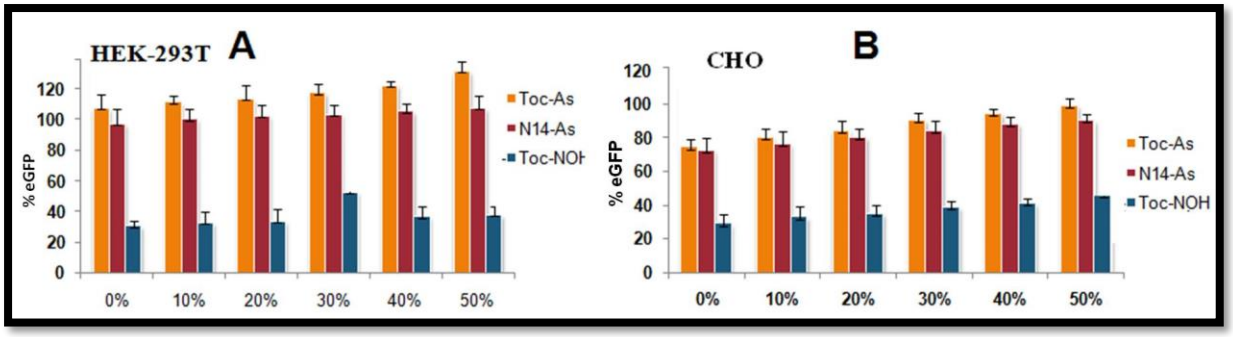

Figure 9. Transfection efficacies of the cationic lipoplexes **Toc-As, N14-As** and **Toc-NOH** in presence of increasing concentration of added serum. *In vitro* transfection efficiencies of liposome-eGFP complexes prepared using GFP reporter gene at a lipid/DNA charge ratio of 4:1 were evaluated in the presence of enhancing concentrations of added serum in (A) HEK-293T and (B) CHO types of cells. The error bar indicates that the standard error.

2.2.10 Cellular uptake

The transfection efficiencies of the non-viral gene delivery systems seem to be linked to the endocytosis of pDNA associated complexes. In order to verify the cellular uptake efficiency of lipoplexes of the present lipids**,** membrane green fluoresce-labeled CHO cell lines were incubated with the lipoplexes comprising of Rhodamine-PE labeled liposomes of lipids (**Toc-As**, **N14-As** and **Toc-NOH**) and *p*CMV-SPORT-β-gal plasmid at 4:1 charge ratio for 4 hrs. The internalization of rhodamine-labeled lipoplexes was observed under an epifluorescence microscope. The intracellular red fluorescence intensity of the cells was quantified using microplate fluorescent reader. **Figure 10** shows the red and green fluorescent images of CHO cells after incubation for 4 h. The results of the cellular uptake experiment show that the % of rhodamine positive cells follows the order: **Toc-As**>**N14-As**>**Toc-NOH**. The lipoplexes particle size may play a vital role in facilitating the cellular uptake. Hence, it is obvious that **Toc-As** lipoplexes having the least particle size at 4:1 is one of the reasons for its high potency for uptake by cell lines. The other reason for the higher uptake efficiency may be the multiple hydroxyl group functionality in its head group region, which may involve in the favorable hydrogen bonding interactions with the biological membrane components. Thus, the higher uptake

efficiency of the lipid **Toc-As** may also an attribute to its superior *in vitro* transfection efficiency compared to **N14-As** and **Toc-NOH.**

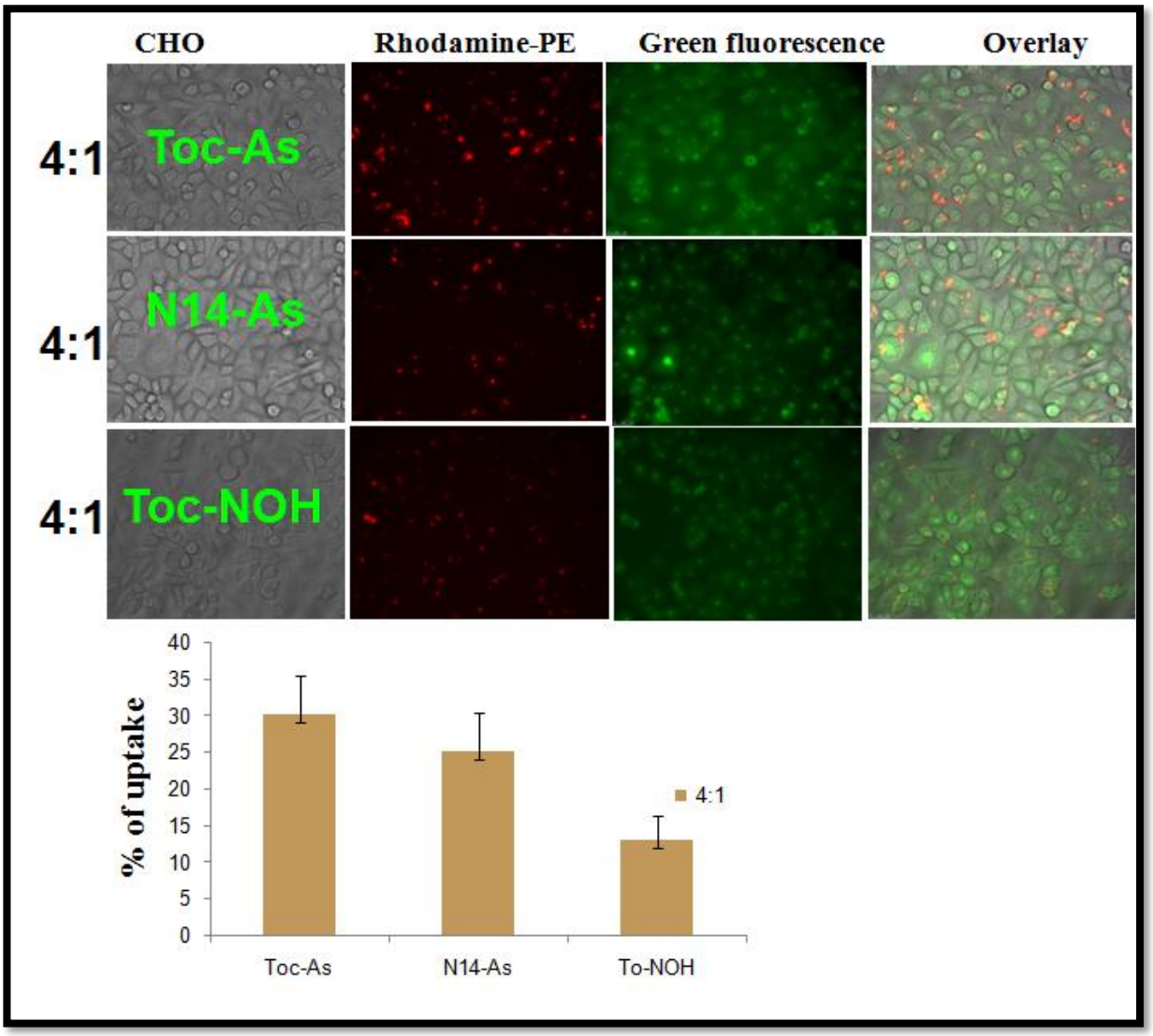

Figure 10. Cellular Uptake of rhodamine-labeled lipoplexes. Fluorescence images (A) and % uptake (B) of CHO cells incubated for 4 h with the complexes of rhodamine-labeled liposomes of **Toc-As**, **N14-As**, and **Toc-NOH** and plasmid DNA. The percentage uptake was calculated using the formula% uptake = 100x (fluorescence intensity of the fluorescence lipoplex treated cell lysate-background) / (fluorescence intensity of lipoplex added to the cells-background).The details of the experiments are as described in the text. Data are shown as mean ± SD (n = 3).

2.2.11 Cytotoxicity assay

The cytotoxicity is a major limiting factor for the success of gene therapy in clinical applications. Especially, in liposomal gene delivery, the cytotoxicity of cationic liposomes is a result of apoptosis[22a, 18, 21, 23,27] and that cationic liposome-induced apoptosis exhibited due to the generation of reactive oxygen species (ROS) [23, 24]. Particularly neurons are vulnerable to increases in ROS levels because these cells have a reduced capacity to detoxify ROS [24, 23]. Towards, this end to observe the cytotoxicities of the lipoplexes of the designed antioxidant lipid **Toc-AS** and control lipids, **N14-As** and **Toc-NOH,** MTT assay was performed in four different cell lines i.e. HepG2, HEK-293, Neuro-2a, and CHO across the charge ratios 1:1 to 8:1. The cell viability results are summarised in **Figure 11**. The results indicate that the lipoplexes of **Toc-As**, **N14-As** and **Toc-NOH** lipids found to be non-toxic up to the charge ratios of 4:1- 1:1 in HepG2, HEK-293T and CHO cell lines and slightly toxic (80%) at 8:1 charge ratio. Whereas in Neuro-2a cell lines the lipid **Toc-NOH** showed less viability i.e.83 % at 4:1 charge ratio, the transfection efficient charge ratio, when compared to lipids (**Toc-As** and **N14-As**) containing ascorbic acid moiety in the head group region. It is clear that the neuro cell line which is vulnerable to ROS related apoptosis could survive in the presence lipids (**Toc-As** and **N14-As**) containing ascorbic acid moiety in the head group region than in the presence of lipid (**Toc-NOH**) not having ascorbic acid in the head group region. Hence, the delivery systems consisting of our designed antioxidant lipid i.e. **TOC-AS** having high radical scavenging ability along with maximum transfection efficiency and least cytotoxicity may be helpful in treating ROS (reactive oxygen species) related diseases such as brain stroke/ischemia and malignancy.

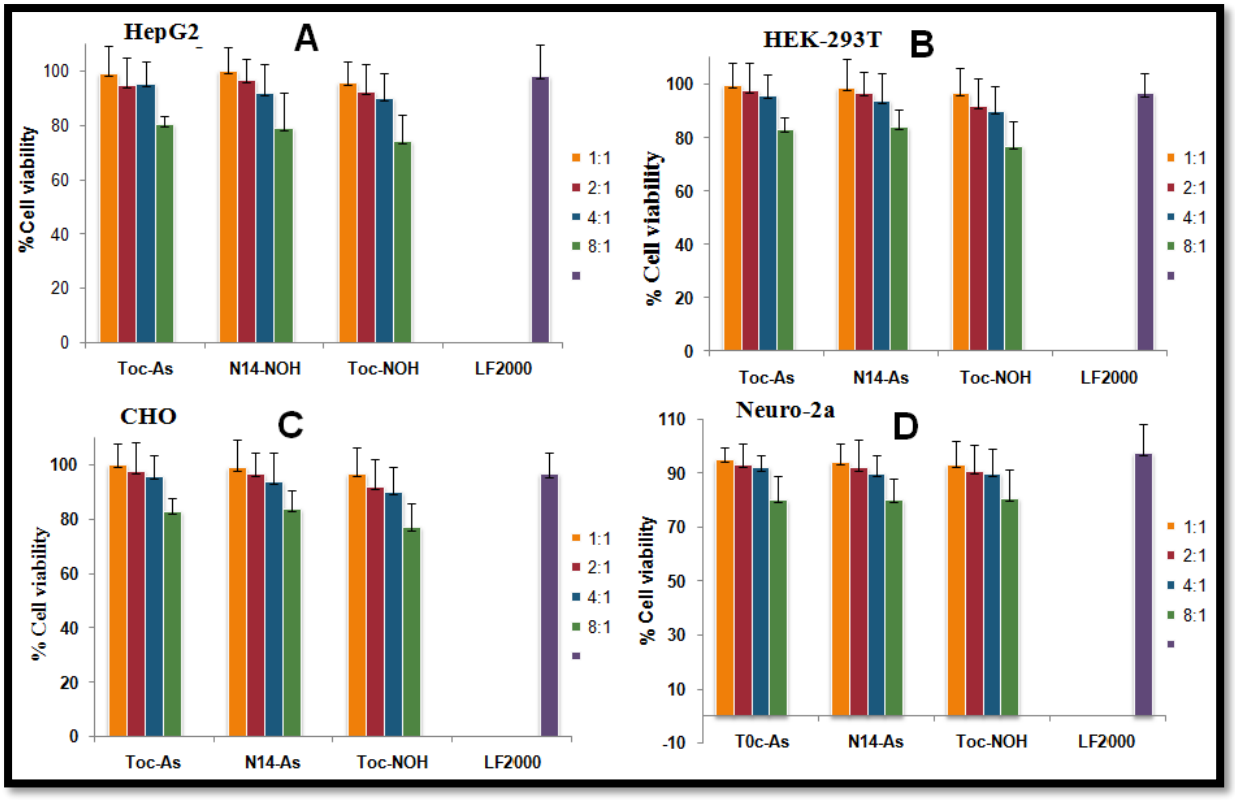

Figure 11. Representative percent of cell viabilities upon treatment of HepG2 (A), HEK-293T (B), CHO (C), and Neuro-2a (D) cells with lipids**Toc-As**, **N14-As** and **Toc-NOH** using MTT assay. The absorbance obtained with reduced formazan with the cell in the absence of cationic lipids was taken to be 100. The toxicity assays were evaluated as depicted in the text. The data obtained is the average values of three independent experiments (n = 3).

2.3 Conclusions

In summary, the synthesized α-tocopherol-ascorbic acid hybrid cationic amphiphile can efficiently deliver genes into multiple culture cells. Among the three cationic lipids studied (**Toc-As**,**N14-As** and **Toc-NOH**), lipid **Toc-As** with ascorbic acid head group showed superior transfection activity. This α-tocopherol-ascorbic acid hybrid lipid has significantly affected the physicochemical and biological properties of cationic lipids. Hence, the ascorbic acid head group might be attractive in designing new lipids for gene delivery and it might be useful for drug delivery. Based on the results it is suggested that **Toc-As** lipid will be a promising non-viral gene delivery vector with superior transfection efficiency, strong radical scavenger activity and least cytotoxicity for treating ROS related diseases in the brain.

2.4 Experimental Section

2.4.1 General procedure and chemicals

The high-resolution mass spectrometric (HRMS) and mass were acquired by using a commercial a Micromass AUTOSPEC-M mass spectrometer (ThermoFinnigan, SanJose, CA, U.S.) equipped with an ESI source.^{1}H NMR and ^{13}C NMR spectra were recorded on a Varian FT400 MHz NMR spectrometer. α-Tocopherol was bought from Sigma Co. Super negatively charged green fluoresces /eGFP plasmid and rhodamine-PE were ample gifts from IICT (Indian Institute of Chemical Technology, Hyderabad, India). Lipofectamine-2000 or Lf2000 was bought from Invitrogen Life Technologies, polyethylene glycol 8000, and o-nitrophenyl-β-D-galactopyranoside was purchased from Sigma (St. Louis, MO, U.S.). NP-40, antibiotics, and agarose were purchased from Hi-media, India. 1,2-dioleoyl-*sn*-glycerol-3-phosphoethanolamine (DOPE) was bought from Fluka (Switzerland). Unless otherwise stated, various organic solvents including dry acetone, ethanol, methylene chloride, and phosphomolybdic acid spray reagent, ethyl bromoacetate, p-toluenesulfonyl chloride, and dry *N*,*N*-dimethylformamide (DMF) were purchased from Sigma-Aldrich Co. and were used without further purification. The progressive of the reaction was monitored by thin-layer chromatography using 0.25 mm silica gel plates. Column chromatography technique was executed with silica gel (Acme Synthetic Chemicals, India; finer than 200 and 60-120mesh). Elemental analyses were performed by High-Resolution Mass Spectrometry (HRMS) using QExactive equipment (Thermo Scientific) and purity of lipids wascharacterized by HPLC (Shimadzu LC Solution) and showed more than 95% purity. HepG2, CHO, Neuro-2a and HEK-293T cells were procured from the National Centre for Cell Sciences (NCCS), Pune, India. The cellwas grown at 37 $^{\circ}$C in Dulbecco's modified Eagle's medium (DMEM) with 10% FBS in a humidified atmosphere containing 5% CO_2 / 95 % air.

2.4.2 Synthesis

Synthesis of *O*-acetic acid-α-tocopherol (1A, scheme 1)

An α-tocopherol (0.5 g, 1.16 mmol) in *N*, *N*-dimethylformamide (DMF) (25 mL) was reacted with ethyl bromoacetate (3.4 g, 8.3 mmol) and finely powdered potassium hydroxide (1.2 g, 30 mmol). The ensuing yellow residue was stirred for 24 h at room temperature. The reaction mixture was acidified with 6N HCl and extracted with (EtOAc) ethyl acetate (3×30 mL). The ethyl acetate layers were washed with water (3×30 mL) and sodium chloride solution (brine) (1×30 mL) and then dried with magnesium sulfate. The ethyl acetate layer was reduced to pale yellow oil and purified by silica gel (100-200 mesh size) chromatography eluting with 15% (v/v) ethyl acetate (EtOAc) and 1% acetic acid in hexanes. This yielded **1A** as yellow color (0.50 g, 85%).

^{1}H NMR (400 MHz, $CDCl_3$) δ/ppm 0.8-0.90 (m, 12H), 1.00-1.5 (m, 25H), 1.77-1.88 (m, 2H), 2.55 (s, 3H), 2.57 (s, 3H), 2.59 (s, 3H), 4.3 (s, 2H), 7.98 (broad, 1H). **ESI-MS**: Calculated 488; found: $[M+NH^+_4]$ 506

Synthesis of *O*-ethyl alcohol -α-tocopherol (1B, scheme 1)

To a solution of lithium aluminum hydride (0.08 g, 1.1 mmol) in 10 mL of dry tetrahydrofuran (THF), a solution of **1A** (2.0 g, 1 mmol) in 5 mL dry THF was added slowly at 0°C with the help of addition funnel about 10 minutes. The reaction combination was stirred for 6 h at room temperature and then the excess $LiAlH_4$ was quenched with ethyl acetate. The ethyl acetate layer was washed with water (3×50 mL), dried with anhydrous Na_2SO_4, filtered, and concentrated under vacuum. The crude product was purified by silica gel column chromatography to give *O*-ethyl alcohol-α-tocopherol **1B** (1.89 g, yield 92%) as a clear oil. Rf = 0.2 (20% EtOAc/hexane, 2:8).

^{1}H NMR (400 MHz, $CDCl_3$) δ/ppm 0.8-0.90 (m, 12H), 1.00-1.5 (m, 25H), 1.77-1.88 (m, 2H), 2.25 (s, 3H), 2.27 (s, 3H), 2.29 (s, 3H), 3.66 (t, 2H), 3.85 (t, 2H).). **ESI-MS**: Calculated 474; found: $[M^+]$ 474

Synthesis of *O*-ethyl-*O*-sulfonyl benzyl -*α*-tocopherol (**1C, Scheme 1**)

To a solution of **1B** (4.0 g, 9.0 mmol) in 10 mL of dry DCM were added tosyl chloride (2.12 g, 18 mmol), pyridine (1.46 g, 18 mmol), and a catalytic amount of DMAP. The reaction mixture was stirred at room temperature for about 12 h. The solvent was evaporated in vacuum to dryness. The residue was dissolved in 25 mL of ethyl acetate and washed twice with 2 ×30 mL of copper sulfate solution to remove any excess pyridine. The organic layer was dried on anhydrous sodiumsulfate, the solvent was evaporated, and the residue was purified by column chromatography by eluting with 2-4% (v/v) ethyl acetate in n-hexane to obtain 4.0 g (yield 85.10%, Rf = 0.4, 10% ethyl acetate in hexane).

^{1}H NMR (400 MHz, $CDCl_3$) δ/ppm 0.8-0.90 (m, 12H), 1.00-1.5 (m, 25 H), 1.77-1.88 (m, 2H), 2.22 (s, 3H), 2.18 (s, 3H), 2.13 (s, 3H), 3.82 (t, 2H), 3.92 (t, 2H), 2.48 (s, 3H,),7.3 (d, 2H), 7.8 (d, 2H)

ESI-MS: calculated 628; found: $[M+NH^+_4]$ = 646

Synthesis *O*-Amino ethyl-[*N*,*O*-(hydroxyethyl), *N* methyl]-*α*-tocopherol (1D & 1E, Scheme 1)

A mixture of *N*-methyl ethanolamine (0.2 g, 8.18 mmol) and **1C** (1.9 g) taken in 10 mL of toluene in around bottomed flask and is refluxed for 24 h. The reaction mixture was poured into ethyl acetate (100 mL), washed with water (2 × 100 mL), dried over anhydrous sodium sulfate, and filtered. Ethyl acetate is removed from the filtrate on a rotary evaporator. The column chromatographic purification of the resulting crude using 60-120 mesh size silica gel and eluting with1-2% methanol (v/v) in chloroform afforded 2.4 g (63.15% yield Rf=0.4, $MeOH/CHCl_3$; 1:19 v/v) of the tertiary amine **1D**. After confirmation of **1D** compound, it was dissolved in 7 mL

of 1N hydrochloric acid in methanol. The reaction mixture was stirred for 12 h and the solvent was evaporated under rota evaporator, then afford pure lipid **Toc-NOH** (**1E**, **scheme 1**) appears as light yellow color.

^{1}H NMR (400 MHz, $CDCl_3$) δ/ppm 0.8-0.90 (m, 12H), 1.00-1.5 (m,25H), 1.77-1.88 (m, 2H), 2.25 (s, 3H), 2.27 (s, 3H), 2.29 (s, 3H), 2.25 (s, 3H, CH_3-N-), 3.84 (t, 4H), 4.33 (t, 4H), **ESI-MS** : Calculated 531.4723; found: [M^+] 531.4731

***O*-Amino ethyl-[*N*,*O*-(hydroxyethyl), *N* methyl] benzene sulfonate-α-tocopherol (3A, Scheme 3)**

To a solution of *O*-amino ethyl-[N, *O*-(hydroxyethyl), N methyl]-α-tocopherol (4.0 g, 9.0 mmol) in 10 mL of dry DCM were added p-toluenesulfonyl chloride (2.12 g, 18 mmol), pyridine (1.46 g, 18 mmol), and a catalytic amount of dimethylaminopyridine (DMAP). Thereaction mixture was stirred at room temperature for 12 h. The total solvent was evaporated in vacuum to dryness. The residue was dissolved in 25 mL of ethyl acetate and washed twice with 2 ×40 mL of copper sulfate solution to remove any excess pyridine. The organic layer was dried on sodiumsulphate, the solvent was evaporated, and the sample was purified by column chromatography, eluting with 2-5% (v/v) ethyl acetate in n-hexane to obtained 4.0 g (yield 85.10%, Rf = 0.5, Ethyl acetate in hexane ; 1:9, v/v) of *O*-tosylation ethyl-α-tocopherol

^{1}H NMR (400 MHz, $CDCl_3$) δ/ppm 0.7-0.81 (m, 12H), 1.00-1.5 (m,25H), 1.77-1.88 (m, 2H), 2.09 (s, 3H), 2.05 (s, 3H), 2.01 (s, 3H), 2.02 (s, 3H, CH_3-N), 2.08 (s, 3H)3.84 (t, 4H), 4.33 (t, 4H), 7.33 (d, 2H), 7.83 (d, 2H); **ESI-MS**: Calculated 686; found: [M^+] 686

Synthesis of *O*-Amino ethyl-[*N*,*O*-(hydroxyethyl), *N* methyl] 5, 6 isopropylidene ascorbic acid -α-tocopherol (3B)

To a solution of 5,6 isopropylidene ascorbic acid (4.0 g, 1 mmol) in 10 mL of dry DCM was added triethylamine (1.46 g, 1.1 mmol), and a catalytic amount of DMAP. The reaction mixture was stirred at room temperature for 15 minutes. The solution *of O*-Amino ethyl-[*N*, *O*-(hydroxyethyl), *N* methyl] benzene sulfonate-α-tocopherol (2.12 g, 18 mmol),in dry DCM, were

added dropwise about 20 minutes. The reaction mixture dissolved in 25 mL of ethyl acetate and washed twice with 2×30 mL of 1N HCl solution to remove any excess triethylamine. The organic layer was dried on anhydrous magnesium sulphate, the solvent was evaporated, and the sample was purified by column chromatography, eluting with 5-8 % (v/v) ethyl acetate in n-hexane to obtain 4.0 g of *O*-Amino ethyl-[*N*,*O*-(hydroxyethyl), *N* methyl] 5, 6 isopropylidene ascorbic acid -α-tocopherol. (Yield 65.4%, Rf = 0.3, Ethyl acetate in hexane, 1:9 v/v)

^{1}H NMR (400 MHz, $CDCl_3$) δ/ppm 0.8-0.90 (m, 12H), 1.00-1.5 (m, 25H), 1.77-1.88 (m, 14H), 2.21 (s, 3H, CH_3-N-), 2.29 (s, 3H), 2.27 (s, 3H), 2.25 (s, 3H), 3.84 (t, 4H), 4.33 (t, 7H), 4.5 (t, 2H), 4.99 (m, 1H); **ESI-MS** ; Calculated 730; found: [M^+] 730.

Synthesis of *O*-Amino ethyl-[*N*,*O*-(hydroxyethyl), *N* methyl] ascorbic acid -α-tocopherol (3C, Scheme 3) (Toc-As lipid)

O-Amino ethyl-[*N*,*O*-(hydroxyethyl), *N* methyl] *5, 6*isopropylidene ascorbic acid -α-tocopherol (1 gm, mmol) was dissolved in 10 mL of 1N hydrochloric acid in methanol in a round bottom flask. The reaction mixture was stirred at room temperature for overnight. The solution was evaporated in vacuum to dryness. The residue was dissolved in hexane, then added diethyl etherdropwise and kept it for overnight at 0-4 ˚C to get solid. No further purification techniques were performed as the compound decomposes on silica gel. To obtain yield 85.5%, Rf= 0.3 ($CHCl_3$/MeOH; 9:1v/v).

^{1}H NMR (400 MHz, $CDCl_3$) δ/ppm: 0.8-0.90 (m,12H), 1.00-1.5 (m,25H), 1.77-1.88 (m, 2H), 2.1 (s, 3H, CH_3-N-), 2.2 (s, 3H), 2.21 (s, 3H), 2.3 (s, 3H), 3.84 (t, 4H), 4.33 (t, 7H), 4.5 (t, 2H), 5.23(m, 1H)

^{13}C NMR (400 MHz, $CDCl_3$) δ 165.80, 147.99, 147.59, 127.71, 125.74, 124.57, 123.01, 117.65, 74.87, 73.64, 70.35, 65.13, 63.35, 62.47, 40.06, 39.38, 37.58, 37.47, 37.40, 37.29, 32.80, 32.70, 31.18, 29.72, 28.00, 24.82, 24.45, 23.89, 22.74, 22.65, 21.05, 20.65, 19.76, 19.70, 12.74, 11.88,

11.81. ESI-Mass: Calculated 690.4949 found 690.97314 + M^+; **ESI-HRMS**: Calculated; 690.49 found: 690. 97314 [M^+].

Synthesis of 5,6 isopropylidene ascorbic acid (2A, Scheme 2)

A mixture of L-Ascorbic acid compound 1 g (2 mmol) and acetone (15 mL) was stirred for 15 minutes. 2, 2-Dimethoxy propane (1.25 mL) and a catalytic amount of tin chloride were added to the reaction mixture and it was refluxed for 6 h. cooled the reaction mixture to 5-10 ˚C and stirred for 45 minutes at room temperature. The precipitated was filtered, washed with acetone and dried to get the compound **2A**.

Yield: 82%; M.P: 206°C. TLC: 100 DCM: 20 EA: 10 ethanol: 1 Acetic acid **^{1}H-NMR**: 11.29 (bs, 1H, OH), 8.48 (bs, 1H, OH), 4.70-4.69 (m, 1H, H_4), 4.25-4.23 (m, 1H, H_5), 4.08-4.06 (m, 1H, H_6), 3.87-3.86 (m, 1H, H_6), 1.24 (s, 6H, CH_3); ^{13}C-NMR: 173.4, 157.1, 117.8, 110.4, 76.6, 76.4, 65.1, 26.3, 25.7; **MS (ESI$^+$)** m/z 219 (M^++1).

Synthesis of *N, N*-di tetradecyl ethanolamine (2B, Scheme 2)

A mixture of tetradecyl bromide (0.066 mmol) and ethanolamine (6.6 mmol) in 20 mL of methanol-acetonitrile solvent mixture (30:70) was refluxed for 48 h on an oil bath. The reaction mixture was evaporated under vacuum and the crude mixture was cooling up to 5 ˚C to obtain a milky white mass. The crude was washed with diethyl ether several times to remove the tetradecylbromide and impurities. Then the crude was recrystallized from methanol and ethyl acetate mixture solvent to get a white solid product. (Yield; 90%)

^{1}H NMR (400 MHz, $CDCl_3$) δ/ppm= 0.863-0.88 (s, 6H), 1.31 (m, 40H), 2.2 (m, 2H), 2.62 (m, 4H), 2.88(t, 2H), 2.91 (t, 2H) **ESI-MS**: Calculated: 453 found: [453 + M^+]

Synthesis of *N, N*-di tetradecyl 2-chloroethyl ammonium (2C, Scheme 2)

N, N-di tetradecyl ethanolamine 0.1 g (1 mmol) was dissolved in 100 mL of dry chloroform followed by the addition of a solution of thionylchloride in chloroform 10 mL was added

dropwise at -5 °C. The reaction mixture was stirred for 1h and refluxed to 90 °C for 6 h. After cool to the room temperature, the reaction mixture was diluted with 100 mL of DCM. Then followed by the reaction mixture was evaporated under vacuum to dryness. The crude was recrystallized with ethyl acetate (EtOAc) Rf= 0.9 (MeOH/DCM: 9:1 v/**v**). Yield: 91%

^{1}H NMR (400 MHz, $CDCl_3$) δ/ppm= 0.863-0.88 (s, 6H), 1.31 (m, 40H), 2.2 (m, 2H), 2.62 (m, 4H), 2.88(t, 2H), 2.91 (t, 2H) **ESI-MS**: Calculated; 458 found: 460 + [M+2]

Synthesis of *N, N*-di tetradecyl 2-(5, 6 isopropylidene ascorbic acid) ethyl ammonium (2D, Scheme 2)

5,6-Isopropylidene ascorbic acid 0.05 mg (0.1 mmol) was dissolved in 15 mL of dry DMSO followed by the addition of anhydrous K_2CO_3 (0.06 mmol) and *N, N*-di tetradecyl 2-chloroethyl ammonium (0.1 mmol) at room temperature. The reaction mixture was stirred for 1h and refluxed to 90 °C for 16 h. After cool to the room temperature, the reaction mixture was diluted with 100 mL of DCM. The dilutedsolution was washed with 50 mL of 10 % aqueous brine solution three times and then dried over anhydrous sodium sulfate, followed by filtration. The filtrate was concentrated under reduced pressure and purified on column chromatography and followed by recrystallizationfrom ether and hexane. Rf=0.2 (MeOH/DCM: 1:19 v/**v**) Yield: 89%

^{1}H NMR (400 MHz, $CDCl_3$) δ/ppm= 0.863-0.88 (s, 6H), 1.31 (m, 40H), 2.2 (m, 2H), 2.62 (m, 4H), 2.88(t, 2H), 2.91 (t, 2H), 3.40 (d, 1H), 3.50 (m, 2H), 4.18 (m, 1H). **ESI-MASS**: Calculated; 652 found: 652 + [M+1].

Synthesis of *N, N*-di tetradecyl 2-(ascorbic acid) ethyl ammonium (2E, Scheme 2)

1 g of *N,N*-di tetradecyl-2-(5,6-isopropylidene ascorbic acid)ethyl ammonium was dissolved in 10 mL of methanol, to which 3 mL of 2N hydrochloric acid (HCl) solution was added. The mixture was refluxed for 2h and evaporated under reduced pressure to give an adhesive liquid product. Ethanol was added to the product, which was then concentrated to give crude crystalline *N, N*-di tetradecyl 2-(ascorbic acid) ethyl ammonium, it was re-crystallized in ethyl acetate/ethanol (8:2) to give an off-white crystalline solid (yield: 75.3%).

^{1}H NMR (400 MHz, $CDCl_3$) δ/ppm= 0.863-0.88 (s, 6H), 1.31 (m, 40H), 2.2 (m, 2H), 2.62 (m, 4H), 2.88(t, 2H), 2.91 (t, 2H), 3.40 (d, 1H), 3.50 (m, 2H), 4.18 (m, 1H); **ESI-HRMS**: Calculated; 612.5249 found: 612.5248 [M+1].

2.4.3 Antioxidant Assay

The inherent antioxidant activity of **Toc-As**, **N14-As** and **Toc-NOH** lipids was carried out by means of the scavenging of 2, 2-diphenyl-1-picrylhydrazyl (DPPH) radicals. The ability of **Toc-As**, **N14-As** and **Toc-NOH** to scavenge radicals was evaluated by incubating different concentrations of the **Toc-As**, **N14-As** and **Toc-NOH** with DPPH (100 μM) radicals in aqueous ethanol for different periods of time and the amount of unscavenged radicals was calculated by measuring the intensity at 490 nm using a microplate reader (Infinite 200 PRO, TECAN). Ascorbic acid (AA, vitamin C) was used as a positive control and untreated DPPH was used as a negative control to measure the antioxidant efficiencies of the **Toc-As**, **N14-As,** and **Toc-NOH**. The antioxidant efficiencies of the **Toc-As**, **N14-As** and **Toc-NOH** are expressed in terms of the percentage of free-radical scavenging activity as a function of concentration and incubation time according to Equation (1)

$$\%\, Scavengeractivity = \frac{Absorbanceofcontrol - Absorbanceofsample}{Absorbanceofcontrol} x\ 100$$

2.4.4 Preparation of liposomes and plasmid DNA

The lipids and the co-lipid DOPE (1 mmol each) were dissolved in chloroform in a glass vial, and a thin film of lipids was made on the wall of the glass tubes while evaporating the total solvent with a thin flow of moisture-free nitrogen gas and dried under high vacuum for 2 h, then 1 ml of sterile deionized water was added to the vacuum-dried lipid film and the mixture was allowed to swell overnight. The vial was then vortexed for 4 min at room temperature to get a transparent or translucent solution and sonicated in a bath sonicator and probe sonicator respectively to produce small unilamellar vesicles (SUVs) from multilamellar vesicles (MLVs).

The resulting clear aqueous liposomes were used to form lipoplexes. The eGFP plasmid was amplified in DH5α-strain of *Escherichia coli*.

2.4.5 Lipoplex preparation and DNA binding assay

Positively charged liposomes were complexed with negatively charged DNA to form lipid-DNA complexes. 1:1 to 8:1 lipid charge ratios were used. 1% agarose gel (pre-stained with ethidium bromide) was used to elucidate the DNA binding capability of liposome with Lipid: DNA charge ratios from 1:1 to 8:1.plasmid DNA (0.3 μg) was complexed with the varying amount of cationic liposomes in that order (from 0.9 μ L to 7.2μL) in a total volume of 30 μL in HEPES buffer (pH 7.4) and incubated at it for 20-25 minutes. 4μL of 6x loading buffer (0.25% Bromophenol blue in 40% (w/v) sucrose with sterile water) was added to it and from the resulting solution, 30 μLwas loaded on each well. The samples were electrophoresed at 80 V for 45 minutes and the agarose gel images for DNA bands were visualized using a Bio-Rad Gel Doc XR+ imaging system (Bio-Rad, Hercules, CA, USA).

2.4.6 Heparin Displacement Assay

Heparin was used to study the anionic dislocation of DNA within the lipoplexes. The lipid: pDNA complexes were prepared as described in the above section (DNA binding assay) and incubated for 20 minutes. Following the incubation, 0.1μg of the sodium salt of heparin was added and incubated for another 30 minutes. The lipoplexes were electrophoresed on an agarose gel (1.5%) for heparin displacement analysis and pDNA bands were visualized as mentioned in the above section.

2.4.6 Zeta potential (ξ) and size measurements

The sizes and the surface charges (zeta potentials) of liposomes and lipoplexes with varying charge ratios (8:1 to 1:1) were measured by photon correlation spectroscopy and electrophoretic mobility on a Zetasizer 3000HSA (Malvern, U.K.). The sizes were measured in serum-free

DMEM media with a sample refractive index of 1.59 and a viscosity of 0.89. The system was calibrated by using the 2005 nm polystyrene polymer (Duke Scientific Corps., Palo Alto, CA, U.S.). The sizes of liposomes and lipoplexes were calculated by using the automatic method. The ζ (zeta potential) was also measured using the following parameters: viscosity, 0.89 cP; dielectric constant, 80; temperature, 25 ˚C; F (Ka), 1.50 (Smoluchowski); the maximum voltage of the current, 80 V. The system was calibrated by using the DTS0050 standard from Malvern. Measurements were done 10 times with the zero-field correction. All the liposomes and lipoplexes of the size measurements were done 10 times in triplicate with the zero field correction and values represented as the average of triplicate measurements. The potentials were measured 10 times and represented as their average values as calculated by using the Smoluchowski approximation.

2.4.7 Cytotoxicity assay

The MTT (3-(4,5-dimethylthiazol-2-yr)-2, 5-diphenyltetrazolium Bromide) based reduction cytotoxicity assays of cationic lipids **Toc-As**, **N14-As** and **Toc-NOH** were carried out in CHO, Neuro-2a, HEK-293T, and HepG2 cells across the lipid: DNA charge ratios of 1:1-8:1in 96-wells plate. Briefly, 24 h after the addition of lipoplexes, MTT (0.5mg/ml in DMEM) was added to cells and incubated for 4 h at 37 ˚C. Results were expressed as percentviability = [A540 (treated cells)-background/A540 (untreated cells)-background] x 100.

2.4.8 Transfection Biology:

A general of the transfection procedure was followed as described below. Eukaryotic cells were cultured at a density of 15000 cells per well in a ninety-six -well plate 18-24 h the day before the transfection. The supercoiled plasmid DNA (0.3 μg) was complexed with varying amounts of desired lipids (0.15 -7.2 mmol) in serum-free DMEM medium (maximum volume should be to 100 μL) for 20 minutes. The charge ratios of cationic liposomes were varied from 0.5:1 to 8:1

(+/-). The liposome -eGFP plasmid complexes were then treated to the cells. After 3 h of the incubation period, 100 μL of Dulbecco's Modified Eagle Medium DMEM with 10% FBS was added to the cells. The serum medium was altered to 10% complete medium after 24 h and the reporter gene activity was estimated after 48 h. The cells were washed two times with PBS (100 μL each) and lysed in 50 μL lysis buffer [0.25 M Tris-HCl pH 8.0, 0.5% NP40]. The Care was taken to ensure complete lysis. The β-galactosidase activity in wells was estimated by addition 50 μL of 2 X-substrate solutions [1.33 mg/mL of ONPG, 0.2 M sodium phosphate (pH 7.3) and 2 mM magnesium chloride] to the lysate in a 96-well plate. The Adsorption at 405 nm was converted to β-galactosidase units using a calibration curve constructed with the commercial β-galactosidase enzyme. The values of β-galactosidase units in three experiments carried out on the same day varied by less than 20%. The transfection experiment was performed in duplicate and the reported transfection efficiency values are the average of triplicate experiments carried out on the same day. Each transfection experiment was repeated three epoch and the day to day changes in average transfection efficiency was found to be within 2-fold. The transfection was obtained on different days were similar.

2.4.9 Cellular eGFP Expression Study.

For cellular α5GFP expression experiments in HEK-293T& HepG2, 50,000 cells were cultured in each well of 24-well plate 18-24 h before the transfection. Then 0.9 μg of eGFP plasmid DNA encoding green fluorescent protein was complexed with liposomes of lipids **Toc-As**, **N14-As** and **Toc-NOH** at charge ratio (lipid/DNA) 2:1 in DMEM medium (total volume made up to 100 μl) for 30 min. Just prior to transfection, cells plated in the 24-wells plate were washed with PBS (2×100 μL) followed by addition of lipoplexes. The media 400 μLwas added after 4 h incubation of the cells. Subsequent to 24 h, the complete medium was removed from each well, and the total cells were washed with PBS (2× 200 μL). Finally, 200 μLof PBS was added to each per good

cells and visualized under the epifluorescent microscope to observe the cells expressing the green fluorescent protein.

2.4.10 Circular Dichroism (CD)

Circular dichroism spectra (CD) were recorded for pDNA and lipoplexes in 6% dextrose solution. Becausethe dextrose is a chiral molecule and it CD (circular dichroism spectra) of dextrose alone was subtracted from that of supercoiled DNA in dextrose solution to obtain the profile for nucleic acid/pDNA. In the same way, the spectra of lipoplexes were recorded with background normalization to the profiles of matching cationic liposomes alone in dextrose solution. Samples were scanned through a wavelength range of 200-500 nm at 25 °C using a 0.5 mL quartz cuvette, with a path length of 1 cm. every sample was scanned four times with an integration time of 5 s, and the values were averaged. Scanning was done at 1 nm steps, and the slit width was 1 nm. Positive charge liposome-nucleic acid complexes were prepared at 4:1 +/- charge ratio at 50 µg/mL supercoiled pDNA concentration.

2.4.11 Transfection Biology in Presence of Serum

Eukaryotic cells were cultured at a density of 15,000 cells (HEK-293T & CHO) per well in a 96-well plate, 18-24 h before the transfection. After that 0.3 µg (0.91 nmol) of eGFP was complexed with a liposome (**Toc-As**, **N14-As** and **Toc-NOH**) in DMEM medium in the presence of increasing concentrations of added serum (10-30% v/v and entire volume made up to 100 µL) for 30 min. The charge ratios of liposome/eGFP were maintained as 4:1, at which all the three lipids showed their maximum transfection efficacies in 2 types of cells used for transfection viz. HEK-293T and CHO. The experimental procedure and determination of eGFP activity per well are similar to that reported for the in vitro transfection experiments.

2.4.12 Cellular Uptake examine by Epifluorescence Microscopy

Eukaryotic cells were harvested at a density of 11 000 cells/ well in a 96-well plate regularly 18−24 h earlier to the treatment in 250 μL of serum contained medium such that the well became 30−60% confluent/ concurrent at the time of transfection. Double helix DNA (0.3 μg of pDNA

diluted to 50 μL with serum-free DMEMmedia) was complexed with rhodamine-PE labeled positively charged cationic liposomes (diluted to 50 μL with DMEM) of lipids **Toc-As**, **N14-As** and **Toc-NOH** using4:1 lipid to DNA charge ratio. The cells were washed with PBS (1 × 200 μL), then treated with lipid-pDNA complexes, and incubated at a humidified atmosphere containing 5% CO_2 (Carbon dioxide) at 37 °C. After 4 h of incubation, the cells were washed with 10% PBS (3 × 200 μL) to remove the dye and fixed with 3.8% paraformaldehyde in PBS at room temperature for 15 min. The red fluorescent cells were recognized under an epifluorescence microscope (Nikon, Japan).

2.5 References

1. Deng, H. X.; Wang, Y.; Ding, Q. R.; Li, D. L.; Wei, Y. Q., Gene therapy research in Asia. *Gene therapy* **2017,***24* (9), 572-577.
2. Griesenbach, U.; Davies, J. C.; Alton, E., Cystic fibrosis gene therapy: a mutation-independent treatment. *Current opinion in pulmonary medicine* **2016,***22* (6), 602-9.
3. Burney, T. J.; Davies, J. C., Gene therapy for the treatment of cystic fibrosis. *The application of clinical genetics* **2012,***5*, 29-36.
4. Porteous, D. J., Current status and future prospects for the treatment of lung disease in cystic fibrosis by gene therapy. *Pulmonary pharmacology* **1994,***7* (3), 153-7.
5. Zhi, D.; Zhang, S.; Wang, B.; Zhao, Y.; Yang, B.; Yu, S., Transfection efficiency of cationic lipids with different hydrophobic domains in gene delivery. *Bioconjugate chemistry* **2010,***21* (4), 563-77.
6. Wang, J.; Guo, X.; Xu, Y.; Barron, L.; Szoka, F. C., Jr., Synthesis, and characterization of long-chain alkyl acylcarnitine esters. Potentially biodegradable cationic lipids for use in gene delivery. *Journal of medicinal chemistry* **1998,***41* (13), 2207-15.
7. Byk, G.; Soto, J.; Mattler, C.; Frederic, M.; Scherman, D., Novel non-viral vectors for gene delivery: synthesis of a second-generation library of mono-functionalized poly-(guanidinium)amines and their introduction into cationic lipids. *Biotechnology and bioengineering* **1998,***61* (2), 81-7.
8. Karmali, P. P.; Kumar, V. V.; Chaudhuri, A., Design, syntheses and in vitro gene delivery efficacies of novel mono-, di- and trypsinated cationic lipids: a structure-activity investigation. *Journal of medicinal chemistry* **2004,***47* (8), 2123-32.
9. Huang, Q. D.; Zhong, G. X.; Zhang, Y.; Ren, J.; Fu, Y.; Zhang, J.; Zhu, W.; Yu, X. Q., Cyclen-based cationic lipids for highly efficient gene delivery towards tumor cells. *PloS one* **2011,***6* (8), e23134.

10. Bhattacharya, S.; Bajaj, A., Advances in gene delivery through molecular design of cationic lipids. *Chem Commun (Camb)* **2009,** (31), 4632-56.

11. Al-Dosari, M. S.; Gao, X., Nonviral gene delivery: principle, limitations, and recent progress. *The AAPS journal* **2009,***11* (4), 671-81.

12. (a) Zhdanov, R. I.; Podobed, O. V.; Vlassov, V. V., Cationic lipid-DNA complexes-lipoplexes-for gene transfer and therapy. *Bioelectrochemistry* **2002,***58* (1), 53-64; (b) Mendell, J. R.; Rodino-Klapac, L.; Sahenk, Z.; Malik, V.; Kaspar, B. K.; Walker, C. M.; Clark, K. R., Gene therapy for muscular dystrophy: lessons learned and path forward. *Neuroscience letters* **2012,***527* (2), 90-9; (c) Bara, J. J.; Clark, T. M.; Remold, S. K., Susceptibility of larval Aedes aegypti and Aedes albopictus (Diptera: Culicidae) to dengue virus. *Journal of medical entomology* **2013,***50* (1), 179-84.

13. (a) Parvizi-Bahktar, P.; Mendez-Campos, J.; Raju, L.; Khalique, N. A.; Jubeli, E.; Larsen, H.; Nicholson, D.; Pungente, M. D.; Fyles, T. M., Structure-activity correlation in transfection promoted by pyridinium cationic lipids. *Organic & biomolecular chemistry* **2016,***14* (11), 3080-90; (b) Doktorovova, S.; Santos, D. L.; Costa, I.; Andreani, T.; Souto, E. B.; Silva, A. M., Cationic solid lipid nanoparticles interfere with the activity of antioxidant enzymes in hepatocellular carcinoma cells. *International journal of pharmaceutics* **2014,***471* (1-2), 18-27.

14. McGregor, C.; Perrin, C.; Monck, M.; Camilleri, P.; Kirby, A. J., Rational approaches to the design of cationic gemini surfactants for gene delivery. *Journal of the American Chemical Society* **2001,***123* (26), 6215-20.

15. (a) Soria, L. F.; Ludwig, E. H.; Clarke, H. R.; Vega, G. L.; Grundy, S. M.; McCarthy, B. J., Association between a specific apolipoprotein B mutation and familial defective apolipoprotein B-100. *Proceedings of the National Academy of Sciences of the United States of America* **1989,***86* (2), 587-91; (b) Watts, D. M.; Bailey, C. L.; Roberts, N. T.; RF, T. A.; Dalrymple, J. M.; Clark, G. C., Maintenance and transmission of Keystone virus by

Aedes atlanticus (Diptera: Culicidae) and the gray squirrel in the Pocomoke Cypress Swamp, Maryland. *Journal of medical entomology* **1988,***25* (6), 493-500; (c) Henriksson, M.; Classon, M.; Ingvarsson, S.; Koskinen, P.; Sumegi, J.; Klein, G.; Thyberg, J., Elevated expression of c-myc and N-myc produces distinct changes in nuclear fine structure and chromatin organization. *Oncogene* **1988,***3* (5), 587-93; (d) Uttara, B.; Singh, A. V.; Zamboni, P.; Mahajan, R. T., Oxidative stress and neurodegenerative diseases: a review of upstream and downstream antioxidant therapeutic options. *Current neuropharmacology* **2009,***7* (1), 65-74.

16. (a) Filion, M. C.; Phillips, N. C., Toxicity and immunomodulatory activity of liposomal vectors formulated with cationic lipids toward immune effector cells. *Biochimica et biophysica acta* **1997,***1329* (2), 345-56; (b) Hahnenberger, K. M.; Baum, M. P.; Polizzi, C. M.; Carbon, J.; Clarke, L., Construction of functional artificial minichromosomes in the fission yeast Schizosaccharomyces pombe. *Proceedings of the National Academy of Sciences of the United States of America* **1989,***86* (2), 577-81.
17. Zhu, J.; Qian, W.; Wang, Y.; Gao, R.; Wang, J.; Xiao, H., Involvement of mitogen-activated protein kinase and NF-kappaB signaling pathways in perfluorooctane sulfonic acid-induced inflammatory reaction in BV2 microglial cells. *Journal of applied toxicology : JAT* **2015,***35* (12), 1539-49.
18. Aramaki, Y.; Takano, S.; Arima, H.; Tsuchiya, S., Induction of apoptosis in WEHI 231 cells by cationic liposomes. *Pharmaceutical research* **2000,***17* (5), 515-20.
19. Lappalainen, K.; Jaaskelainen, I.; Syrjanen, K.; Urtti, A.; Syrjanen, S., Comparison of cell proliferation and toxicity assays using two cationic liposomes. *Pharmaceutical research* **1994,***11* (8), 1127-31.
20. Nagata, S., Apoptosis by death factor. *Cell* **1997,***88* (3), 355-65.

21. Takano, S.; Aramaki, Y.; Tsuchiya, S., Physicochemical properties of liposomes affecting apoptosis induced by cationic liposomes in macrophages. *Pharmaceutical research* **2003,***20* (7), 962-8.

22. (a) Aramaki, Y.; Takano, S.; Tsuchiya, S., Induction of apoptosis in macrophages by cationic liposomes. *FEBS letters* **1999,***460* (3), 472-6; (b) Shirley, R.; Ord, E. N.; Work, L. M., Oxidative Stress and the Use of Antioxidants in Stroke. *Antioxidants (Basel)* **2014,***3* (3), 472-501.

23. Aramaki, Y.; Takano, S.; Tsuchiya, S., Cationic liposomes induce macrophage apoptosis through mitochondrial pathway. *Archives of biochemistry and biophysics* **2001,***392* (2), 245-50.

24. Iwaoka, S.; Nakamura, T.; Takano, S.; Tsuchiya, S.; Aramaki, Y., Cationic liposomes induce apoptosis through p38 MAP kinase-caspase-8-Bid pathway in macrophage-like RAW264.7 cells. *Journal of leukocyte biology* **2006,***79* (1), 184-91.

25. Raff, M., Cell suicide for beginners. *Nature* **1998,***396* (6707), 119-22.

26. Dharmalingam, P.; Marrapu, B.; Voshavar, C.; Nadella, R.; Rangasami, V. K.; Shaji, R. V.; Abbas, S.; Prasad, R. B.; Kaki, S. S.; Marepally, S., An anti-oxidant, alpha-lipoic acid conjugated oleoyl-sn-phosphatidylcholineas a helper lipid in cationic liposomal formulations. *Colloids and surfaces. B, Biointerfaces* **2017,***152*, 133-142.

27. Dringen, R.; Pawlowski, P. G.; Hirrlinger, J., Peroxide detoxification by brain cells. *Journal of neuroscience research* **2005,***79* (1-2), 157-65.

28. Habiro, A.; Tanno, S.; Koizumi, K.; Izawa, T.; Nakano, Y.; Osanai, M.; Mizukami, Y.; Okumura, T.; Kohgo, Y., Involvement of p38 mitogen-activated protein kinase in gemcitabine-induced apoptosis in human pancreatic cancer cells. *Biochemical and biophysical research communications* **2004,***316* (1), 71-7.

29. Ambrosi, M.; Fratini, E.; Alfredsson, V.; Ninham, B. W.; Giorgi, R.; Lo Nostro, P.; Baglioni, P., Nanotubes from a vitamin C-based bolaamphiphile. *Journal of the American Chemical Society* **2006,***128* (22), 7209-14.

30. Jin, X.; Kennedy, S. W.; Di Muccio, T.; Moon, T. W., Role of oxidative stress and antioxidant defense in 3,3',4,4',5-pentachlorobiphenyl-induced toxicity and species-differential sensitivity in chicken and duck embryos. *Toxicology and applied pharmacology* **2001,***172* (3), 241-8.

31. El-Senousey, H. K.; Chen, B.; Wang, J. Y.; Atta, A. M.; Mohamed, F. R.; Nie, Q. H., Effects of dietary vitamin C, vitamin E, and alpha-lipoic acid supplementation on the antioxidant defense system and immune-related gene expression in broilers exposed to oxidative stress by dexamethasone. *Poultry science* **2017**.

32. (a) Khor, S. C.; Wan Ngah, W. Z.; Mohd Yusof, Y. A.; Abdul Karim, N.; Makpol, S., Tocotrienol-Rich Fraction Ameliorates Antioxidant Defense Mechanisms and Improves Replicative Senescence-Associated Oxidative Stress in Human Myoblasts. *Oxidative medicine and cellular longevity* **2017,***2017*, 3868305; (b) Kalmodia, S.; Vandhana, S.; Tejaswini Rama, B. R.; Jayashree, B.; Sreenivasan Seethalakshmi, T.; Umashankar, V.; Yang, W.; Barrow, C. J.; Krishnakumar, S.; Elchuri, S. V., Bio-conjugation of antioxidant peptide on surface-modified gold nanoparticles: a novel approach to enhance the radical scavenging property in cancer cell. *Cancer nanotechnology* **2016,***7*, 1.

33. Almofti, M. R.; Harashima, H.; Shinohara, Y.; Almofti, A.; Li, W.; Kiwada, H., Lipoplex size determines lipofection efficiency with or without serum. *Molecular membrane biology* **2003,***20* (1), 35-43.

34. Ross, P. C.; Hui, S. W., Lipoplex size is a major determinant of in vitro lipofection efficiency. *Gene therapy* **1999,***6* (4), 651-9.

35. Lai, E.; van Zanten, J. H., Real time monitoring of lipoplex molar mass, size and density. *Journal of controlled release : official journal of the Controlled Release Society* **2002,***82* (1), 149-58.

36. Liu, S.; Zhou, D.; Yang, J.; Zhou, H.; Chen, J.; Guo, T., Bioreducible Zinc(II)-Coordinative Polyethylenimine with Low Molecular Weight for Robust Gene Delivery of Primary and Stem Cells. *Journal of the American Chemical Society* **2017**.

37. Kedika, B.; Patri, S. V., Design, synthesis, and in vitro transfection biology of novel tocopherol based monocationic lipids: a structure-activity investigation. *Journal of medicinal chemistry* **2011,***54* (2), 548-61.

38. Neault, J. F.; Naoui, M.; Tajmir-Riahi, H. A., DNA-drug interaction. The effects of vitamin C on the solution structure of Calf-thymus DNA studied by FTIR and laser Raman difference spectroscopy. *Journal of biomolecular structure & dynamics* **1995,***13* (2), 387-97.

39. Yoshikawa, Y.; Suzuki, M.; Chen, N.; Zinchenko, A. A.; Murata, S.; Kanbe, T.; Nakai, T.; Oana, H.; Yoshikawa, K., Ascorbic acid induces a marked conformational change in long duplex DNA. *European journal of biochemistry* **2003,***270* (14), 3101-6.

40. (a) Bloomfield, V. A., DNA condensation by multivalent cations. *Biopolymers* **1997,***44* (3), 269-82; (b) Fang, Y.; Hoh, J. H., Surface-directed DNA condensation in the absence of soluble multivalent cations. *Nucleic acids research* **1998,***26* (2), 588-93; (c) Bloomfield, V. A., Condensation of DNA by multivalent cations: considerations on mechanism. *Biopolymers* **1991,***31* (13), 1471-81; (d) He, S.; Arscott, P. G.; Bloomfield, V. A., Condensation of DNA by multivalent cations: experimental studies of condensation kinetics. *Biopolymers* **2000,***53* (4), 329-41.

41. Gao, X.; Huang, L., Cationic liposome-mediated gene transfer. *Gene therapy* **1995,***2* (10), 710-22.

42. Herz, J.; Gotthardt, M.; Willnow, T. E., Cellular signalling by lipoprotein receptors. *Current opinion in lipidology* **2000,***11* (2), 161-6.

43. Kedika, B.; Patri, S. V., Benzothiazole head group based cationic lipids: synthesis and application for gene delivery. *European journal of medicinal chemistry* **2014,***74*, 703-16.

44. Mukthavaram, R.; Marepally, S.; Venkata, M. Y.; Vegi, G. N.; Sistla, R.; Chaudhuri, A., Cationic glycolipids with cyclic and open galactose head groups for the selective targeting of genes to mouse liver. *Biomaterials* **2009,***30* (12), 2369-84.

CHAPTER 3

Hepatocellular targeted α-tocopherol based pH sensitive galactosylated lipid: design, synthesis and transfection Studies

3.1 Introduction

Cationic lipid-based delivery systems hold great promise among the non-viral transfection vectors for nucleic acid delivery applications.[1,2] These delivery systems are considered as safest alternatives for viral counterparts owing to their ease in preparation, non-immunogenic nature and efficiency in forming stable, injectable complexes even with large-size DNA (up to 10,000 bp).[3,4] Typical non-viral cationic agent/lipid delivery system used for pDNA delivery contains a hydrophilic head group with a positive charge and a hydrophobic domain of steroidal origin (Cholesterol or similar skeletons) or aliphatic long chains separated with/without a spacer/linker.[5] Cationic liposomes can deliver a therapeutic payload to specific body cells by tethering receptor-specific ligands in a target-guided manner with enhanced efficacies.[6]Liver-targeted gene therapy can make a maximum impact in the treatment of genetic disorders such as hemophilia, hereditary tyrosinemia type I (HTI).[78] Prior findings demonstrated that galactosylated cationic lipids could effectively deliver a therapeutic payload to the liver through asialoglycoprotein receptors (ASGPRs).[9] However, cationic liposomes exhibit necroptosis due to the high density of positive charges at the surface of liposomes which depolarize the negatively charged cell surface, leading to trigger up-regulation of intracellular reactive oxygen species (ROS) in turn leading to necroptosis mechanism. To address these issues, we developed cationic lipids with α-tocopherol as the hydrophobic core. α-tocopherol, a form of Vitamin-E is a membrane antioxidant, helps in preventing lipid peroxidation compared to cholesterol.[10] Other analogs such as Vitamin-E-TPGSs, are used extensively as a solubilizer in nanoparticles formulations and in clinical use.[11] In our continued efforts for developing safer and efficient transfection reagents, α-tocopherol derivatized cationic lipids found to be effective and safe in multiple cultured cell lines. [12] More importantly, α-tocopherol based lipids exhibited improved transfections in presence of serum.[13] The reasoning for using triazole as a linker between hydrophilic moiety and the hydrophobic core is that triazole imparts pH sensitivity, stability and

improves DNA binding property.[14] Triazole linker facilitates the escape of lipoplexes from endosomes in a pH-responsive manner.[15] V.V. Kumar et al. demonstrated that cysteinylated cationic lipids containing triazole group facilitated lipoplexes to escape from the early endosomes by modulating endosomal pH, prevented lysosomal degradation and maximized transfection.[16],[17]. Taking cues from our previous findings, in the present study, we developed α-tocopherol based ASGPR targeted liposomal delivery system by conjugating galactose ligand to tocopherol through a triazole linker for efficient delivery of nucleic acids into hepatocytes. In addition, we synthesized a control non-targeting lipid, Toc-OH similar to Toc-Gal lipid except conjugating ASGPR targeting ligand (D-Galactose). We characterized the biophysical properties such as size, potentials and DNA binding studies with liposomes of **Toc-Gal** and **Toc-OH** lipids. Cell viabilities, Transfection efficacies, and ASGPR receptor specific targeting property were evaluated in ASGPR receptor positive and negative cell lines (HepG2 and SK-HEP-1) using reporter gene assays and receptor saturation studies. In addition, serum compatibility studies were also performed in representative HepG2 cells.

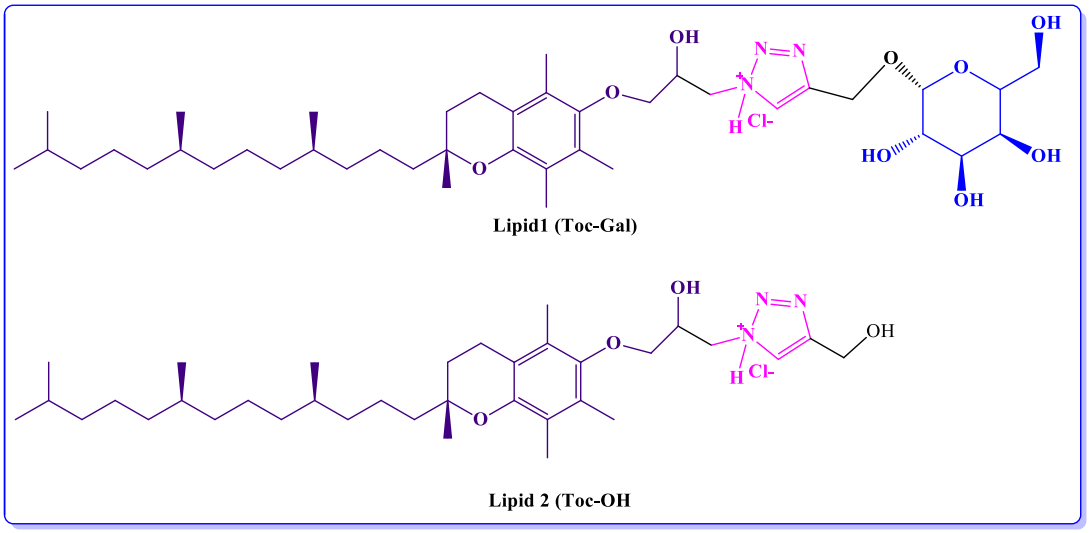

Chemical structures of cationic lipids

3. 2 Results and discussion:

3.2.1 Chemistry

Synthetic routes adopted for preparing the α-tocopherol based cationic glycolipids, **Toc-Gal**, and its control lipid, **Toc-OH** are shown schematically in **Schemes 1A** and **1B** respectively. The precursor intermediate α-tocopheryl-1, 2-azido alcohol (**2A**, **Scheme 1A,** 82%) for the synthesis of both the lipids, **Toc-Gal** and **Toc-OH** was prepared conventionally in 2 steps. Briefly, *O*-alkylation of α-tocopherol with epichlorohydrin in presence of 50% sodium hydroxide and tetra butyl ammonium hydrogen sulfate provided the epoxide linked α-tocopherol, 1A which upon epoxide opening with sodium azide afforded intermediate **2A (**88%) (**Scheme 1**A). The intermediate **2A** upon treatment with β-D-galactose tetraacetate *O*- propargyl glycoside, $CuSO_4.5H_2O$, sodium ascorbic acid provided the intermediate **3A** (89 %) (**Scheme 1A**). The intermediate **3A** upon *O*-acetyl deprotection using sodium methoxide in presence of dry methanol yielded intermediate **4A (**89%) (**Scheme 1A).** Protonation/Quaternization of intermediate **4A** (92%) with 6N hydrochloric acid afforded the title glycolipid, **Toc-Gal** (**Scheme 1**A). Control lipid, **Toc-OH** was synthesized by reacting intermediate **2A** (**from Scheme 1A**) with propargyl alcohol in presence of $CuSO_4.5H_2O$ and Sodium ascorbate yielded α-Tocopherol-triazole intermediate **1B** (78%) (**Scheme 1B**). The resulting triazole ether intermediate **1B** (**Scheme 1B**) was quaternized/protonated with 6N hydrochloric acid to afford target compound **Toc-OH** (92%) (**Scheme 1B**). Structures of all the synthetic intermediates as shown in **Schemes 1A** and **1B** were confirmed by ^{1}H NMR and ESI-MS. Structures of target lipids, **Toc-Gal** &**Toc-OH** were confirmed by ^{1}H NMR, ^{13}C NMR, ESI-MS, and HRMS. Severe line broadening (particularly in the range δ 3-5 ppm) was observed in ^{1}H NMR spectra of **Toc-Gal** presumably due to the presence of multiple exchangeable hydroxyl protons thus; **Toc-Gal** was characterized by the molecular ion peaks in ESI-MS and HRMS spectra. The purity of the

target lipids, **Toc-Gal** &**Toc-OH** were confirmed by reverse phase HPLC analysis using methanol as mobile phase. The purity of the target lipids was found to be more than 95%.

Scheme 1A: Synthesis of Galactosylated Lipid (Toc-Gal)

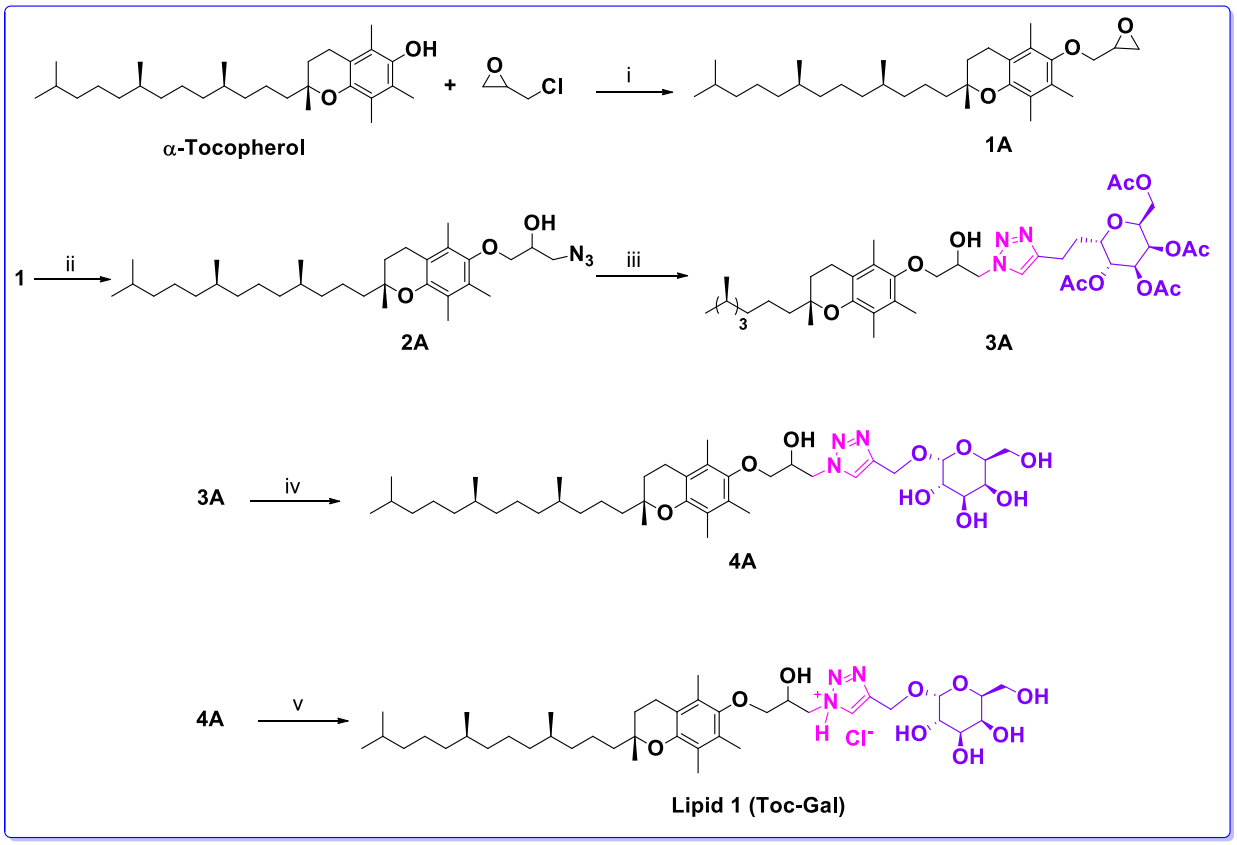

Reagents: i) 50% NaOH solution, Tetra butyl ammonium hydrogen sulphate; 82% ii) NaN_3, 1:1 THF/H_2O, 12 h Reflux; 88% iii) β-D-galactose tetra acetate *O*-propargyl glycoside, $CuSO_4.5H_2O$, Sodium Ascorbic acid, 1:1 THF/H_2O, 18 h RT.;89 % iv) Dry MeOH, NaOMe, 12 h, RT; 89 % v) 6N HCl, Diethyl ether, 0.5 h, RT 92%

Scheme IB: Synthesis of Control Lipid (Toc-OH)

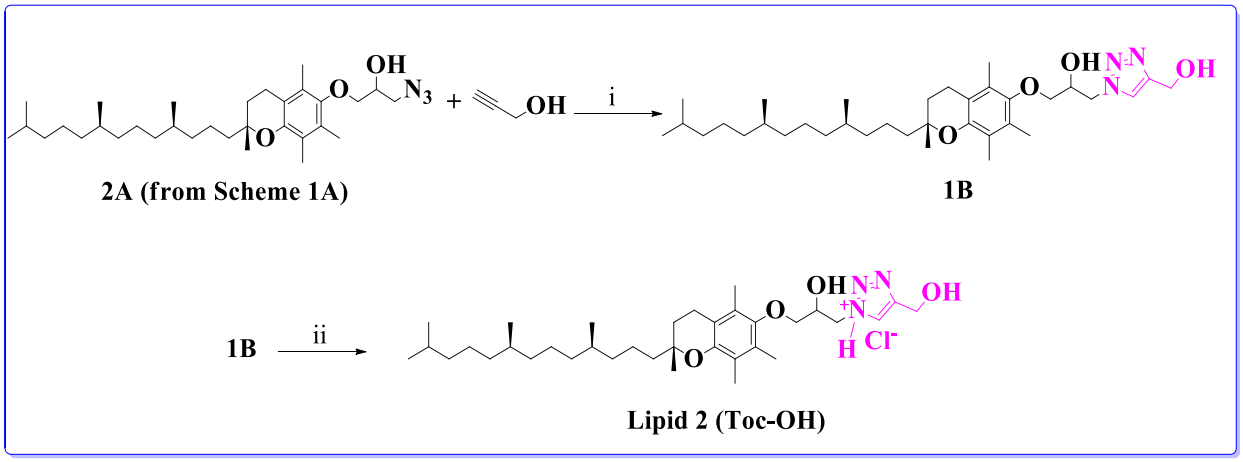

Reagents') $CuSO_4.5H_2O$, Sodium Ascorbate, 1:1 THF/H_2O, 24 h, RT ; 78%ii) dry Acetonitrile, 6N HCl, 24 h, Reflux. 92%

3.2.2 Liposomal Formulations

Initially, we used **Toc-Gal** and **Toc-OH** with cholesterol as co-lipid at 1:1 molar ratio (1 mM concentration w.r.t **Toc-Gal/Toc-OH**) to prepare liposomes, which didn't yield uniform vesicle formation resulting in precipitation. Subsequently, we used DOPC and DOPE (conventionally used co-lipids) to prepare liposomes with **Toc-Gal** & **Toc-OH** in above-indicated ratio and concentration. We observed the formation of the uniform liposomal solution with DOPE: **Toc-Gal/Toc-OH** only. However, the liposomal formulation prepared with DOPE as co-lipid at 1:1 DOPE: **Toc-Gal/Toc-OH** ratio exhibited poor DNA binding efficacies (discussed in the following section). Hence, we had to opt for next formulation using DOPE with **Toc-Gal/Toc-OH** at 2:1 ratio and performed all the experiments with above formulation.

3. 2.3 Physico-chemical Characterizations of Liposomes and Lipoplexes

2.3.3.1 DNA binding & Heparin displacement study

To begin with, we employed conventional agarose gel electrophoresis assay towards evaluating the relative DNA binding efficiencies of above prepared liposomal formulations at varying lipid: DNA charge ratios. Initially, we used liposomal formulations of **Toc-Gal** and **Toc-OH** with DOPE at equimolar ratio i.e. 1:1 DOPE: **Toc-Gal**/**Toc-OH**. Liposomal preparation involving **Toc-Gal** at 1:1 molar ratio showed optimal binding at 8:1 and 4:1 lipid: DNA charge ratios. The binding efficiencies drastically reduced at 2:1 charge ratio, while there was poor binding of DNA at 1:1 charge ratio (**Figure S1**, Supplementary Information). However, Liposomal preparation of **Toc-OH** showed little/no binding across the lipid:DNA charge ratio of 8:1-1:1 (**Figure S1**, Supplementary Information). The reason for compromised DNA binding could be due to an aromatic planar ring of tocopherol that might be limiting binding efficiencies. To overcome the limitation, we used liposomal formulations with DOPE and **Toc-Gal**/**Toc-OH** at 2:1 ratio for DNA binding studies. Results from the gel electrophoresis experiment demonstrated excellent pDNA binding interactions for **Toc-Gal** across 10:1 to 2:1 lipid: pDNA charge ratio with a slight reduction of binding at 1:1 charge ratio (**Figure 1**). However, **Toc-OH** exhibited high binding at 10:1 and 8:1 charge ratios only. We observed optimal pDNA binding at 4:1 charge ratio while at 2:1 & 1:1 charge ratio showed poor DNA binding (**Figure 1A**). Further, heparin displacement experiment was performed to confirm the DNA binding data obtained with the above liposomal formulations. Liposomal formulation with **Toc-Gal** resisted displacement of pDNA with heparin across the lipid: DNA charge ratio 10:1-1:1 (**Figure 1B**). However, **Toc-OH** formulation could survive DNA displacement at 10:1 and 8:1 charge ratios. pDNA from **Toc-OH** lipoplexes gradually displaced as the lipid: pDNA charge ratio decreased from 4:1 to 1:1 (**Figure 1B**). Results from above experiments suggest that **Toc-Gal** has better binding efficiencies than **Toc-OH** at lower charge ratios i.e. 4:1 to 1:1 and showed similar DNA binding efficiencies at higher lipid: pDNA charge ratios i.e. 10:1 and 8:1. This may be due to more hydrogen bonding interactions of **Toc-Gal** with pDNA when compared to **Toc-OH**.

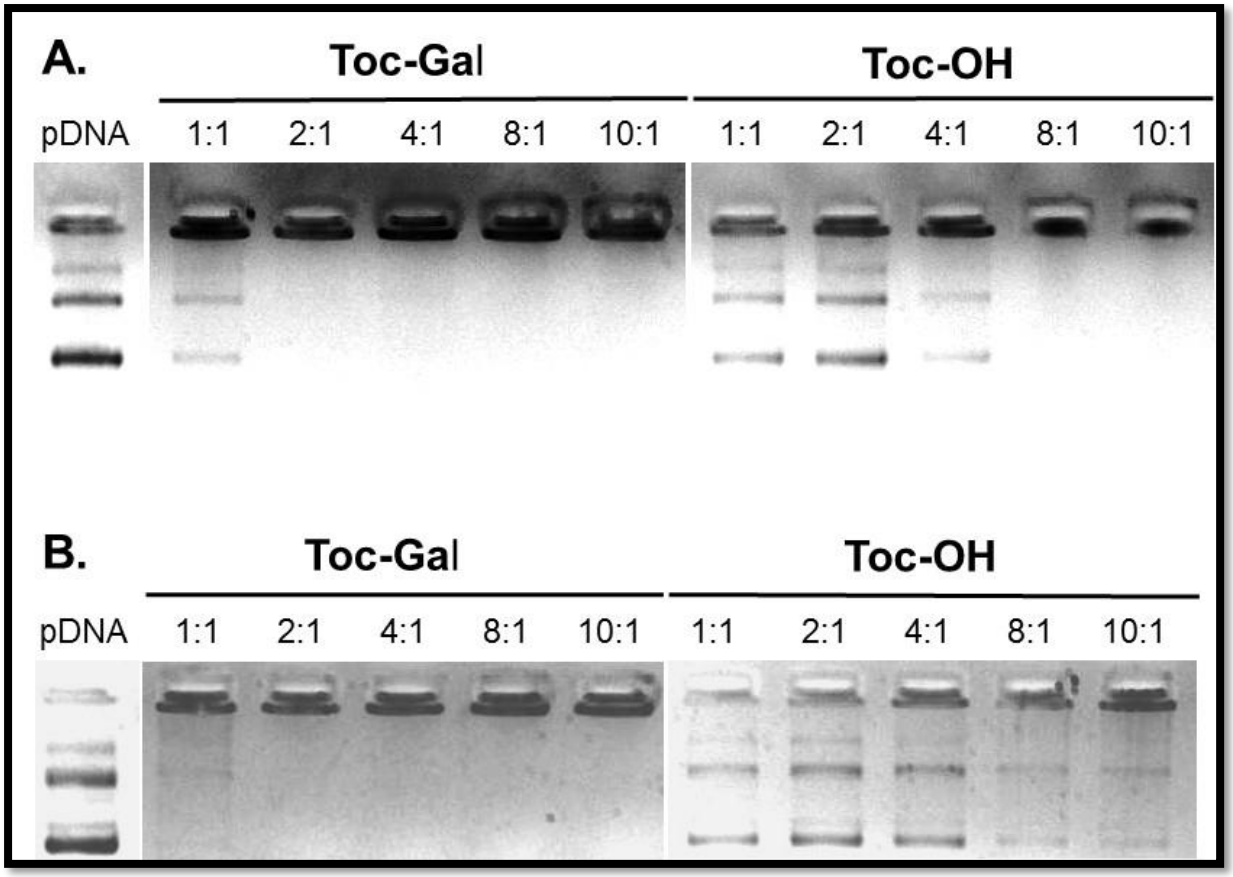

Figure 1. Electrophoretic gel patterns for lipoplex-associated DNA in agarose gel retardation assay (**A**) and Heparin displacement assay (**B**). The lipid/DNA charge ratios are indicated at the top of each lane.

3.2.3.2 Circular Dichroism (CD)

Circulardichroism (CD) is use to investigate the structure of pDNA and the conformational changes produced by ligand or cationic lipid binding[18], [19], [20]. Generally, CD spectra of pDNA occur due to the electronic transitions of nucleobases. The interactions in between these nucleobases and cationic lipids give the intense CD, which is very sensitive to the total confirmation of these biomolecules. The correlations between a few characteristic CD spectral features and the structure of various DNA-liposome complexes (B-DNA, A-DNA, C-DNA etc.,) might be useful to get the information about the mechanistic pathway for gene delivery. In this paper, we report the characterization of DNA- liposome complexes (**Toc-Gal** and **Toc-OH**) by Circulardichroism (CD) at a charge ratio of 10:1, which were shown in Fig 2. The CD spectra

were recorded from 200 nm to 500 nm to find the changes in the confirmation of pDNA arising due to interaction with the cationic liposome. The CD spectrum of pDNA presented was in canonical B form, a positive band at 225 nm, the negative signal at 240 nm, and crossover point near 305 nm, which were changed to 250nm, 218nm,and 260nm respectively for the cationic liposome **To-Gal** (**Figure 2**). Whereas the CD spectrum of cationic liposome **Toc-OH** exhibits a positive band at 210 nm, the negative band at 212 nm. The liposomes of **Toc-Gal** and **Toc-OH** showed significant conformational changes when interacted with pDNA.

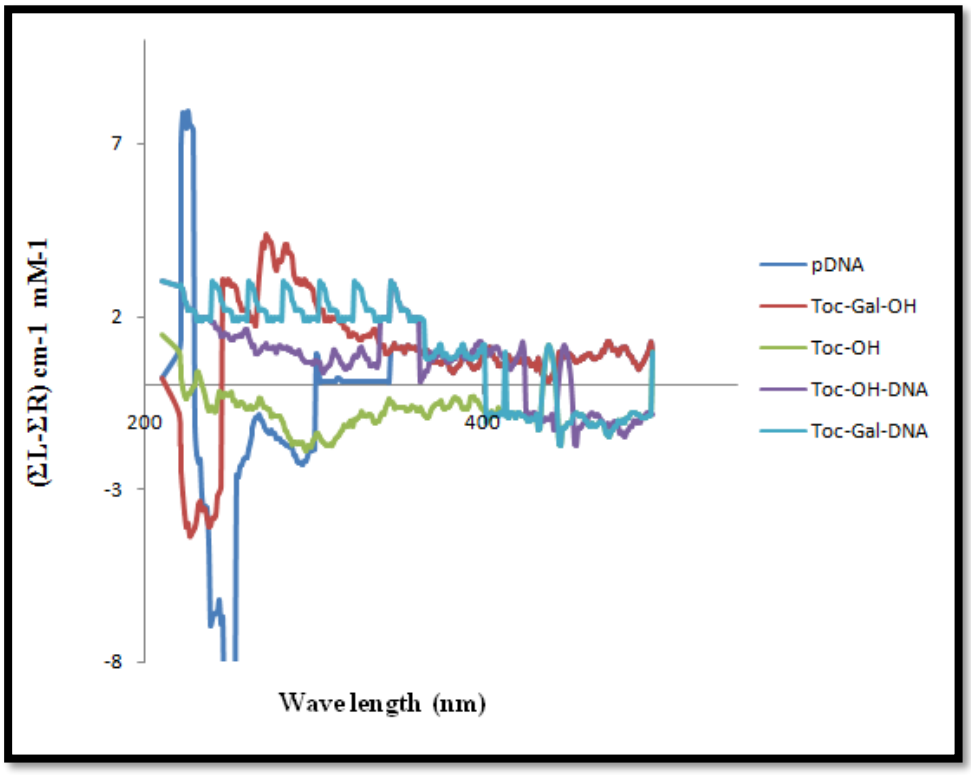

Figure 2. Circular dichroism (CD) spectra of lipid-pDNA complexes. Liposomes were prepared at 2:1 molar ratio of lipid DOPE and cationic lipids i.e. (**Toc-Gal** and **Toc-OH**) Complexes were prepared at the charge ratio of 10:1 and CD was recorded at a pDNA concentration of 50 µg/mL. The CD spectrum has been compared to the profile for pDNA alone. Spectral profiles of liposomes with milliQ water alone were subtracted as blank.

3. 2.3.3 Liposome sizes and Zeta potentials (ξ)

Following DNA binding studies, we have evaluated the physicochemical properties such as hydrodynamic diameter and zeta potentials of liposomes and lipoplexes of **Toc-Gal** and **Toc-OH**

using Dynamic Laser Scattering (DLS) method. Initially, liposomes of **Toc-Gal** and **Toc-OH** showed hydrodynamic sizes of 500 nm and 367 nm respectively while potentials were comparable with +7.12 mV for Toc-Gal and +6.3 mV for **Toc-OH** (**Figure 3**). Next, size data from lipoplexes showed significant variation for **Toc-Gal** and **Toc-OH** across the lipid:DNA charge ratio of 1:1 to 10:1 (**Figure 3A**). Lipoplexes prepared from liposomes of **Toc-OH** showed 600 nm at 1:1 charge ratio and were further found to be within a range of 324 nm - 484 nm across 2:1 to 10:1 charge ratios (**Figure 3B**). Interestingly, we observed an incremental pattern for lipoplexes of **Toc-Gal**, which showed 855 nm and 985 nm at 1:1-2:1 charge ratios. However, we found a slight decrease in size at 4:1 charge ratio (953 nm) when compared with 2:1 charge ratio. At higher charge ratios of 8:1 and 10:1, sizes of lipoplexes were found to be 1068 nm and 1154 nm respectively (**Figure 3A**). Unlike the variation observed in hydrodynamic sizes of lipoplexes for **Toc-Gal** and **Toc-OH**, global surface potentials were found to be comparable to each other across 1:1-10:1 lipid:DNA charge ratio (**Figure 3A**). Zeta potential data for lipoplexes at 1:1 and 2:1 charge ratios indicated less cationic in nature showing negative values of -15.8 mV and -11.5 mV for **Toc-Gal** and **Toc-OH** respectively (**Figure 3B**). However the global surface charges were found to be increasing for lipoplexes of **Toc-Gal** and **Toc-OH** across 4:1-10:1 charge ratios (3.9 mV, 9 mV & 16 mV for **Toc-Gal**, 4.5 mV, 8 mV & 14 mV for **Toc-OH**) (**Figure 3B**). Results from DLS experiment reveals that hydrodynamic sizes of liposomes, global surface charges of both liposomes and lipoplexes of **Toc-Gal** and **Toc-OH** didn't show significant variation. However, there was an increase in the hydrodynamic diameters of lipoplexes prepared using liposomes of **Toc-Gal** as the lipid: DNA charge ratio increased. It can be argued that the observed increment in the sizes of **Toc-Gal** lipoplexes could be due to higher hydration at the surface of liposomes. Since, **Toc-Gal** contains a galactose head-group, which has 3 additional hydroxyl groups when compared with **Toc-OH** which may add a higher degree of hydration. Hence, the observed size increase with an increase in a lipid:DNA charge ratio could be due to additional hydroxyl groups present in the head-group of **Toc-Gal**.[2]

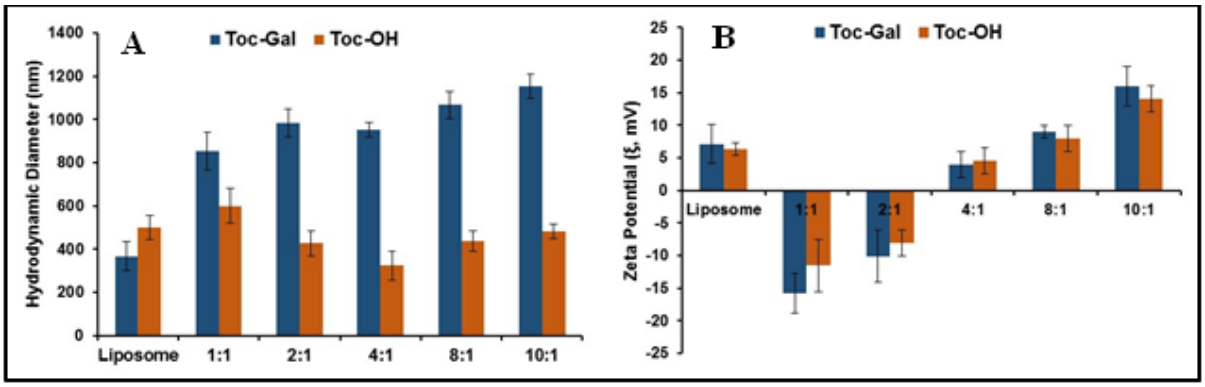

Figure 3. Graphical representation of Hydrodynamic Diameters (**A**) and Zeta Potentials (ξ, mV) (**B**) of the lipoplex-associated DNAin plain DMEM.

3.**2.4 Cell viability**

The cell viabilities using cationic liposomes of **Toc-Gal** &**Toc-OH** in complexation with pDNA (pCMV-SPORT-β-galactosidase) were assessed by MTT assay in 2 cell lines, HepG2 and SK-HEP-1. Results from the study showed that lipoplexes of both **Toc-Gal** and **Toc-OH** exhibited minimal cytotoxicity across 1:1-10:1 lipid:DNA charge ratio in both the cell lines. Cell viability was found to be more than 90% up to 8:1 lipid:DNA charge ratio for both the lipids and it was ~85% viable cells at 10:1 charge ratio (**Figure 4**). It is evident from the cell viability data that variation/enhancement in transfection efficacies of **Toc-Gal** and **Toc-OH** lipids cannot be attributed to their cytotoxic effects.

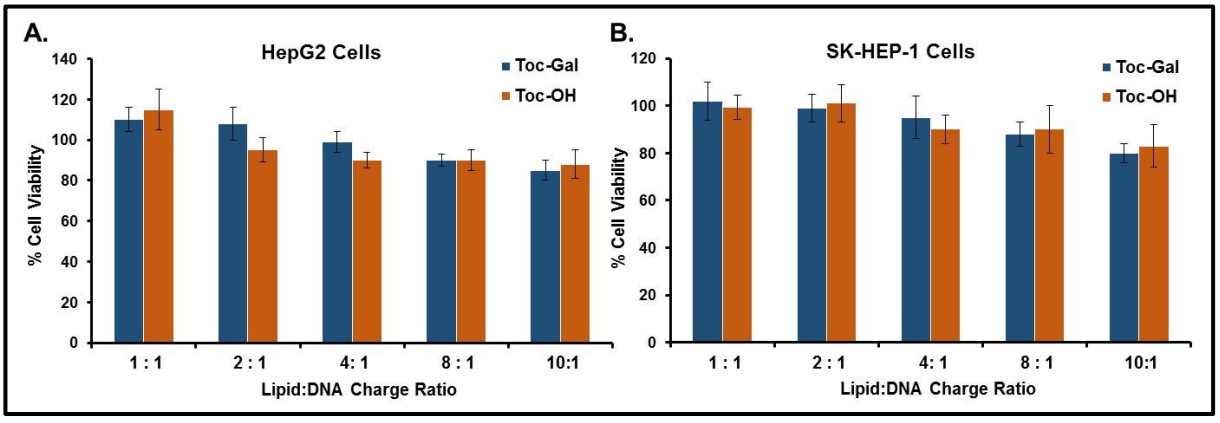

Figure 4. MTT assay based percent cell viabilities in HepG2 (A) and SK Hep-1 cells (B). Cells were treated with lipoplexes of lipids (Toc-Gal & Toc-OH) and pDNA (pCMV-SPORT-β-gal) with lipid:DNA charge ratios 1:1-10:1.

3.2.5 Transfection biology

The relative *in vitro* transfection efficacies of **Toc-Gal** and **Toc-OH** were initially evaluated using pEGFP (a plasmid DNA encoding green fluorescence protein) in ASGPR positive and negative cells, HepG2 & SK-HEP-1 at lipid:DNA charge ratios of 10:1 & 8:1 (optimal charge ratios as revealed by DNA binding studies). Transfection efficacies obtained in HepG2 cells treated with lipoplexes of **Toc-Gal** were found to be expressing higher percentages of green fluorescent protein than control lipid, **Toc-OH** at 8:1 charge ratio followed by 10:1 charge ratio (**Figure 5A**). Further, SK-HEP-1 cells revealed similar transfection profiles for both **Toc-Gal** and **Toc-OH** at 10:1 & 8:1 charge ratios (**Figure 5B**). Interestingly, the transfection activities obtained for **Toc-Gal** in HepG2 cells were found to be 2-3 fold higher when compared with transfection activities in SK-HEP-1 cells. However, no such variation was observed for **Toc-OH** transfection activity (**Figure 5B**). Microscopic image data obtained from cellular uptake and expression study revealed highest GFP expression for **Toc-Gal** at 8:1 charge ratio. Surprisingly, **Toc-Gal** at 10:1 charge ratio showed ~20% less fluorescence as compared to **Toc-Gal** at 8:1 charge ratio. Further, GFP expression in **Toc-OH** treated HepG2 cells was found to be ~60% less when compared with **Toc-Gal** at their respective lipid:DNA charge ratios (**Figure 5C**). In addition, GFP expression for **Toc-Gal** was found to be 2-fold higher than Lipofectamine 2000 in HepG2 cell lines (**Figure 5**). Enhanced transfection activity for **Toc-Gal** in HepG2 cells could be due to the presence of ASGPR receptors on the cell surface of HepG2 cells which might increase the endocytosis through receptor-mediated lipoplex internalization resulting in enhanced protein expression. Since SK-HEP-1 cells do not express ASGPR receptors on their cell surfaces leading to reduced transfection activities for lipoplexes of **Toc-Gal** when compared with HepG2 cells. This is supported by transfection data obtained in HepG2 & SK-HEP-1 cells for lipoplexes

of **Toc-OH** (which does not have ASGPR receptor targeting ligand) which showed comparable activity in both cell lines. Plasmid DNA expression results suggested that receptor-mediated endocytosis of **Toc-Gal** had better transfection efficiencies.

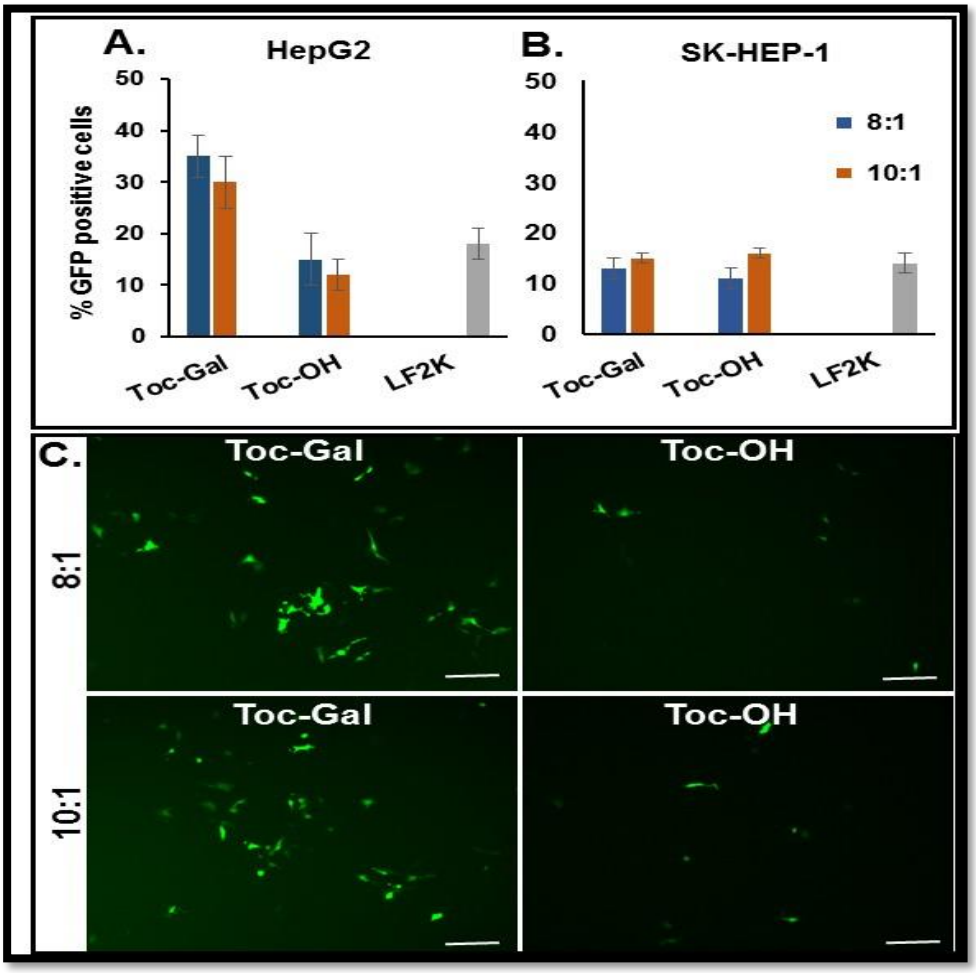

Figure 5. *In vitro* Transfection studies for Liver targeted lipid, Toc-Gal, and control lipid, Toc-OH in HepG2 (A) and SK Hep-1 (**B**) cells. % of GFP positives cells quantitated by FACS. Representative epifluorescence microscopic images of HepG2 cells transfected with lipoplexes of Toc-Gal & Toc-OH with eGFP encoded plasmid DNA at Lipid/DNA charge ratios 8:1 & 10:1 (**C**).

3.2.6 ASGPR receptor specificity of Toc-Gal

High-affinity ASGPR receptors are over-expressed in hepatocytes (liver cells).[21] D-Galactose is one of the well-known ligands for ASGPR receptors as such ligands play a key role in the targeted delivery of nucleic acids.[9a] **Toc-Gal** was designed for targeting ASGPR receptors

expressed in hepatocytes along with a negative control lipid, **Toc-OH** (without galactose head-group) to establish the receptor specificity of **Toc-Gal** in ASGPR +ve HepG2 cells. Towards determining the ASGPR receptor specificity of newly synthesized lipid **Toc-Gal** and its control lipid **Toc-OH**, we performed cellular uptake studies in ASGPR receptor-positive cells (HepG2) with concentration-dependent ligand saturation experiment. Asialofetuin, a naturally occurring ligand for the ASGPR receptors was used as saturating ligand at 0-100 µg and liposomes were labeled with rhodamine (Rh). The uptake efficiency for **Toc-Gal** without ligand saturation was found to be highest (35% Rh positive cells) and the activity significantly diminished dose-dependently in HepG2 cells pre-treated with Asialofetuin, a natural ligand for ASGPR receptors (Figure 6A). Upon receptor saturation with 25 µg asialofetuin, transfection activity reduced by 20% for **Toc-Gal** (showing 28% Rh positive cells, normalized value) and ~70% reduction with 100 µg asialofetuin (**Figure 6**). However, control lipid, **Toc-OH** in HepG2 cells did not show significant variation in the transfection activity in both normal (no receptor saturation) and asialofetuin pre-treated (receptor saturation) cells (**Figure 6**). This data was further supported with microscope images obtained using HepG2 with/without ligand pre-treatment for **Toc-Gal** and **Toc-OH** transfections. In microscopic images of **Toc-Gal** lipoplex treatment, the number of Rh positive cells were found to be remarkably less when cells were pre-incubated with asialofetuin than for untreated cells while a number of Rh positive cells didn't change with **Toc-OH** lipoplex treated cells (**Figure 6**). Together, these findings confirmed that cellular uptake of the **Toc-Gal** is likely to be mediated via ASGPR receptors present in the cell surface of HepG2 cells.

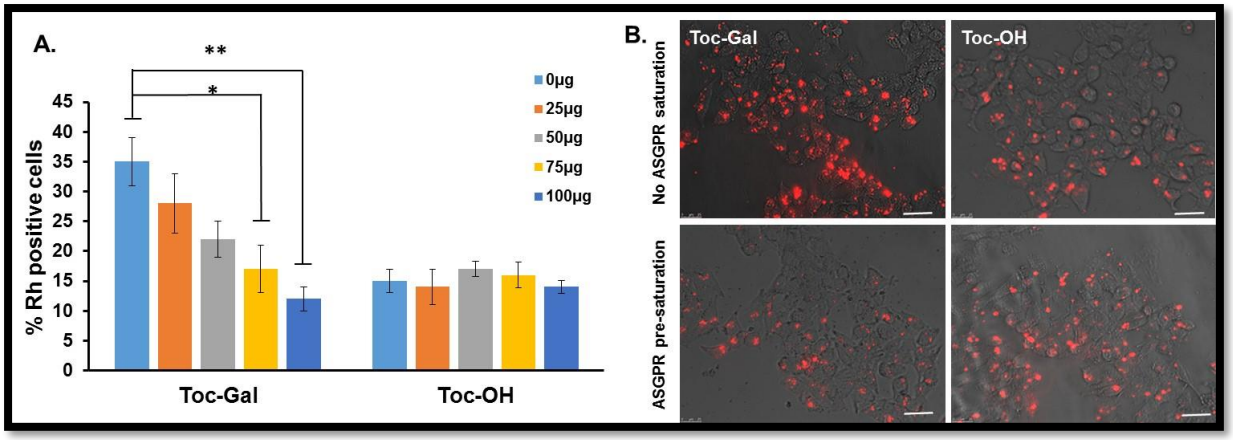

Figure 6. Transfection properties of **Toc-Gal** and control lipid, **Toc-OH** after ASGPR receptor saturation with asialofetuin at varying concentration in HepG2 cells (**A**). Representative epifluorescence microscopic images of HepG2 cells transfected with lipoplexes of Rhodamine labeled **Toc-Gal** & **Toc-OH** liposomes with and without ASGPR receptor saturation (**B**).

3. 2.7 Serum stability

In general, transfection activities of liposomes (prepared using different cationic lipids) are evaluated mostly in complete media i.e. media containing 10% (v/v) serum or in serum-free media.[16, 22]. It is believed that transfection activity of cationic lipids decreases drastically due to the interaction of negatively charged serum proteins with liposomes containing cationic charge ultimately hampering the efficient interaction with the cell surface and reduced internalization of lipoplexes.[23] Clinical success of *in vitro* transfection efficient cationic lipids also depends on the serum stability/serum compatibility. Hence, it is necessary to evaluate the compatibility of such transfection efficient lipids with varying serum concentrations. Towards evaluating the serum compatibility of **Toc-Gal** and **Toc-OH** lipids, we have performed transfection studies in representative HepG2 cells with increasing amounts of added serum (from 10-90%) at 8:1 lipid:DNA charge ratio. As shown in Figure 6, the transfection efficacies of **Toc-Gal** increased as the percentage of added serum increased (up to 50% added serum). For **Toc-Gal**, we observed ~30% enhancement in the gene transfer activity at 50% added serum (**Figure 6**). However, transfection activity of Toc-Gal was found to be decreasing at high concentrations of

added serum (60-90% added serum) (**Figure 7**). Contrastingly, the transfection activity of **Toc-OH** lipid showed poor serum compatibility with increasing amounts of added serum. Further, we observed that gene transfer efficacy of **Toc-OH** was drastically reduced with 40-90% of added serum (**Figure 7**). The enhanced serum compatible transfection activities of the **Toc-Gal** lipid, when compared with **Toc-OH** lipid, could be due to multiple hydroxyl functionalities of galactose moiety present in the polar head-group region which might be shielding the surface charge of the lipid:DNA complexes. Overall, such enhanced transfection efficacies of **Toc-Gal** lipid with increasing amounts of serum (up to 50% added serum) shows the serum stability of lipoplexes prepared using **Toc-Gal** liposomes and is likely to find use in transfecting cells under systemic settings.

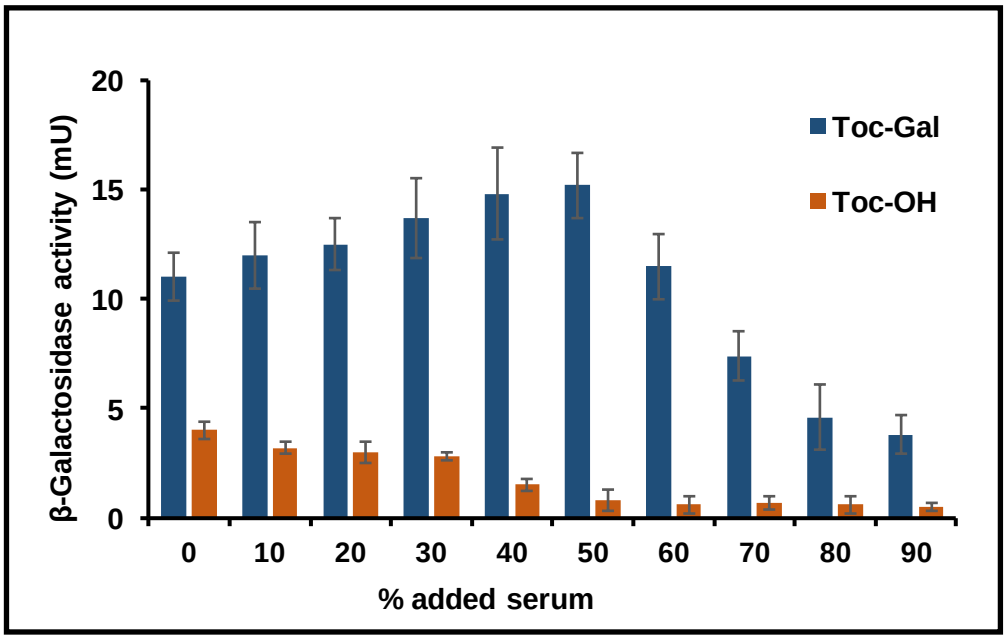

Figure 7. Transfection efficacies of **Toc-Gal** & **Toc-OH** in presence of increasing concentrations of added serum. *In vitro* transfection efficiencies of lipid:DNA complexes prepared using pCMV-β-gal-SPORT reporter gene at lipid:DNA charge ratio of 8:1 were evaluated in the presence of increasing concentrations of added serum in representative HepG2 cells.

3.3 Conclusions

In summary, we demonstrated that cationic galactosylated lipid-linked with triazole moiety to an anti-oxidant tocopherol hydrophobic tail efficiently delivered genes into hepatocellular carcinoma cells (HepG2) through ASGPR Receptors. The novel cationic lipids found to be safe in both liver cells, HepG2 and liver endothelial cells, SK-HEP-1. Presaturation of ASGPRs with a synthetic ligand asialofetuin retarded the cellular uptake of **Toc-Gal** lipoplexes, whereas, uptake of **Toc-OH** lipoplexes were unchanged. Further, **Toc-Gal** was found to be serum compatible with enhanced transfection activity (up to 50% added serum). These findings collectively suggested that **Toc-Gal** could be used for liver-specific gene delivery without damaging liver cells.

3.4. Materials and methods:

3. 4.1 General procedures and reagents

Mass spectral data were acquired by using a commercial LCQ ion trap mass spectrometer (ThermoFinnigan, SanJose, CA, USA) equipped with an ESI source or micromassQuatroLC-triple quadrupole mass spectrometer for ESI analysis. ^{1}H NMR spectra were recorded on AV 400 MHz NMR Spectrometer. Unless or else stated, all reagents were purchased from local commercial suppliers and were used without further purification. Column chromatography was carr out with silica gel (Acme Synthetic Chemicals, India, 60-120 mesh. Cell culture media, fetal bovine serum, 3-(4,5-Dimethylthiazol-2-yr)-2,5-diphenyltetrazolium bromide (MTT), HepG2 (Human hepatocarcinoma cell) cell line was procured from the National Centre for Cell Sciences (NCCS), Pune, India and SK-HEP-1 Cells from ATCC. Cells were grown at 37°C in Dulbecco's modified Eagle's medium (DMEM) with 10% FBS in a humidified atmosphere containing 5% CO_2, 95% air.

3.4.2 Synthesis

3.4.2.1. Synthesis of Liver targeted Lipid 1 (Toc-Gal), Scheme 1A

a. Synthesis of α-tocopherylglycidyl ether (1A)

A mixture of α-tocopherol (8.2 g, 20 mmol), epichlorohydrin (5.6 g, 60.5 mmol), NaOH sodium hydroxide pellets (2.4 g, 60 mmol), water (1 mL)) and tetrabutylammonium hydrogen sulfate (0.322 g, 1 mmol) was stirred for 24 h at 40 °C. The crude was filtered off and filtrate obtained was extracted with dichloromethane (DCM) (3 x 20 mL). The combined organic layers were dried over anhydrous magnesium sulfate. The solvent and excess epichlorohydrin was distilled off under vacuum and the obtained residue was purified by gel column chromatography (v/v 40: 1, Pet ether/Ethyl Acetate) to give Intermediate **1A** as oil (7.8 g, 82% yield).

^{1}H NMR (400 MHz, $CDCl_3$): δ/ppm = 0.85 (s, 12H), 1.05–1.61 (m, 24H), 1.80 (m, 2H), 2.08 (s, 3H), 2.14 (s, 3H), 2.18 (s, 3H), 2.57 (t, 6.7 Hz, 2H), 2.71 (m, 1H), 2.88 (t,4.6 Hz, 1H), 3.35 (m, 1H), 3.65 (m, 1H), 3.90 (m, 1H).

ESI-MS *m/z*: Calculated 486 (for $C_{32}H_{54}O_3$); found: 487 [M^+]

b. Synthesis of α-tocopherol 1, 2-azido alcohol (2A)

To a mixture of tocopherol epoxide (0.486 g, 1 mmol) and $CeCl_3.7H_2O$ (0.18609 g, 0.5 mmol) in acetonitrile & water mixture (9:1, 10 mL) was added NaN_3 (0.0715 g, 1.1 mmol) and refluxed for 12 h. The reaction progress was monitored by TLC. After completion of the reaction, the reaction mixture was diluted with water (20 mL) and extracted with ethyl acetate (3 x 20 mL). The combined organic layers were washed with saturated sodium chloride solution (brine), dried over anhydrous sodium sulfate and evaporated to dryness under reduced pressure. The crude product was purified by column chromatography with 60-120 mesh silica gel using hexane in

ethyl acetate as the eluent (10:90, v/v) to give Intermediate **2A** as a yellow liquid (0.4 g, 88 % yield).

^{1}H NMR (400 MHz, $CDCl_3$): δ/ppm = 0.83-0.87 (m, 12H), 1.12-1.37 (m, 26H), 2.08 (s, 3H), 2.12 (s, 3H), 2.17 (s, 3H), 2.58 (m, 2H), 2.3 (m, 2H), 3.8 (m, 1H), 4.2 (m, 2H).

ESI-MS *m/z*: Calculated 529.243 (for $C_{32}H_{55}O_3N_3$); found: 552 [M^++Na]

c. Synthesis of Liver targeted Lipid Intermediate (3A)

A mixture of $CuSO_4.5H_2O$ (15 mg, 0.06 mmol), sodium ascorbate (30 mg, 0.12 mmol), α-tocopherol-2-azido-alcohol (347 mg, 0.65 mmol) and β-D-galactose tetraacetate ***O***-propargylglycoside (1.1 mmol,) in THF/H_2O (7 mL, 1:1) were heated for 1 h under microwave irradiation (100 $^\circ$C). The product was precipitated by the addition of methanol (20 mL). The precipitated was washed with methanol and dried over reduced pressure. The mixture of crude product was purified by column chromatography $CHCl_3$/Methanol. The yield of product was 89 % as a yellow liquid.

^{1}H NMR (400 MHz, $CDCl_3$): δ/ppm = 0.83-0.87 (m, 12H), 1.12-1.37 (m, 26H), 2.08 (s, 3H), 2.12 (s, 3H), 2.17 (s, 15H), 2.58 (m, 2H), 3.24 (s,broad OH, 1H), 3.34 (s, broad 4H), 3.39 (m, 2H), 3.4 (m, 1s), 3.7 (m, 2H), 3.8 (m, 1H), 3.81 (m, 1H), 3.84 (d, 1H), 3.94 (d, 1H), 4.95 (d, 1H), 8.01 (s, 1H).

ESI-MS *m/z*: Calculated 915.546 (for $C_{49}H_{77}O_{13}N_3$); found: 916 [M^+].

d. Synthesis of Liver targeted Lipid (Toc-Gal) (4A)

In a 25 mL round bottom flask, 0.5 mL of sodium methoxide (0.5 N) (freshly prepared by dissolving 0.13 g of sodium in dry methanol) was added to a solution of intermediate 3A (30 mg, 0.035 mmol, prepared above in step h) in dry methanol (1 mL). The reaction mixture was stirred at room temperature for 1 h, neutralized with Amberlite IR120 (H^+), filtered and the filtrate was dried over anhydrous sodium sulfate and concentrated on a rotary evaporator.

Column chromatographic purification of the residue (using 60–120 mesh size silicagel and 9–10% methanol in chloroform as eluent) followed by the compound was quaternized with anhydrous HCl. The yield of product was 92% as a yellow liquid.

^{1}H NMR (400 MHz, $CDCl_3$): δ/ppm = 0.83-0.87 (m, 12H), 1.12-1.37 (m, 26H), 2.08 (s, 3H), 2.12 (s, 3H), 2.17 (s, 3H), 2.58 (m, 2H), 3.24 (s,broad OH, 1H), 3.34 (s, broad 4H), 3.39 (m, 2H), 3.4 (m, 1s), 3.7 (m, 2H), 3.8 (m, 1H), 3.81 (m, 1H), 3.84 (d, 1H), 3.94 (d, 1H), 4.95 (d, 1H), 8.01 (s, 1H).

^{13}C NMR (400 MHz, $CDCl_3$): δ/ppm = 155.67, 148.00, 147.86, 131.14, 128.91, 127.73, 127.68, 125.78, 125.71, 122.98, 117.61, 74.84, 73.75, 73.69, 69.75, 59.19, 52.68, 50.61, 44.66, 40.07, 39.40, 37.59, 37.49, 37.43, 37.32, 32.81, 32.71, 31.28, 28.01, 24.85, 24.47, 23.90, 22.77, 22.68, 21.06, 20.67, 19.79, 19.72, 12.76, 12.66, 11.89, 11.81.

ESI-MS *m/z*: Calculated 748.51 (for $C_{41}H_{70}O_9N_3$); found: 748.5110 [M^+]

3.4.2.2 Synthesis of Control Lipid 2 (Toc-OH), Scheme 1B

A mixture of Intermediate **2A** (0.347 g, 0.6 mmol) (Scheme **1A**), $CuSO_4.5H_2O$ (0.015 g, 94 mmol), Sodium ascorbate (0.030 g, 0.15 mmol), propargyl alcohol (0.0109 g, 0.7 mmol) in THF/H_2O (7mL, 1:1) were heated for 1 h under microwave irradiation (100 °C). The product was precipitated by the addition of methanol (20 mL). The precipitated product was collected, washed with methanol and dried under reduced pressure. The crude product was subjected to column chromatography purification with the $CHCl_3$/MeOH solvent system to obtain pure Intermediate **1B** (78%) as a yellow compound and followed by quaternization with anhydrous HCl afforded the title compound Lipid 2. The yield of product was 92% as a yellow liquid. (0.092 g yield).

^{1}H NMR (400 MHz, $CDCl_3$): δ/ppm = 0.83-0.87 (m, 12H), 1.12-1.37 (m, 26H), 2.08 (s, 3H), 2.12 (s, 3H), 2.17 (s, 3H), 2.58 (m, 2H), 3.42 (s, OH broad), 3.64 (s, OH broad), 3.7 (m, 2H), 3.82 (m, 1H), 4.21 (m, 2H), 4.3 (s, 2H), 7.7 (s, 1H).

ESI-MS *m/z*: Calculated 586.47 (for $C_{35}H_{60}O_4N_3$); found: 586.47110 [M^+]

3.4.3 Preparation of liposomes and formulations

1mM **Toc-gal** and **Toc-OH** with DOPE were dissolved in 100 µL of chloroform in a glass vial. The solvent was removed with help of a thin flow of moisture-free nitrogen gas and the glass vial was kept for drying under high vacuum for 3 hr. After that 1 mL of sterile deionized water was added to dried lipid films and the mixtures were kept to stay overnight. The vials were then vortexed for 2-3 minutes at room temperature to produce unstill multilamellar vesicles (MLVs) formed. After formation of the MLVs were sonicated initially in a water bath followed by probe sonication with help of a Branson 450 sonifier at 100% duty cycle and 25 W output power to produce small unilamellar vesicles (SUVs). The eGFP plasmid was amplified in DH5α-strain of *Escherichia coli*, the purity of plasmid was checked by A_{260}/A_{280} ratio (around 1.9).

3.4.4 Zeta potential (ξ) and size measurements

The sizes and the surface charges (zeta potentials) of liposomes and lipoplexes with varying charge ratios (8:1 to 1:1) were measured by photon correlation spectroscopy and electrophoretic mobility on a Zetasizer 3000HSA (Malvern, U.K.). The sizes were measured in serum-free DMEM media with a sample refractive index of 1.59 and a viscosity of 0.89. The system was calibrated by using the 2005 nm polystyrene polymer (Duke Scientific Corps., Palo Alto, CA, U.S.). The sizes of liposomes and lipoplexes were calculated by using the automatic method. The ζ (zeta potential) was also measured using the following parameters: viscosity, 0.89 cP; dielectric constant, 80; temperature, 25°C; F (Ka), 1.50 (Smoluchowski); the maximum voltage of the current, 80 V. The system was calibrated by using the DTS0050 standard from Malvern.

Measurements were done 10 times with the zero-field correction. All the liposomes and lipoplexes of the size measurements were done 10 times in triplicate with the zero field correction and values represented as the average of triplicate measurements. The potentials were measured 10 times and represented as their average values as calculated by using the Smoluchowski approximation.

3.4.5 DNA-binding assay

The DNA binding ability of **Toc-Gal** and **Toc-OH** liposomal formulations at varying lipid:DNA charge ratios were evaluated by agarose gel retardation assay.[22b, 24] 1% agarose gel (pre-stained with ethidium bromide) was used for the assay. Briefly, lipoplexes were prepared using pCMV-β-gal (0.30 μg) with the varying amount of liposomes in a total volume of 20 μL in Hepes buffer, pH 7.40 and incubated at room temperature for 20-25 minutes. 4 μL of 6X loading buffer (0.25% Bromophenol blue in 40% (w/v) sucrose in H_2O) was added to each of the samples and resulting solution (24 μL) was loaded on to each well of agarose gel. The samples were electrophoresed at 80 V for 45 minutes and the DNA bands were visualized in the Gel documentation unit.

3.4.6 Heparin Displacement Assay

Heparin was used to study the anionic displacement of DNA within the lipoplexes. The lipid:DNA complexes were prepared as described in the above section (DNA binding assay) and incubated for 20 minutes. Following incubation, 0.1 μg of the sodium salt of heparin was added and further incubated for another 30 minutes. The samples were electrophoresed on an agarose gel (1.5%) for Heparin displacement analysis and DNA bands were visualized as mentioned in the above section.

3.4.7 Circular Dichroism

Circular dichroism (CD) spectra of plasmid DNA and pDNA-liposome complexes were obtained using the Aviv 62A spectrometer (Lakewood, NJ). Samples were scanned through a wavelength

range of 200-500 nm at 25 °C using a 0.5 mL quartz cuvette, with a path length of 1 cm. Each sample was scanned four times with an integration time of 5 s, and the values were averaged. Scanning was done at 1 nm steps, and the slit width was 1 nm. Liposome-pDNA complexes were prepared at 10:1 +/-charge ratio at 50 µg/mL pDNA concentration. Sample values were subtracted from those obtained for milliQ water (for pDNA).

3.4.8 Toxicity Assay

Cytotoxicities of Toc-Gal and Toc-OH liposomal formulations at varying lipid:DNA charge ratios were evaluated using conventional - (4, 5-dimethylthiazol-2-yl)-2,5-diphenyltetrazolium bromide (MTT) based colorimetric cell viability assay as reported previously [9a]. The assay was performed in 2 different cell lines (HepG2 and SK-HEP-1 cells) in similar conditions as maintained for transfection experiments. After 48 h of lipoplex incubation, MTT was added directly to the 96-well plates and further incubated for 3-4 h. Next, media was removed without disturbing the formazan crystals following the addition of DMSO. Well-plates were kept for 15-20 gentle shaking and absorbance values were recorded using microplate reader. Results were expressed as percent viability = [A_{540}(treated cells)-background/A_{540}(untreated cells)-background] x100.

3.4.9 Transfection Biology

A general of the transfection procedure was followed as described below. Eukaryotic cells were cultured at a density of 15000 cells per well in a ninety-six-well plate 18-24 h the day before the transfection. The supercoiled plasmid DNA (0.3 µg) was complexed with varying amounts of desired lipids (0.15 -7.2 nmol) in serum-free DMEM medium (maximum volume should be to 100 µL) for 20 minutes. The charge ratios of cationic liposomes were varied from 0.5:1 to 8:1 (+/-). The liposome -eGFP plasmid complexes were then treated to the cells. After 3 h of the incubation period, 100 µL of Dulbecco's Modified Eagle Medium DMEM with 10% FBS was added to the cells. The serum medium was altered to 10% complete medium after 24 h and the

reporter gene activity was estimated after 48 h. The cells were washed two times with PBS (100 µL each) and lysed in 50 µLlysis buffer [0.25 M Tris-HCl pH 8.0, 0.5% NP40]. The Care was taken to ensure complete lysis. The β-galactosidase activity in wells we estimated by addition 50 µL of 2 X-substrate solutions [1.33 mg/mL of ONPG, 0.2 M sodium phosphate (pH 7.3) and 2 mM magnesium chloride] to the lysate in a 96-well plate. The Adsorption at 405 nm was converted to β-galactosidase units using a calibration curve constructed with the commercial β-galactosidase enzyme. The values of β-galactosidase units in three experiments carried out on the same day varied by less than 20%. The transfection experiment was performed in duplicate and the reported transfection efficiency values are the average of triplicate experiments carried out on the same day. Each transfection experiment was repeated three epoch and the day to day changes in average transfection efficiency was found to be within 2-fold. The transfection was obtained on different days were similar.

3.4.10 Cellular uptake study

For Cellular uptake experiments, 1,00,000 HepG2 cells were seeded in 24-well plate (Corning Inc., Corning, NY) in 500 µL of DMEM medium with 10% FBS 12-18 h before the uptake experiment. Care was taken to maintain 60-70% confluent at the time of uptake. For preparing Rhodamine-PE labelled liposomes, 0.5 mM liposomes (**Toc-Gal** &**Toc-OH**) were prepared as described in the above section of 'Preparation of Liposomes' with additional step of adding 0.005 mM Rhodamine-PE (i.e., 1% w.r.t the total formulation content, Avanti-Polar Lipids, USA) to the liposomal solution before evaporating the chloroform. Glass vials containing labelled liposomes were wrapped with aluminium foils to avoid exposure. Rhodamine-PE labeled liposomes of **Toc-Gal** & **Toc-OH** were complexed with pCMV-SPORT-β-gal (0.3 µg/well) at lipid/DNA charge ratio of 8:1 (total volume of 100 µL DMEM) for 15-20 min. 30 mins before the transfection, cells were pretreated with asialofetuin in varying concentrations from 0µM to 100 µM. The lipoplexes were then added to the cells and incubated for 3-4 h. After 4 h

incubation, cells were washed with PBS (2X100 µL) and fixed with 3.8% paraformaldehyde in PBS at room temperature for 10 min. The red fluorescent cells were detected under an inverted fluorescence microscope (Nikon, Japan). FACS analysis, same transfection procedure is followed except, after 4 h, media was removed; cells were washed with PBS (2 X 200 mL) and trypsinized with 0.1% Trypsin/EDTA solution. 500 mL completemedium was added to the trypsinized cell suspension, centrifuged for 3 min at2000 rpm and the complete medium was removed. PBS (500 mL) was added to thecells and the cell suspension was once more centrifuged for 3 min at 2000 rpm. The supernatant was removed and the cell pellets were resuspended in 100 µL in PBS for FACS analysis.

3.4.11 Serum compatibility study

Serum compatibility studies were carried in representative HepG2 cells at 8:1 lipid:DNA charge ratio. Briefly, cells were seeded at a density of 15,000 cells per well in a 96-well plate 18-24 h the day before the transfection. Plasmid DNA (0.3 µg) was complexed with 7.2 nmol of individual liposomes (at 8:1 lipid:DNA charge ratio) in serum-free DMEM medium (volume of the lipoplex was maintained within 10 µL) for 20 minutes. Lipoplexes prepared in serum-free media were made up to 100 µL by addition of necessary volumes of serum-free DMEM and FBS (increasing amounts of added serum, 10-90%) so that the final serum concentrations ranged from 10-90% (for example, to make-up 10% added serum with 100 µL total volume, 10 µL of FBS and 80 µL of DMEM were added to 10 µL of lipoplex solution prepared in serum-free DMEM). The lipid:DNA complexes with varying amounts of serum (10-90%) was added to the cells and incubated. After 3-4 h of incubation, DMEM was removed, DMEM with 10% FBS i.e. complete medium was added to the cells. The reporter gene activity was estimated between 36 and 48 h following the same protocol as described in Transfection Biology section of Materials and methods.

3.4. 12 Cellular α5GFP Expression Study

For cellular α5GFP expression experiments in HeG2 and SKHep-1 50, 000 cells were cultured in well of 24-well plate 18-24 h before the transfection. Then 0.9 μg of α5GFP plasmid DNA encoding green fluorescent protein was complexed with liposomes of lipids **Toc-Gal** and **Toc-OH** at charge ratio (lipid-DNA complexes) 10:1& 8:1 in plain DMEM medium (total volume made up to 100 μL) for 30 min. Just prior to transfection, cells plated in the 24-well plate were washed with PBS (2×100 μL) followed by addition of lipoplexes. The media 400 μL was added after 4 h incubation of the cells. After 48 h, the complete medium was removed from each well, and the total cells were washed with PBS (2× 200 μL). Finally, 200 μL of PBS was added to each per good cells and visualized under the inverted fluorescent microscope to observe the cells expressing the green fluorescent protein.

3.5 References

1. Srinivas, R.; Samanta, S.; Chaudhuri, A., Cationic amphiphiles: promising carriers of genetic materials in gene therapy. *Chemical Society reviews* **2009,***38* (12), 3326-38.
2. var, C.; Meka, R. C.; Samanta, S.; Marepally, S.; Chaudhuri, A., Enhanced Spacer Length between Mannose Mimicking Shikimoyl and Quinoyl Headgroups and Hydrophobic Region of Cationic Amphiphile Increases Efficiency of Dendritic Cell-Based DNA Vaccination: A Structure-Activity Investigation. *Journal of medicinal chemistry* **2017,***60* (4), 1605-1610.
3. (a) Nayerossadat, N.; Maedeh, T.; Ali, P. A., Viral and nonviral delivery systems for gene delivery. *Advanced biomedical research* **2012,***1*, 27; (b) Hardee, C. L.; Arevalo-Soliz, L. M.; Hornstein, B. D.; Zechiedrich, L., Advances in Non-Viral DNA Vectors for Gene Therapy. *Genes* **2017,***8* (2).
4. Marepally, S.; Boakye, C. H.; Shah, P. P.; Etukala, J. R.; Vemuri, A.; Singh, M., Design, synthesis of novel lipids as chemical permeation enhancers and development of nanoparticle system for transdermal drug delivery. *PloS one* **2013,***8* (12), e82581.
5. (a) Martin, B.; Sainlos, M.; Aissaoui, A.; Oudrhiri, N.; Hauchecorne, M.; Vigneron, J. P.; Lehn, J. M.; Lehn, P., The design of cationic lipids for gene delivery. *Current pharmaceutical design* **2005,***11* (3), 375-94; (b) Bhattacharya, S.; Bajaj, A., Advances in gene delivery through molecular design of cationic lipids. *Chem. Commun. (Camb.)* **2009,** (31), 4632-56.
6. (a) Schatzlein, A. G., Targeting of Synthetic Gene Delivery Systems. *J. Biomed. Biotechnol.* **2003,***2003* (2), 149-158; (b) Zylberberg, C.; Gaskill, K.; Pasley, S.; Matosevic, S., Engineering liposomal nanoparticles for targeted gene therapy. *Gene Ther.* **2017**.
7. (a) Murphy, S. L.; High, K. A., Gene therapy for haemophilia. *British journal of haematology* **2008,***140* (5), 479-87; (b) Azuma, H.; Paulk, N.; Ranade, A.; Dorrell, C.; Al-

Dhalimy, M.; Ellis, E.; Strom, S.; Kay, M. A.; Finegold, M.; Grompe, M., Robust expansion of human hepatocytes in Fah-/-/Rag2-/-/Il2rg-/- mice. *Nature biotechnology* **2007,***25* (8), 903-10.

8. Yin, H.; Song, C. Q.; Dorkin, J. R.; Zhu, L. J.; Li, Y.; Wu, Q.; Park, A.; Yang, J.; Suresh, S.; Bizhanova, A.; Gupta, A.; Bolukbasi, M. F.; Walsh, S.; Bogorad, R. L.; Gao, G.; Weng, Z.; Dong, Y.; Koteliansky, V.; Wolfe, S. A.; Langer, R.; Xue, W.; Anderson, D. G., Therapeutic genome editing by combined viral and non-viral delivery of CRISPR system components in vivo. *Nature biotechnology* **2016,***34* (3), 328-33.
9. (a) Mukthavaram, R.; Marepally, S.; Venkata, M. Y.; Vegi, G. N.; Sistla, R.; Chaudhuri, A., Cationic glycolipids with cyclic and open galactose head groups for the selective targeting of genes to mouse liver. *Biomaterials* **2009,***30* (12), 2369-84; (b) Mahidhar, Y. V.; Rajesh, M.; Chaudhuri, A., Spacer-arm modulated gene delivery efficacy of novel cationic glycolipids: design, synthesis, and in vitro transfection biology. *Journal of medicinal chemistry* **2004,***47* (16), 3938-48.
10. Wiseman, H., Vitamin D is a membrane antioxidant. Ability to inhibit iron-dependent lipid peroxidation in liposomes compared to cholesterol, ergosterol and tamoxifen and relevance to anticancer action. *FEBS letters* **1993,***326* (1-3), 285-8.
11. (a) Gaspar, V. M.; Moreira, A. F.; Costa, E. C.; Queiroz, J. A.; Sousa, F.; Pichon, C.; Correia, I. J., Gas-generating TPGS-PLGA microspheres loaded with nanoparticles (NIMPS) for co-delivery of minicircle DNA and anti-tumoral drugs. *Colloids and surfaces. B, Biointerfaces* **2015,***134*, 287-94; (b) Zhao, J.; Feng, S. S., Effects of PEG tethering chain length of vitamin E TPGS with a Herceptin-functionalized nanoparticle formulation for targeted delivery of anticancer drugs. *Biomaterials* **2014,***35* (10), 3340-7.
12. (a) Kedika, B.; Patri, S. V., Design, synthesis, and in vitro transfection biology of novel tocopherol based monocationic lipids: a structure-activity investigation. *Journal of medicinal chemistry* **2011,***54* (2), 548-61; (b) Kedika, B.; Patri, S. V., Influence of minor

backbone structural variations in modulating the in vitro gene transfer efficacies of alpha-tocopherol based cationic transfection lipids. *Bioconjugate chemistry* **2011,***22* (12), 2581-92.

13. Kedika, B.; Patri, S. V., Synthesis and gene transfer activities of novel serum compatible reducible tocopherol-based cationic lipids. *Mol. Pharm.* **2012,***9* (5), 1146-62.
14. Midoux, P.; Pichon, C.; Yaouanc, J. J.; Jaffres, P. A., Chemical vectors for gene delivery: a current review on polymers, peptides and lipids containing histidine or imidazole as nucleic acids carriers. *British journal of pharmacology* **2009,***157* (2), 166-78.
15. (a) Midoux, P.; LeCam, E.; Coulaud, D.; Delain, E.; Pichon, C., Histidine containing peptides and polypeptides as nucleic acid vectors. *Somatic cell and molecular genetics* **2002,***27* (1-6), 27-47; (b) Singh, R. S.; Goncalves, C.; Sandrin, P.; Pichon, C.; Midoux, P.; Chaudhuri, A., On the gene delivery efficacies of pH-sensitive cationic lipids via endosomal protonation: a chemical biology investigation. *Chemistry & biology* **2004,***11* (5), 713-23.
16. Kumar, V. V.; Pichon, C.; Refregiers, M.; Guerin, B.; Midoux, P.; Chaudhuri, A., Single histidine residue in head-group region is sufficient to impart remarkable gene transfection properties to cationic lipids: evidence for histidine-mediated membrane fusion at acidic pH. *Gene therapy* **2003,***10* (15), 1206-15.
17. Gosangi, M.; Rapaka, H.; Ravula, V.; Patri, S. V., Evolution of New "Bolaliposomes" using Novel alpha-Tocopheryl Succinate Based Cationic Lipid and 1,12-Disubstituted Dodecane-Based Bolaamphiphile for Efficient Gene Delivery. *Bioconjugate chemistry* **2017,***28* (7), 1965-1977.
18. Narang, A. S.; Thoma, L.; Miller, D. D.; Mahato, R. I., Cationic lipids with increased DNA binding affinity for nonviral gene transfer in dividing and nondividing cells. *Bioconjugate chemistry* **2005,***16* (1), 156-68.

19. Carvlin, M. J.; Datta-Gupta, N.; Fiel, R. J., Circular dichroism spectroscopy of a cationic porphyrin bound to DNA. *Biochemical and biophysical research communications* **1982,***108* (1), 66-73.

20. Sipski, M. L.; Wagner, T. E., Probing DNA quaternary ordering with circular dichroism spectroscopy: studies of equine sperm chromosomal fibers. *Biopolymers* **1977,***16* (3), 573-82.

21. D'Souza, A. A.; Devarajan, P. V., Asialoglycoprotein receptor mediated hepatocyte targeting - strategies and applications. *Journal of controlled release : official journal of the Controlled Release Society* **2015,***203*, 126-39.

22. (a) Banerjee, R.; Das, P. K.; Srilakshmi, G. V.; Chaudhuri, A.; Rao, N. M., Novel series of non-glycerol-based cationic transfection lipids for use in liposomal gene delivery. *Journal of medicinal chemistry* **1999,***42* (21), 4292-9; (b) Chandrashekhar, V.; Srujan, M.; Prabhakar, R.; Reddy, R. C.; Sreedhar, B.; Rentam, K. K.; Kanjilal, S.; Chaudhuri, A., Cationic amphiphiles with fatty acyl chain asymmetry of coconut oil deliver genes selectively to mouse lung. *Bioconjugate chemistry* **2011,***22* (3), 497-509; (c) Prata, C. A.; Zhao, Y.; Barthelemy, P.; Li, Y.; Luo, D.; McIntosh, T. J.; Lee, S. J.; Grinstaff, M. W., Charge-reversal amphiphiles for gene delivery. *J. Am. Chem. Soc.* **2004,***126* (39), 12196-7.

23. (a) Li, S.; Tseng, W. C.; Stolz, D. B.; Wu, S. P.; Watkins, S. C.; Huang, L., Dynamic changes in the characteristics of cationic lipidic vectors after exposure to mouse serum: implications for intravenous lipofection. *Gene Ther.* **1999,***6* (4), 585-94; (b) Zelphati, O.; Uyechi, L. S.; Barron, L. G.; Szoka, F. C., Jr., Effect of serum components on the physico-chemical properties of cationic lipid/oligonucleotide complexes and on their interactions with cells. *Biochim. Biophys. Acta* **1998,***1390* (2), 119-33.

24. Srujan, M.; Chandrashekhar, V.; Reddy, R. C.; Prabhakar, R.; Sreedhar, B.; Chaudhuri, A., The influence of the structural orientation of amide linkers on the serum compatibility and lung transfection properties of cationic amphiphiles. *Biomaterials* **2011,***32* (22), 5231-40.

CHAPTER 4

Azasugar head group based cationic lipids for gene delivery: design, synthesis and transfection studies

4.1 Introduction

Gene therapy appears to be a very promising technique in modern medicine that grasps a profound assurance for the treatment of a wide range of both genetic and sporadic diseases[1]. The treatments of genetic diseases have been carried out by using viral and non-viral gene delivery vectors[2]. The high transfection efficiency and long-term gene expression are less achieved by viral vectors vis-à-vis non-viral vectors because of the restricted DNA packaging capacity of viral vectors to transport larger genes into the cells[3]. But, non-viral vectors are gaining attention because of their relatively safe, less toxic nature, ability to transfer larger sized genes, and potential for up-scaling attributes[4]. Till date, different types of non-viral vectors like synthetic cationic polymers, polysaccharides, lipid nanoparticles, polypeptide nano-complexes, and inorganic nanoparticles etc., have been developed and their potential for intracellular delivery of drugs and nucleic acid has been verified. Moreover, the most of the non-viral vectors have manifested their effective intracellular gene delivery *in vitro* as well as *in vivo*[5]. However, the development of novel synthetic vectors needs to be more efficient and safe, to pave the way for the therapeutic applications and to translate gene therapy into a reality[6]. The cationic lipoplexes are formed due to the electrostatic interaction between the positively charged head group of cationic lipids and the negative charge of phosphates in nucleic acids[7]. The hydrophobic moiety of the lipids is involved in the condensation of the complexes into discrete particles by a spontaneous self-assembling process. In general, the lipoplexes are bound to negatively charged cell-surface proteoglycans and enter the cells primarily by endocytosis[8]. Most of the particles remain trapped in the endosome and undergo degradation upon fusion of endosome with lysosomes. Liposome/DNA complex that succeeds in endosomal escape gets separated in the cytosol and their released DNA can migrate towards the nucleus, under the threat of degradation by nucleases, for the nuclear import[9].

Some methods have been developed to make efficient and safe delivery of pDNA vectors into the cytosol. These include the introduction of a zwitterions group to the non-viral gene

delivery vectors, which can fail the reaction ability between the carrier and negatively charged serum components[10]. These approaches often demonstrated better biocompatibility and serum-stability. Most of the researchers have reported that a high number of -OH groups on the gene transfecting vectors might help reduce their cytotoxicity as well as the gene delivery efficiency and serum-tolerance ability. Towards the improvement of potency, bioavailability and serum compatibility of tocopherol based lipids, in the present study, azasugar (possessed 4 OH groups) and pyrrolidine (without OH groups) head groups have been coupled with tocopherol (**Toc-aza** and **Toc-pyr** (**Scheme 1& 2**) to form new head group based lipids. Furthermore, the structure-activityrelationship (SAR) of **Toc-Aza** and **Toc-pyr** lipids, relative pDNA interactions of the lipids, physicochemical properties like size &zeta potential and gene delivery efficiency are discussed in the present chapter. It is found that lipid **Toc-Aza** lipid may serve as an efficient on-viral gene delivery vector with the least cytotoxicity.

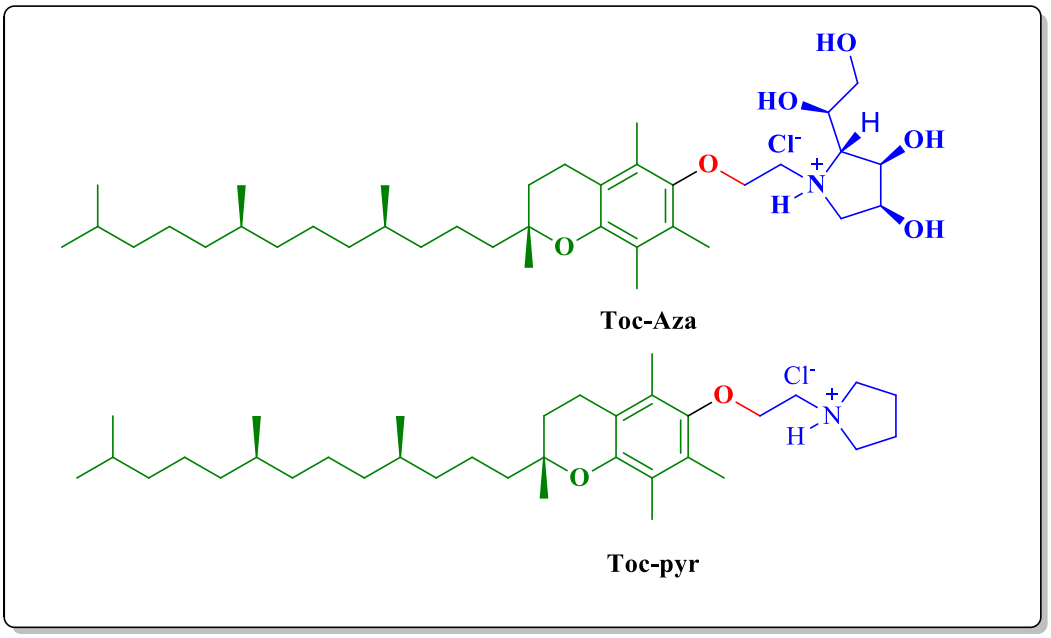

Chart 1 Chemical structure of cationic lipids

4.2 Results & Discussion

The current research work illustrates the synthesis of novel cationic lipids (i.e. **Toc-Aza** and **Toc-pyr**) and their physicochemical characteristics. The relative *in vitro* transfection efficiencies

of lipid **Toc-Aza** and control lipid **Toc-pyr** performed against three types of cell lines are reported. In addition, the epifluorescence microscopes experiments in support of the results obtained in *in-vitro* transfection examine are reported. The cytotoxicity and serum stability in three different types of cell lines for lipids **Toc-Aza** and **Toc-pyr** are also reported. The two cationic lipids were designed and synthesized in order to probe whether the favorable H-bonding interaction between cell membrane pDNA and hydroxy groups present in the azasugar-headgroup region of tocopherol based lipids could play a major role in stabilizing liposomes/nucleic acid complexes and enhancing transfection efficiency of the cationic lipids. The stability, transfection efficiencies and the cellular uptake of lipoplexes of lipids **Toc-Aza** and **Toc-pyr** are compared with each other.

4.2.1 Chemistry

The key structural elements general to both the cationic lipids **Toc-Aza** and **Toc-Pyr**(Chart 1) described herein include (i) tocopherol as anchoring group common for both the lipids (ii) the presence of azasugar the hydrophilic group in lipid **Toc-Aza**(iii) ether linker common to both **Toc-Aza** and **Toc-pyr** lipids, and (iv) the presence of d pyrrolidine ring without OH groups in the head region in lipids**Toc-pyr**. The synthetic procedures of novel transfection lipids shown in Chart 1are described in the Experimental Section. As outlined in Schemes 1-2, the chemistries involved in preparing these new cationic lipids are straightforward. The cationic lipids **Toc-Aza** and **Toc-pyr** were synthesized from two different syntheticintermediates, i.e. 2-aminoethyl-α-tocopheryl-ether for the synthesis of lipid **Toc-Aza**(**Scheme 1**) and 2-chloroethyl-α-tocopheryl-ether for the synthesis of lipid **Toc-pyr** (**Scheme 2**).The intermediate **ATE** (2-aminoethyl-α-tocopheryl-ether) was synthesised by conversion of mesylated tocopherol, to 2-aminoethyl-α-tocopheryl-ether using 2-aminoethanol in presence of base KOH.ATE was then treated with intermediate 2, 3, 4, 6-Di-*O*-isopropylidene-l, 5-άi-*O*-methanesulfonyl-D-mannitol (two-step synthesis), where the resulting intermediate 2, 3, 4, 6-Di-*O*-isopropylidene-l, α-tocopheryl-D-mannitol was formed, upon deprotection with trifluoroacetic acid (TFA), afforded lipid **Toc-Aza**

(Scheme 1). Whereas, **Toc-pyr** lipid was taken four steps for the final product and it was obtained from the alkylation of pyrrolidine with 2-chloroethyl-α-tocopheryl-ether, afforded lipid **Toc-Pry.** Initially, 2-chloroethyl-α-tocopheryl-ether was synthesized by chlorination of ethanol-α-tocopheryl-ether, which was obtained by the reduction of α- tocopherol acetic acid. The acetic acid derivative of tocopherol is synthesized as per scheme mentioned procedure. The chemical structures of all the synthetic intermediates and final cationic lipids shown in **Schemes 1-2** are confirmed by ^{1}H NMR and molecular ion peaks in their ESI mass spectra. The purity of final lipids is also characterized by HPLC analysis data, as described.

Scheme 1: Synthesis of Lipid **Toc-Aza**

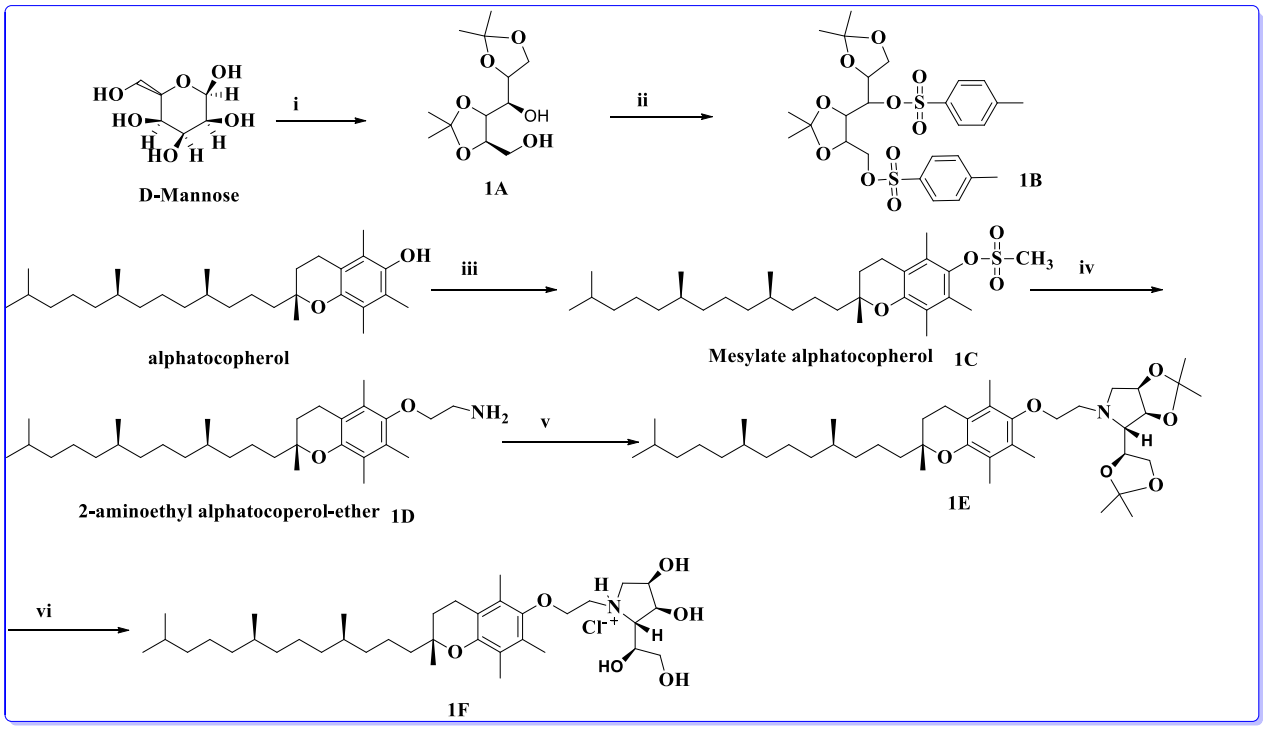

Reagents : i) Dry Acetone, *p*-toluene sulphonylchloride monohydrate, 2, 2- dimethoxy propane, Na_2CO_3, 12 h RT, dry Methanol, $NaBH_4$ and 12 h RT67%, ii) DCM, Tosyl chloride, DMAP, 12 h RT 85%, iii) dry DCM, pyridine, DMAP, methane sulphonylchloride, 12 h RT 85.1%, iv) ethanolamine, toluene, KOH, refluxed 63.15%, v) toluene, di-O-isopropylidene-l,5-άi-O-methanesulfonyl-D-mannitol, triethylamine, refluxed 12 h 58.15%, vi) 1:1 HCl/MeOH, refluxed 12 h 60.5%.

Scheme 2: Synthesis of Lipid **Toc-pyr**

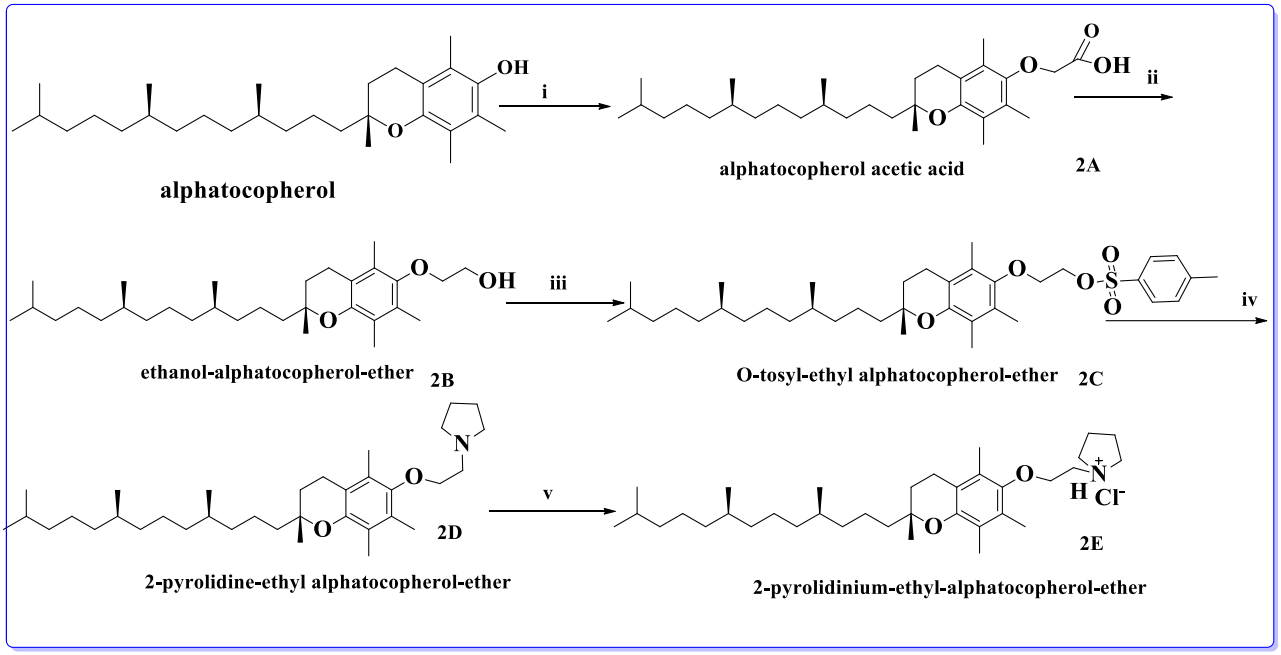

Reagents: i) Ethyl bromoacetate, DMF, KOH and 24 h RT 85%, ii) Dry THF, $LiALH_4$, 6 h RT 86%, iii) Dry DCM, tosylchloride, triethylamine, DMAP, 12 h RT 92% , iv) Pyrrolidine, MeOH, refluxed 12 h 72%, , v) 1:1 HCl/MeOH, 12 h RT 92% .

4.3 Toc-Aza and Toc-Pyr liposomes preparation

Cationic liposomes were prepared by the dry lipid hydration method as described earlier[11]. The cationic liposomes were formulated by varying molar ratios (0.5 and 1:1) of synthesized cationic lipids, **Toc-Aza & Toc-pyr** and a well-known co-lipid DOPE (1, 2-dioleoyl-sn-glycerol-3-phosphoethanolamine). Subsequently, liposomes were prepared under sterile conditions followed by sonication for five min at room temperature. The liposomes of both the lipids (**Toc-Aza** & **Toc-pyr**) are observed to form stable uniform liposomes at 1:1 molar ratio of lipid: DOPE with high efficacy of DNA binding. The suspensions were stable and no precipitation was observed even after 2 months when stored at 4 °C

4.4 Physico-chemical characterization of Toc-aza and Toc-Pyr liposomes and their Lipoplexes

The physicochemical features of the cationic liposome may change due to the complexation of the liposomes with nucleic acids. The Proper sizes and surface charge of DNA: liposome complexes are important factors for efficient gene delivery. Dynamic light scattering (DLS) was used to characterize the liposomes and lipid:DNA (+/-) complexes. pDNA is complexed with liposomes (**Toc-Aza/**DOPE and **Toc-pyr/**DOPE) varying charge ratios 1:1, 2:1, 4:1 & 8:1in presence of Dulbecco's Modified Eagle's medium (DMEM). **Figure 1** clearly indicates that hydrodynamic diameter of liposomes of **Toc-Aza** and **Toc-pyr** are found to be 145 nm 230 nm respectively, while liposome complexes with pDNA showed more than two-fold increase in the size at 1:1 charge ratio. On further increasing the charge ratio of lipid/pDNA complexes of lipids **Toc-Aza** and **Toc-pyr** from 1:1 to 8:1 reduction in size is observed that is from 380 nm to 130 nm and 545 nm to 150 nm respectively. The reduction in size with increase in charge ratio may be due to the improved condensation at higher lipid concentrations. The ζ potential of liposomes **Toc-Aza** and **Toc-Pyr** (+15 mV and + 21 mV respectively). As expected, ζ potential was increased by increasing the fraction of cationic lipids from 1:1 to 8:1 charge ratio. More interestingly, the lipoplexes of lipid **Toc-Aza**2: 1 charge ratio showed size in the range of 250 nm and ζ potential of +5 mV, which are believed to be suitable for the efficient gene transfections. Whereas, the lipoplexes of **Toc-pyr** showed the optimal diameter 296.3 nm and ζ potential of +13 mV at 4:1 charge ratio. The results suggesting that the efficient transfection requires the optimal size and zeta potentials of lipoplexes.

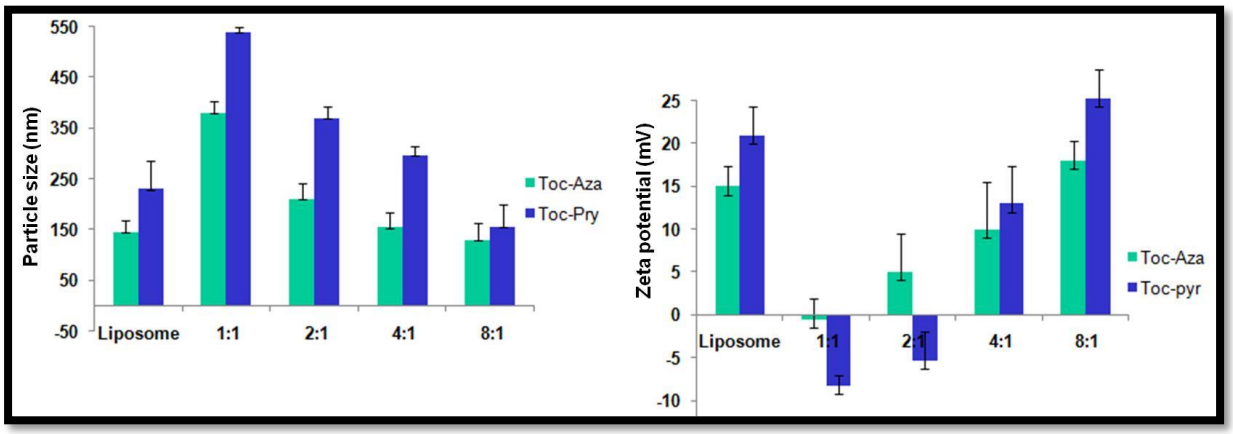

Figure 1. Mean particle sizes (A) and zeta-potentials (B) of lipid-DNA complexes at various N/P ratios (DLS at room temperature in DMEM). Data represent mean ± SD (n = 3).

4.4.1 Interaction of Toc-Aza and Toc-pry liposomes with pDNA and their characterization

To characterize the electrostatic interactions between the nucleic acid and the present lipids **Toc-Aza & Toc-pyr** as a function of lipid: DNA charge ratio, electrophoretic gel retardation assay, and heparin displacement assay are carried out using conventional gel electrophoresis. The liposomal formulations with DOPE and **Toc-Aza**/**Toc-pry** at 1: 1-mole ratio were used for pDNA binding studies. Results from this gel electrophoresis study revealed the excellent DNA binding interactions for lipid **Toc-Aza** across 8:1 - 1:1 lipid: DNA charge ratio (**Figure 2A**). However, lipid **Toc-pyr** exhibited good binding only at higher charge ratios i.e. 4:1 and 8:1. It also shows that while for the lipid **Toc-Aza** the finest pDNA binding at 2:1 charge ratio, whereas, for lipid **Toc-pyr,** at 4:1 charge ratio showed good binding and at 2:1 charge ratio showed poor DNA binding (**Figure 2A**). These differences in the binding efficiencies may lead to a difference in transfection efficiencies of the two lipids. Further, heparin displacement experiment was also carried out to confirm the DNA binding data obtained with the above liposomal formulations. Liposome complexed with **Toc-Aza** resisted displacement of pDNA with heparin across the lipid: DNA charge ratio 8:1 - 1:1 (**Figure 2B**). However, **Toc-pyr** formulation could not survive DNA displacement with heparin at 1:1 to 4:1 charge ratios. DNA from **Toc-pyr** lipoplexes gradually displaced as the lipid: DNA charge ratio decreased from 8:1-1:1 (**Figure 2B**). A gel retardation experiment showed that the lipid **Toc-Aza** was able to bind effectively pDNA than the lipid **Toc-pyr**. This result emphasizes that the structure of the azasugar -OHs function contributed to the interaction of the liposomes and nucleic acid. The stability of lipoplexes of lipid **Toc-Aza** may be attributed to the favorable hydrogen-bonding interactions between pDNA and the hydroxyl functionalities present in the polar head group region of lipid **Toc-Aza**

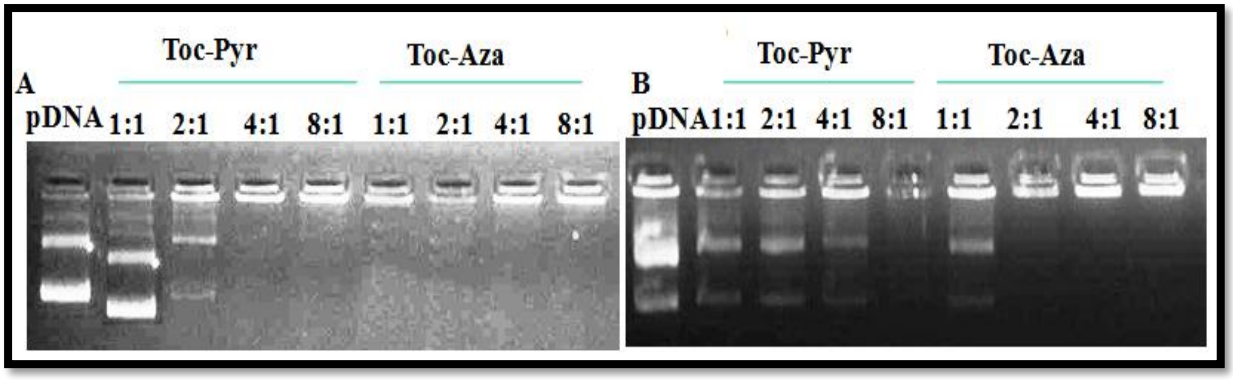

Figure 2. Electrophoretic gel patterns for **Toc-Aza** & **Toc-Pyr** lipoplexes-associated DNA in agarose gel retardation assay (**A**) and Heparin displacement assay (**B**). The lipid/DNA charge ratios are indicated at the top of each lane

4.5 Transfection biology of Toc-Aza and Toc-pyr lipoplexes

The transfection efficiencies of lipoplexes of lipids **Toc-Aza** and **Toc-pyr** were studied in three cultured mammalian cells (i.e., HepG2, HEK-293T and CHO) The three cultured mammalian cells (i.e., HepG2, HEK-293T and CHO) *p*-CMVSPORT- *β*-gal pDNA was taken as the reporter gene encoding the enzyme *β*-galactosidase to prepare lipoplexes of lipids **Toc-Aza** and **Toc-pyr** across the lipid/pDNA charge ratios of 1:1 to 8:1.Despite the presence of azasugar and pyrrolidine head groups being the only structural differences between the lipids **Toc-Aza** and **Toc-pyr**, liposomes of lipid**s Toc-Aza** could deliver reporter gene into all the three cell lines studied efficiently particularly at charge ratio 2:1(**Figure 3A−C**). **Toc-Aza** lipoplex showed its maximum transfection efficacies at lipid/pDNA (+/-) charge ratio of 2:1 in CHO, HEK-293T & HepG2cells (Figure 3, A−C, respectively). Whereas, **Toc-pyr** lipoplex was showed their maximum transfection activity at 4:1 charge ratio in aforementioned three cell lines (**Figure 3**).The figure 3 clearly indicating that lipoplexes of **Toc-Aza** promoted transfection revealed the maximum % of protein expression at 2:1 charge ratio; this may be due to the fact that the least particle size (195 nm) and optimal binding of lipoplex, and minimum cytotoxicity. Moreover, **Toc-Aza** lipoplexes were found to be 2times better in transfecting HepG2, equal activity in CHO and nearly 1.8 times in transfecting HEK-293T cells compared to commercially available

lipofection 2000. The lowest transfection efficiency (TE) of **Toc-pyr** may be due to the absence of hydroxyl groups hence, the less binding interactions between pDNA: lipid and which lead to the larger size of lipoplexes. The superior transfection efficiencies of **Toc-Aza**/DOPE liposomes compared with **Toc-pyr**/DOPE liposomes and lipofectamine 2000, indicating that the azasugar-based vectors have great potential as efficient non-viral gene delivery vectors. Thus, the relative transfection profiles of **Toc-Aza** and **Toc-pyr** lipoplexes outline in parts A−C of **Figure 3**indicating that the azasugar head group-*α*-tocopherol hybrid transfecting lipoplexes is a vital parameter able of greatly influencing the gene transfer efficacies of *α*-tocopherol based cationic lipids. After the observed transfection results, it can be concluded that only a sugar molecule other than cationic polymer issue to have maximum specific interaction with pDNA hence,sugarmodification lipid is a useful strategy for efficient gene delivery.

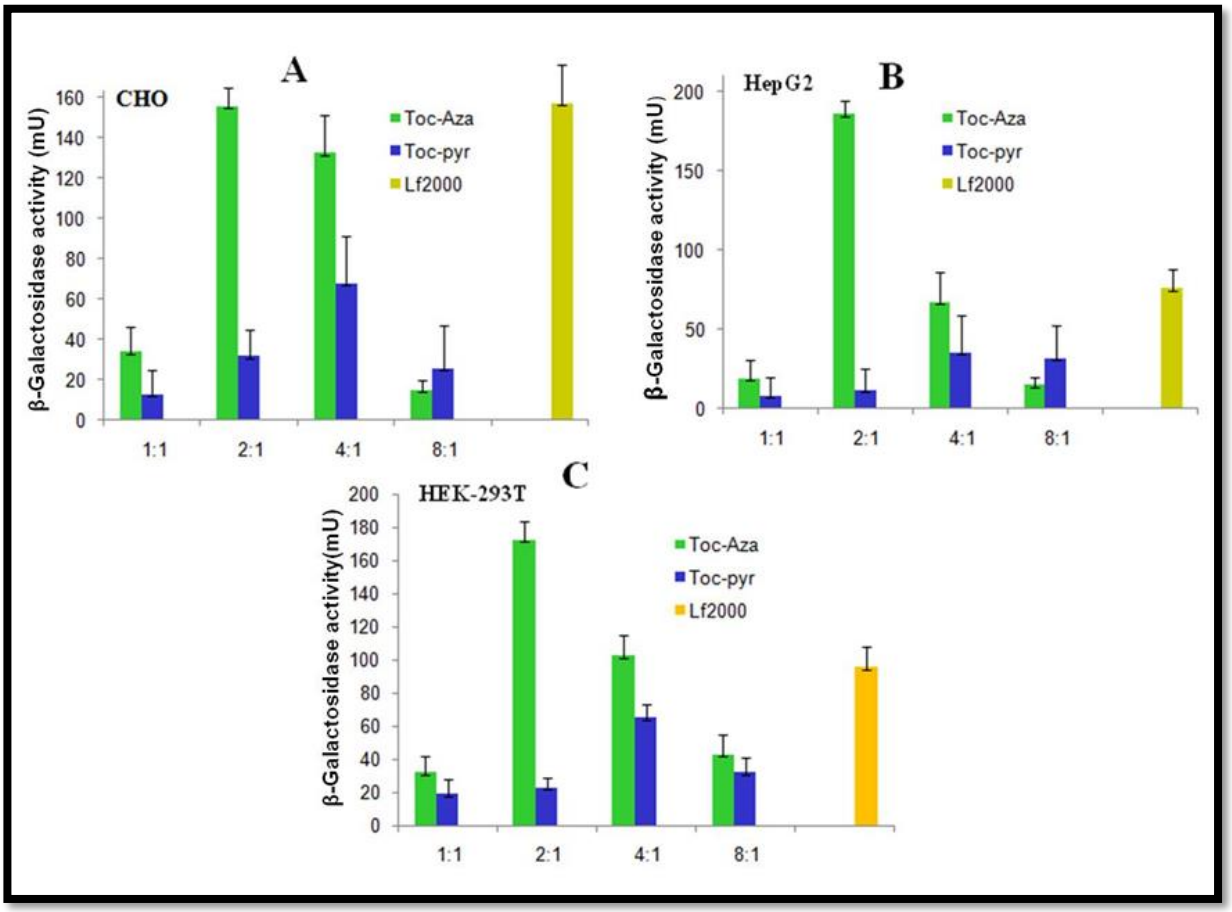

Figure 3. (A-C) Transfection efficiencies of lipids **Toc-Aza and Toc-pyr** in (A) HepG2 cells, (B) HEK-293 cells, and (C) CHO cells with DOPE as co-lipid (each lipid formulated with co-lipid in 1:1 molar ratio respectively). All the lipids were tested on the same day, and the data presented are the average of three experiments performed on three different days. The error bar represents the standard error. The difference in the data obtained is statistically significant in all charge ratios.

4.5. 1 Cellular expression of eGFP with Toc-Aza and Toc-pyr lipids

To get further support the β-gal reporter gene expressionresults, qualitative and quantitative eGFP assays were carried out at eGFP/cationic liposome complex (2:1& 4:1) charge ratios in HEK-293T cells. It is necessary to probe at this point that, whether the pDNA expression (eGFP) attains its utmost value at this given charge ratio (2:1) or not. The cellular expression of green fluorescence protein (eGFP) in HEK-293T was monitored by using epifluorescence microscope. The % of the expression of green fluorescence protein (eGFP) in HEK-293T is found to be more for lipid **Toc-Aza**, and moderate for **Toc-pyr** at 2:1 charge ratios (**Figure 4**). The expression of eGFP with cationic lipid **Toc-Aza** is found to be on par with that of lipofectamine 2000 at 2:1 charge ratio. The transfection activity of **Toc-Aza** lipoplex was found to be more compared to **Toc-pyr** lipoplex at 2:1 charge ratios (**Figure 4**).The obtained quantitative results (**Figure 4**) summarizes that **Toc-Aza** lipoplexes were showed ~120% of GFP positive cells at 2:1 charge ratio, whereas, it showed ~65% of eGFP positive cells at 4:1charge ratio. It is also confirmed by the quantitative analysis of GFP expression that the percentage of GFP positive cells for lipoplexes of **Toc-Aza** at 2:1 charge ratio is on par with that of lipofectamine 2000.

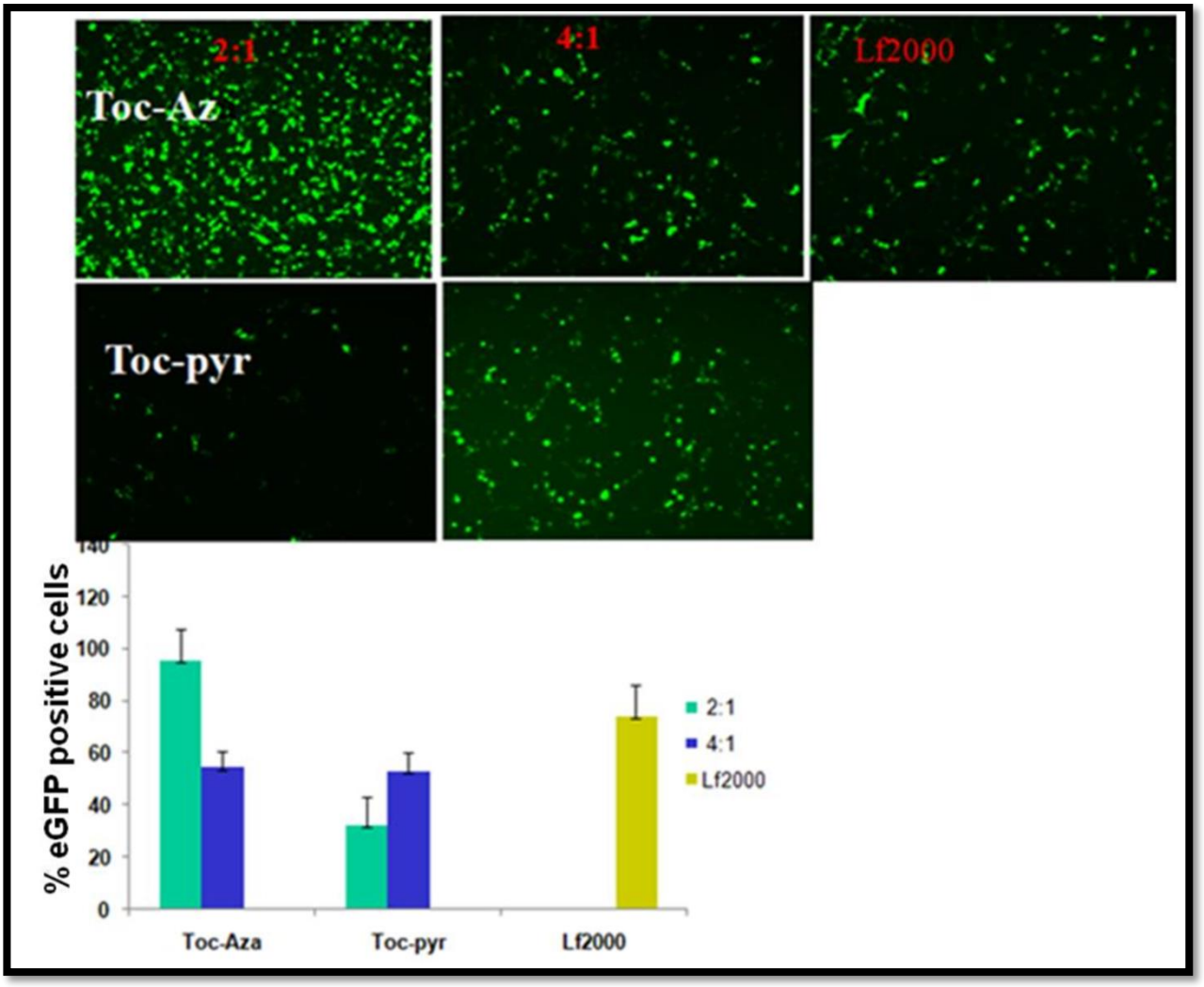

Figure 4. (A) Cellular expression of eGFP. Inverted microscopic images of HEK-293T cells transfected with lipoplexes of lipids **Toc-Aza** and **Toc-pyr** prepared at high in vitro transfection lipid:DNA charge ratios of 2:1 and 4:1.The details of the experiments are as described in the text. Bars = 100µm. standards shown are means ± SD of three independent experiments carryout in Triplicates. Statistical analysis was carried out by two-way ANOVA ($P<0.01$). **(B)** % positive GFP cells of eGFP plasmid transfection in HEK293 cell lines using lipoplexes of **Toc-Aza** and **Toc-pyr** and eGFP at 2:1 and 4:1 N/P charge ratios. Lipofectamine 2000 (Lf2000) is taken as positive control.

4.6 Effect of serum on transfection efficiency of Toc-aza and Toc-pyr lipids

In general, transfection efficiency studies of cationic liposomes are carried out either in the absence of serum or in presence of only 10% (v/v) serum as reported in many earlier investigations. However, the serum incompatibility/ serum stability still remains the major setback retarding clinical success of cationic lipid-mediated gene delivery system. Generally,*in*

vitro gene transfer activities of cationic lipids are frequently affected in the presence of serum. Such common serum incompatibility of cationic lipids is due to adsorption of negatively charged serum proteins onto the positively charged cationic liposome surfaces, which reduces their efficient interaction and internalization. Obviously, an opinion of gene transfer efficacies across a range of lipid-DNA complex charge ratios in multiple cultured cells in the presence of increasing concentrations of added serum is necessary for the significant systemic potential of any *in vitro* efficient cationic transfection lipid. Towards this, the serum-stability study was carried out for lipids **Toc-Aza** and **Toc-pyr** at lipid-DNA charge ratio 2:1 (at which one of the lipids showed its highest transfection capability in all three types of cells) in the presence of 10 % serum. The transfection efficiency results of lipoplexes of **Toc-Aza** and **Toc-pyr** and in presence of 10% added serum were quantified by flow cytometry (**Figure 5**). The MFI was significantly enhanced i.e. 93-97%with an MFI of 172 for the lipoplexes of **Toc-Aza** compared to **Toc-pyr** lipoplexes in the presence of 10 % serum (**Figure 5**).at2:1 N/P ratio in HepG2 cell line. The results clearly indicating that the serum may help in the transfection activity of lipoplexes prepared from **Toc-Aza** lipid. In CHO and HEK-293T cells, **Toc-Aza** lipoplexes showed % eGFP 78 % with an MFI of 109 % in HEK-293T cells and%eGFP83 % with an MFI125in CHO cells whereas lipoplexes of Toc-pyr showed low % eGFP and MFI in both these cell lines. High serum compatible transfection characteristics of lipid **Toc-Aza** might be due to the large surface charge shielding of the lipid-DNA complexes induced by the -OHs (hydroxy groups) of **Toc-Aza** lipid in its polar head group region. Moreover, the finding results clearly indicated that both the -OHs group and the tocopherol hydrophobic tail together as a hybrid is responsible for its higher transfection efficiency of **Toc-Aza** cationic lipid.

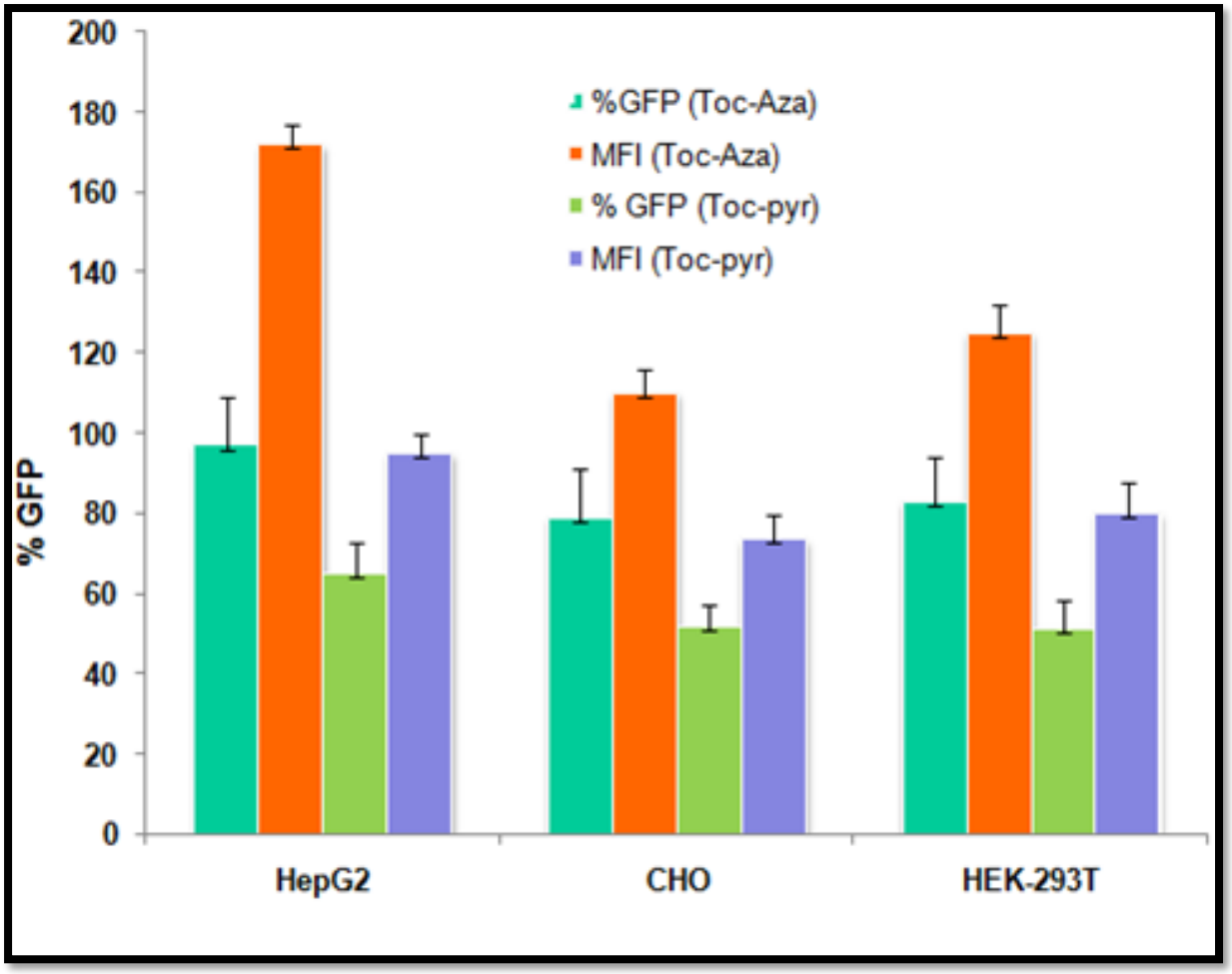

Figure 5. Optimized (2:1) charge ratio of **Toc-Aza** and **Toc-pyr** lipids. (A) The transfection efficiency of **Toc-Aza** and **Toc-pyr** lipids in presence of 10% serum. Concentration of pDNA = 0.8 mg/well. Data are expressed as a number of positive transfected cells eGFP and MFI as obtained from flow cytometry.

4.6.2 Cytotoxicity study of lipids Toc-Aza and Toc-pyr.

The minimum cytotoxicity of a synthetic gene delivery vector is another key factor that increases its possible use in medical gene therapy. MTT assay was carried out to determine the safety of the synthetic cationic lipids under investigation. The cell viability of **Toc-Aza** and **Toc-pyr** liposomes/ pDNA complexes were evaluated (**Figure 6**) in CHO, HepG2, and HEK-293T cell lines across the charge ratios 1:1-8:1. The cell viabilities of lipoplexes of both the lipid formulations are found to be remarkably high (more than 85%) particularly up to the lipid:DNA charge ratios of 4:1(**Figure 6)**. The cell viabilities of **Toc-Aza** and **Toc-pyr** lipoplexes are found

to be greater than 70% even at a higher charge ratio of 8:1(**Figure 6**). Thus, the contrasting *in vitro* gene transfer efficacies of **Toc-Aza** and **Toc-pyr** lipoplexes (**Figure 6**) are unlikely to originate from varying cell cytotoxicities of the lipids. The experimental results in all the three cell lines studied indicate that the **Toc-Aza** and **Toc-pyr** based formulations when compared to lipofectamine2000, (**Figure 6**) are less toxic. Thus in comparison to the conventional cytofectins tocopherol-azasugar hybrid cationic lipids are better transfection reagents with least cytotoxicity, which is an essential parameter of transfecting reagents for *in vitro* and *in vivo* applications.

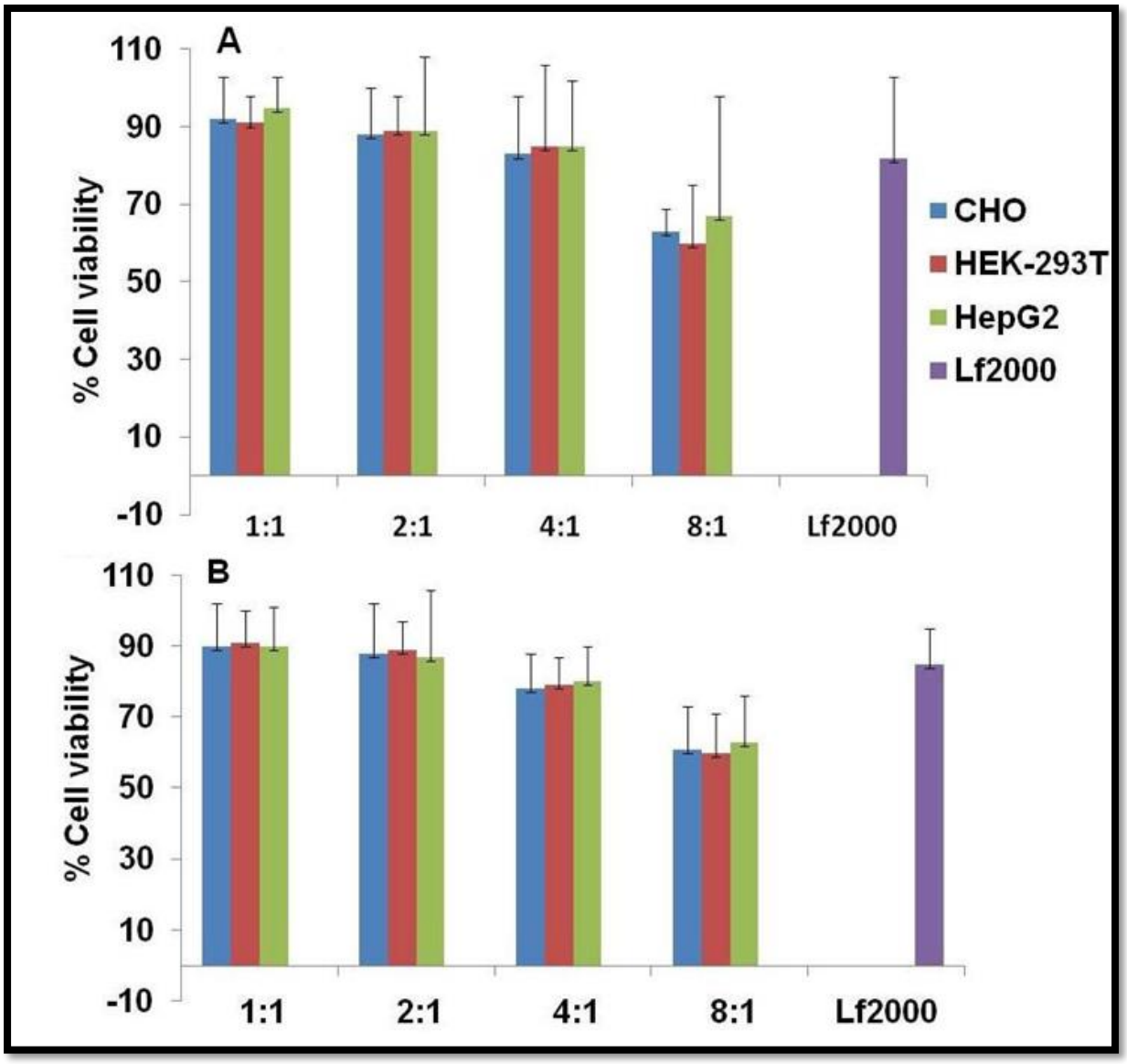

Figure 11. Tetrazolium-based colorimetric assay (MTT assay) results to represent the viabilities of various cell lines treated with the complexes derived from lipid **Toc-Aza** (A) & lipid **Toc- pyr**

(B) complexes of both lipoplexes were prepared using the plasmid DNA (0.3 μg/well) across the charge ratios ranging from 2:1 to 8:1.The data obtained is the average values of three independent experiments (n = 3). Statistical analysis was performed by Two-way ANOVA ($P<0.005$).

4.7 Experimental section

General procedure and chemicals reagents

Mass spectral data were acquired by using a commercial LCQ ion trap mass spectrometer (ThermoFinnigan, SanJose, CA, U.S.) equipped with an ESI source.^{1}H NMR and ^{13}C NMR spectra were recorded on a Varian FT400 MHz NMR spectrometer. D mannose, p-toluene sulfonicacid, 2,2dimethoxy propane, pyrrolidine,and α-tocopherol were purchased from Sigma Co. Super negatively charged eGFP plasmid, and rhodamine-PE were ample gifts from CSCR (Centre for Stem cell Research, Tamilnadu, India). Lipofectamine-2000 was purchased from Invitrogen Life Technologies, polyethylene glycol 8000, and o-nitrophenyl-β-D-galactopyranoside (pDNA) was purchased from Sigma (St. Louis, MO, U.S.). NP-40, antibiotics, and agarose were purchased from Hi-media, India. 1,2-dioleoyl-*sn*-glycerol-3-phosphoethanolamine (DOPE)was purchased from Fluka (Switzerland). Unless otherwise stated, various organic solvents including, pyridine, $NaBH_4$, triethylamine, methanol, methylene chloride (DCM), phosphomolybdicacid spray reagent, epichlorohydrin, and potassium hydroxide (KOH) were purchased from Sigma-Aldrich Co. and were used without further purification. The progress of the reaction was monitored by thin-layer chromatography using 0.25 mm silica gel plates. Column chromatography technique was executed with silica gel (Acme Synthetic Chemicals, India; finer than 200 and 60-120mesh). Elemental analyses were performed by High-Resolution Mass Spectrometry (HRMS) using QExactive equipment (Thermo Scientific) and purity of lipids wascharacterized by HPLC (Shimadzu LC Solution) and showed more than 95% purity. HepG2, CHO and HEK-293T cells were procured from the National Centre for Cell

Sciences (NCCS), Pune, India. The cells were grown at 37 ˚C in Dulbecco's modified Eagle's medium (DMEM) with 10% FBS in a humidified atmosphere containing 5% CO2 / 95 % air.

2, 3, 4, 6-Di-isopropylidene-1,5-di-*O*-hydroxy-D-mannitol (**1A, Scheme 1**).

To a suspension of D-mannose (10 g, 55.5 mmol) and p-toluenesulfonic acid monohydrate (1.06 g, 5.55 mmol) over 4 Å molecular sieves in dry DMF (80 mL) at 0 ˚C was added 2, 2 dimethoxypropene (10.6 mL, 8.0 g, 222 mmol) dropwise over 30 minutes. The suspension was maintained at 5 - 10 °C for 8 hours and allowed to warm to room temperature. The resulting pale yellow solution was quenched by the addition of $NaCO_3$ (2 g). Filtration and removal of the solvent in vacuo gave a yellow oil. The residue was partitioned between EtOAc (200 mL) and water (200 mL) and the organic layer was separated. The aqueous phase was extracted with EtOAc (3 x 100 mL) and the combined organic extracts were washed with brine (2 x 80 mL) and dried over $MgSO_4$. Evaporation afforded the crude di-isopropylidene as the major of three products, two of which were inseparable by column chromatography Rf: 0.18 (Hex: EtOAc 3:1). The crude mixture was then dissolved in anhydrous MeOH (100 mL) under nitrogen at 0 °C before the portion-wise addition of $NaBH_4$ (2.9 g, 77 mmol). Vigorous effervescence occurred and the solution was stirred at 0 °C for 30 minutes and then at room temperature for 4 hours. Two new products were observed by TLC, the major of which is the desired diol (Rf: 0.36) the minor product (Rf 0.52, Hex: EtOAc 1:2) was not able to be separated. The solvent was removed in vacuo and the residue was partitioned between EtOAc (150 mL) and water (150 mL) and the organic layer was separated. The aqueous phase was extracted with EtOAc (5 x 50 mL) and the combined organic extracts were washed with brine (2 x 50 mL) and dried over MgSO4. Evaporation and followed by column chromatography (25% - 67% EtOAc in Pet.) afforded the diol as a colourless syrup (9.36 g, 36 mmol, 67% over 2 steps). Rf= 0.36 (Hex: EtOAc 1:2);

^{1}H NMR (400 MHz, CDCl3) 4.47 (dd, J = 2.3, 6.7 Hz, 1H), 4.31 (dt, J = 4.8, 6.7 Hz, 1H), 3.97 - 3.89 (m, 2H), 3.81 (m, 2H), 3.70 (dd, J = 2.3, 8.8 Hz, 1H), 3.64 (td, J = 2.6, 10.3 Hz, 1H), 1.53

(s, 3H), 1.49 (s, 3H), 1.41 (s, 3H), 1.38 (s, 3H); MS (ESI+) m/z 285.09 [100, (M+Na)+]; (ESI+) m/z 262.1489 (263.1489 Calcd for $C_{12}H_{22}O_6Na$).

2, 3, 4, 6-Di-*O*-isopropylidene-1,5-di-*O*-benzylsulfonyl-D-mannitol (**1B**, **Scheme 1**).

To a mixture of stirred solution of the diol (5 g, 19 mmol), DMAP (250 mg, 2 mmol) and anhydrous pyridine (10 mL) in dry DCM (150 mL) under nitrogen at 0 °C added dropwise methanesulfonyl chloride (4.5 mL, 59 mmol). The solution was stirred at 0 °C for 30 minutes and then warmed to room temperature and stirred for 6 hours. The reaction was quenched by the addition of saturated $NaHCO_3$ (50 mL) before being extracted with DCM (3 x 50 mL). The combined organic extracts were then washed with brine (2 x 100 mL) and dried over $MgSO_4$. Evaporation of the solvent chromatography (Hex: EtOAc 1:1) afforded dimesylate as a white amorphous solid (6.76 g, 16 mmol, 85%). Rf = 0.15 (Hex: EtOAc 3:1).

^{1} H NMR (400 MHz, $CDCl_3$): δ/ppm= 4.82 (ddd, J = 5.1, 7.3, 8.8 Hz, 1H), 4.55 (ddd, J = 4.1, 6.3, 7.5 Hz, 1H), 4.50 (dd, J = 7.5, 10.3 Hz, 1H) 4.40 (dd, J = 1.1, 6.3 Hz, 1H), 4.38 (dd, J = 4.1, 10.3 Hz, 1H), 4.13 (dd, J = 5.1, 12.0 Hz, 1H), 3.88 (dd, J = 7.3, 12.1 Hz, 1H), 3.81 (dd, J = 1.1, 8.8 Hz, 1H), 3.08 (s, 3H), 3.07 (s, 3H), 1.52 (s, 3H), 1.50 (s, 3H), 1.41 (s, 3H), 1.37 (s, 3H); MS (ESI+) m/z (intensity) 569.18 [100, (M+Na)+]; m/z 592.0860

Synthesis of *O*-Mesyl-α-tocopherol (1C, Scheme 1)

To α-tocopherol (4.0 g, 9.0 mmol) in 10 mL of dry DCM added methane sulfonyl chloride (2.12 g, 18 mmol), pyridine(1.46 g, 18 mmol), and a catalytic amount of DMAP. The combined mixture was vigorously stirred at room temperature for12 h. The solvent was reduced in vacuum to dryness. The crude was dissolved in 25 mL of ethyl acetate and washed twice with2 × 20 mL of copper sulfate solution to remove any excess pyridine. The organic layer was dried on anhydrous sodiumsulfate, the solvent was evaporated, and the sample was purified by column chromatography, eluting with 2-3% (v/v) ethyl acetate in n-hexane to obtain 4.0 g (yield 85.10%, Rf = 0.4, 10% ethyl acetate in hexane) of *O*-mesyl-α-tocopherol.

^{1}H NMR (400 MHz, $CDCl_3$) δ/ppm = 0.8-0.90 [m, 12H, CH-CH_3], 1.00-1.4 [m,18H, -$(CH_2)_9$], 1.56 [s,3H, CH_3], 1.6-1.9 [m, 3H, CH-CH_3],2.05 [s, 3H, CH_3-5], 2.19 [s, 3H, CH_3-8],2.22 [s, 3H, CH_3-7], 2.55-2.6 [t, 2H, CH_2-4], 3.22 [s, 3H, SO_2-CH_3].

Synthesis of *O*-Aminoethyl-α-tocopherol (**1D**, **Scheme 1**)

A combined solution of ethanolamine (~4.1 g, 90 mmol) and finely powder potassium hydroxide (~4.5 g, 8.18 mmol) was taken in a two-necked round-bottomed flask and added 10 mL of toluene. The mixture contained two-necked round bottom flask was fitted with a Dean-Stark apparatus and is refluxed for 2 h to remove the water as azeotrope combined mixture. The mesylate tocopherol (4.16 g, 8.18 mmol) was added to the reaction mixture and it refluxed at 83 ˚C for 48 h. The totally combined mixture was taken into ethyl acetate (100 mL) and the ethyl acetate layer was twice washed with H_2O (2 ×100 mL), dried over anhydrous sodiumsulfate, and filtered. Ethyl acetate is separate from the filtrate on a rotary machine. The column chromatography technique was used to purify the residue using 100-200 mesh size silica gel eluting with 1-5% methanol (v/v) in chloroform afforded 2.3 g (63.15% yield Rf: 0.4, 10% methanol in chloroform) of the primary amine (**1D**).

^{1}H NMR (400 MHz, $CDCl_3$) δ/ppm= 0.85-0.90 [m, 12H, CH-CH_3tocopheryl], 1.35 [s, 3H, CH_3 -2], 1.00-1.4 [m, 18H, - $(CH_2)_9$], 1.7-1.8 [m, 2H, CH_2-3 tocopheryl], 2.05 [s, 3H, CH3-5 tocopheryl], 2.15 [s, 3H, CH_3-8], 2.18 [s, 3H, CH_3-7], 2.55-2.6 [t, 2H, CH_2-4], 3.1-3.3 [t, 2H, N-CH_2-CH_2-O-], 3.7-3.9 [m, 2H, NCH_2 -CH_2-O-], 6.3-6.4 [s, 3H,NH_2-CH_2-CH_2-O-].ESIMS m/z: calc 474 found 474

2, 3, 4, 6-Di-O-isopropylidene-1,5-O-amino ethyl α-tocopherol-D-mannitol(1E, Scheme 1)

A solution of the ditosylate derivative (1 g, 9.5mmol) and *O*-amino ethyl α-tocopherol (0.9 g, 0.444mmol) in 10 mL of toluene was taken in a one-necked round bottomed flask. The reaction mixture was refluxed at 110 °C for overnight. After TLC analysis the toluene solvent was evaporated under rotary evaporator and then reaction mixture was taken in to diethyl ether. The

ether layer was twice washed with H_2O (2 ×100 mL), dried over anhydrous sodiumsulfate, and filtered. The ether layer was evaporate under vacuum followed by column chromatography (Hexane: EtOAc, 7:3) to give **1E** as a pale yellow colour oil. (58.15% yield Rf= 0.5, 40 % Hexane: EtOAc,) of the primary amine (**1E**).

^{1} H NMR 400 MHz, CDCl3)δ/ppm = 0.85-0.90 [m, 12H], 1.35 [s, 3H], 1.00-1.4 [m, 30H], 1.7-1.8 [m, 2H], 2.05 [s, 3H], 2.15 [s, 3H, CH_3-8], 2.18 [s, 3H, CH_3-7], 2.55-2.6 [t, 2H, CH_2-4],[t, 2H, CH_2], 3.1-3.3 [t, 2H, N-CH_2-CH_2-O-],(4.47 (dd, 1H), 4.31 (dt, 1H), 3.97 - 3.89 (m, 2H), 3.81 (m, 2H), 3.70 (dd, 1H), 3.64 (td, 1H), 1.53 (s, 3H), 1.49 (s, 3H), 1.41 (s, 3H), 1.38 (s, 3H). ESIMS m/z: calc 700 found: 700

Synthesis of 1,5-Anhydro-5-*O*-ethyl amino – *α*-tocopherol -L-gulitol (final lipid) (1F, Scheme 1)

The protected coupling azasugar –tocopherol hybrid product was dissolved in dry MeOH (2 mL), HCl (2 mL) was then added, and the reaction mixture was vigorously stirred for 6-8 h at room temperature. The progress of the reaction mixture was followed by TLC analysis of aliquots (developing solvent $CHCl_3$: MeOH 8:2 v/v). When the starting material had been consumed, the solvent was evaporated under reduced pressure. The residue was rinsed with hexane (4 x 2 mL) and the hexane was decanted. The remaining gum was dissolved in MeOH/DCM and purified by column chromatography ($CHCl_3$: MeOH 2-4 % v/v) to give the final purified compounds in yellow color. (60.5% yield Rf= 0.4, 10% methanol in chloroform) of the primary amine (**1F**).

^{1} H NMR 400 MHz, CDCl3)! δ/ppm=0.85-0.90 [m, 12H, CH-CH_3], 1.35 [s, 3H, CH_3 -2], 1.00-1.4 [m, 18H, - $(CH_2)_9$], 1.7-1.8 [m, 2H, CH_2-3], 2.05 [s, 3H, CH3-5], 2.15 [s, 3H, CH_3-8], 2.18 [s, 3H, CH_3-7], 2.55-2.6 [t, 2H, CH_2-4],[t, 2H, CH_2], 3.1-3.3 [t, 2H, N-CH_2-CH_2-O-],
4.30 (td, 1H), 4.24 (dd, 1H), 3.70 (ddd, 1H), 3.63 (dd, 1H), 3.48 (ddd, 1H), 3.42 (dd, 1H), 2.98 (dd, 1H), 2.79 (dd, 1H); ESI-HRMS m/z: calc 620.4934 found: 620. 49503

Synthesis of *O*-acetic acid-*α*-tocopherol (2A, scheme 2)

α-Tocopherol (0.5 g, 1.16 mmol) in *N*, *N*-dimethylformamide (DMF) (25 mL) was reacted with ethyl bromoacetate (3.4 g, 8.3 mmol) and finely powdered potassium hydroxide (1.2 g, 30 mmol). The ensuing mixture was stirred for 24 h at room temperature. The crude was acidified with 6N HCl and extracted with ethyl acetate (3×30 mL). The ethyl acetate layers were washed with water (3×30 mL) and sodium chloride solution (brine) (1×30 mL) and then dried with magnesium sulfate. The residue pale yellow oil was purified by silica gel (100-200 mesh size) chromatography eluting with 15% (v/v) ethyl acetate (EtOAc) and 1% acetic acid in hexanes. This yielded **2A** as yellow-colored compound (0.50 g, 85%).

^{1}H NMR (400 MHz, $CDCl_3$) δ/ppm = 0.8-0.90 (12H), 1.00-1.5 (m, 25H), 1.77-1.88 (m, 2H), 2.55 (s, 3H), 2.57 (s, 3H), 2.59 (s, 3H), 4.3 (s, 2H), 7.98 (broad, 1H).**ESI-MS**: Calculated 488; found: $[M+NH^+_4]$ 506

Synthesis of *O*-ethyl alcohol -α-tocopherol (2B, scheme 2)

To a solution of lithium aluminum hydride (0.08 g, 1.1 mmol) in 10 mL of dry Tetrahydrofuran solvent, a solution of **1A** (2.0 g, 1 mmol) in 5 mL dry tetrahydrofuran was added slowly at 0 ˚C with the help of addition funnel about 10 minutes. The reaction was vigorously stirred for 6 h at room temperature and then followed by quenching of excess $LiAlH_4$with ethyl acetate. The ethyl acetate layer was two times washed with H_2O (2×50 mL), dried over anhydrous Na_2SO_4, filtered, and concentrated under reduced pressure. The crude product was purified by silica gel column chromatography to give *O*-ethyl alcohol-α-tocopherol **1B** (1.89 g), 86%) as a clear oil. Rf = 0.2 (20% EtOAc/hexane, 2:8).

^{1}H NMR (400 MHz, $CDCl_3$) δ/ppm= 0.8-0.90 (12H), 1.00-1.5 (m, 25H), 1.77-1.88 (m, 2H), 2.55 (s, 3H), 2.57 (s, 3H), 2.59 (s, 3H), 3.66 (t, 2H), 3.85 (t, 2H).). **ESI-MS**: Calculated 474; found: $[M^+]$ 474

Synthesis of *O*-ethyl chloro -α-tocopherol (2C, Scheme 2)

To a stirred solution of *O*-ethyl alcohol -α-tocopherol 0.1 g (1 mmol) in chloroform 100 mL a solution of thionylchloride in chloroform 10 mL was added dropwise at -5 ˚C. After removing ice

bath the reaction mixture was allowed to reach the room temperature and refluxed for 150 minutes. Then the solvent was evaporated in vacuum and the residue was treated with 20 mL of methanol and evaporated to dryness again. The crude product was purified by column chromatography. (Yield: 92%)

^{1}H NMR (400 MHz, $CDCl_3$) δ/ppm= 0.8-0.90 (12H), 1.00-1.5 (m, 25H), 1.77-1.88 (m, 2H), 2.55 (s, 3H), 2.57 (s, 3H), 2.59 (s, 3H), 3.76 (t, 2H), 3.95 (t, 2H).).**ESI-MS**: Calculated 474; found: [M^++ 3] 495

Synthesis of pyrrolidinium-*O*-ethyl-α-tocopherol lipid (**2D**&**EScheme 2**)

Pyrrolidine 0.05 mg (0.72 mmol) was dissolved in 15 mL of dry methanol followed by the addition of dry K_2CO_3 (0.06 mmol) and *O*-ethyl chloro -α-tocopherol (0.495mmol). The combined reaction mixture was heated to 90 °C for 16 h. After TLC analysis the reaction mixture is cooled to room temperature and then diluted with 100 mL of DCM. The diluted solution was washed with 50 mL of 10 % aqueous brine solution three times and then dried over anhydrous sodium chloride, followed by filtration. The filtrate was evaporated under reduced pressure. The crude was purified by column chromatography using 100-200 mesh silica gels (72% yields). After purification of tertiaryamine, 0.5 g (1.05 mmol) was dissolved in 5 mLof (2:2 v/v) a mixture of chloroform and methanol, and 1 mL of 1 N HCl was added at 0 ˚C. The resulting solution was stirred at room temperature for 12 h. Excess HCl was removed by flushing with nitrogen to give the title compound as a hydrochloride salt. The crude was purified by column chromatographic using 60-120 mesh size silica gel and 3-5 % (v/v) methanol/chloroform as eluent afforded final lipid as a pale yellow liquid (0.92 g, yield 92%, Rf = 0.2, 5% methanol in chloroform).

^{1}H NMR (400 MHz, $CDCl_3$) δ/ppm = 0.8-0.87 (12H), 1.80-1.54 (m, 25H), 1.08-1.88 (m, 2H), 2.55 (s, 3H), 2.57 (s, 3H), 2.59 (s, 3H), 2.82 (t, 2H), 4.20 (t, 2H).) **ESI-HRMS** Mass m/z: Calculated 528.48090; found: [$M^{+]}$ 528.48070

4.8 Preparation of liposomes and plasmid DNA

The cationic lipid and the auxiliary lipid DOPE (concentration of each lipid and co-lipid is 1 mol, respectively) were dissolved in dry chloroform in an autoclaved dry glass vial. The solvent was evaporated with a thin flow of moisture-free nitrogen gas, and further dried the thin film under high vacuum for 6 h. Then 1 ml of milliQ water was added to dried lipid film and the mixture was allowed to swell for 12 h. The vial was then vortexed for 2-3 min at room temperature till transparent solution appears and occasionally sonicated in a bath sonicator to produce multilamellar vesicles (MLVs). MLVs were then sonicated in an ice bath until clarity using a Branson 450 sonifier at 100% duty cycle and 25W output power. The resulting clear aqueous liposomes were used in forming lipid-DNA complexes. *p*CMV-SPORT-β-gal and eGFP plasmids were amplified in a DH5α strain of *Escherichia coli*, isolated by alkaline lysis procedure, and finally purified by PEG-8000 precipitation as described previously[10c]. The purity of plasmid was checked by A_{260}/A_{280}ratio (around 1.9) and 1% agarose gel electrophoresis.

4.9 DNA binding assay

Lipoplexes were formed by mixing 3 μL of supercoiled pDNA (0.1 μg/μL in 10 mm HEPES buffer, pH 7.4) with deferent amounts of lipids so that the final lipid: pDNA charge ratios were maintained at 1:1 to 8:1 in a total volume of 30 μL. Lipoplexes were incubated for 30 minutes at room temperature after which 15 μL of each lipoplex was loaded on a 1% agarose gel (pre-stained with ethidium bromide) and electrophoresed (80 V, 45 min.). The bands were visualized using a Bio-Rad Gel Doc XR+ imaging system (Bio-Rad, Hercules, CA, USA)

4.10 Heparin Displacement Assay

Heparin helps to study the anionic dislocation of DNA within the lipoplexes. The lipid: DNA complexes were prepared as described in the above section (DNA binding assay) and incubated for 20 minutes. These lipids: DNA complexes were further incubated for 30 minutes with 0.1µg

of the sodium salt of heparin. The samples were electrophoresed in an agarose gel (1.5%) for heparin displacement analysis and DNA bands were visualized as mentioned in the above section.

4.11 Zeta potential (ξ) and size measurements

The sizes and the surface charges (zeta potentials) of liposomes and lipoplexes with varying charge ratios (8:1 to 1:1) were measured by photon correlation spectroscopy and electrophoretic mobility on a Zetasizer 3000HSA (Malvern, U.K.). The sizes were measured in deionized water with a sample refractive index of 1.59 and a viscosity of 0.89cP. The system was calibrated using 200 nm $\pm$ 5 nm polystyrene polymers (Duke Scientific Corps., Palo Alto, CA). The diameters of liposomes and lipoplexes were calculated by using the automatic method in triplicate and represented as average values. The sizes were measured in triplicate. The zeta potential was measured using the following parameters: viscosity, 0.89 cP; dielectric constant, 79; temperature, 25°C; F (Ka), 1.50 (Smoluchowski); the maximum voltage of the current, 80 V. The system was calibrated by using the DTS0050 standard from Malvern. Measurements were done 10 times with the zero-field correction. The potentials were measured 10 times and represented as their average values as calculated by using the Smoluchowski approximation.

4.12 Transfection Biology

A general transfection procedure was followed as described below. Eukaryotic cells were cultured at a density of 15000 cells per well in a ninety-six-well plate 18-24 h the day before the transfection. The supercoiled plasmid DNA (0.3 μg) was complexed with varying amounts of desired lipids (0.15 -7.2 mmol) in serum-free DMEM medium (maximum volume should be to 100 μL) for 20 minutes. The charge ratios of cationic liposomes were varied from 0.5:1 to 8:1 (+/-). The liposome pDNA plasmid complexes were then treated with the cells. After 3 h of the incubation period, 100 μL of Dulbecco's Modified Eagle Medium DMEM with 10% FBS was added to the cells. The serum medium was altered to 10% complete medium after 24 h and the

reporter gene activity was estimated after 48 h. The cells were washed two times with PBS (100 µL each) and lysed in 50 µLlysis buffer [0.25 M Tris-HCl pH 8.0, 0.5% NP40]. The care was taken to ensure complete lysis. The β-galactosidase activity in wells was estimated by addition 50 µL of 2 X-substrate solutions [1.33 mg/mL of ONPG, 0.2 M sodium phosphate (pH 7.3) and 2 mM magnesium chloride] to the lysate in a 96-well plate. The adsorption at 405 nm was converted to β-galactosidase units using a calibration curve constructed with the commercial β-galactosidase enzyme. The values of β-galactosidase units in three experiments carried out on the same day varied by less than 20%. The transfection experiment was performed in duplicate and the reported transfection efficiency values are the average of triplicate experiments carried out on the same day. Each transfection experiment was repeated three epoch and the day to day changes in average transfection efficiency was found to be within 2-fold. The transfection was obtained on different days were similar.

4.13 Cellular α5GFP Expression Study

For cellular α5GFP expression experiment in HEK-293 50, 000 cells were cultured in well of 24-well plate 18-24 h before the transfection. Then 0.9 µg of α5GFP plasmid DNA encoding green fluorescent protein was complexed with liposomes of lipids **Toc-Aza and Toc-pyr** at charge ratio (lipid-DNA complexes) 2:1 in carbonate-free DMEM medium (total volume should be to 100 µL) for 30 min. Just prior to transfection, cells plated in the 24-well plate were washed with PBS (2×100 µL) followed by addition of lipoplexes. The media 400 µL was added after 4 h incubation of the cells. After 24 h, the complete medium was removed from each well, and the total cells were washed with PBS (2× 200 µL). Finally 200 µL of PBS was added to each per well and visualized under the inverted fluorescent microscope to observe the cells expressing the green fluorescent protein and after that the cells expressing eGFP was quantified using a FACS Calibur flow cytometer (Becton-Dickinson) equipped with an argon ion laser at 488 nm for excitation and detection at 530 nm. 10,000 cells were analyzed for each sample using the

software, Cell Quest. Nontransfected cells served as live cell controls for gate settings which in turn provided the cut off thresholds for quantification of the fluorescent cell population.

4.14 Serum-stability of Lipoplexes

Eukaryotic cells were cultured at a density of 15, 000 cells (HEK-293T, CHO, and HepG2) per well in a ninety-six-well plate 18-24 h prior to the transfection. Then 0.3 μg (0.91 nmol) of pDNA was complexed with cationic liposomes (**Toc-Aza** and **Toc-pyr**) in DMEM medium in the presence of added serum 10% v/v and (total volume should be 100 μL) incubated for 30 min. The charge ratios of lipoplexes were maintained as 2: 1, at which one of the lipid **Toc-Aza** showed their maximum transfection efficacies in three different types of cells used for transfection HepG2, HEK-293T, and CHO. The experimental procedure and determination of β-galactosidase activity per well are similar to that reported for the *in vitro* transfection procedure.

4.15 Cytotoxicity assay

The cytotoxicities of cationic lipids (**Toc-Aza & Toc-pyr)** in CHO, HEK-293T and HepG2 cells across the lipoplexes charge ratios of 1:1-1:8 as used in the authentic transfection experiments were assessed with the help of MTT (3-(4, 5-dimethyathiazol-2-yl)-2, 5-diphenyltetrazolium Bromide) based reduction assay as reported previously. The MMT assay was carried out in 96-well plates by maintaining the same ratio of a number of cells to an amount of cationic lipid: DNA complexes, as used in the transfection experiments. Briefly, the cells were incubated with lipoplexes for 3 h followed by the addition of 100 μL of DMEM containing 20% FBS and 10 μL MTT (5mg/mL in PBS). After 3-4 h of incubation at 37 °C, the medium was removed and 100 μL of DMSO: Methanol (50:50, v/v) was added to the cells. The absorbance was measured at 550 nm and results were expressed as percent viability = [A_{540} (treated cells)-background/A_{540} (untreated cells)-background] x100.

4.5 References

1. (a) Wu, P.; Chen, H.; Jin, R.; Weng, T.; Ho, J. K.; You, C.; Zhang, L.; Wang, X.; Han, C., Non-viral gene delivery systems for tissue repair and regeneration. *Journal of translational medicine* **2018,***16* (1), 29; (b) Sun, D.; Schur, R. M.; Lu, Z. R., A novel nonviral gene delivery system for treating Leber's congenital amaurosis. *Therapeutic delivery* **2017,***8* (10), 823-826; (c) Fernandez-Pineiro, I.; Pensado, A.; Badiola, I.; Sanchez, A., Development and characterisation of chondroitin sulfate- and hyaluronic acid-incorporated sorbitan ester nanoparticles as gene delivery systems. *European journal of pharmaceutics and biopharmaceutics : official journal of Arbeitsgemeinschaft fur Pharmazeutische Verfahrenstechnik e.V* **2018,***125*, 85-94; (d) McMillan, A.; Nguyen, M. K.; Gonzalez-Fernandez, T.; Ge, P.; Yu, X.; Murphy, W. L.; Kelly, D. J.; Alsberg, E., Dual non-viral gene delivery from microparticles within 3D high-density stem cell constructs for enhanced bone tissue engineering. *Biomaterials* **2018,***161*, 240-255; (e) Holstein, M.; Mesa-Nunez, C.; Miskey, C.; Almarza, E.; Poletti, V.; Schmeer, M.; Grueso, E.; Ordonez Flores, J. C.; Kobelt, D.; Walther, W.; Aneja, M. K.; Geiger, J.; Bonig, H. B.; Izsvak, Z.; Schleef, M.; Rudolph, C.; Mavilio, F.; Bueren, J. A.; Guenechea, G.; Ivics, Z., Efficient Non-viral Gene Delivery into Human Hematopoietic Stem Cells by Minicircle Sleeping Beauty Transposon Vectors. *Molecular therapy : the journal of the American Society of Gene Therapy* **2018**.
2. (a) Badamchi-Zadeh, A.; Tartaglia, L. J.; Abbink, P.; Bricault, C. A.; Liu, P. T.; Boyd, M.; Kirilova, M.; Mercado, N. B.; Nanayakkara, O. S.; Vrbanac, V. D.; Tager, A. M.; Larocca, R. A.; Seaman, M. S.; Barouch, D. H., Therapeutic Efficacy of Vectored PGT121 Gene Delivery in HIV-1-Infected Humanized Mice. *Journal of virology* **2018,***92* (7); (b) Kodama, Y.; Hanamura, H.; Muro, T.; Nakagawa, H.; Kurosaki, T.; Nakamura, T.; Kitahara, T.; Kawakami, S.; Nakashima, M.; Sasaki, H., Gene delivery system of pDNA using the blood glycoprotein fetuin. *Journal of drug targeting* **2017**, 1-6; (c) Jeong, G. W.;

Nah, J. W., Evaluation of disulfide bond-conjugated LMWSC-g-bPEI as non-viral vector for low cytotoxicity and efficient gene delivery. *Carbohydrate polymers* **2017,***178*, 322-330.

3. (a) Caroline Diana, S. M.; Rekha, M. R., Efficacy of vinyl imidazole grafted cationized pullulan and dextran as gene delivery vectors: A comparative study. *International journal of biological macromolecules* **2017,***105* (Pt 1), 947-955; (b) Nakatsuji, H.; Kawabata Galbraith, K.; Kurisu, J.; Imahori, H.; Murakami, T.; Kengaku, M., Surface chemistry for cytosolic gene delivery and photothermal transgene expression by gold nanorods. *Scientific reports* **2017,***7* (1), 4694; (c) Pacheco-Lugo, L.; Diaz-Olmos, Y.; Saenz-Garcia, J.; Probst, C. M.; DaRocha, W. D., Effective gene delivery to Trypanosoma cruzi epimastigotes through nucleofection. *Parasitology international* **2017,***66* (3), 236-239; (d) Zhang, T. Y.; Wu, J. H.; Xu, Q. H.; Wang, X. R.; Lu, J.; Hu, Y.; Jo, J. I.; Yamamoto, M.; Ling, D.; Tabata, Y.; Gao, J. Q., Design of magnetic gene complexes as effective and serum resistant gene delivery systems for mesenchymal stem cells. *International journal of pharmaceutics* **2017,***520* (1-2), 1-13.

4. (a) Ohta, T.; Hashida, Y.; Higuchi, Y.; Yamashita, F.; Hashida, M., In Vitro Cellular Gene Delivery Employing a Novel Composite Material of Single-Walled Carbon Nanotubes Associated With Designed Peptides With Pegylation. *Journal of pharmaceutical sciences* **2017,***106* (3), 792-802; (b) Miller, J. B.; Zhang, S.; Kos, P.; Xiong, H.; Zhou, K.; Perelman, S. S.; Zhu, H.; Siegwart, D. J., Non-Viral CRISPR/Cas Gene Editing In Vitro and In Vivo Enabled by Synthetic Nanoparticle Co-Delivery of Cas9 mRNA and sgRNA. *Angew Chem Int Ed Engl* **2017,***56* (4), 1059-1063; (c) Zhang, B.; Zhang, Y.; Yu, D., Lung cancer gene therapy: Transferrin and hyaluronic acid dual ligand-decorated novel lipid carriers for targeted gene delivery. *Oncology reports* **2017,***37* (2), 937-944.

5. (a) Laskar, P.; Dey, J.; Banik, P.; Mandal, M.; Ghosh, S. K., In Vitro Drug and Gene Delivery Using Random Cationic Copolymers Forming Stable and pH-Sensitive

Polymersomes. *Macromolecular bioscience* **2017,***17* (4); (b) Liu, J.; Shui, S. L., Delivery methods for site-specific nucleases: Achieving the full potential of therapeutic gene editing. *Journal of controlled release : official journal of the Controlled Release Society* **2016,***244* (Pt A), 83-97.

6. (a) Pflueger, I.; Charrat, C.; Mellet, C. O.; Garcia Fernandez, J. M.; Di Giorgio, C.; Benito, J. M., Cyclodextrin-based facial amphiphiles: assessing the impact of the hydrophilic-lipophilic balance in the self-assembly, DNA complexation and gene delivery capabilities. *Organic & biomolecular chemistry* **2016,***14* (42), 10037-10049; (b) Chen, M.; Tang, Y.; Wang, T.; Long, Q.; Zeng, Z.; Chen, H.; Feng, X., Enhanced gene delivery of low molecular weight PEI by flower-like ZnO microparticles. *Materials science & engineering. C, Materials for biological applications* **2016,***69*, 1367-72; (c) Shekhar, S.; Roy, A.; Hong, D.; Kumta, P. N., Nanostructured silicate substituted calcium phosphate (NanoSiCaPs) nanoparticles - Efficient calcium phosphate based non-viral gene delivery systems. *Materials science & engineering. C, Materials for biological applications* **2016,***69*, 486-95; (d) McErlean, E. M.; McCrudden, C. M.; McCarthy, H. O., Delivery of nucleic acids for cancer gene therapy: overcoming extra- and intra-cellular barriers. *Therapeutic delivery* **2016,***7* (9), 619-37; (e) Yu, J.; Zhang, J.; Xing, H.; Yang, Z.; Cai, C.; Zhang, C.; Zhao, X.; Wei, M.; Yang, L.; Ding, P., Guanidinylated bioresponsive poly(amido amine)s designed for intranuclear gene delivery. *International journal of nanomedicine* **2016,***11*, 4011-24; (f) S, P. S.; R, R. M., Disulphide cross linked pullulan based cationic polymer for improved gene delivery and efflux pump inhibition. *Colloids and surfaces. B, Biointerfaces* **2016,***146*, 879-87; (g) Wu, G. H.; Hsu, S. H., Synthesis of water-based cationic polyurethane for antibacterial and gene delivery applications. *Colloids and surfaces. B, Biointerfaces* **2016,***146*, 825-32; (h) Cui, S. H.; Zhi, D. F.; Zhao, Y. N.; Chen, H. Y.; Meng, Y.; Zhang, C. M.; Zhang, S. B., Cationic lioposomes with folic acid as targeting ligand for gene delivery. *Bioorganic & medicinal chemistry letters* **2016,***26* (16), 4025-9.

7. (a) Wang, L. H.; Wu, T.; Wu, D. C.; You, Y. Z., Bioreducible Gene Delivery Vector Capable of Self-Scavenging the Intracellular-Generated ROS Exhibiting High Gene Transfection. *ACS applied materials & interfaces* **2016,***8* (30), 19238-44; (b) Pierrat, P.; Kereselidze, D.; Lux, M.; Lebeau, L.; Pons, F., Enhanced gene delivery to the lung using biodegradable polyunsaturated cationic phosphatidylcholine-detergent conjugates. *International journal of pharmaceutics* **2016,***511* (1), 205-218; (c) Thibault, M.; Lavertu, M.; Astolfi, M.; Buschmann, M. D., Structure Dependence of Lysosomal Transit of Chitosan-Based Polyplexes for Gene Delivery. *Molecular biotechnology* **2016,***58* (10), 648-656.

8. (a) Das, J.; Han, J. W.; Choi, Y. J.; Song, H.; Cho, S. G.; Park, C.; Seo, H. G.; Kim, J. H., Cationic lipid-nanoceria hybrids, a novel nonviral vector-mediated gene delivery into mammalian cells: investigation of the cellular uptake mechanism. *Scientific reports* **2016,***6*, 29197; (b) Wang, W.; Dong, B.; Ittmann, M. M.; Yang, F., A Versatile Gene Delivery System for Efficient and Tumor Specific Gene Manipulation in vivo. *Discoveries (Craiova)* **2016,***4* (2); (c) Majidi, A.; Nikkhah, M.; Sadeghian, F.; Hosseinkhani, S., Development of novel recombinant biomimetic chimeric MPG-based peptide as nanocarriers for gene delivery: Imitation of a real cargo. *European journal of pharmaceutics and biopharmaceutics : official journal of Arbeitsgemeinschaft fur Pharmazeutische Verfahrenstechnik e.V* **2016,***107*, 191-204.

9. (a) Rezaee, M.; Oskuee, R. K.; Nassirli, H.; Malaekeh-Nikouei, B., Progress in the development of lipopolyplexes as efficient non-viral gene delivery systems. *Journal of controlled release : official journal of the Controlled Release Society* **2016,***236*, 1-14; (b) Hill, A. B.; Chen, M.; Chen, C. K.; Pfeifer, B. A.; Jones, C. H., Overcoming Gene-Delivery Hurdles: Physiological Considerations for Nonviral Vectors. *Trends in biotechnology* **2016,***34* (2), 91-105; (c) Yang, Z.; Li, Y.; Gao, J.; Cao, Z.; Jiang, Q.; Liu, J., pH and redox dual-responsive multifunctional gene delivery with enhanced capability of

transporting DNA into the nucleus. *Colloids and surfaces. B, Biointerfaces* **2017,***153*, 111-122; (d) Feng, T.; Tian, H.; Dong, X.; Lam, M. H.; Liang, H.; Chen, X., pH-sensitive OEI-poly(aspartic acid-b-lysine) as charge shielding system for gene delivery. *Journal of controlled release : official journal of the Controlled Release Society* **2015,***213*, e104.

10. (a) Zhang, Y.; Anchordoquy, T. J., The role of lipid charge density in the serum stability of cationic lipid/DNA complexes. *Biochimica et biophysica acta* **2004,***1663* (1-2), 143-57; (b) Kedika, B.; Patri, S. V., Benzothiazole head group based cationic lipids: synthesis and application for gene delivery. *European journal of medicinal chemistry* **2014,***74*, 703-16; (c) Kedika, B.; Patri, S. V., Synthesis and gene transfer activities of novel serum compatible reducible tocopherol-based cationic lipids. *Molecular pharmaceutics* **2012,***9* (5), 1146-62; (d) Kedika, B.; Patri, S. V., Influence of minor backbone structural variations in modulating the in vitro gene transfer efficacies of alpha-tocopherol based cationic transfection lipids. *Bioconjugate chemistry* **2011,***22* (12), 2581-92; (e) Kedika, B.; Patri, S. V., Design, synthesis, and in vitro transfection biology of novel tocopherol based monocationic lipids: a structure-activity investigation. *Journal of medicinal chemistry* **2011,***54* (2), 548-61.
11. Muripiti, V.; Rachamalla, H. K.; Banerjee, R.; Patri, S. V., alpha-Tocopherol-based cationic amphiphiles with a novel pH sensitive hybrid linker for gene delivery. *Organic & biomolecular chemistry* **2018,***16* (16), 2932-2946.

CHAPTER 5

Structure-activity analysis of serotonin modified tocopherol based lipids: design, synthesis and transfection biology

5.1 Introduction

In the context of gene therapy, non-viral nucleic acid delivery is a viable alternative for the intervention of various human diseases[1]. The approach mainly utilizes cationic lipid formulations, engineered nanoparticles or peptides and their derivatives for delivering DNA *in vitro* and *in vivo*[2]. Among these, cationic lipid-based vectors have contributed to the diversity and repertoire of gene delivery vehicles and have been widely used for nucleic acid therapy and clinical applications [3]. Essentially, these approaches facilitate targeted delivery of plasmid DNA in a cell-specific and non-toxic manner while simultaneously increasing the therapeutic efficacy. Selective targeting of the liposome/pDNA (+/-) complexes may be achieved through the incorporation of cell specific ligands on the liposomal surface through direct formulation or by covalent coupling [3c, d, 4]. In order to fully realize the therapeutic potential, he delivery vehicle must protect the genetic material or nucleic acid against nucleases in serum-rich biological milieu to enable selective transport to the targeted tissues while fostering uptake and consequential endosomal escape[5]. Although cationic vectors can mediate effective gene transfer, tissue specific delivery *in vivo* is still a major hurdle. Till date, tissue-specific targeting of cationic liposome/DNA (+/-) has been accomplished primarily by two different methods. The first approach involves transfection of selected tissues, such as nasal epithelium, neuronal, arterial endothelium, lung, or tumors following local delivery of lipid-based complexes to distinct regions. This straightforward approach has led to its early success in the clinic for the intervention of several diseases that include cystic fibrosis and cancer. The second approach entails target selectivity by coupling cell- binding ligands to enhance cell selectivity. Examples include, conjugation of serotonin targeting 5-HT receptor[6] transferrin carbohydrates to liposomes for the purpose of complementing the intrinsic activities of lipids with ligands that can target a specific receptor.

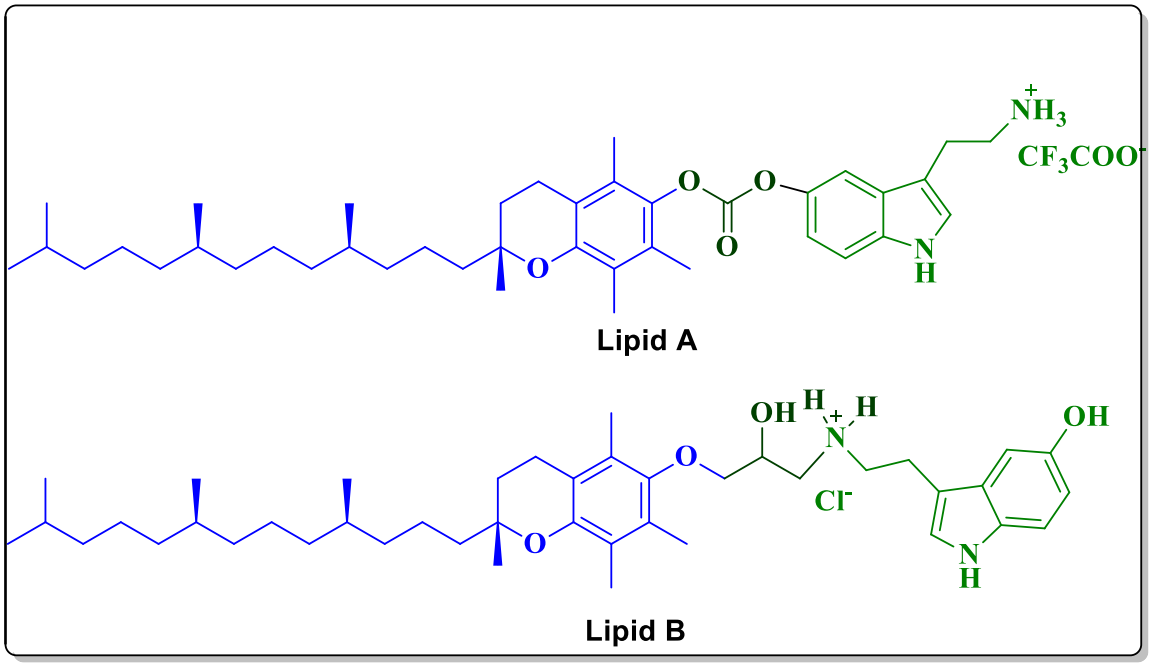

Figure.1. Chemical structures of targeted Cationic Lipids

Receptors for serotonin (5-hydroxytryptamine [5-HT], a neuro transmitters are abundant in neural as well as non-neural tissues. Serotonin is an important member of the GPCR (G-protein coupled receptors) super family acts as a neuro transmitter and is involved in the etiology of large number of neuro degenerative diseases. Dizeyi et al has confirmed the over expression of 5-HT receptors in prostate cancer tissues through ligand binding assays[7]. Recent studies have shown the involvement of serotonin in the peripheral tissues. These non-pharmacological functions have been linked to its chemical properties through receptor-independent mechanisms [8]with potent antioxidant properties. Besides, the antioxidative properties of □-tocopherol has been demonstrated and the molecule has been used in treating ROS(reactiveoxygenspecies)related diseases[9]. Serotonin possesses two reactive functional groups i.e. phenolic hydroxyl and primary amine. Through mutagenesis studies, Ho et al., established the involvement of hydroxyl and amine groups indirect receptor binding through interaction with serine, as partateand threonine residues present in different transmembrane helices of the receptor. Importantly, mutational and modeling studies reveal that serotonin

receptor prefers ligands with a hydrogen bond acceptor at a position corresponding to the hydroxyl group in serotonin. In this study, we explored the potential of the hybrid conjugate to enhance DNA delivery to 5-HT receptor-enriched cells. This is with the anticipation that serotonin upon conjugation to α-tocopherol through the reactive groups will retain the combined properties and at the same time reduce the toxicity while increasing cell viability upon transfection. We covalently linked serotonin to α-tocopherol through the reactive -$NH_2$and -OH groups and characterized the molecules by examining the structure-activity relationship (SAR) arising from subtle differences in lipid architecture. This is with the premise that the structure may influence transfection efficiency and which was examined through functional and computational studies. To the best of our knowledge, this is the first study reporting the synthesis and use of 5-HT-derived tocopherol lipid as a unique non-toxic conjugate for nucleic acid delivery specifically into cells that express the serotonin receptor

5.2 Results & Discussion

5.2.1 Chemical characterization of serotonin conjugates

To examine structure-based activity and functionality of serotonin derived tocopherol lipids, two cationic **Lipids A (-NH2)** and **Lipid B (-OH)** (**Schemes 1 & 2**) were designed and synthesized. Design in **LipidA** depicts the conjugation of α-tocopherol to serotonin, through a carbonate linker at –OH group of 5-HT ligand, while **Lipid B** was prepared by conjugating 5-HT to tocopherylglycidyl ether through a β-hydroxy linker at –NH group of 5-HT ligand. While **LipidA** was synthesized by the coupling of tocopherylchloroformate with Boc-protected serotonin, followed by deprotection of the intermediate compound with trifluoro acetic acid (**Scheme1**),**LipidB** (**Scheme2**) (α-tocopherylglycidyl ether) in triethylamine at -10 to 0 □C for ~12 h followed by quaternization using HCl in dry methanol. The structures of all the intermediates (**Scheme 1**) were confirmed by both ^{1}HNMR and mass spectral analysis. The purity of the final conjugates was confirmed by High Resolution Mass Spectrometry

(HRMS) and analytical High Performance Liquid Chromatography (HPLC) methods. ^{1}H NMR spectra of all the intermediates **I-V** (**Scheme1**), $^{1}HNMR$ and HRMS-mass spectra of the final **LipidA** and **LipidB** and the HPLC chromatograms for the final conjugates **Lipid A** (**-NH_2**) and **Lipid B (-OH)** in two different mobile phases (100%methanol and95:5methanol/water v/v), are depicted in **FiguresS1-S12** of the Supporting Information.

Scheme 1

Synthesis of Lipid A

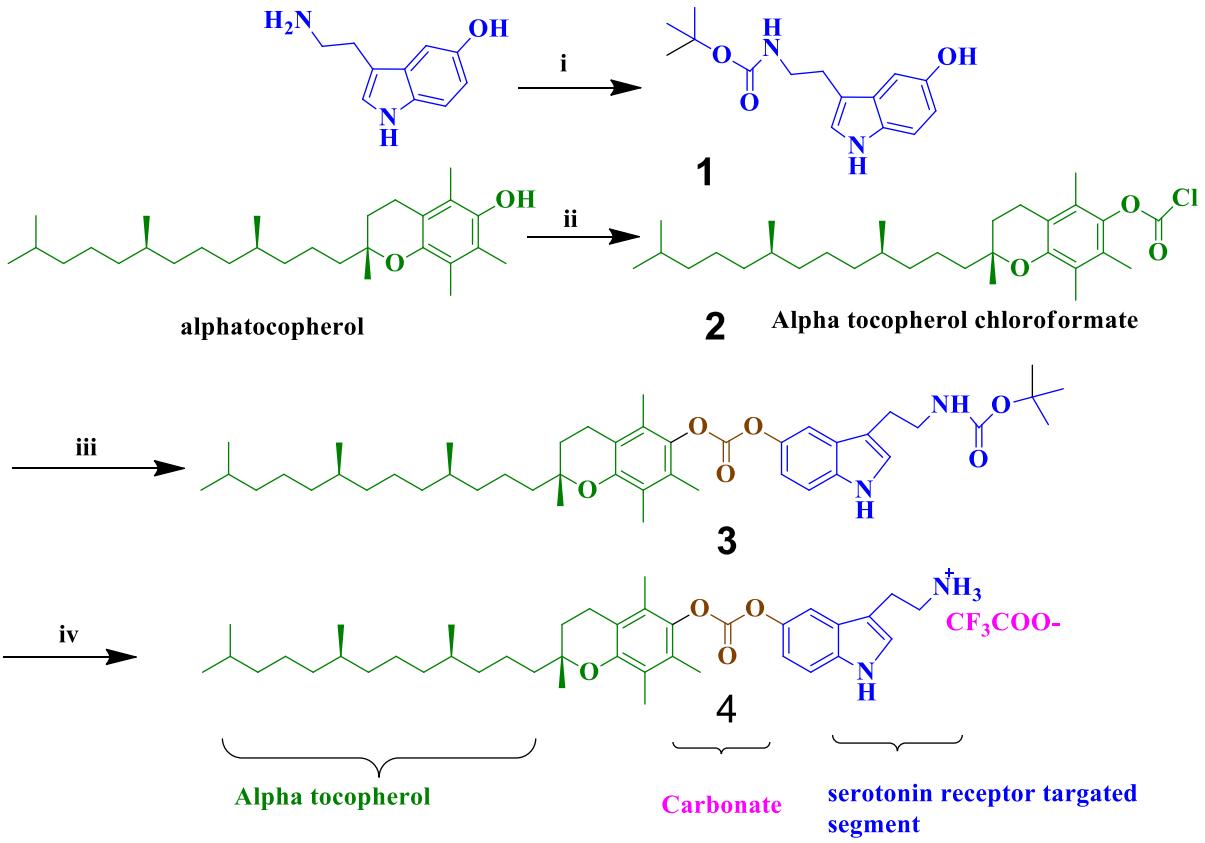

Reagents: i) Dry DCM, Et_3N, BOC_2O, 12h RT, 93%, ii) Dry THF, Et_3N, Diphosgene, 12h RT, 90% , iii) Boc serotonin, dry DCM, 12h,90%, RT iv) dry DCM, CF_3COOH, 12h RT, 95%

Scheme 2

Synthesis of Lipid B

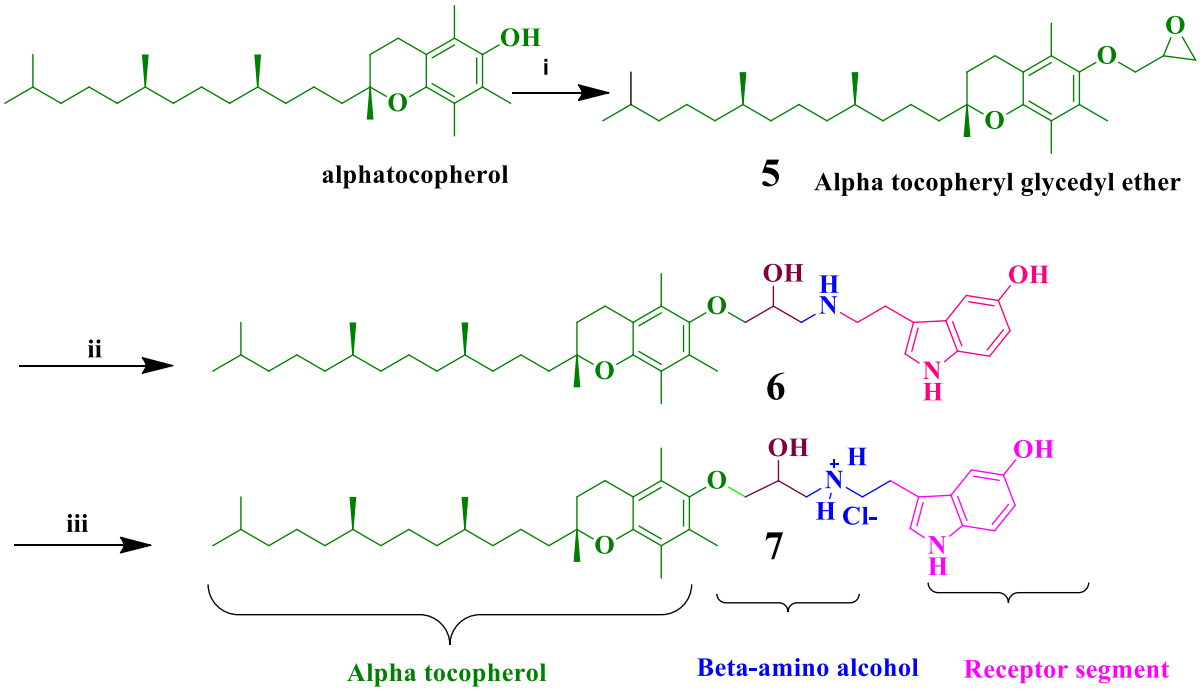

Regents: i) Epichlorohydrin, 50% KOH solution, tetra butyl ammonium hydrogen sulfate ($Bu_4N^+HSO_4$) and 5 h RT 96%, ii) Serotonin, -10 $^{\circ}$C, Et_3N, 12 h RT 70%, iii) Dry MeOH in HCl, 12 h RT 86%.

5.2.2 Physico chemical characterization

5.2.3 Preparation of Liposomes

Cationic liposomes were prepared with **Lipid A** (**-NH_2**) and **Lipid B (-OH)** by the dry lipid film hydration method as described[10] at varying molar ratios(0.5:1,1:1and2:1)and formulated with co-lipids DOPC and DOPE. Following thin film preparation and drying, lipids were hydrated in sterile water (or buffer at pH 7.4) and subsequently sonicated at room temperature for ~6 min. All the formulations i.e. **Lipid A: DOPE, Lipid A: DOPC, Lipid B: DOPE** and **Lipid B: DOPC** were observed to form stable uniform liposomal suspensions at 2:1 molar ratio. No precipitation was observed for 8 weeks following storage at 4 °C.

5.2.4 DNA binding ability of Lipid A and Lipid

To evaluate the extent of DNA binding, **Lipid A** and **Lipid B** formulated with co-lipids **DOPE** and **DOPC** were complexed with plasmid DNA and evaluated through agarose gel electrophoresis and heparin binding assays. Following electrophoresis, binding was observed at very low charge ratio of 1:1 in the case **Lipid A: DOPE, Lipid B: DOPE, Lipid A: DOPC** and **Lipid B: DOPC**. It was also observed that ~ >90% of plasmid DNA was bound at 2:1 and4:1N/P charge ratios. Complete bindingofDNAwasachievedat8:1 N/P charge ratio (**Figure 2A**) as seen by the retention of the lipoplexes in the well, indicating net neutrality of lipoplexes at the higher charge ratio. This was further supported by surface potential measurement of lipoplexes, **Figure 2B**, which indicates neutralization of negatively charged DNA upon the addition of cationic liposomal conjugates. **LipidA: DOPE, LipidB: DOPE, Lipid A: DOPC** and **LipidB: DOPC** were positive at low charge ratio of 1:1 (5-9 mV). Further increase was observed at8:1 charge ratio (28-30 mV) (**Figure 2B**). To further elucidate the strength of binding and stability, lipoplexes were treated with heparin, an anionic mucopolysaccharide, which competes with negatively charged DNA (**Figure 2B)**. As observed, binding efficiency of all the formulations were found to be similar (**Figure 2B**) even in the presence of heparin, indicating strong liposome-DNA interactions that are unaffected in the presence of heparin. The stability of the lipoplexes may also be attributed to the favorable hydrogen-bonding interactions between DNA and quaternary amine and hydroxyl functionalities present in the polar head group region of **Lipid A** and **Lipid B** respectively**.** Together these studies reveal that the formulations possess suitable attributes at 2:1 lipid/DNA charge ratios and hence considered optimal for *in vitro* DNA delivery applications.

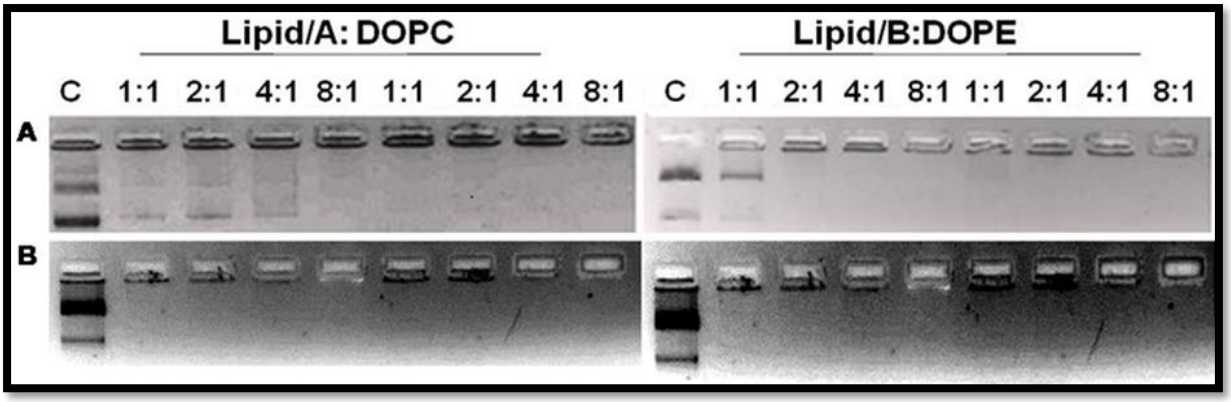

Figure 2 Gel-binding assays of lipids Lipid **A** and Lipid **B**. Electrophoretic migration patterns for liposome-pDNA in gel retardation assay in the absence **(**A) and presence of Heparin (B) in the displacement assay at indicated charge ratios. The details of the treatment are as described in the text.

5.2.5 **Characterization of lipoplexes**

As gene delivery is governed by parameters such as surface charge and size, we analyzed these aspects by measuring the zeta potential and hydrodynamic diameter through dynamic light scattering (DLS). Lipoplexes prepared with **Lipid A** and **Lipid B** formulated with DOPE or DOPC were in the size range of 180-190 nm. In comparison, formulations prepared with DOPC were 850-950 nm. These results suggest that the co-lipid may have an effect on the liposome dimension (**Figure 3A**). Lipoplexes with DOPE as the co-lipid were 400-800 nm in dimension at all charge ratios of (1:1-8:1). In contrast, formulations with DOPC were larger, measuring between 450-1250 nm. It was observed that this kinetic increase in lipoplex size at increasing lipid concentration may be due to polyanion induced aggregation[11]. The resultant increase at higher charge ratios may also possibly be due to the dilution of lipoplexes in bicarbonate ion enriched media during incubation[12]. Moreover, formulations of both **Lipid A** and **Lipid B**, at 2:1 charge ratios were < 500 nm, a dimension that may enhance uptake. Interestingly, at 2:1 charge ratio, both lipids formulated with DOPE were<300 nm. Surface charge of lipoplexes prepared with **LipidA** and **LipidB** (N/P) also measured, **Figure**

3A. Free cationic liposomes have a surface potential of <40mV and all the lipoplexes at the charge ratios tested (1:1to4:1) have a positive surface potential below 32 mV. At 8:1 charge ratios, all four lipoplexes displayed a surface potential of >35 mV, which suggests increase in the rate of condensation of DNA and positive surface charge upon lipid binding and as a function of charge ratio. Interestingly, the surface potential at 2:1 charge ratio measured < 9 mV.

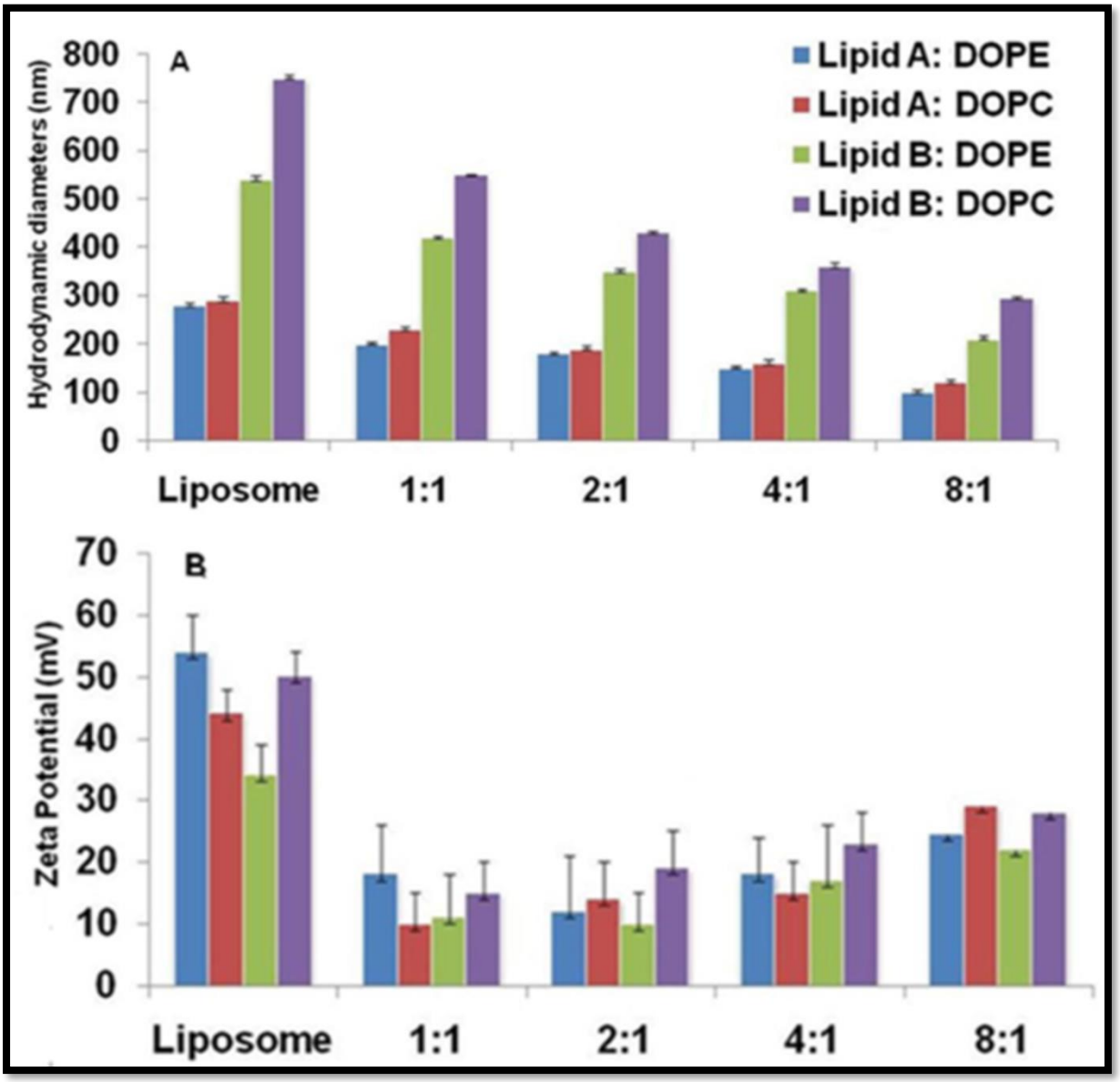

Figure 3. Graphical representations of hydrodynamic diameters (**A**) & Zeta Potentials (ξ, mV) (**B**) of the Lipoplexes in DMEM (without serum). Data represent mean ± SD (n = 3).Statistical analysis was performed by Two-way ANOVA.

5.2.6 Transient transfection: Target specificity of serotonin conjugates

We investigated the cell specificity and transfection potential of serotonin-α-tocopherol hybrid conjugate formulations through reporter gene expression assays using HEK-293T, Neuro-2a, and HepG2 cells **(Figure 4A)**. Cells were treated with lipoplexes that were prepared using **Lipid A** and **Lipid B** formulated with DOPE and DOPC using plasmid pCMVβ-gal DNA at charge ratios of 2:1and4:1, with Lipofectamine as the bench mark standard. Enhanced activity was observed at charge ratio 2:1 than at 4:1 with both formulations with DOPE as the co-lipid, (**Figure 4A**). Lipids formulated with DOPE were observed to be far more efficient than their DOPC counter parts. This may be due to smaller size of lipoplexes prepared with DOPE than DOPC. Moreover, when compared to **Lipid A**, **Lipid B** showed greater activity in all cells except HEK 293T.Comparingthestructuresof **LipidA** and **B**, the longer linker plus the exposed hydroxyl moiety of **LipidB** may evoke synergistic interactions as well as enantiospecific interactions with the DNA and cell membrane receptor for providing higher transfection rates. It was also observed that among HEK293T, HepG2 and Neuro-2a, the transfection efficiency mediated by both lipids in HEK293Tcells was maximal when lipids were formulated with DOPE. Moreover, compared to Lipofectamine 3000, both formulations showed higher transfection efficiency in HEK293T at 2:1 charge ratio. To further gain insight into the target specificity to 5-HT receptor, transfection assays were performed using T-CHO cells which express the serotonin receptors ($5\text{-}HT_{1A}R$)[13]. For comparison and as control, CHO cells were identically transfected in parallel. It was observed that both the lipids showed higher transfection efficiency when

formulated with DOPE than with DOPC (**Figure 4B**) as seen from enhanced reporter gene expression, which reiterates the role of auxiliary lipid DOPE in influencing the morphology and size of lipoplexes and subsequent internalization of nucleic acids. It was earlier observed that formulations that included serotonin lipid-conjugates mediated selective uptake of plasmid DNA in TCHO cells stably expressing serotonin receptors than CHO[14]. Subsequent experiments (**Figure4A**) further confirmed the target ability of **LipidA** and **Lipid B** which delineates that formulations of both the lipids demonstrate greater activity in T-CHO compared to CHO, due to higher (~14 times) greater receptor density in T-CHO cell lines[14b], Moreover, transfection mediated by lipoplexes prepared with **Lipid B**: DOPE exhibited ~2-2.5-foldhigheractivityin T-CHOandlipoplexespreparedwith**LipidA**:DOPEshowed1.5-2 fold higher efficacy compared to control (**Figure 4A**). Specific and efficient uptake of lipoplexesintoCHO-5-HT_{1A} R cells, were also conclusively demonstrated by flow cytometry studies (**Figure7**). Collectively, our results suggest the increased uptake of lipoplexes may have led to enhanced reporter gene expression specifically in TCHO cells, hence following the overall rank order **Lipid B:DOPE**>**Lipid A: DOPE**>**Lipid B**:**DOPC**>**Lipid A: DOPC** in mediating target-selectivity. The differential transfection potential of **Lipid A** and **B** indicate that the chemical structure of serotonin conjugate head group and linker length plays an important role in determining. The higher activity of **Lipid B** possibly denotes better hydrogen bonding of the exposed hydroxyl terminal of **Lipid B** in contrast to the N-H amide bonds of **Lipid A** and this promotes favorable head group conformation at specific binding sites on serotonin receptor to invoke higher vesicle internalization as well as transfection in serotonin receptor-enriched cells.

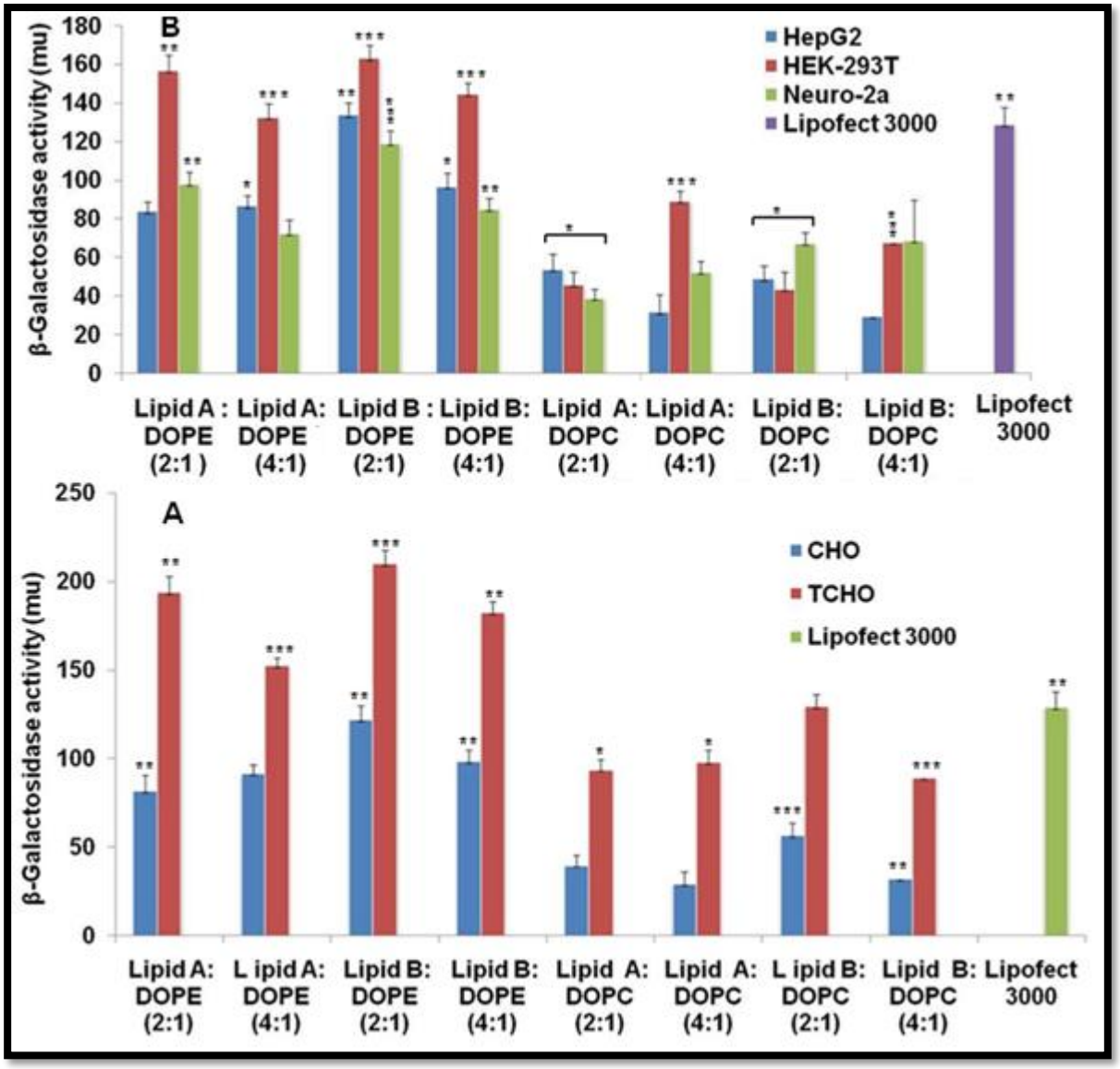

Figure 4. Transient transfection in vitro: TCHO, HepG2, CHO, Neuro-2a and HEK-293T cells were treated with **LipidA** and **LipidB** formulated with DOPE/DOPC using pCMVβ-Gal in the absence of serum. Statistical analysis was performed by Two-way ANOVA (*P<0.05, **P<0.01,***P<0.001).

Transfection w as also evaluated using pEGFP plasmid as the reporter gene encoding green fluorescence protein in HEK-293T and HepG2 cells using four formulations. (**Figure 5-6**) Following an incubation period of 48 h, cells were visualized by fluorescence microscopy and quantitated. Analysis of GFP expression revealed the superior efficiency of **Lipid B: DOPE**

compared to **Lipid A: DOPC** or **Lipid B: DOPC** and Lipofectamine, which in line with our aforesaid observations (**Figure 5 &6**).

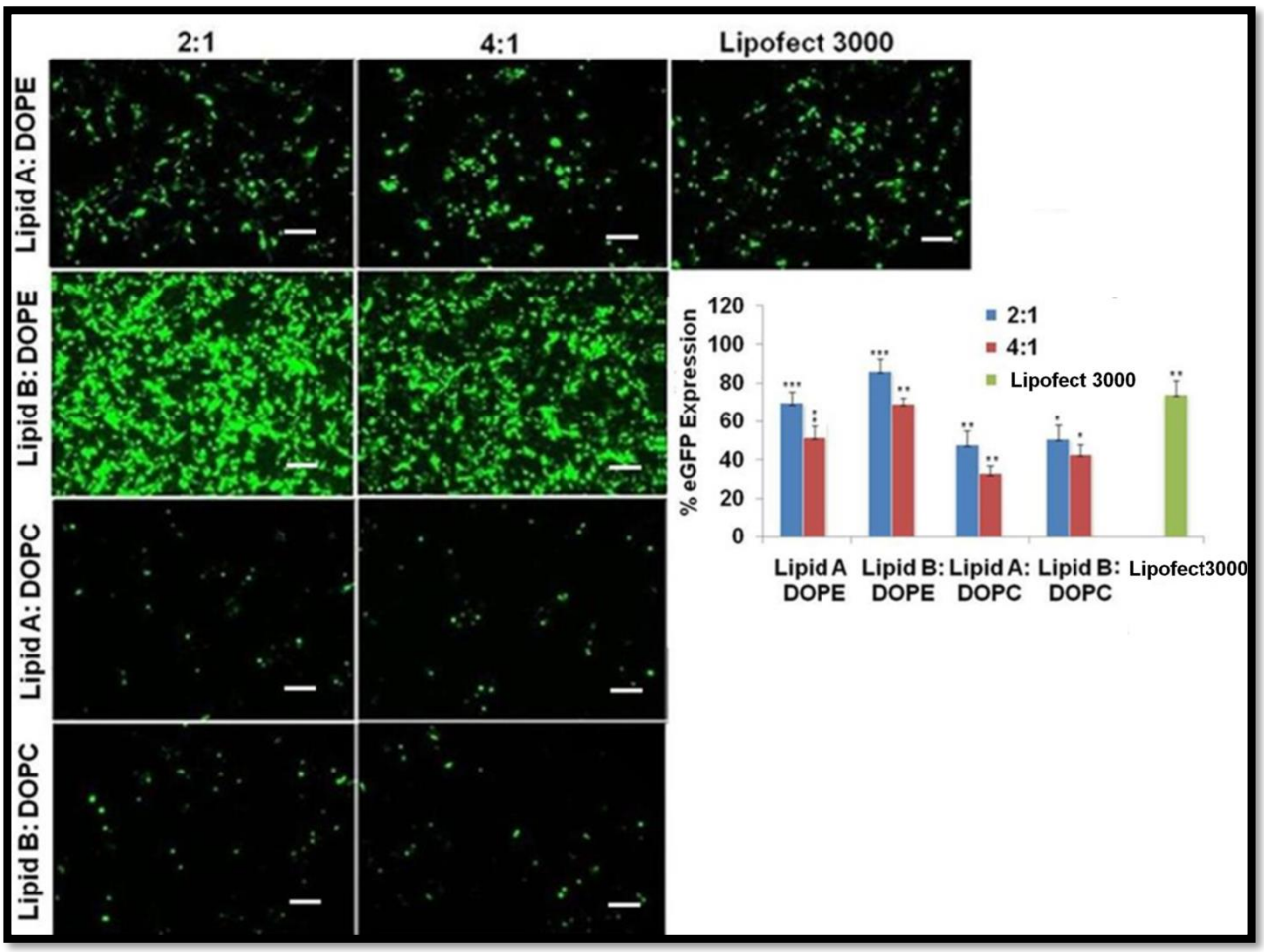

Figure 5. Transfection in HEK-293T cells. A) Images depict GFP fluorescence following transfection mediated by **Lipid A** and **Lipid B** formulations at charge ratios 2:1 and 4:1.Lipoplexes were prepared and incubated with HEK-293T cell lines for 4 h in presence of 10% serum subsequently replaced with complete medium and images acquired by fluorescence. Microscopy 48 h post transfection B) Representative graph depicts the transfection efficiencies in terms of percentage GFP positive cells. Statistical analysis was performed by Two-way ANOVA (*P<0.005, **P<0.01, ***P<0.001) (Magnification/scale Bars = 100 μm.)

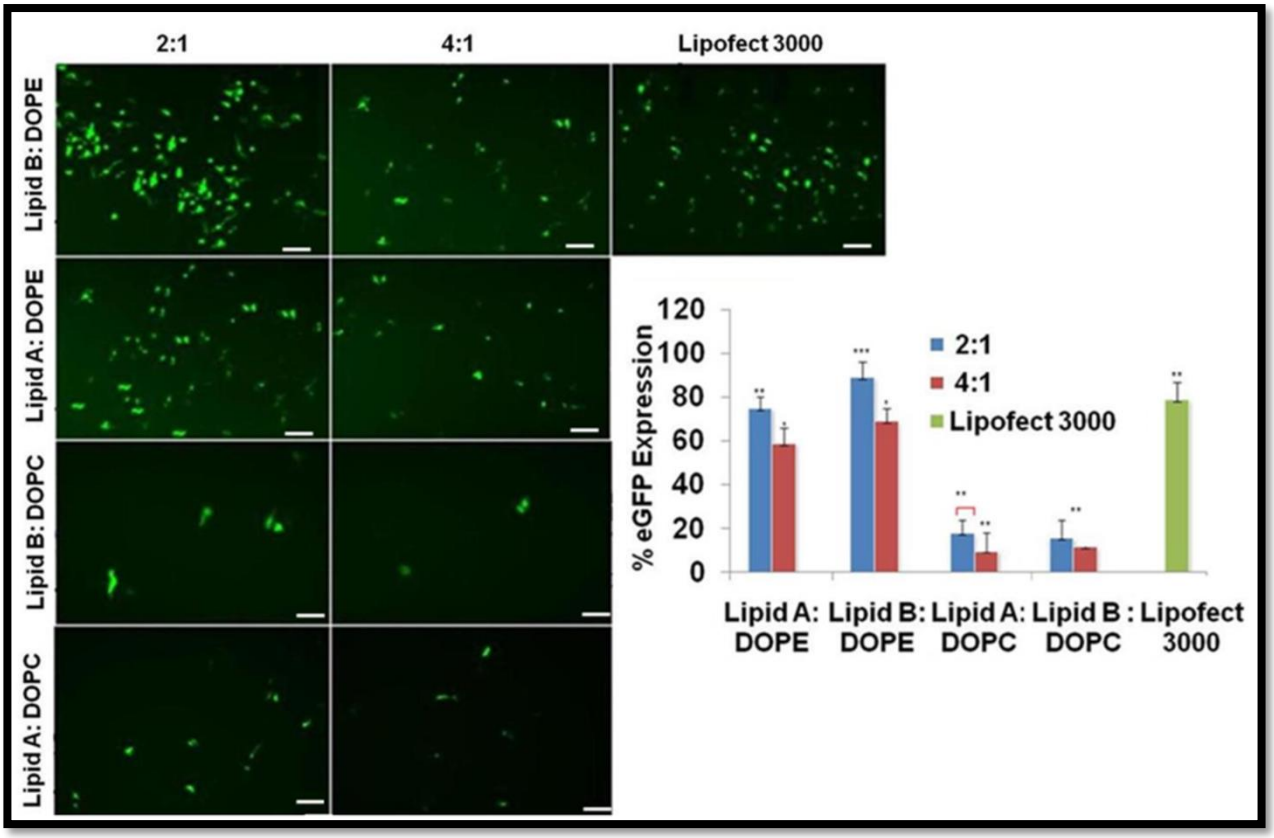

Figure6.Transient transfection in HepG2 cells using plasmid DNA pEGFP: A) Representative fluorescence images depicting GFP expression DNA at charge ratios 2:1 and 4:1.Lipoplexes with either DOPE or DOPC (1:2) was prepared. Cells were treated and incubated for 4 h in presence of 10% serum later changed to complete media and incubated for 48 h. Images were acquired 48 h post transfection). Representative graph depicts the transfection efficiencies in terms of percentage GFP positive cells. Statistical analysis was performed by Two-way ANOVA (*P<0.05,*P<0.01,***P<0.001). (Scale Bars=100µm)

5.2.7 Cellular uptake study of Lipid A& Lipid B:

As transfection efficiencies are directly linked to the extent of internalization, we then monitored uptake behavior of lipoplexes prepared with **Lipid A: DOPE, Lipid B**: **DOPE**, **Lipid A: DOPC** and **Lipid B: DOPC** in both TCHO (CHO-5-HT_{1A}R) and CHO cells. Cells were incubated with lipoplexes labeled with Rhodamine-PE and complexed with *p*CMV-β-gal plasmid at 2:1 charge ratio for 4 h. Following uptake, cells displaying fluorescence were analyzed and quantified. It was observed that fluorescence was maximal in

TCHO cells with **Lipid B: DOPE** (**Figure 7),** following the rank order: **Lipid B: DOPE**>**LipidA**: **DOPE**>**LipidB**: **DOPC**>**LipidA: DOPC.** We believe that particle sizes of lipoplexes may play a vital role in facilitating cell uptake. This is evident from data obtained with **LipidB: DOPE** where the size at 2:1, being the lowest, may contribute to its high activity. The other reason for these observations is the presence of the β-hydroxyl linker functionality in its spacer region in **Lipid B** that may promote hydrogen bonding interactions with the serotonin receptor [15]leading to higher transfection

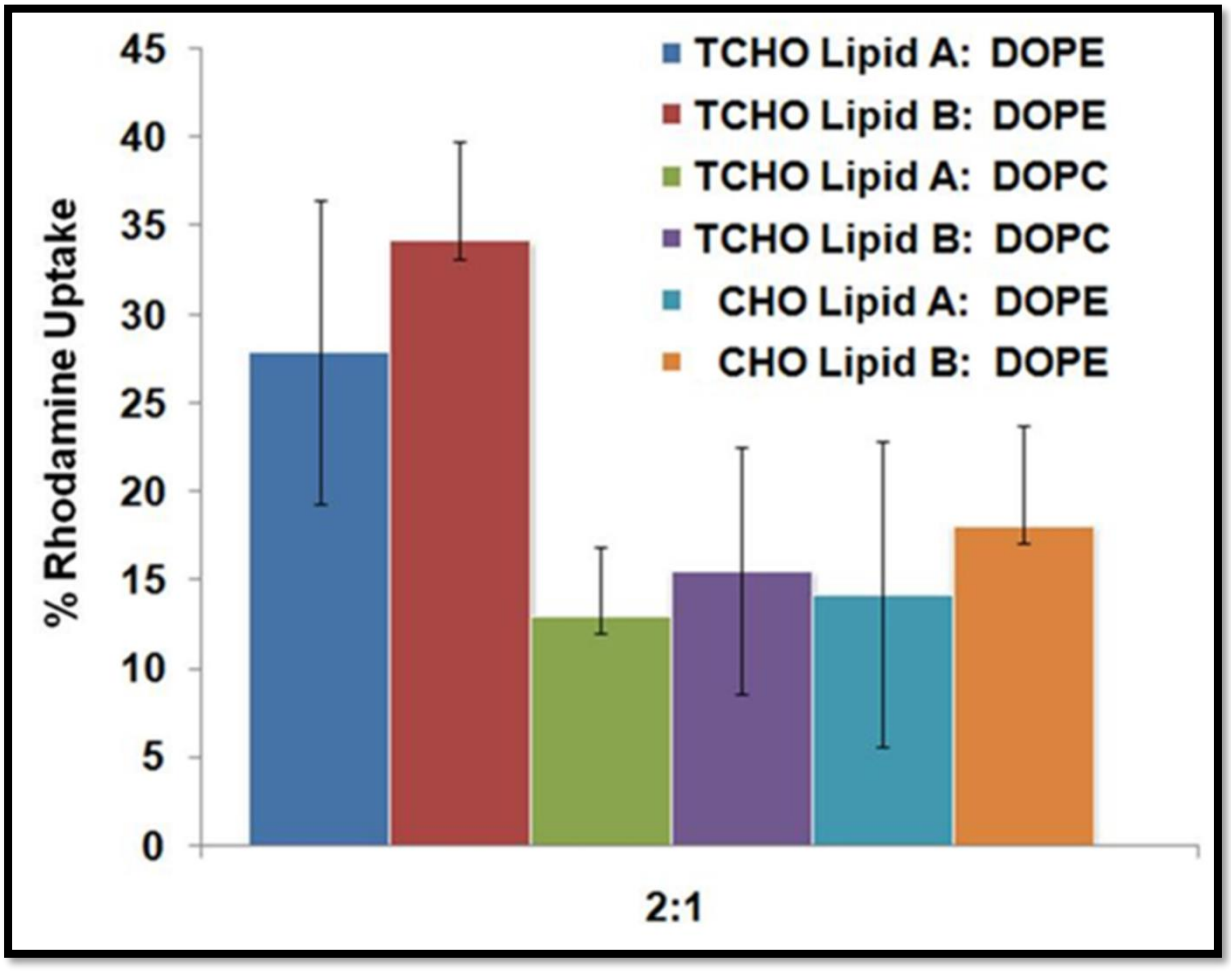

Figure7. Quantitative uptake of rhodamine-labeled lipoplexes prepared with **Lipid A** and **Lipid B** formulated with DOPE and DOPC using pCMV-β-gal plasmid DNA at 2:1charge ratio in TCHO &CHO cells. Cells were incubated for 4h following measurement of rhodamine uptake by flow cytometry. Statistical

analysis was performed by Two-way ANOVA ($P<0.005$). The details of the experiments are as described in the text.

5.2.9 Effect of serum on transfection mediated by Lipid A and Lipid B

One of the major drawbacks of cationic lipids, being positively charged, is the lack of stability in serum which hinders its use in *in-vivo*. This is believed to be due to the fact that transfection activity of cationic lipids decreases drastically upon interaction of negatively charged serum proteins eventually hampering the efficient interaction with cell surface leading to reduced internalization of lipoplexes[16]. Hence, there is a need to develop strategies that foster the stability of lipoplexes in serum. Unfortunately, the details of lipoplex-serum interactions are still poorly understood. In order to investigate stability of the conjugates under study, **Lipid A** and **Lipid B** formulations, were evaluated in the presence of increasing amounts of serum in CHO, TCHO, HepG2 and Neuro- 2a cells. Reporter gene expression assays, in the presence of serum with lipids formulated with DOPE led to enhancement in transfection efficiency. In contrast, formulations with either **Lipid A** or **Lipid B** with **DOPC**, the activity was drastically reduced (**Figure 8**). We surmise that negatively charged serum proteins upon interaction within lipoplexes prepared with DOPE may alter the morphology favourably following aggregation of lipoplexes. Moreover, size-dependent uptake of lipoplexes and the increase in transfection efficiency in serum may arise due to the serum-induced switch from a clathrin- dependent to a caveolae-mediated mechanism of lipoplex internalization[17].

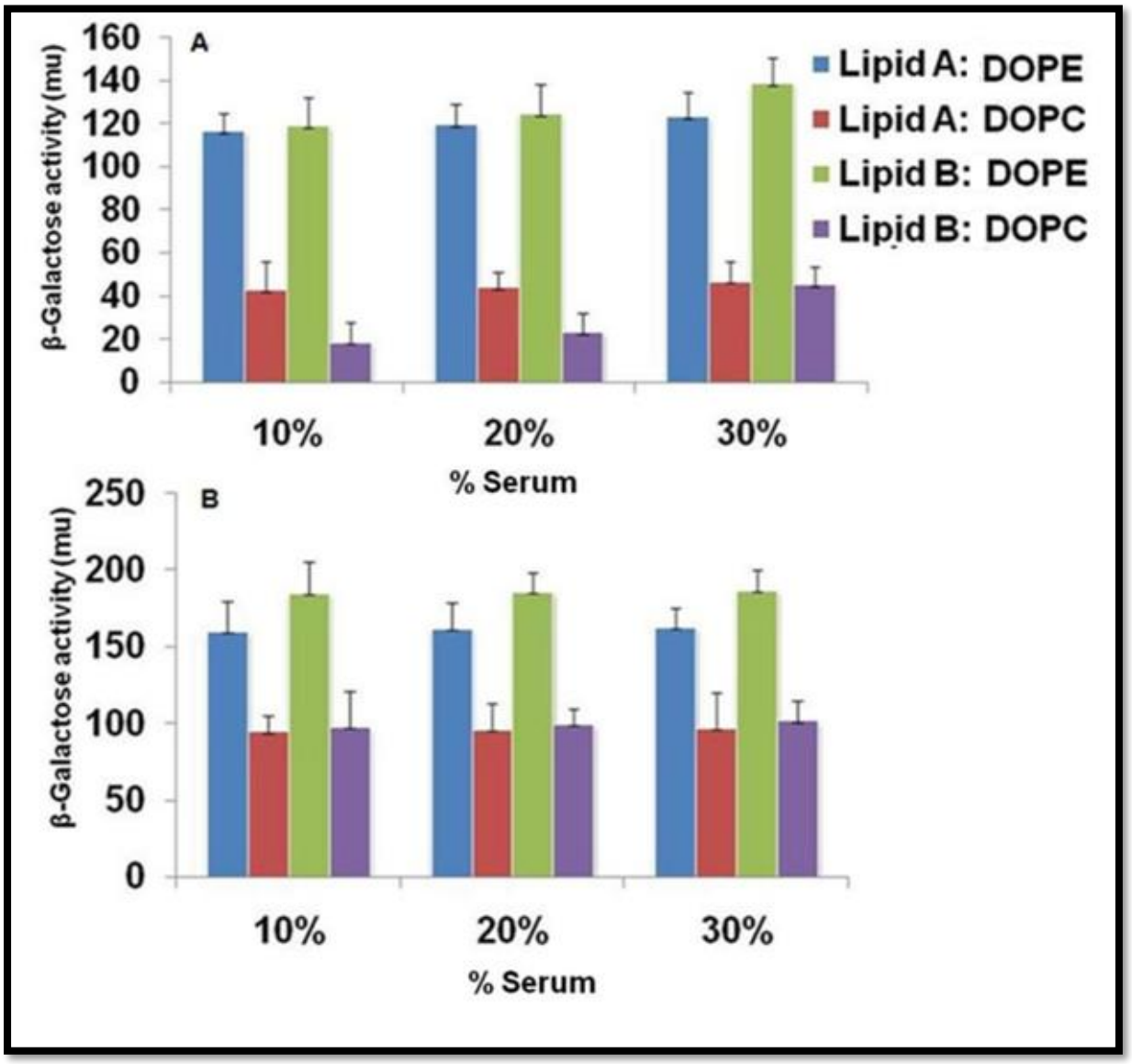

Figure 8.Transfection in the presence of serum. Lipoplexes prepared with **LipidA and Lipid B** in the presence of increasing concentrations of serum in (A) CHO (B) and TCHO. *In vitro* transfection efficiencies of formulations prepared using pCMV-b- Gal at charge ratio of 2:1. The error bar indicates that the standard error. The difference in the data obtained is statistically significant in all charge ratios ($P < 0.003$).

5.2.10 Intracellular trafficking

Poor intracellular trafficking is often associated with limitations such as size and hydrophilic nature of formulations that affect the transfection efficiency. Also, size of lipoplexes having a

direct bearing on internalization and affects transfection by impeding movement across the plasma. Friend and Labat-Moleur et al. established endocytosis as the major mechanism [18]for the cellular entry of non-viral vectors. Following endocytosis, internalized lipoplexes tend to be trapped in intracellular vesicles that eventually fuse with lysosomes and are degraded [18] .To overcome these problems, strategies that circumvent clathrin-mediated endocytosis can be used to deliver DNA [17, 19]. Our observations encouraged us to explore this aspect by evaluating their entry mechanisms using various inhibitors, **Figure 9.** Towards probing the internalization mechanism of lipoplexes prepared with **Lipid A** and **Lipid B**, cells were pre-treated with inhibitors namely chlorpromazine a clathrin pathway inhibitor, filipin-III,acaveolae pathway inhibitor and m-β-cyclodextrin, cholesterol depletion/clathrin and caveolae pathway inhibitor prior to transfection with **LipidA** and **Lipid B** formulations. Gene expression results clearly indicate uptake of lipoplexes occurs predominantly *via* clathrin path way (**Figure 11**).

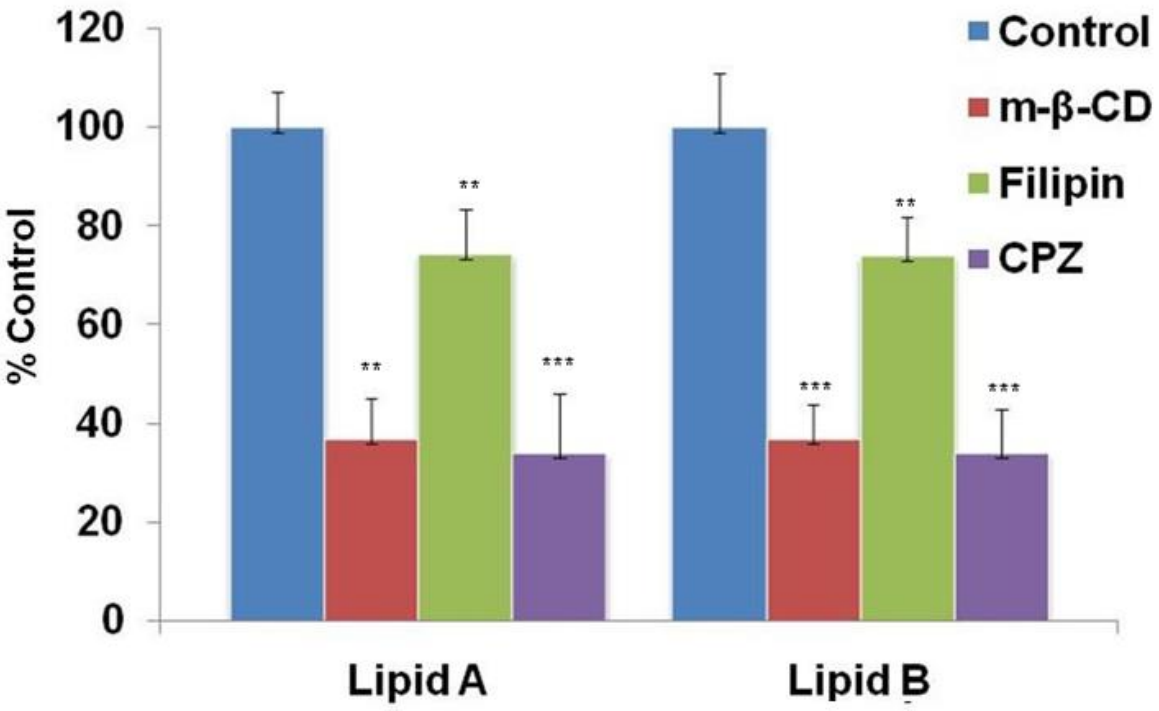

Figure. 9. Transfection using pEGFP plasmid (0.8µg/well)in HepG2 cell line in the presence of endocytosis inhibitors: Normalized % of GFP +ve cells were obtained from GFP

fluorescent quantification of three individual experiments 48 h of post transfection. Cells were pretreated with the inhibitors (control: sky blue), methyl-β-cyclodextrin (m-β-CD, 10 µg mL^{-1}orange),Filipin-III(5µgmL^{-1}blue)and chlorpromazine(CPZ,10µgmL^{-1}green)for1h prior to lipoplex addition. Cells and incubated for further 4 h after treatment with lipoplexes. Statistical analysis was performed by Two-way ANOVA (**P<0.01,***P<0.001).

5.2.11 Intracellular trafficking

The size of lipoplexes has a direct bearing on internalization and most of the non-viral gene delivery vectors developed impede movement across the plasma membrane because of their large size and hydrophilic nature of formulations, rendering them transfection incompetent. A friend and Labat-Moleur et al. reported that endocytosis has been established as the major mechanism[25] for the cellular entry of non-viral vectors. Following endocytosis, internalized lipoplexes tend to be trapped in intracellular vesicles that eventually fuse with lysosomes and eventually degrade[25] (Bally et al., 1999).To avoid problems associated with endocytosis, other specific receptor sites strategies can be used to deliver pDNA in a manner that circumvents clathrin-mediated endocytosis[26](Dokka and Rojanasakul, 2000). Poor intracellular trafficking is often associated with these limitations that affect the transfection efficiency. The aforesaid results of formulated α-tocopherol-serotonin hybrid cationic lipids further encouraged us to explore their cellular entry mechanism, **Figure 11.** Towards probing the internalization mechanism of lipoplexes of **Lipid A** and **Lipid B**, the cells were pre-treated for 1 h with various inhibitors namely chlorpromazine (Braeckmans K andVercauteren D, 2010), a clathrin pathway inhibitor, filipin-III, a caveolae pathway inhibitor and m-β-cyclodextrin, a cholesterol depletion/clathrin and caveolae pathway inhibitor and transfected with the lipoplexes of **Lipid A** and **Lipid B**. Our results clearly indicate uptake of lipoplexes *via*clathrinpathwaythan the caveolar pathway, (**Figure 11**) which indicates that these lipoplexes are sensitive to cholesterol depletion. The results clearly suggest that internalization *via* a clathrin-independent mechanism significantly contributes to the efficient internalization of **Lipids A** and **B** lipoplexes.

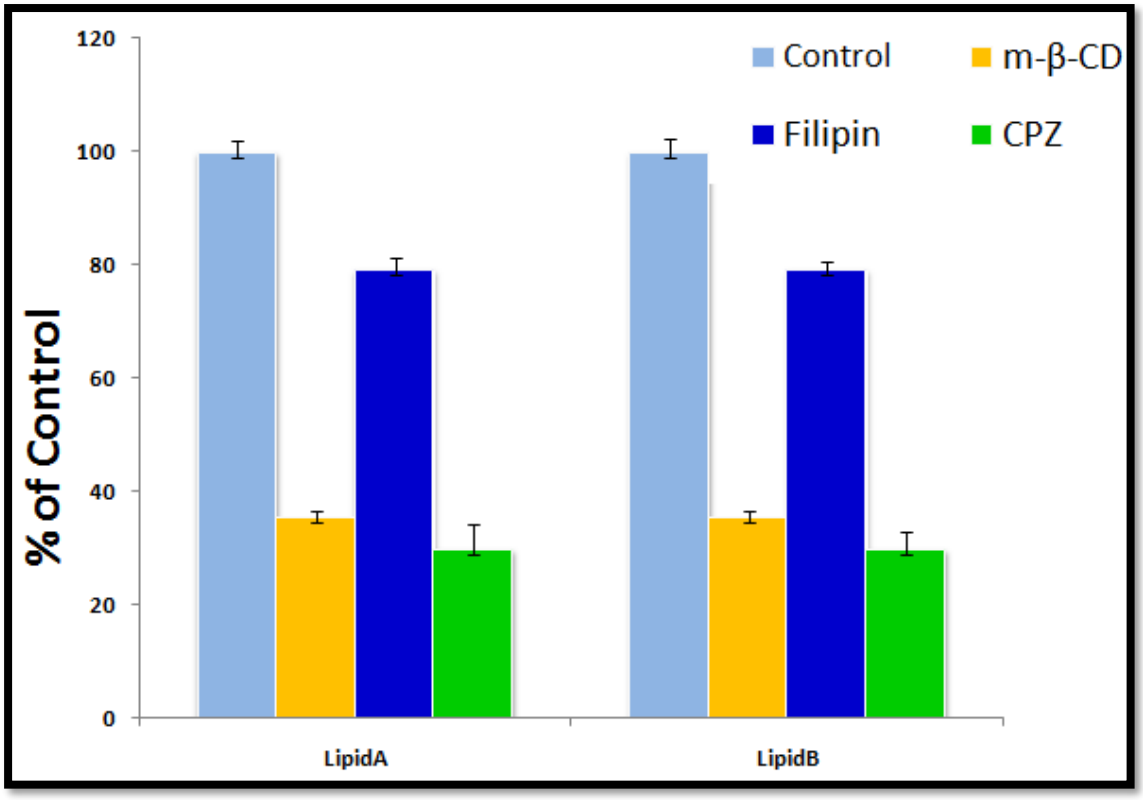

Figure.11 Transfection using pEGFP plasmid (0.8 µg /well) in HepG2 cell line in the presence of endocytosis inhibitors: Normalized % of GFP +ve cells were obtained from GFP fluorescent quantification of three individual experiments at 48 h of post-transfection. Cells were pretreated with the inhibitors (control: sky blue), methyl-β-cyclodextrin (m-β-CD, 10 µg mL^{-1} orange), Filipin-III (5µg mL^{-1} blue) and chlorpromazine (CPZ, 10 µg mL^{-1} green) for 1 h prior to lipoplexes aaddition. Lipoplexes were added to cells and incubated for further 4 h. Statistical analysis was performed by Two-way ANOVA (**P<0.01,***P<0.001).

5.2.12 Evaluation of ROS levels:

Cancer cells constantly generate high levels of reactive oxygen species (ROS) leading to non-specific damage of protein and consequent cell death. Moreover, ROS level can induce lipid peroxidation and disrupt the membrane lipid bilayer structure that inactivate the membrane-bound receptors. In addition, cationic lipids are known to induce ROS levels [20] that could trigger the necroptosis cascade. The diverse pharmacological properties of α-tocopherol and

their anti- oxidant properties have been established. Along with, the indole amine derivatives, serotonin possesses strong antioxidant and radical scavenging activity. In combination with surface active phospholipids such as DOPC and DOPE may induce cooperative antioxidant potential through the regeneration of tocopheryloxyl radical [21]. To examine this property, we conducted a fluorescence-based assay using HEK- 293T cells and dichlorofluorescin diacetate (DCFDA) as the fluorescent probe and tested the ability of **Lipid A** and **Lipid B** in ROS quenching. N-acetyl cysteine (NAC), a powerful antioxidant was taken as a negative control. Piperlongumine, a ROS inducer and enhancer of ROS levels, was used as a positive control. Lipoplex formulations of **Lipid B: DOPE** induced maximum ROS quenching at 2:1 charge ratio when compared to **Lipid B**: **DOPC, Lipid A**: **DOPE** and **Lipid A: DOPC** complexes at 2:1 charge ratio, **Figure 10**. The greater ROS quenching potential of **Lipid B** formulated with DOPE is not surprising as the primary amine head group of DOPE but not DOPC, increased the anti-oxidant activity of alpha-tocopherol by regeneration of the alpha-tocopherol quinone. Besides, antioxidant and membrane binding properties of serotonin protect lipids from oxidation. This indicates that the quenching, which relies on the size of the lipoplex, may compromise cellular uptake of lipoplexes, thereby resulting in reduced activity. In comparison, the functional **Lipid A: DOPE** and **Lipid A: DOPC** complexes showed a moderate decrease in the ROS levels which substantiates the efficient ROS quenching attribute of **Lipid B**: **DOPE**.

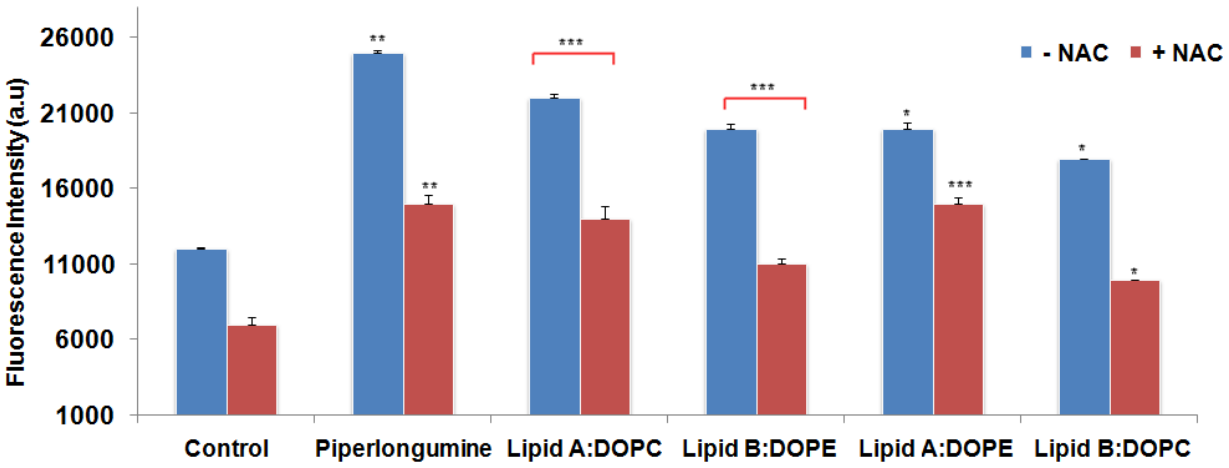

Figure.10 ROS Assay in HEK-293Tcells following treatment with liposomal formulations by flow cytometry. *In vitro* ROS measurement was carried using DCFDA fluorescence assay. Statistical analysis was performed by Two-way ANOVA (*P<0.05, **P<0.01,***P<0.001).

5.2.13 Toxicity studies

Cell viability being a major limiting factor for biological applications, we next evaluated the toxicity of **Lipid A** and **Lipid B**. This is with the anticipation that the conjugate will retain the potent anti-oxidant properties while reducing the toxicity, leading to an increase in cell viability upon transfection in vitro. CHO, TCHO, HepG2, HEK-293T and Neuro-2acellswere plated as described in the methods and then examined using MTT (**Figure11**). This was followed by further incubation in serum for 48h.As seen in **Figure 12;** more than 85%cells were viable at charge ratio 4:1. At higher charge ratio 8:1, > 70% of cells were viable (**Figure 11**), which indicates that difference observed in the transfection assays are unlikely to originate from lipid toxicity and that the α-tocopherol-serotonin hybrid based formulations, when compared to Lipofectamine 3000, are non-toxic. The presence of biodegradable carbonate and β-hydroxy based linker group may have further contributed to reduction in toxicity and transfection efficiency compared to Lipofectamine 3000.

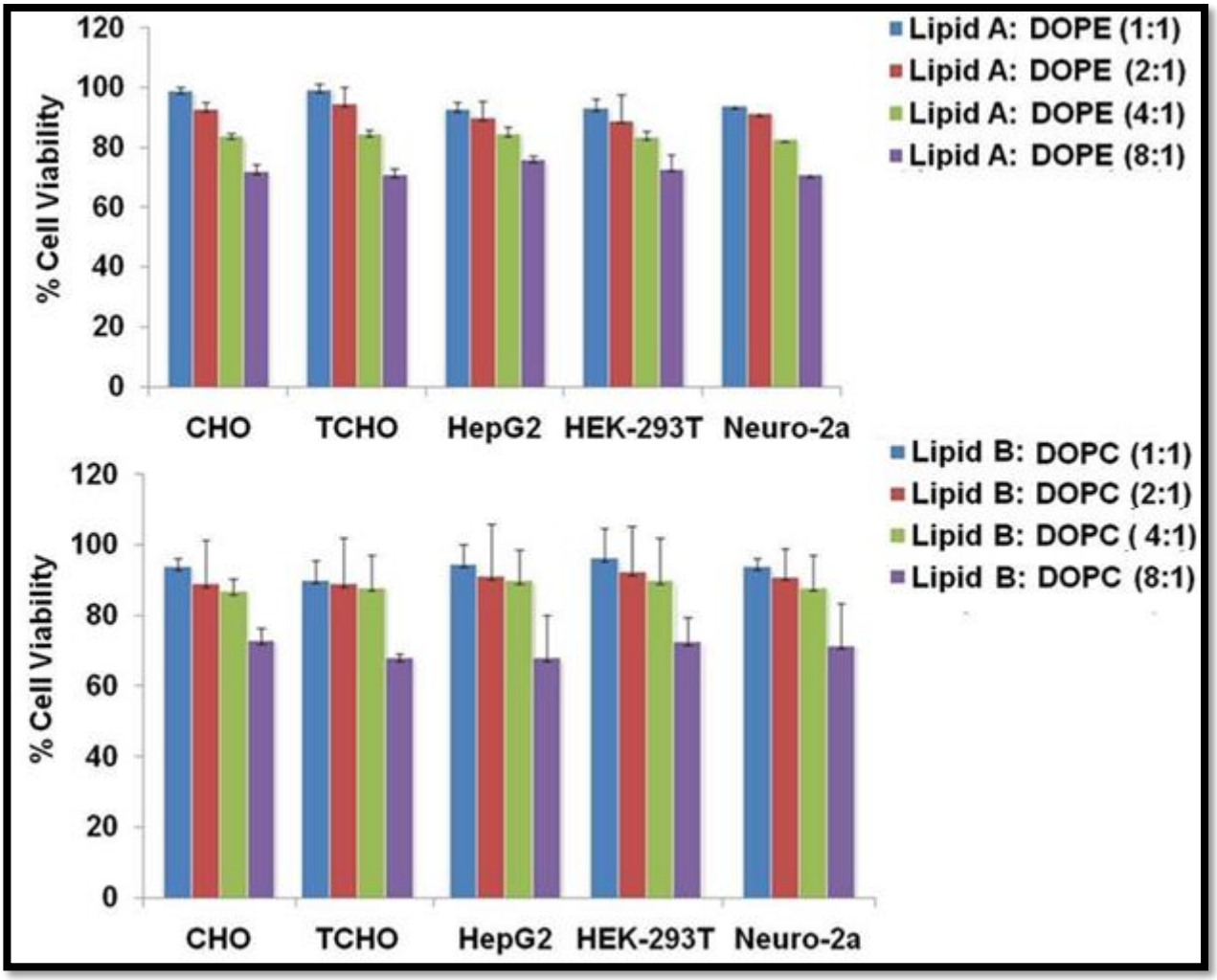

Figure 11. Tetrazolium-based colorimetric assay (MTT assay). Graph represents % viability of cells treated with **Lipid A** (A) and **Lipid B** formulations (B) Lipoplexes were prepared using the plasmidDNA(0.3μg/well) across the charge ratios ranging from2:1to8:1.The data obtained is the average values of three independent experiments(n=3).Statistical analysis was performed by Two-way ANOVA ($P<0.001$).

5.2.14 Molecular Docking studies

Having demonstrated the potential of **Lipid A** and **Lipid B** to mediate receptor-specific gene transfection, we then examined the binding mode of the lipids to the endogenous neurotransmitter serotonin through molecular docking studies *in silico*. Also, lack of structural information of serotonin1A receptor (5-HT_{1A})[22]motivated us to evaluate the binding geometry of the conjugates upon interaction with the corresponding receptor, however using well-known available structures of serotonin and5-HT_{1B} receptor that has 39% sequence similarity with that of 5-HT_{1A}**(Figure13**).This was implemented in Maestro (version9.2,Schrödinger,LLC, New York, NY, 2011) and the most favorable binding conformations of the docked complex from these analyses were selected. Glide scores obtained from these studies as depicted in **Table 1**, enable the estimation of binding affinity of the ligand conjugated to **Lipid A** and **Lipid B** with the receptor[23].

Table1: Glide scores obtained through docking studies

Compound	**Glide score (kcal/mole)**
Serotonin	-5.7
Lipid A	-10.9
Lipid B	-4.9

Figure 12. Sequence alignment of serotonin-1A receptor with serotonin-1B receptor shows goodsimilarityinthetransmembraneregionsofthetworeceptors.Theseare theregionswhich contain the conserved residues Y109, D129, T134, F331 and F332, involved in the binding of serotonin. A structural alignment of serotonin-1B (PDB id: 4IAR) and a model structure of serotonin-1A shows a good superposition of the two structures in the transmembrane regions, with an RMSD of3.03A^{o}.

(A) **(B)** **(C)**

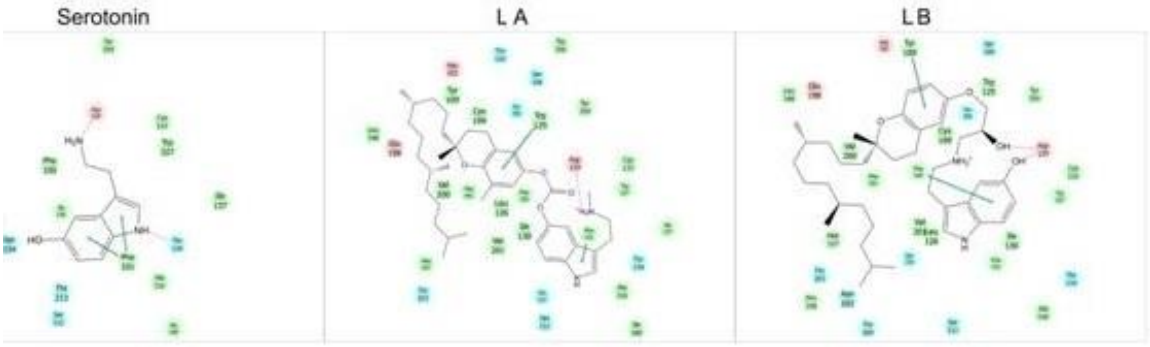

Figure 13. 2D Ligand-receptor interaction diagram of A) Serotonin, B) **Lipid A** and C) **Lipid B** making optimal interactions with serotonin receptor. The dotted lines indicate hydrogen bond interactions and solid lines indicate π-π stacking interactions.

Studies reveal that **Lipid A** exhibits greater affinity to serotonin receptor than **Lipid B, Table 1.** Interestingly, the **Lipid B** and serotonin having similar G scores suggest similar binding affinity. Additionally, interaction of the ligand to the active site ontherecepto risconservedandwhereAsp129, Thr134 and Phe331 were shown to interact with serotonin as reported earlier[24][29]**Figure 12**and **Figure 13**. The indole ring of serotonin molecule displays π-π stacking interactions with Phe 331and N-H of pyrrole, there is hydrogen bonding with Thr134and free-NH_2groupwithAsp 129 (**Figure 13A**). Pyrrole ring in **Lipid A** was shown to have π-π stacking interactions with Phe331and fused tetra hydropyran with Trp125 along with hydrogen bond interactions of free amino ethyl group with Asp 129 (**Figure 13B**). Phenyl group of indole ring in **Lipid B** was shown to have π-π stacking interactions with Phe 330 and fused tetrahydropyran with Tyr

109 and 5-hydroxyl group of indole and hydroxyl group in linker was shown to have hydrogen bondinteractionswithAsp129(**Figure13C**).The involvement of hydroxyl group of serotonin moiety may favour hydrogen bonding interactions with the receptor, in accordance with the reported mutational and modeling studies[25] where serotonin$_{1A}$ receptor prefers ligands with hydrogen bond acceptor at a position corresponding to the hydroxyl group in serotonin. The docking studies similarly show that **Lipid B** with the free hydroxyl group is available for interaction with serotonin$_{1A}$ receptor, (**Figure 13)**. The present study also offers a unique insight into how a differentially tethered serotonin head group to the lipid tocopherol affects the overall receptor binding and efficiency, signifying that higher G scores may not be an indicator of biological activity observed. Here, the differential conjugation of serotonin to tocopherol enables the formulation of two different lipids similar in all structural components but differing in the functional moiety freely present in the distal end of the head group. The significance is that the activity differences between **Lipid A** and **B** could be directly linked to the presence of either amino or hydroxy terminal or their subsequent interactions with the 5-HT1a receptor promoting sequential adhesion, endocytosis and transfection. Earlier agonist binding studies of 5-HT1a receptor indicated the involvement of ion-pair formation between the protonated amino group as well as the hydroxyl group of serotonin with the aspartate or serine/threonine residues of the 5-HT1a receptor respectively [26] which sheds light on the significance of both the functional group in serotonin-receptor interactions. However when formulated with the co-lipid DOPE, multiple parameters determine the receptor binding affinity such as the liposomal surface structural reorganization (liposome-ligand length from receptor), flexibility of the tethered ligand to overcome the hydrodynamic drag force of the solvent on the liposome, receptor segregation induced by ligand adhesion and plasma membrane deformation induced by curvature of the

respective liposomes[27]. Comparative transfection studies of the formulations showed greater activity in the cells examined except in HEK293T. These findings suggest the involvement of phenolic hydroxyl group of serotonin moiety in the hydrogen bonding interactions with the receptor. This is also in accordance with earlier mutational studies wherein the involvement of reactive hydroxyl was first demonstrated[26] by Ho et al. 1992. Subsequent mutational studies together with molecular modeling also demonstrated preference of serotonin$_{1A}$ receptor to ligands corresponding to hydroxyl group in serotonin [27] Taking cues from these studies, in a different approach, Gopal et al., covalently conjugated serotonin to DSPE- PEG – 2000 to the amino group to reconstitute formulations to mediate selective targeting [14a, 28] (Gopal etal.2011). In this study, computational simulations of serotonin, reported here provide insights into the binding mode of the ligand to the receptor. The modeling studies (**Table I**, **Figure13A-C**) show that free ligand serotonin and **LipidB** with the free hydroxyl group that is available for interaction with serotonin1$_A$ receptor prefer ligands with a hydrogen bond acceptor have similar Gscore predicts similar binding mode when compared to **LipidB**. This is also validated through our experiments wherein transfection of **Lipid A** is surpassed by that of **Lipid B** influenced by co-lipid DOPE. Docking studies reveal that **Lipid A** has a higher affinity than **Lipid B**, and in vitro studies showed greater activity with **Lipid B**. It is possible that a conformational change in the receptor could arise from the differential binding orientation of the tethered ligands (**amino** vs **hydroxyl**). The results indicate that both the amino and hydroxyl tethered serotonin conjugated liposomes interacted with the same active site of 5-HT1a receptor similar to native serotonin, thus promoting transfection. Importantly, this explains the higher transfection rate of **LipidB** and scope for further development of non- viral vectors for nucleic acid delivery to the central nervous system.

Conclusion

Our studies conclusively demonstrate the efficacy and utility of the designed and developed tocopherol formulation i.e. **Lipid B:** DOPE for targeted delivery of nucleic acids. The methodology, in principle, may be applicable for targeted delivery of nucleic acids in vitro to neuronal cells and cancer cell lines that express serotonin receptors. Additionally supported by molecular docking studies, **Lipid B** with the hydroxy functionality exhibits specific targeting with higher transfection efficiency *in vitro* and serum compatibility thus having considerable scope for the development of non-toxic tocopherol formulations for targeted *in vivo* applications.

5.4 Experimental section

5.4.1 General procedure and chemicals reagents

Mass spectral data were acquired by using a commercial LCQ ion trap mass spectrometer (ThermoFinnigan, SanJose, CA, U.S.) equipped with an ESI source.^{1}H NMR and ^{13}C NMR spectra were recorded on a Varian FT400 MHz NMR spectrometer. Serotonin and α-Tocopherol were purchased from Sigma Co. Super negatively charged eGFP plasmid, and rhodamine-PE were ample gifts from IICT (Indian Institute of Chemical Technology, Hyderabad, India). Lipofectamine-3000 was purchased from Invitrogen Life Technologies, polyethylene glycol 8000, and o-nitrophenyl-β-D-galactopyranoside (pDNA) were purchased from Sigma (St. Louis, MO, U.S.). NP-40, antibiotics, and agarose were purchased from Hi-media, India. 1,2-dioleoyl-*sn*-glycerol-3-phosphoethanolamine (DOPE) and DOPCwere purchased from Fluka (Switzerland). Unless otherwise stated, various organic solvents including, pyridine, triethylamine, methanol, methylene chloride (DCM), phosphomolybdic acid spray reagent, epichlorohydrin, and potassium hydroxide (KOH) were purchased from Sigma-Aldrich Co. and were used without further purification. The progressive of the reaction was monitored by thin-layer chromatography using 0.25 mm silica gel plates. Column chromatography technique was executed with silica gel (Acme Synthetic Chemicals,

India; finer than 200 and 60-120mesh). Elemental analyses were performed by High-Resolution Mass Spectrometry (HRMS) using QExactive equipment (Thermo Scientific) and purity of lipids wascharacterized by HPLC (Shimadzu LC Solution) and showed more than 95% purity. HepG2, CHO, Neuro-2a and HEK-293T cells were procured from the National Centre for Cell Sciences (NCCS), Pune, India. The cellwas grown at 37 ˚C in Dulbecco's modified Eagle's medium (DMEM) with 10% FBS in a humidified atmosphere containing 5% CO2 / 95 % air.

Synthesis of tert-butyl (2-(5-hydroxy-1H-indol-3-yl) ethyl) carbonate from serotonin (1, Scheme 1)

1.0 g of serotonin hydrochloride (4.7 mmol) in dry methanol solution was taken in aflame-dried Schlenk flask under an argon atmosphere. To this triethyl amine (1.51 mL, 10.3 mmol) was added and the solution is cooled to 0°C. Boc_2O (1.54 g, 7.05 mmol) dissolved in methanol was added drop wise to the above solution. After 3 h of stirring, the resulting mixture was quenched with water, transferred to a separation funnel, and extracted three times with DCM. The combined organic phases were dried (Na_2SO_4), filtered under suction, and concentrated in vacuum. The product was purified by column chromatography (EtOAc / pentane 1:1) and isolated as a yellow solid (1.21 g, 4.38mmol, 93%).

^{1}H NMR (400 MHz, $CDCl_3$) : δ 8.05 (s, 1H), 7.25 (d, J = 8.8, 1H), 7.06 (d, J = 1.8, 1H), 7.00 (s, 1H), 6.90 (dd, J = 2.4, 8.8, 1H), 6.33−5.96 (m, 1H), 5.45 (dq, J = 1.6, 17.3, 1H), 5.29 (dq, J = 1.4, 10.5, 1H), 4.65 (brs, 1H), 4.59 (dt, J = 1.4, 5.3, 2H), 3.63−3.30 (m, 2H), 2.91 (t, J = 6.5, 2H), 1.44 (s, 9H). 13C NMR (100 MHz, CDCl3): δ 156.2, 152.7, 133.9, 131.8, 127.6, 123.1, 117.3, 112.6, 112.3, 112.0, 102.2, 79.2, 69.9, 40.9, 28.4, 25.7. ESI Mass m/z: - 299.

Synthesis of Tocopheryl chloroformate from Tocopherol (2, Scheme 1)

To a 250 mL of round bottom flask 1g of (+/_)-α-tocopherol in 10 mL dry THF, 0.2 mL of NEt_3 was added, stirred for 10 minutes and then 0.5 mL of diphosgene in dry THF was added drop wise with pressure equalizing funnel about 30 minutes at 0°C. The reaction mixture was stirred overnight. Charcoal was added to reaction mixture, stirred for 10 minutes and then filtered. The solvent was removed under rotary evaporator. The residue was purified with column by using 60-120 mesh size silicagel. The compound was eluted by hexane. The yield of the compound was 90%. (Rf: 0.7 TLC; Hexane).

^{1}H NMR (400 MHz, $CDCl_3$): 0.8-0.9 [m, 12H, CH-CH_3tocopheryl], 1.00-1.4 [m, 18H, -$(CH_2)_9$tocopheryl], 1.7-1.8 [[m, 2H, CH2-3 tocopheryl], 2.05 [s, 3H, CH3-5 tocopheryl], 2.15 [s, 3H, CH3-8 tocopheryl], 2.18 [s, 3H, CH3-7 tocopheryl], 2.55-2.6 [t, 2H, CH2-4 tocopheryl] ppm. ESI Mass calculated ; m/z: 492, found : m/z 492+NH_4=510.

***O*-Acylation of BOC-Protected Serotonin with Tocopheryl chloroformate (3, Scheme 1)**

To 0.5 g (1mmol) of tocopheryl chloroformate dissolved in dry DCM in 100mL round bottom flask added triethyl amine (0.5mmol). The above mixture was added drop wise about 20 minutes to tert-Butyl (2-(5-hydroxy-1H-indol-3-yl) ethyl) carbonate (1.1mmol) with the help of pressure equalizing funnel. The reaction mixture was stirred for 12h at room temperature. The resulting mixture was quenched with 2N HCl and water, transferred to a separation funnel, and extracted three times with DCM. The combined organic phases were dried (Na_2SO_4), filtered and concentrated in vacuum. The product was purified by column (Rf: - 0.3 10% EtOAc/ hexane). The product yield is 95%.

^{1}H NMR (400 MHz, $CDCl_3$): 9.4 [s,1H- indole], 7.6 [s, 1H,-imidazole=CH], 7.4 [s, 1H-aromatic], 7.2 [d, 1H-aromatic], 7.4 [d, 1H-aromatic], 7.8 [s, 1 CO-NH amide-broad], 1.8

(s, 9H –C(CH_3)$_3$, 2.9 [t, 2H], 2.8 [t, 2H], 0.8-0.9 [m, 12H, CH-CH_3tocopheryl], 1.00-1.4 [m, 18H, -(CH_2)$_9$tocopheryl], 1.7-1.8 [[m, 2H, CH2-3 tocopheryl], 2.05 [s, 3H, CH3-5 tocopheryl], 2.15 [m, 9H, tocopheryl], 2.18 [s, 3H, CH3-7 tocopheryl], 2.55-2.6 [t, 2H, CH2-4 tocopheryl] ppm. ESI-mass ; calculated m/z: 755, found: 755

Deprotection of BOC Protected Serotonin lipid (4, Scheme 1)

0.1 g of Boc-serotonin tocopheryl chloroformate was dissolved in 5mL of dry DCM in 100mL Round bottom flask under inert atmosphere. To this solution 0.05mL of TFA was added. The reaction mixture was stirred for 12h at room temperature. The resulting mixture was concentrated in vacuum about 20 min for removing excess TFA. The residue was purified by column chromatography (100-200 size silica gel) (Rf: - 0.1 10% Methanol/ chloroform v/v). The product of yield is 95%.

^{1}H NMR (400 MHz, $CDCl_3$): 9.4 [s,1H- indole], 7.6 [s, 1H,-imidazole=CH], 7.4 [s, 1H-aromatic], 7.2 [d, 1H-aromatic], 7.4 [d, 1H-aromatic], 7.8 [s, 1 CO-NH amide-broad], [t, 2H], 2.8 [t, 2H], 0.8-0.9 [m, 12H, CH-CH_3tocopheryl], 1.00-1.4 [m, 18H, -(CH_2)$_9$tocopheryl], 1.7-1.8 [[m, 2H, CH2-3 tocopheryl], 2.05 [s, 3H, CH3-5 tocopheryl], 2.15 [m, 9H, tocopheryl], 2.18 [s, 3H, CH3-7 tocopheryl], 2.55-2.6 [t, 2H, CH2-4 tocopheryl] ppm.

^{13}C NMR (100 MHz, $CDCl_3$) δ 154.17, 153.74, 149.72, 144.46, 144.26, 141.08, 139.30, 134.43, 133.28, 129.31, 126.80, 126.72, 126.00, 125.43, 125.08, 124.01, 123.51, 123.28, 117.69, 115.91, 115.21, 114.41, 114.11, 113.97, 112.34, 110.06, 109.60, 109.30, 107.68, 75.23, 55.99, 40.22, 39.75, 39.40, 37.59, 37.49, 37.44, 37.32, 34.75, 33.87, 32.82, 32.73, 31.97, 31.65, 31.00, 30.20, 29.95, 29.74, 29.59, 29.41, 29.20, 28.99, 28.01, 24.85, 24.49, 23.67, 22.76, 22.66, 21.06, 20.52, 19.78, 19.71, 14.17, 12.77, 11.91, 11.81.

HRMS (ES) m/z: - calculated 633.46302, found. 633.46256., HPLC: purity 95%

Synthesis of epoxidation of alpha-tocopherol with Epichlorohydrin (5, Scheme 2)

To a stirred mixture of (+/_)-α-tocopherol (5.42 g, 12.58 mmol), rac-epichlorohydrin (1.74 g, 18.87 mmol), and tetra-butylammonium hydrogensulfate (0.43 g, 1.13 mmol) at 0 °C, added 50 % KOH solution (3.24 g, 57. 8 mmol) in water (6.5 mL). The reaction mixture was warmed to room temperature and stirred for 4 h, extracted with Et_2O, washed with water, dried with anhydrous Na_2SO_4, filtered, and concentrated under reduced pressure. The crude product was purified by silica gel column chromatography to give α-tocopherylglycidyl ether 1 (5.89 g, 12.10 mmol, 96 %) as a clear oil. The yield of compound was 96%. Rf = 0.69 (EtOAc/hexane).

^{1}H,NMR (400 MHz, $CDCl_3$): δ = 0.84 (d, J = 6.4 Hz, 3 H), 0.85 (d, J = 6.4 Hz, 3 H), 0.87 (d, J = 6.4 Hz, 6 H), 1.00–1.60 (m, 21 H), 1.23 (s, 3 H), 1.71–1.85 (m, 2 H), 2.08 (s, 3 H), 2.14 (s, 3 H), 2.18 (s, 3 H), 2.57 (t, J = 6.8 Hz, 2 H), 2.70 (dd, J = 5.0, 2.6 Hz, 1 H), 2.87 (dd, J = 5.0, 4.0 Hz, 1 H), 3.35 (dddd, J = 5.8, 4.0, 3.2, 2.6 Hz, 1 H), 3.66 (ddd, J = 11.0, 5.8, 1.8 Hz, 1 H), 3.90 (ddd, J = 11.0, 3.2, 1.6 Hz, 1 H) ppm. ESI Mass m/z :(486+1) =487.

Synthesis of regioselective epoxide ring opening (α-tocopheryl glycidyl ether) with Serotonin (6, Scheme 2)

To a solution of serotonin in (1.85 g, 0.01 mol) 2 mL of dry pyridine was added and stirred at −10 °C for 1h. A solution of alphatocopherylglycidyl ether (1.9 g, 0.01 mol) in 1 mL of methylene chloride (DCM) was cooled to –10 °C and was added drop-wise to the above mixture about 30 min. After 12 h of stirring at -10°C, the reaction mixture was diluted with 20 mL of toluene and concentrated in vacuo. The residue was purified with 60-120 mesh silicagel. The compound was eluted by 4% Chloroform in Methanol. The yield of the compound was 70% (Rf: 0.3 TLC; 3-4% Chloroform in Methanol)

NMR (400 MHz, DMSO) δ/ppm 10.6 [s, indole NH], 8.6 [s, imidazole =CH], 7.2 [d,1H aromatic],6.8 [d, 1H-aromatic], 6.9 [s, 1H-aromatic], 5.8 [m, 1H CH_2-COH_2-CH_2], 5.0 [d, 2H], 4.6 [d, 2H], 4.1[2H,broad- CH_2-NH,-CH_2OH-CH_2], 2.8 [t,2H-NH-CH_2-CH_2-], 3.3 [t, 2H], 0.8-0.9 [m, 12H, CH-CH_3tocopheryl], 1.00-1.4 [m, 18H, -$(CH_2)_9$tocopheryl], 1.7-1.8 [m, 2H, CH2-3 tocopheryl], 2.05 [s, 3H, CH3-5 tocopheryl], 2.15 [s, 3H, CH3-8 tocopheryl], 2.18 [s, 3H, CH3-7 tocopheryl], 2.55-2.6 [t, 2H, CH2-4 tocopheryl] ppm.

^{13}C NMR (100 MHz, $CDCl_3$) δ 207.06, 149.82, 148.03, 146.82, 131.25, 127.46, 127.32, 125.62, 124.01, 122.80, 117.53, 114.07, 112.28, 108.58, 100.43, 85.55, 78.12, 77.92, 74.80, 66.09, 40.54, 39.38, 37.45, 37.30, 33.83, 32.80, 31.93, 30.93, 29.70, 29.52, 29.37, 29.17, 28.96, 27.98, 24.81, 24.48, 23.43, 22.73, 22.64, 21.07, 20.52, 19.76, 19.69, 14.12, 12.55, 11.70. HRMS (ES) m/z: calculated 662.45687 found: 663.45667

Quaternization of Serotonin Lipid B. (7, Scheme 2)

To a stirred solution of the tertiary serotonin α-tocopherol in dry methanol, excess anhydrous HCl was added. The reaction mixture was stirred for 12h at room temperature. The residue was concentrated under vacuum. The crude product was purified by column chromatography (MeOH: $CHCl_3$1:9 v/v) to afford the quaternized α-tocopherol-serotonin lipid as a yellow color.

NMR (400 MHz, DMSO) δ/ppm 10.6 [s, indole NH], 8.6 [s, imidazole =CH], 7.2 [d,1H aromatic],6.8 [d, 1H-aromatic], 6.9 [s, 1H-aromatic], 5.8 [m, 1H CH_2-COH_2-CH_2], 5.0 [d, 2H], 4.6 [d, 2H], 4.1[2H,broad- CH_2-NH,-CH_2OH-CH_2], 2.8 [t,2H-NH-CH_2-CH_2-], 3.3 [t, 2H], 0.8-0.9 [m, 12H, CH-CH_3tocopheryl], 1.00-1.4 [m, 18H, -$(CH_2)_9$tocopheryl], 1.7-1.8 [[m, 2H, CH2-3 tocopheryl], 2.05 [s, 3H, CH3-5 tocopheryl], 2.15 [s, 3H, CH3-8 tocopheryl], 2.18 [s, 3H, CH3-7 tocopheryl], 2.55-2.6 [t, 2H, CH2-4 tocopheryl] ppm.

^{13}C NMR (100 MHz, $CDCl_3$) δ 207.06, 149.82, 148.03, 146.82, 131.25, 127.46, 127.32, 125.62, 124.01, 122.80, 117.53, 114.07, 112.28, 108.58, 100.43, 85.55, 78.12, 77.92, 74.80, 66.09, 40.54, 39.38, 37.45, 37.30, 33.83, 32.80, 31.93, 30.93, 29.70, 29.52, 29.37, 29.17, 28.96, 27.98, 24.81, 24.48, 23.43, 22.73, 22.64, 21.07, 20.52, 19.76, 19.69, 14.12, 12.55, 11.70. HRMS (ES) m/z: calculated 663.45687 found: 663.50954. , HPLC: 96% purity.

5.4.2 DNA binding assay

To elucidate the DNA binding capability of liposomes with Lipid: DNA, lipoplexes were prepared at charge ratios ranging from 1:1 to 8:1 using 0.3µgplasmid DNA in a total volume of 30µL in HEPES buffer (pH 7.4) and further incubated at room temperature for 20-25 minutes.4µL of 6x loading buffer (0.25% Bromophenol blue in 40% (w/v) sucrose with sterile H_2O) was added to it and from the resulting solution, 30µL was loaded on each well. The samples were electrophoresed at 80 V for 45 minutes and the agarose gel (pertained with EtBr) was imaged following visualization using a Bio-Rad Gel Doc XR+ imaging system (Bio-Rad, Hercules, CA, USA) and analyzed.

5.4.3 Heparin Displacement Assay

Heparin was used to study the anionic displacement of pDNA from lipoplexes. Lipid: pDNA complexes were prepared as described in the above section (pDNA binding assay) and incubated for 20 min. Following the incubation, 0.1µg of the sodium salt of heparin was added and incubated for another 30 min. Samples were electrophoresed in an agarose gel (1.5%) and pDNA bands were visualized as mentioned in the above section.

5.4.4 Zeta potential (ξ) and size measurements

Size and the surface charge (zeta potentials) of liposomes and lipoplexes with varying charge ratios (8:1 to 1:1) were measured by photon correlation spectroscopy and electrophoretic

mobility on a Zetasizer 3000HSA (Malvern, U.K.). Measurements were carried out in DMEM media with a sample refractive index of 1.59 and a viscosity of 0.89cP. The system was calibrated by using the 2005 nm polystyrene polymer (Duke Scientific Corps., Palo Alto, CA, U.S.). The diameters of liposomes and lipoplexes were calculated by using the automatic method. Zeta potential was also measured using the following parameters: viscosity, 0.89 cP; dielectric constant, 79; temperature, 25°C; F (Ka), 1.50 (Smoluchowski); the maximum voltage of the current, V. The system was calibrated by using the DTS0050 standard from Malvern. Measurements were done 10 times with the zero-field correction. All the liposomes and lipoplexes of the size measurements were done 10 times in triplicate with the zero field correction and values represented as the average of triplicate measurements. The potentials were measured 10 times and represented as their average values calculated by using the Smoluchowski approximation.

5.4.5 Cytotoxicity (MTT) assay (Mitochondrial activity)

The MTT (3-(4,5-dimethylthiazol-2-yl)-2, 5-diphenyltetrazolium Bromide) based reduction cytotoxicity assays of cationic lipids **A & B** were carried out in CHO, Neuro-2a, HEK-293T, and HepG2 cells across the lipid: DNA charge ratios of 1:1-8:1in 96-wells plate. Briefly, 24 h after the adding of lipoplexes, MTT (0.5mg/ml in DMEM) was added to cells and incubated for 4 h at 37 ˚C. Results were expressed as percent viability = [A540 (treated cells)-background/A540 (untreated cells)-background] x 100.

5.4.6 Transfection Biology

CHO, TCHO, Neuro-2a, HEK-293T, and HepG2 cells were seeded at a density of 10,000 per well, in a 96-well plate, 18-24 h before transfection. Then 0.3 μg (0.91 nmol) of plasmid

DNA was complexed with different concentrations of liposomal formulations of Lipids **A** and **B** i.e. 1:1 to 8:1 in DMEM medium (total volume made up to 100 µL) for 30 min. Just prior to transfection, cells plated in the 96-well plate were washed twice with PBS (100 µL) followed by the addition of lipoplexes (lipid-DNA complexes). After 4 h of incubation, 100 µL of DMEM with 20% FBS was added to the cells. The medium was replaced with 10% complete medium after 24 h, and reporter gene activity was estimated after 48 h. Cells were washed twice with PBS (100 µL each) and lysed in 50 µLlysis buffer [0.25 M Tris-HCl (pH 8.0) and 0.5% NP40]. The β-galactosidase activity per well was estimated by adding 50 µL of 2 substrate solution [1.33 mg/mL ONPG, 0.2 M sodium phosphate (pH 7.3), and 2mM magnesium chloride] to the lysate. The absorbance of the product ortho-nitrophenol at 405 nm was converted to β-galactosidase units by using a calibration curve constructed using a pure commercial β-galactosidase enzyme. Each transfection experiment was repeated 3 times on 3 different days. The transfection values were noted as an average of three replicate transfection plates, performed on three different days. The values of β-galactosidase units in replicate plates assayed on the same day varied by less than 20%.

5.4.7 ROS assay

Intracellular ROS generation was measured by 2', 7'–dichlorofluorescein diacetate (DCF-DA)method given by Kim *et al.,* 2010 with slight modifications. HEK-293 Cells were seeded into a 24 well plate 12h before the transfections. After 24h of the treatment with the liposome/p DNA, the cells were incubated with 10µM DCF-DA at 37°C for 15 min. Qualitative cellular fluorescence images were captured by fluorescence microscopy by exiting at 488nmand emitting at 525 nm (Leica DMI6000B inverted Microscope).

5.4.8 Treatment with inhibitors

Cells were incubated with chlorpromazine (CPZ, 10 μg mL−1), filipin-III (5 μg mL−1) and methyl-β-cyclodextrin (m-β-CD, 10 mg mL−1) (all from Sigma) in normal cell culture medium for 1 at 37 °C prior to the addition of lipoplexes formulated with Lipid **A** and **B**. Consequently, cells were incubated for 4 h, trypsinized and collected in 10% FBS containing PBS, followed by analysis using FACS. The concentration of chlorpromazine (CPZ) employed in the study was such that uptake of fluorescently labeled lipoplexes and **B**, which is widely recognized as a ligand exclusively internalized via clathrin-independent endocytosis, was inhibited by 80–95 % since it has been reported that this lipoplexis exclusively internalized via a clathrin-independent mechanism.

5.4.10 Cellular eGFP Expression Study

For cellular α5GFP expression experiments in HEK-293T and HepG2, 50,000 cells were cultured in 24-wells plate, 18-24 h before transfection. Then 0.9 μg of eGFP plasmid DNA encoding green fluorescent protein was complexed with liposomes of lipids **A**&**B** at charge ratio (lipid/DNA) 2:1 in DMEM medium (total volume made up to 100 μL) for 30 min. Just prior to transfection, cells plated in the 24-wells plate were washed with PBS (2×100 μL) followed by addition of lipoplexes. The media 400 μLwas added after 4 h incubation of the cells. After 24 h, the complete medium was removed, and cells were washed with PBS (2× 200 μl). Finally, 200 μL of PBS was added to each per good cells and visualized under the epifluorescence microscope to observe green fluorescent protein.

5.4.11 Transfection Biology in Presence of Serum

Cells were plated at a density of 15,000 cells (HEK-293T and CHO) per well in a 96-well plate, 18-24 h prior to transfection. Then 0.3 μg (0.91 nmol) of eGFP was complexed with

lipids **A**&**B** in DMEM medium in the presence of increasing concentrations of added serum (10-30% v/v and total volume made up to 100 μL) for 30 min. The charge ratios of lipid/eGFP plasmid were maintained at2:1, at which the two lipids exhibited their highest transfection ability in four different types of viz. HepG2, Neuro-2a, HEK-293T and CHO and TCHO (TCHO-5HT$_{1A}$R). TCHO stably expresses the human serotonin$_{1A}$ receptor compared to CHO cells. The experimental procedure and determination of eGFP activity per well are similar to that reported for the in vitro transfection experiments.

5.4. 12 Statistical analysis

The results were expressed as (mean standard deviation). Statistical importance between treatments was assessed by the ANOVA test followed by the Dennett multiple comparison tests (*p<0.05, **P<0.01, ***P<0.001).

5.4.13 Cellular Uptake examine by Epifluorescence Microscopy

Cells were cultured at a density of 10 000 cells/ well in a 96-well plate 16−24 h prior to treatment in 200 μL of growth medium until cells are 30−50% confluent at the time of transfection. 2DDNA (0.3 μg of pDNA diluted to 50 μL with serum-free DMEMmedia) was complexed with rhodamine-PE labeled cationic liposomes (diluted to 50 μL with DMEM) of **Lipids A** and **B** using 2:1 lipid to pDNA charge ratio. The cells were washed with PBS (1 × 200 μL) and then treated with lipoplexes, and incubated in a humidified chamber containing 5% CO2 at 37 °C. After 4 h of incubation, the cells were washed with PBS (3 × 200 μL) to remove the dye and fixed with 3.8% paraformaldehyde in PBS at room temperature for 10 min. Cells exhibiting Rhodamine fluorescence was detected under an epifluorescence microscope (Nikon, Japan).

5.4.14 Docking studies

Preparation of Ligands

To predict the docking poses and scores of Lipid **A** and Lipid **B** with the 5-HT1B receptor, we used serotonin as a reference molecule. The ligands were built using ChemDraw 13.0 and were saved as MOL file. The ligands were loaded into Maestro 9.2 software and optimized using LigPrep tool. The possible ionization states at pH 7 ± 2 were generated using an OPLS2005 force field. Single conformation with lowest potential energy for each minimized compound was retained for further docking.

Preparation of the receptor protein

The crystal structure of 5-HT1B (PDB id: 4IAR) having bound ergotamine to the active site Asp 129 was taken for the study. The protein structure was prepared using Protein Preparation Wizard tool. The missing side chains were added to the structure using Schrödinger Prime 3.0 (Prime version 3.0, Schrödinger, LLC, New York, NY, 2011). Hydrogens were added and water molecules were deleted within 5 A^o from the crystal chain. The entire process was adjusted to a pH range of 7.0 ± 4. The optimization was performed to a maximum root mean square deviation (RMSD) of 0.3 A^o using OPLS2005 force field.

GRID generation

The receptor grid was generated with dimensions (10 x 10 x 10 A^o) at the centroid of co-crystallized ligand, ergotamine. The resultant GRID file was used for docking.

Docking

The receptor GRID was selected using Ligand Docking tool and docking was set in XP (extra precision). The minimized ligands were imported for docking to the grid selected. Epik

state penalties were added to docking score and XP descriptor file was generated (.xpdes). The resultant docking study was visualized in XP visualizer.

5.5 References

1. (a) Ramamoorth, M.; Narvekar, A., Non viral vectors in gene therapy- an overview. *Journal of clinical and diagnostic research : JCDR* **2015,** *9* (1), GE01-6; (b) Kay, M. A., State-of-the-art gene-based therapies: the road ahead. *Nature reviews. Genetics* **2011,** *12* (5), 316-28; (c) Pahle, J.; Walther, W., Vectors and strategies for nonviral cancer gene therapy. *Expert opinion on biological therapy* **2016,** *16* (4), 443-61.
2. (a) Schwartz, B.; Ivanov, M. A.; Pitard, B.; Escriou, V.; Rangara, R.; Byk, G.; Wils, P.; Crouzet, J.; Scherman, D., Synthetic DNA-compacting peptides derived from human sequence enhance cationic lipid-mediated gene transfer in vitro and in vivo. *Gene therapy* **1999,** *6* (2), 282-92; (b) Katz, M. G.; Fargnoli, A. S.; Williams, R. D.; Bridges, C. R., Gene therapy delivery systems for enhancing viral and nonviral vectors for cardiac diseases: current concepts and future applications. *Human gene therapy* **2013,** *24* (11), 914-27; (c) Nayerossadat, N.; Maedeh, T.; Ali, P. A., Viral and nonviral delivery systems for gene delivery. *Advanced biomedical research* **2012,** *1*, 27; (d) Boisguerin, P.; Deshayes, S.; Gait, M. J.; O'Donovan, L.; Godfrey, C.; Betts, C. A.; Wood, M. J.; Lebleu, B., Delivery of therapeutic oligonucleotides with cell penetrating peptides. *Advanced drug delivery reviews* **2015,** *87*, 52-67.
3. (a) Dorraj, G.; Carreras, J. J.; Nunez, H.; Abushammala, I.; Melero, A., Lipid Nanoparticles as Potential Gene Therapeutic Delivery Systems for Oral Administration. *Current gene therapy* **2017,** *17* (2), 89-104; (b) Zhu, L.; Torchilin, V. P., Stimulus-responsive nanopreparations for tumor targeting. *Integrative biology : quantitative biosciences from nano to macro* **2013,** *5* (1), 96-107; (c) Zhang, L.; Zhang, P.; Zhao, Q.; Zhang, Y.; Cao, L.; Luan, Y., Doxorubicin-loaded polypeptide nanorods based on electrostatic interactions for cancer therapy. *Journal of colloid and interface science* **2016,** *464*, 126-36; (d) Jiang, Y.; Li, F.; Luan, Y.; Cao, W.; Ji, X.; Zhao, L.; Zhang, L.; Li, Z., Formation of drug/surfactant catanionic vesicles and their application in sustained drug release. *International journal of pharmaceutics* **2012,** *436* (1-2), 806-14.
4. Schwendener, R. A., Liposomes as vaccine delivery systems: a review of the recent advances. *Therapeutic advances in vaccines* **2014,** *2* (6), 159-82.
5. Sahay, G.; Alakhova, D. Y.; Kabanov, A. V., Endocytosis of nanomedicines. *Journal of controlled release : official journal of the Controlled Release Society* **2010,** *145* (3), 182-95.

6. (a) Lembo, P. M.; Ghahremani, M. H.; Albert, P. R., Receptor selectivity of the cloned opossum G protein-coupled receptor kinase 2 (GRK2) in intact opossum kidney cells: role in desensitization of endogenous alpha2C-adrenergic but not serotonin 1B receptors. *Mol Endocrinol* **1999,** *13* (1), 138-47; (b) Albert, P. R., Transcriptional regulation of the 5-HT1A receptor: implications for mental illness. *Philosophical transactions of the Royal Society of London. Series B, Biological sciences* **2012,** *367* (1601), 2402-15; (c) Stiedl, O.; Pappa, E.; Konradsson-Geuken, A.; Ogren, S. O., The role of the serotonin receptor subtypes 5-HT1A and 5-HT7 and its interaction in emotional learning and memory. *Frontiers in pharmacology* **2015,** *6*, 162.

7. (a) Gurbuz, N.; Ashour, A. A.; Alpay, S. N.; Ozpolat, B., Down-regulation of 5-HT1B and 5-HT1D receptors inhibits proliferation, clonogenicity and invasion of human pancreatic cancer cells. *PloS one* **2014,** *9* (9), e110067; (b) Dizeyi, N.; Bjartell, A.; Nilsson, E.; Hansson, J.; Gadaleanu, V.; Cross, N.; Abrahamsson, P. A., Expression of serotonin receptors and role of serotonin in human prostate cancer tissue and cell lines. *The Prostate* **2004,** *59* (3), 328-36.

8. Azouzi, S.; Santuz, H.; Morandat, S.; Pereira, C.; Cote, F.; Hermine, O.; El Kirat, K.; Colin, Y.; Le Van Kim, C.; Etchebest, C.; Amireault, P., Antioxidant and Membrane Binding Properties of Serotonin Protect Lipids from Oxidation. *Biophysical journal* **2017,** *112* (9), 1863-1873.

9. Waris, G.; Ahsan, H., Reactive oxygen species: role in the development of cancer and various chronic conditions. *Journal of carcinogenesis* **2006,** *5*, 14.

10. Muripiti, V.; Rachamalla, H. K.; Banerjee, R.; Patri, S. V., alpha-Tocopherol-based cationic amphiphiles with a novel pH sensitive hybrid linker for gene delivery. *Organic & biomolecular chemistry* **2018,** *16* (16), 2932-2946.

11. (a) Pires, P.; Simoes, S.; Nir, S.; Gaspar, R.; Duzgunes, N.; Pedroso de Lima, M. C., Interaction of cationic liposomes and their DNA complexes with monocytic leukemia cells. *Biochimica et biophysica acta* **1999,** *1418* (1), 71-84; (b) Maccarrone, M.; Dini, L.; Di Marzio, L.; Di Giulio, A.; Rossi, A.; Mossa, G.; Finazzi-Agro, A., Interaction of DNA with cationic liposomes: ability of transfecting lentil protoplasts. *Biochemical and biophysical research communications* **1992,** *186* (3), 1417-22; (c) Bordi, F.; Cametti, C.; Sennato, S.; Diociaiuti, M., Direct evidence of multicompartment aggregates in polyelectrolyte-charged liposome complexes. *Biophysical journal* **2006,** *91* (4), 1513-20.

12. (a) Brgles, M.; Santak, M.; Halassy, B.; Forcic, D.; Tomasic, J., Influence of charge ratio of liposome/DNA complexes on their size after extrusion and transfection efficiency. *International journal of nanomedicine* **2012,** *7*, 393-401; (b) Khatri, N.; Baradia, D.; Vhora, I.; Rathi, M.; Misra, A., Development and characterization of siRNA lipoplexes: Effect of different lipids, in vitro evaluation in cancerous cell lines and in vivo toxicity study. *AAPS PharmSciTech* **2014,** *15* (6), 1630-43.

13. Abdouh, M.; Storring, J. M.; Riad, M.; Paquette, Y.; Albert, P. R.; Drobetsky, E.; Kouassi, E., Transcriptional mechanisms for induction of 5-HT1A receptor mRNA and protein in activated B and T lymphocytes. *The Journal of biological chemistry* **2001,** *276* (6), 4382-8.

14. (a) Fantini, J.; Barrantes, F. J., Sphingolipid/cholesterol regulation of neurotransmitter receptor conformation and function. *Biochimica et biophysica acta* **2009,** *1788* (11), 2345-61; (b) Lukasiewicz, S.; Blasiak, E.; Szafran-Pilch, K.; Dziedzicka-Wasylewska, M., Dopamine D2 and serotonin 5-HT1A receptor interaction in the context of the effects of antipsychotics - in vitro studies. *Journal of neurochemistry* **2016,** *137* (4), 549-60.

15. (a) Huang, Y.; Thathiah, A., Regulation of neuronal communication by G protein-coupled receptors. *FEBS letters* **2015,** *589* (14), 1607-19; (b) Yin, W.; Zhou, X. E.; Yang, D.; de Waal, P. W.; Wang, M.; Dai, A.; Cai, X.; Huang, C.-Y.; Liu, P.; Wang, X.; Yin, Y.; Liu, B.; Zhou, Y.; Wang, J.; Liu, H.; Caffrey, M.; Melcher, K.; Xu, Y.; Wang, M.-W.; Xu, H. E.; Jiang, Y., Crystal structure of the human 5-HT1B serotonin receptor bound to an inverse agonist. *Cell discovery* **2018,** *4* (1), 12; (c) Borroni, M. V.; Valles, A. S.; Barrantes, F. J., The lipid habitats of neurotransmitter receptors in brain. *Biochimica et biophysica acta* **2016,** *1858* (11), 2662-2670; (d) Zhang, X. X.; McIntosh, T. J.; Grinstaff, M. W., Functional lipids and lipoplexes for improved gene delivery. *Biochimie* **2012,** *94* (1), 42-58; (e) Corbo, C.; Molinaro, R.; Parodi, A.; Toledano Furman, N. E.; Salvatore, F.; Tasciotti, E., The impact of nanoparticle protein corona on cytotoxicity, immunotoxicity and target drug delivery. *Nanomedicine (Lond)* **2016,** *11* (1), 81-100.

16. (a) Marchini, C.; Montani, M.; Amici, A.; Amenitsch, H.; Marianecci, C.; Pozzi, D.; Caracciolo, G., Structural stability and increase in size rationalize the efficiency of lipoplexes in serum. *Langmuir : the ACS journal of surfaces and colloids* **2009,** *25* (5), 3013-21; (b) Nakai, T.; Kanamori, T.; Sando, S.; Aoyama, Y., Remarkably size-regulated cell invasion by artificial viruses. Saccharide-dependent self-aggregation of

glycoviruses and its consequences in glycoviral gene delivery. *Journal of the American Chemical Society* **2003,** *125* (28), 8465-75.

17. Khalil, I. A.; Kogure, K.; Akita, H.; Harashima, H., Uptake pathways and subsequent intracellular trafficking in nonviral gene delivery. *Pharmacological reviews* **2006,** *58* (1), 32-45.
18. Bareford, L. M.; Swaan, P. W., Endocytic mechanisms for targeted drug delivery. *Advanced drug delivery reviews* **2007,** *59* (8), 748-58.
19. Gong, Q.; Huntsman, C.; Ma, D., Clathrin-independent internalization and recycling. *Journal of cellular and molecular medicine* **2008,** *12* (1), 126-44.
20. (a) Dhanasekaran, D. N.; Reddy, E. P., JNK-signaling: A multiplexing hub in programmed cell death. *Genes & cancer* **2017,** *8* (9-10), 682-694; (b) Andon, F. T.; Fadeel, B., Programmed cell death: molecular mechanisms and implications for safety assessment of nanomaterials. *Accounts of chemical research* **2013,** *46* (3), 733-42.
21. Bisby, R. H.; Ahmed, S.; Cundall, R. B.; Thomas, E. W., Free radical reactions with alpha-tocopherol and N-stearoyl tryptophan methyl ester in micellar solutions. *Free radical research communications* **1986,** *1* (4), 251-61.
22. Wang, C.; Jiang, Y.; Ma, J.; Wu, H.; Wacker, D.; Katritch, V.; Han, G. W.; Liu, W.; Huang, X. P.; Vardy, E.; McCorvy, J. D.; Gao, X.; Zhou, X. E.; Melcher, K.; Zhang, C.; Bai, F.; Yang, H.; Yang, L.; Jiang, H.; Roth, B. L.; Cherezov, V.; Stevens, R. C.; Xu, H. E., Structural basis for molecular recognition at serotonin receptors. *Science* **2013,** *340* (6132), 610-4.
23. Gu, R. X.; Ingolfsson, H. I.; de Vries, A. H.; Marrink, S. J.; Tieleman, D. P., Ganglioside-Lipid and Ganglioside-Protein Interactions Revealed by Coarse-Grained and Atomistic Molecular Dynamics Simulations. *The journal of physical chemistry. B* **2017,** *121* (15), 3262-3275.
24. Friesner, R. A.; Murphy, R. B.; Repasky, M. P.; Frye, L. L.; Greenwood, J. R.; Halgren, T. A.; Sanschagrin, P. C.; Mainz, D. T., Extra precision glide: docking and scoring incorporating a model of hydrophobic enclosure for protein-ligand complexes. *Journal of medicinal chemistry* **2006,** *49* (21), 6177-96.
25. (a) Kitson, S. L., 5-hydroxytryptamine (5-HT) receptor ligands. *Current pharmaceutical design* **2007,** *13* (25), 2621-37; (b) Cheng, C. H.; Costall, B.; Naylor, R. J.; Rudd, J. A., The effect of 5-HT receptor ligands on the uptake of [3H]5-hydroxytryptamine into rat cortical synaptosomes. *European journal of pharmacology* **1993,** *239* (1-3), 211-4.

26. Li, Z.; Gorfe, A. A., Receptor-mediated membrane adhesion of lipid-polymer hybrid (LPH) nanoparticles studied by dissipative particle dynamics simulations. *Nanoscale* **2015,** *7* (2), 814-24.
27. Raymond, J. R.; Mukhin, Y. V.; Gettys, T. W.; Garnovskaya, M. N., The recombinant 5-HT1A receptor: G protein coupling and signalling pathways. *British journal of pharmacology* **1999,** *127* (8), 1751-64.
28. Gopal, V.; Xavier, J.; Dar, G. H.; Jafurulla, M.; Chattopadhyay, A.; Rao, N. M., Targeted liposomes to deliver DNA to cells expressing 5-HT receptors. *International journal of pharmaceutics* **2011,** *419* (1-2), 347-54.

CHAPTER 6

α-Tocopherol-based cationic amphiphiles with a novel pH sensitive hybrid linker for gene delivery

6.1 Introduction

Gene delivery is a route of inserting a genetic material in to host cells, which mainly depends on developing efficient and safe vectors for delivering genes. Till date, numerous viral and non-viral vectors have been adopted to introduce naked DNA into the cells [1-3]. Non-viral or synthetic vectors as promising delivery agents became the primary area of research owing to their several significant factors, *viz*., greater carrier capacity, simple structure, safety, ease of large-scale preparation, stability, potential to incorporate targeting ligands and unlimited vector size[4, 5]. Among non-viral vectors, cationic liposomes and polymer based vectors have gained increasing interest due to their high transfection efficacy and ideal characteristics. Generally, the structure of cationic lipids which determines their transfection efficiency consists of head group, hydrophobic domain and the linker[6]. The transfection efficacy of cationic lipids depends on the length of hydrophobic alkyl chains, nature of hydrophilic head group and nature of pH sensitive linkers (like carbamate, imidazole, ester etc.,).The transfection efficacy of cationic lipids also depends on means of internalisation into the cytoplasm, endosomal escape, and their entry into the nucleus[6]. Despite tremendous progresses, the therapeutic efficiency of cationic lipid-based transfection systems remains relatively low as compared to viral ones. Because of the complexity of transfection pathway and cellular barriers, the exact structural requirement for efficient gene delivery is still an ambiguous challenge. Hence, there is a dire need to develop non-viral gene transfer reagents that possess good transfection efficiency (TE), less toxic and biocompatibility. Many research groups have been focused in developing the structurally modified transfection vectors[7-9]. Towards the search for new efficient transfection potent lipid vector, recently we demonstrate the potential of tocopherol based lipids in transfecting pDNA to various cell lines[10-12]. α-tocopherol (vitamin E) is a lipid-soluble natural amphiphilic molecule and this is the only vitamin that is non-toxic even at high doses[13]. It plays vital role in many physiological

pathways. It can circulate the lipoproteins by the radical-trapping antioxidant present in human plasma[14]. Even minor modifications of chemical structures account for improved transfection efficacy of cationic lipids, thus playing a crucial role for potential gene delivery.

Our previous reports claimed that *α*-tocopherol-based cationic lipids having ether linker showed excellent transfection activity, least toxic and serum compatible[10-12]. Based on earlier results; we elaborated chemical modifications on tocopherol cationic lipids by introducing a novel hybrid linker "ether-β-hydroxy-triazole" between tocopherol, the anchoring moiety and the basic tris (2-hydroxy ethyl)quarternary ammonium head group. The rationale behind approaching ether-β-hydroxy-triazole hybrid linker is to help in the rupture of endosomes and enhance biocompatibility of the lipids. The linker also determines the chemical destabilization of lipoplexes and biodegradability of the lipids in both cell environment and biological fluids. Triazole also imparts pH sensitivity, binding affinity with oligonucleotides and contributes to the escape of lipoplexes from endosomes in pH responsive behaviour [15](Figure 1). To demonstrate the importance of the hybrid linker i.e. ether-β-hydroxy-triazole, we synthesized three lipids **Lp1-Lp3**. The lipid **Lp1** consists of only 'ether-β-hydroxy' linker connecting tocopherol moiety and tris(2- hydroxyl ethyl) ammonium head group. Whereas lipid **Lp2** consists of the hybrid linker 'ether-β hydroxyl-triazole' between tocopherol moiety and tris(2-hydroxy ethyl) ammonium head group. Lipid **Lp3** has the same hybrid linker and anchoring group as **Lp2** only difference is instead of tris(2-hydroxy ethyl) ammonium, tris(ethyl) ammonium as the head group. The transfection efficiencies of these three lipids were evaluated and showed correlation between the *in vitro* transfection efficacies of with (without) triazole-ether hybrid functionalities linker and with (without) trihydroxy functionalities in the polar head group regions for potent α-tocopherol cationic amphiphiles. Our findings demonstrate that the relative *in vitro* gene transfer efficacies of the presently

described triazole hybrid linker based cationic amphiphiles are due to the remarkable pH sensitivity of the novel hybrid linker group.

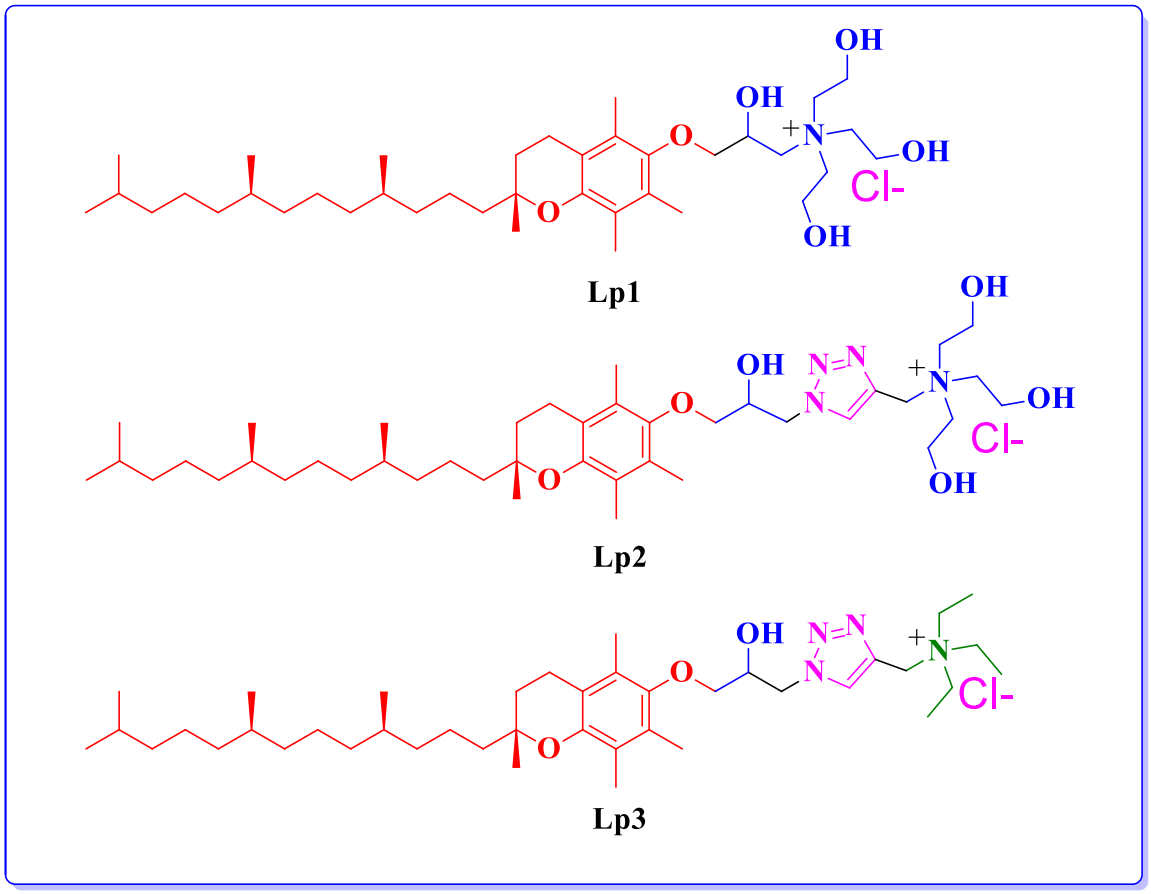

Fig.1. Chemical structures of Cationic lipids

6.2 Results and Discussion

6.2.1 *Chemistry*

The final lipids **Lp1-Lp3** were synthesized as described in the Schemes **1, 2 and 3**. All the three cationic lipids consist of a common α-tocopherol as the hydrophobic group. Lipid **Lp1** contains ether-beta hydroxy linker group, lipids **Lp2** and **Lp3** contain ether-hydroxy-triazole hybrid linker. **Lp1** and **Lp2** has tris-2-hydroxyethyl-ammonium group as the head group where as in **Lp3** there are no hydroxy groups in the head group region it consists of tris-ethyl-ammonium group as the head group. The precursor intermediate α-tocopherol azido ether

(**2B**, **Scheme 2**) for the synthesis of both lipids, **Lp2** and **Lp3** was prepared conventionally in 2 steps. Briefly, *O*-alkylation of α-tocopherol with epichlorohydrin in presence of 50% sodium hydroxide and tetra butyl ammonium hydrogen sulphate provided the epoxide linked α-tocopherol (86% yield), **1A** which upon epoxide opening with sodium azide gave intermediate **2B** (86% yield) (**Scheme 2**). Whereas, the intermediate **1B** (78% yield) is obtained by opening epoxide **1A** using diethanolamine. Subsequently the lipid **Lp1** is (88% yield) obtained by the quarternization of intermediate **1B** with chloroethanol (Scheme 1).The intermediate **2B** upon treatment with *N*, *N*, *N*-tris(2-hydroxyethyl)prop-2yn-1-aminium or*N*,*N*,*N*-triethylprop-2-yn-1-aminium, $CuSO_4.5H_2O$, sodium Ascorbate using click chemistry[16, 17] provided the intermediates **2C** (90% yield)and **3B** (88% yield) respectively (**Scheme 2** and **3**). The intermediate **2C** and **3B** upon chloride ion exchange over amberlyst-26 yielded final lipids **Lp2** (90% yield) and **Lp3** (92% yield) respectively (**Scheme 2** and **3).** Structures of all the synthetic intermediates were confirmed by ^{1}H-NMR, ESI-MASS and final lipids shown in **Schemes 1-3** are confirmed by ^{1}H NMR,^{13}C NMR and molecular ion peaks in their ESI –HRMS mass spectra. The purity of final lipids was characterized by RP-HPLC, as described in the Experimental Section.

Scheme 1: Synthesis of **Lp1**

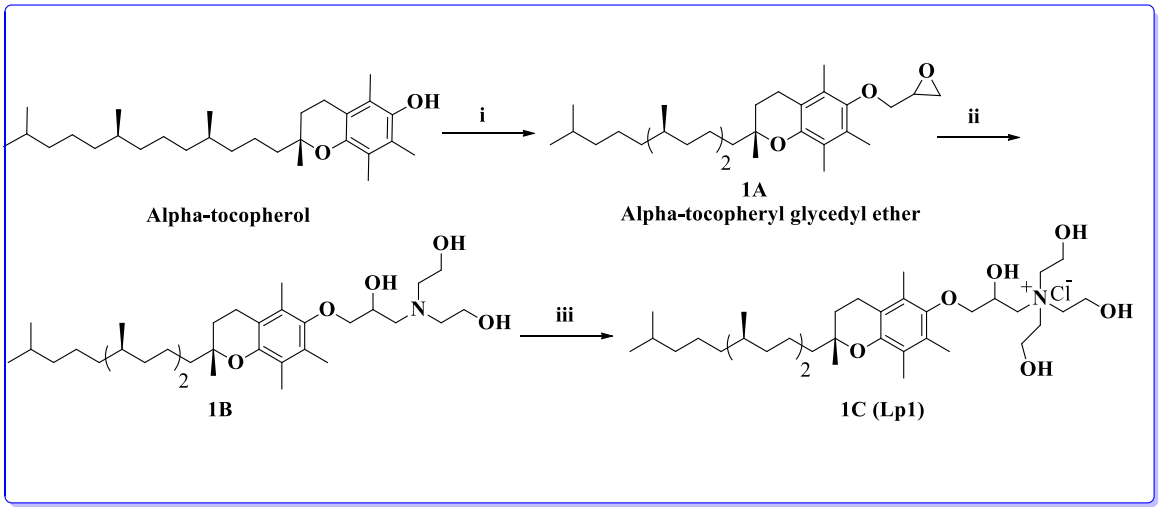

Reagents: (i) Epichlorohydrin, 50% aq KOH solution, Bu_4NHSO_4 and 0 ˚C 6 h (88% yield); (ii) Ethanol in toluene 1:1, Diethanolamine and refluxed 24 h (78% yield); (iii) Anhydrous K_2CO_3, excess 2-chloroethanol and reflux 36 h (88% yield).

Scheme. 2. Synthesis of **Lp2**

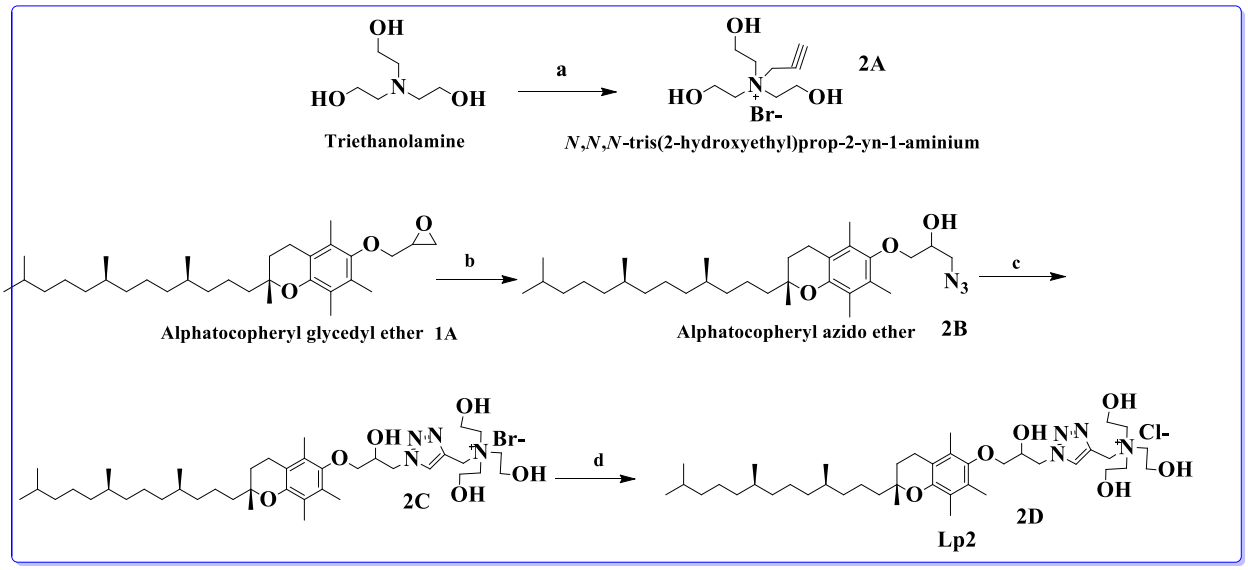

Reagents: (a) propargylbromide, *n*-propanol in toluene 1:1 and 4 ºC 12 h (95% yield); (b) NaN_3, $CeCl_3.7H_2O$, CH_3CN, H_2O 9:1 3 h reflux (86% yield); (c) *N*,*N*,*N*-tris(2-hydroxyethyl)prop-2-yn-1-aminium, *α*-tocopheryl azido ether, $CuSO_4$:$6H_2O$, sodium ascorbate and 12 h RT (79% yield); (d) amberlyst anion exchange resin

Scheme. 3. Synthesis of **Lp3**.

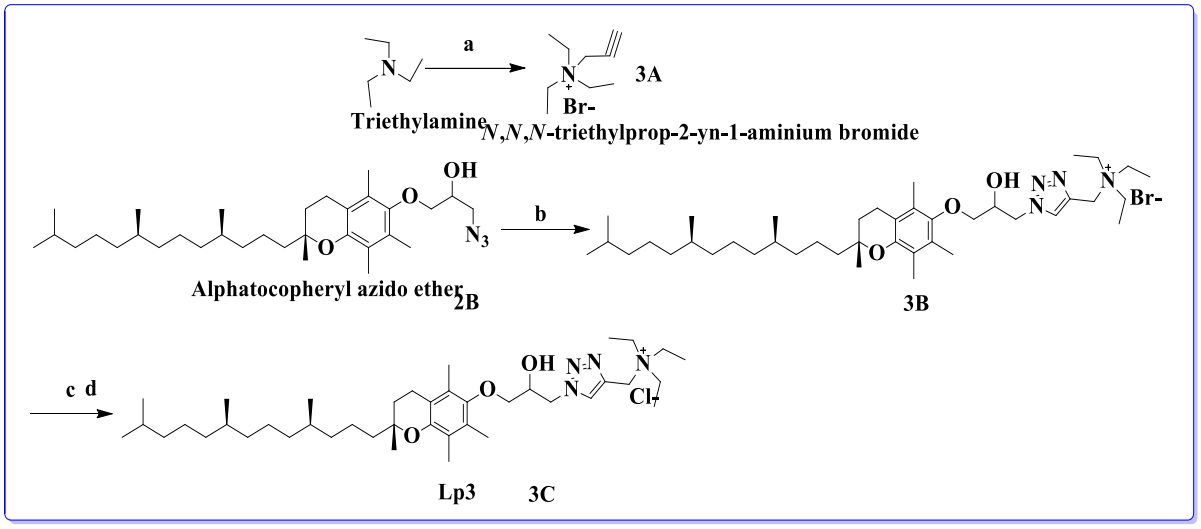

Reagents: (a) propargylbromide, n-propanol in toluene 1:1 and 4 ˚C 12 h (95% yield); (b) *N*,*N*,*N*-tris(2-ethyl)prop-2-yn-1-aminium (88% yield), (c) α-tocopheryl azido ether, $CuSO_4$:$6H_2O$, sodiumascorbate and 12 h RT (93% yield) ; (d) amberlyst anion exchange resin.

6.2.2 Liposomes preparations

Cationic liposomes were prepared by the dry lipid hydration method as described earlier [10, 15,16]. The cationic liposomes were formulated by varying molar ratios (0.5:1 and 1:1) of synthesized cationic lipids, **Lp1-Lp3** and a well-known co-lipid DOPE (1, 2-dioleoyl-sn-glycero-3-phosphoethanolamine). Subsequently, liposomes were prepared under sterile conditions followed by sonication for 5 min at room temperature. The liposomes of all the three lipids (**Lp1**, **Lp2** and **Lp3**) observed to form stable uniform liposomes at 1:1 molar ratio of lipid: DOPE with high efficacy of DNA binding. The suspensions were stable and no precipitation was observed even after 2 months when stored at 4 °C. Hence, the molar ratio of lipid: DOPE, 1:1 is used for all further studies.

6.2.3 Nano-sizes and surface charges of the lipoplexes

Towards physicochemical characterization of cationic lipids (**Lp1-Lp3**), the nano sizes and the surface charges of the liposomes and lipoplexes of all three cationic lipids (**Lp1-Lp3**) prepared were measured. The sizes and surface charges of these lipids (**Lp1-Lp3**) were measured with the help of a dynamic laser light scattering (DLS) instrument with a ζ-sizing capacity across the lipid-DNA charge ratios of 1:1 to 8:1 in presence of DMEM. It was found that the hydrodynamic sizes of the liposomes of lipids **Lp1-Lp3**varies between 200 nm to 310 nm and their respective lipoplexes (**Lp1-Lp3**) ranged from 248.86 to 608 nm as shown in **Figure 2**. It was observed that the nano-sizes of lipoplexes prepared, either transfection efficient or incompetent lipids, similarly increased with increasing lipid-DNA charge ratios as depicted in **Figure 2.** The sizes of the lipoplexes of lipid **Lp2** is found to be the least among

the three lipids at 1:1 and 2:1 charge ratios where the maximum transfection of all the three lipids is observed. The rate of increase of sizes of the lipoplexes of lipid **Lp3** with increase in charge ratio is observed to be more than that of lipid **Lp1** and **Lp2 (Figure 2)**.The maximum size of lipoplexes of lipid **Lp3** may be because of the absence of the hydroxyl groups in the head group region, which are responsible for hydrogen boding interactions between DNA and lipid for effective condensation[18-20.]

The surface potentials of lipid-DNA complexes were determined in presence of DMEM. It is observed that all the lipid-DNA complexes the positive charge is increasing with increasing lipid: DNA charge ratios. The surface charges of lipoplexes of lipids **Lp1-Lp3**increased in the range of 5 to 30 mV (**Figure 2**). As the charge increases the rate of neutralization of DNA also increases and hence the zeta potential on the lipoplexes increases. It is observed that the rate of increase of zeta potential on the lipoplexes of **Lp1** is more when compared to **Lp2** and **Lp3**. This suggests that maybe triazole moiety in the linker region also play role in the neutralization of DNA.

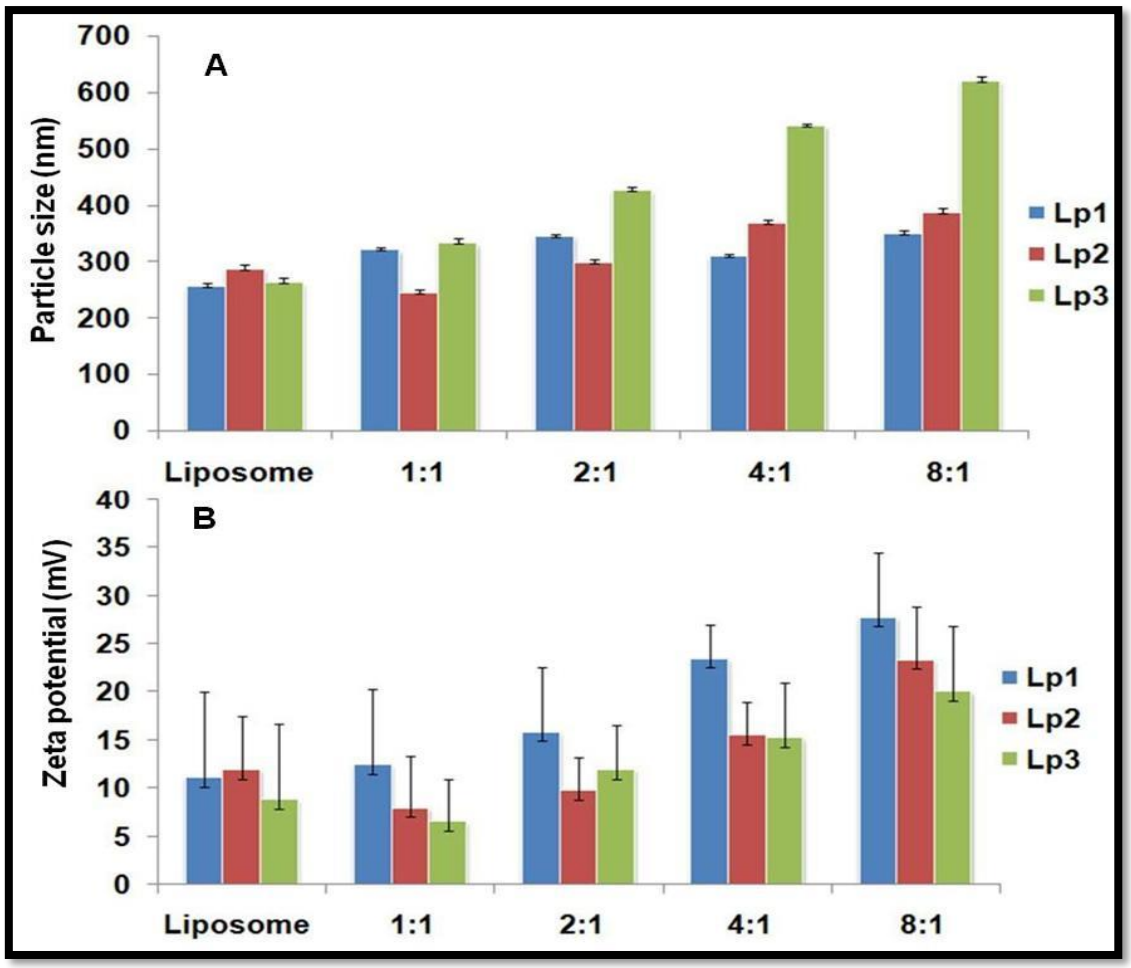

Figure.2 Mean particle sizes (A) and zeta-potentials (B) of lipid-DNA complexes at various N/P ratios (DLS at room temperature in DMEM). Data represent mean ± SD (n = 3).Statistical analysis was performed by Two-way ANOVA post hoc test (*P<0.05, **P< 0.01, ***P<0.001).

6.2.4 Lipid-DNA binding interaction and heparin displacement assay

To characterize the electrostatic interactions between the plasmid DNA and the present lipids **Lp1-Lp3** as a function of lipid: DNA charge ratio, electrophoretic gel retardation assay and heparin displacement assay are carried out using conventional gel electrophoresis. The electrophoretic mobility pattern of gel retardation assay revealed that the retardation of DNA was initiated even at very low charge ratio at 1:1, in case of all the lipids **Lp1-Lp3**. It is also observed that for all the lipids, about 90% of DNA mobility was retarded at 2:1 and 4:1 N/P

charge ratios and complete retardation of DNA was achieved at 8:1 N/P charge ratio (Figure 3). This was further supported by measuring the zeta potential of complexes derived from the charge ratios mentioned in Figure 2 which represents the neutralization of negative charge of DNA with successive addition of liposomes. The complexes surface potentials of all the lipids **Lp1-Lp3** were positive (5-12 mV) at lower charge ratio,1:1 itself and which was increased up to 20-30 mV respectively at 8:1 (**Figure 3A**).

To further elucidate the strength of lipoplexes in holding the plasmid, the lipoplexes were treated with Heparin; an anticoagulant. The finest stability of lipoplexes formed with lipids was confirmed by monitoring the sensitivities of the lipoplexes upon treatment with Heparin displacement. Similar binding efficacies were obtained for the liposomes of all lipids as observed in gel retardation assay (**Figure 3B**). Thus, the lipid-DNA complexes of lipids **Lp1-Lp3** having optimally strong lipid-DNA interactions may effectively contribute to the release of plasmid DNA in the cytoplasm. The stability of lipid-DNA complexes of lipids **Lp1-Lp2** may be attributed to the favourable hydrogen-bonding interactions betweenDNA and the hydroxyl functionalities present in the polar head group region of lipids **Lp1-Lp2.**

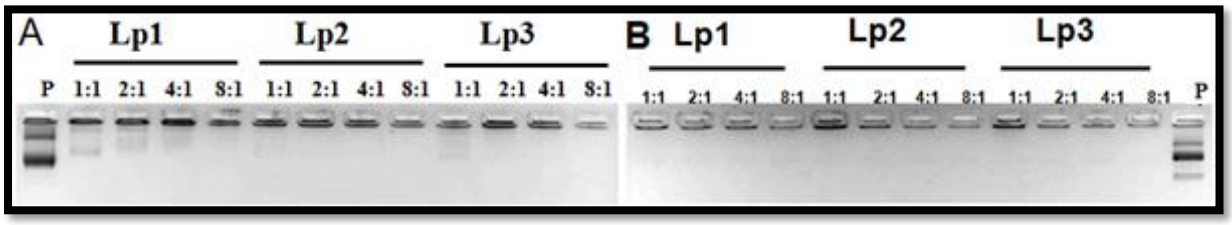

Figure 3(A) Electrophoretic gel patterns for lipoplex-associated DNA in gel retardation assay. (A) Refer to lipids **Lp1-Lp3**. The lipid: DNA charge ratios are indicated at the top of each line.**(**B) Electrophoretic gel patterns for lipid-DNA complexes-associated DNA in Heparin displacement assay for lipids **Lp1-Lp3**.The lipid: DNA charge ratios are indicated at the top of each line. The details of the treatment are as described in the text.

6.2.5 Buffering capacities of cationic lipids Lp1, Lp2 & Lp3

Endosomal escape is a major bottleneck for efficient non-viral gene delivery. Recent studies of Yun-jaie and Chong-Su Cho indicated that the buffering capacity of the polymers/lipids primarily impacts the endosomal escape and subsequent transfection efficiency[21]. Furthermore, the highlighted the significance of linkers in optimizing the buffering capacity when designing polymers or lipids for gene delivery. The studies demonstrated the mechanism of endocytosis and formation of endosomes prone to lysomallysis of polyplexes/lipoplexes having weak buffering capacity. Towards this end, to observe whether the introduction of triazole in the present ether-β-hydroxy-triazole hybrid linker contribute to its endosomal pH buffering or not, the buffering capacities of the lipids **Lp1**, **Lp2** and **Lp3** were studied by acid-base titration experiments and branched PEI was used as the control. The results revealed that the ether-β-hydroxy- triazole hybrid molecules gave a relatively slow pH increase with the addition of NaOH, indicating their good buffering capacities (**Figure 4**). The buffering capacity of the lipid **Lp2** is observed to be the maximum among the three lipids studied and also almost equal to the buffering capacity of PEI. The lipid **Lp3,** having the same linker group as **Lp2** is also showing high buffering capacities. Whereas, the buffering capacity of the lipid **Lp1**is found to be the least in which triazole moiety in the linker is absent**.** The pKa of the three lipids were determined using the above titration curve for the three lipids **Lp1**, **Lp2** and **Lp3** as about 4.4, 5.5 and 4.8 respectively. In the endosomal DNA escape mechanism mediated by pH-sensitive cationic transfection lipids, it is believed that the endosomal release of DNA into the cytosol should critically depend upon efficient protonation of the weakly basic head groups of pH-sensitive lipids in the acidic lumen of endosomes. The pKa of the lipids also clearly demonstrate that at endosomal pH **Lp2** will get protonated which may leads to the change in the morphology of the liposomes and hence release of the endosomal content into the cytoplasm. Hence, the results clearly

demonstrate the role of the triazole moiety of the linker in the endosomal escape through the endosomal pH buffering.

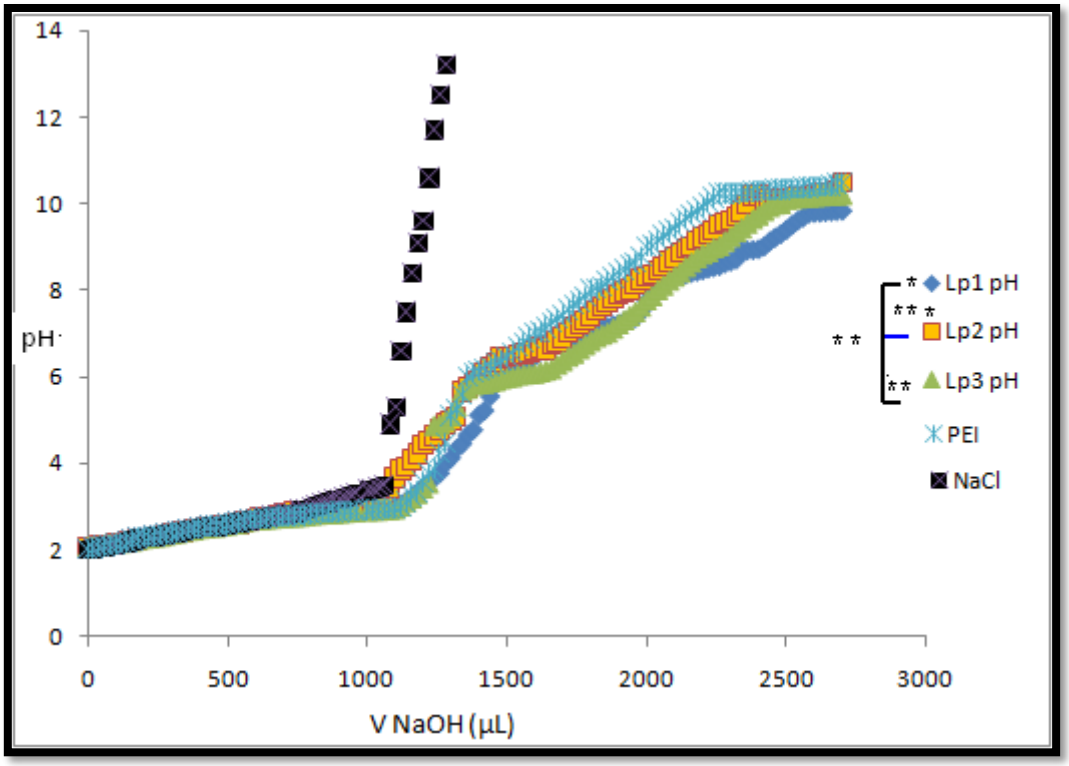

Figure 4. Acid-base titration profiles of 25 kDa PEI, 150 mM NaCl and lipid solutions. Lipids or PEI (0.050 mmol of cationic lipids **Lp1**, **Lp2** & **Lp3**) was first treated with 1 N HCl to adjust pH to 2.0, and then the solution pH was measured after each addition of 20 mL of0.1 N NaOH solution; Statistical analysis was performed by One-way ANOVA post hoc test (*P<0.05, **P< 0.01, ***P<0.001).

6.2.6 Hydrolysis Kinetics (HPLC) studies of Lipids Lp1, Lp2 and Lp3

To determine the pH sensitivity of the lipids **Lp1**, **Lp2** and **Lp3,** the rate of hydrolysis of the lipids (10 mg/mL) at different pHs 4.5, 5.5 and 7.4 were analysed using HPLC. The lipids were incubated in acetate buffer at pH s 4.5, 5.5 and 7.4 for different time intervals. The hydrolysis kinetics/degradation of lipids was quantitatively analyzed by HPLC, calculating the ratio between the peak area corresponding to the lipids hydrolysed product and the starting material, respectively (**Figure 5**). All the three lipids did not hydrolyze/degraded at

pH 7.4 even after 60 minutes. Rate constants were determined by plotting the cationic lipids (**Lp1**, **Lp2** & **Lp3**) versus time. After 45 min of incubation lipid **Lp1** is found to be degraded up to 30% at pH 5.5, and upto56% at pH 4.5. Whereas, the lipid **Lp2** (ether- β-hydroxy-triazole linker) was completely hydrolyzed at pH 4.5 and 70% degraded at pH 5.5. The lipid **Lp3** having the same linker as **Lp2** degraded to 60% at pH 4.5 and 34 % at 5.5. It was hypothesized that this variation may be due to the greater hydrophilic nature **Lp2** than **Lp3**, which helps in drawing more water around the lipid, hence faster degradation. These observed results are consistent with the qualitative acid-base titration results. In other words, the ether-β-hydroxy-triazole linker and hydroxy groups in the head group region may be a potent influence on their hydrolysis rates. Herein, we expected that the higher rate of hydrolysis and buffering capacity of lipid **Lp2**which might be contributed to the early endosome release compare to lipids **Lp3** and **Lp1.**

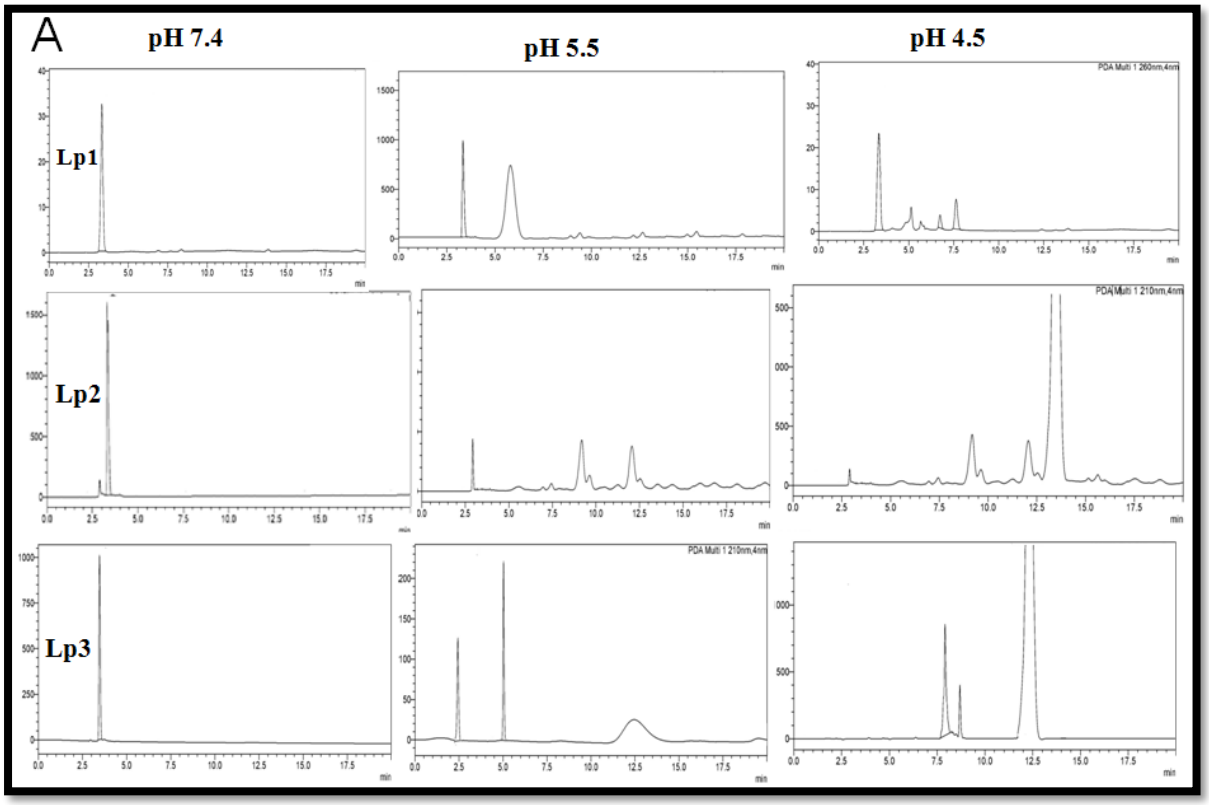

Figure 5 (A): Chromatograms of **Lp1, Lp2 & Lp3** cationic lipids**:** Determination of the rate of hydrolysis of the acid-sensitive lipids (10 mg/mL), which were incubated in acetate buffer at pH 4.5, 5.5 and 7.4 at 45 min. and 60 min. respectively.

6.2.7 pH- triggered size changes of lipoplexes of Lp1, Lp2 and Lp3 cationic lipids

To assess whether the acid-catalyzed hydrolysis of **Lp1**, **Lp2** and **Lp3** cationic lipids can trigger the changes in their liposome/pDNA complexes morphology, the hydrodynamic diameter of the lipoplexes was monitored after incubation [22] at different pH values i.e. 7.4, 5.5 and 4.5 (**Figure 6A**). As shown in figure 8 clearly indicating that the particle size of three liposome/DNA complexes was increased at lower buffer pH values, suggesting membrane fusion. The particle size of **Lp2** liposome permanently changed when compared to **Lp1** and **Lp3**liposomes at lower pH 4.5 value and also larger than **Lp1** and **Lp3.** whereas, the increase in particle size of**Lp3** liposomes with decrease in pH is less compared to **Lp2** liposome, this may be due to less hydration. The time dependent enhancement of size of the liposomes at pH4.5 was also studied (**Figure 6B**). It is observed that at pH 4.5, **Lp2** liposome particle diameter increased rapidly within the first ten minutes of incubation when compared to **Lp3**, **Lp1** liposomes. The sizes of the liposomes of **Lp1**, **Lp2** and **Lp3** were continue to increase at a slower rate upon prolonged incubation time. This clearly emphasize that to acidic environment destabilization and aggregation of **Lp2** liposome occurs, which might depend upon the hydrolysable group i.e. ether- β-hydroxy-triazole linker.

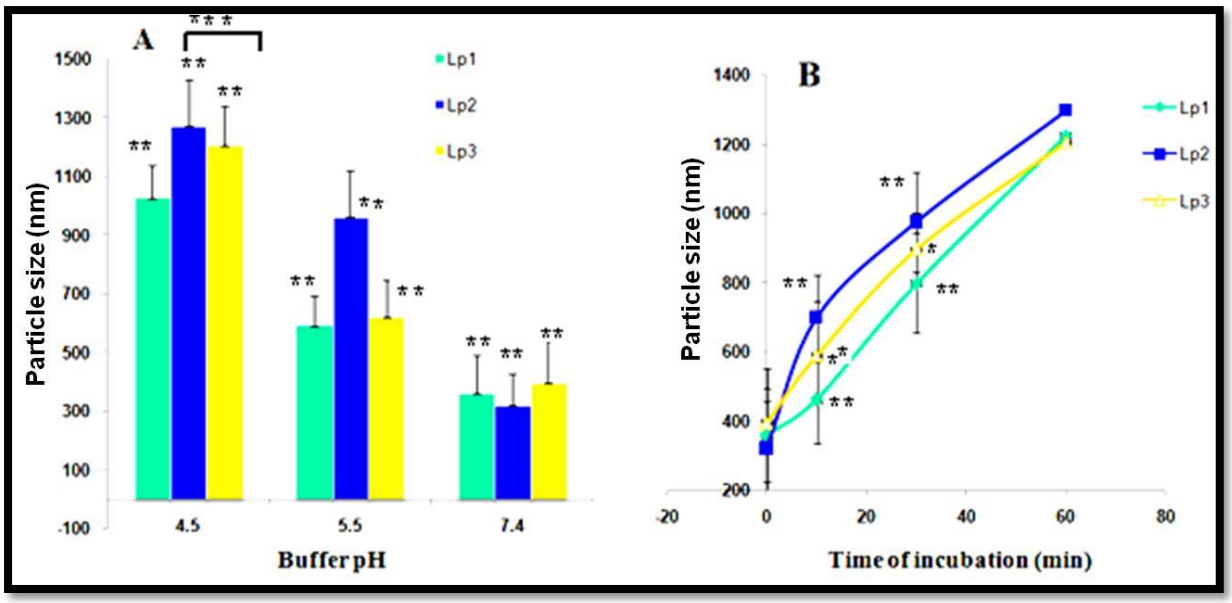

Figure.6 Increase in liposome particle size in response to buffer pH. (**A**) The size of the liposomes following 30 minutes incubation at 37 ˚C at various buffer pH; (**B**) time-dependent enhance in liposome diameter at pH 4.5. The liposome composition used was lipid/DOPE (1:1); Statistical analysis was performed by Two-way ANOVA (P<0.005) Statistical analysis was performed by t-test paired (* P<0.05, **P< 0.01, *** P<0.001).

6.2.8 Transfection biology: *in vitro* transfection studies

The transfection efficiencies of synthesized cationic lipids **Lp1-Lp3** compared with that of the commercial formulation lipofectamine3000 in NIH3T3, B16F10, HEK-293, and HepG2 cell lines are summarized in **Figure 7**. Higher gene transfection efficiencies of lipoplexes of all the synthesized lipids were observed at 2:1 and 4:1 lipid: DNA charge ratios. In the reporter gene assay, the *in vitro* gene transfer efficiencies of lipids **Lp1-Lp3** were observed to be higher in HepG2 and HEK-293 cells compared to B16F10and NIH3T3 cells. The lipids **Lp1-Lp3** showed moderate transfection activity in NIH3T3 cells and least activity in B16F10 cells. The high transfection activity of tocopherol based synthesized cationic lipids in HepG2 cells might be due to the presence of TTP (tocopherol transfer protein) in liver cells which contributed in the transfer of tocopherol and its analogues to HepG2 cells as reported previously [23, 24]. Among the tested lipids, lipoplex formed from lipid **Lp2** having the hybrid

linker ‘ether-β hydroxyl-triazole’ and triethyl hydroxyl groups on the head group region showed superior gene-transfection activity at 2:1 lipid: DNA complexes ratio against all the tested cell-lines.Moreover, transfection effieciency of **Lp2** in HEK-293, and HepG-2 cell lines is equal to that of the transfection observed in Lipofectamine 3000 (**Figure 7**). The higher transfection activity of lipid **Lp2** may be due to pH sensitivity[22, 25-27] of ‘ether-β hydroxyl-triazole’ linker and hydrogen bonding formation of hydroxyl groups with the cell-membrane to enable endosomal escape and release of the nucleic acid. Lipid **Lp1** contained triethyl hydroxyl groups on the head group region and no triazole moiety in the liker region showed less transfection efficacy than **Lp2** in the entire cell lines studied at 2:1 and 4:1 charge ratios. Whereas, the lipid **Lp3** with triethyl groups on head region showed the least transfection efficiency among the three lipids in all the cell lines and charge ratios studied (**Figure 7**). The least transfection efficiency of **Lp3** may be due to the absence of hydroxyl groups hence, the less binding interactions between DNA: lipid and which lead to larger size of lipoplexes.

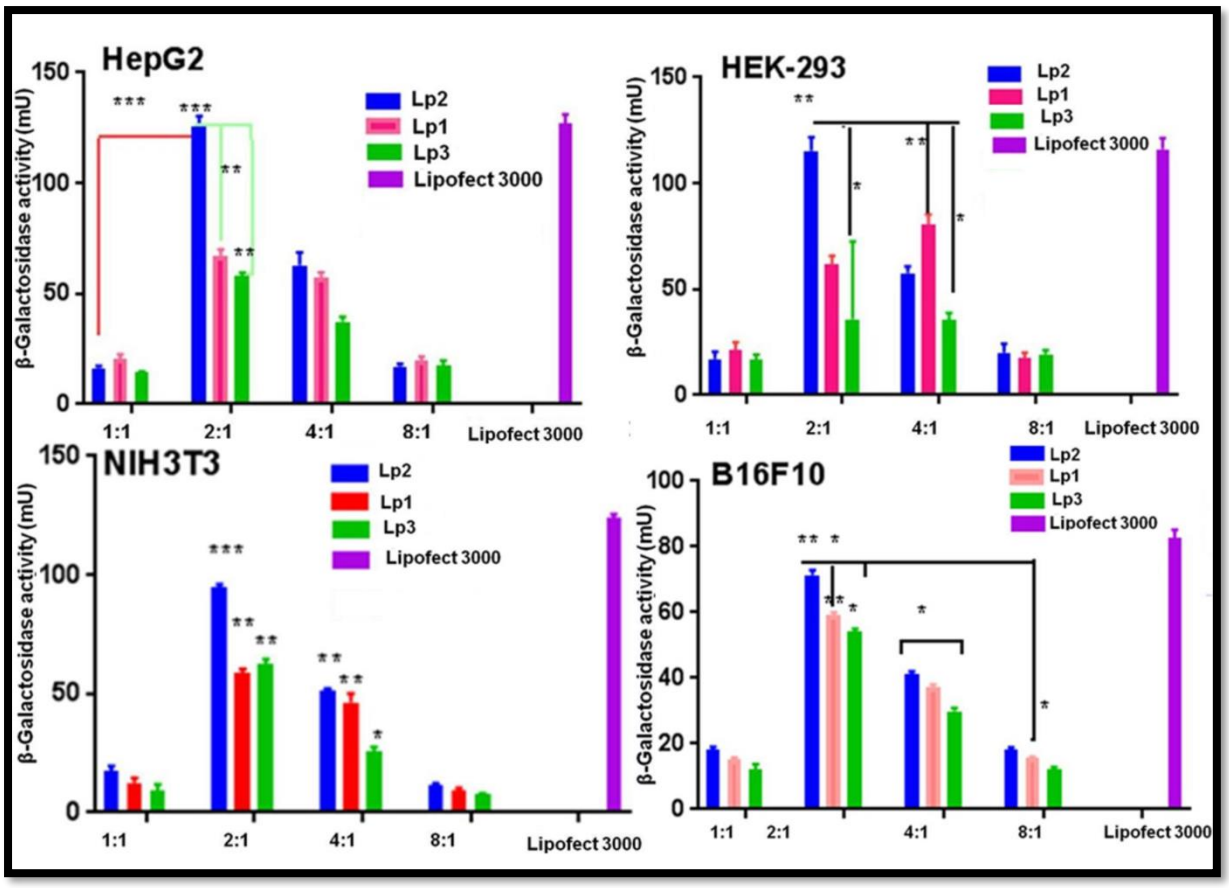

Figure. 7(A-D) Transfection efficiencies of lipids **Lp1-Lp3** in (A) HepG2 cells, (B) HEK-293 cells, (C) NIH3T3 cells and (D) B16F10 cells with DOPE as co-lipid (each lipid formulated with co-lipid in 1:1 molar ratio respectively).The transfection efficiencies of the lipids were compared to that of commercial formulation. Transfection experiments were performed as described in the text. All the lipids were tested on the same day, and the data presented are the average of three experiments performed on three different days. The error bar represents the standard error. Statistical analysis was performed by Two-way ANOVA.*P < 0.05; **P < 0.01; ***P < 0.001

6.2.9 Cellular expression of eGFP

Based on the pCMV-SPORT-β-galactosidase transfection results, the maximum transfection for the synthesized cationic lipids in tested cell-lines (B16F10, HepG2, NIH3T3 and HEK-293) was observed at 2:1 and 4:1 lipid: DNA charge ratios. It is obligatory to investigate at this point that, whether the DNA expression (eGFP) attains its utmost value at this given charge ratio or not. Herein, we selected HEK-293 cell line in order to study the transfection

efficacies of lipoplexes of green fluorescent protein encoded eGFP plasmid DNA. Consequently, the cellular expression of eGFP in HEK-293 was monitored by using inverted fluorescent microscope. The same results that observed in case of transfection activity studies are reflected here also. The expression of eGFP in HEK-293 is found to be high for lipid **Lp2**, moderate for **Lp1** and least for **Lp3** at 2:1 and 4:1 charge ratios studied (**Figure 8**). In addition, all the three lipids showed more eGFP expression at 2:1 charge ratio compared to the charge ratio at 4:1.The expression of eGFP with lipid **Lp2** is found to be on par with that of Lipofectamine 3000 at 2:1 charge ratio.

The eGFP expression quantitatively evaluated using FACS and the results indicate that all the three cationic lipoplexes (**Lp1, Lp2** and **Lp3**) showed their maximum % GFP positive cells at 2:1 charge ratio than 4:1 charge ratio (**Figure 8**).The obtained quantitative results (**Figure 8**) summarizes that **Lp2** lipoplexes showed ~90% of GFP positive cells at 2:1 charge ratio, whereas, it showed ~78% of GFP positive cells at 4:1charge ratio. It is also confirmed from the quantitative analysis of GFP expression that the percentage of GFP positive cells for lipoplexes of **Lp2** at 2:1 charge ratio is on par with that of lipofectamine 3000. The lipoplexes of **Lp1** and **Lp3** were showed lower% GFP positive cells compared to **Lp2** lipoplexes. The order of transfection efficiency of cationic lipids were mentioned according to their % GFP positive cells **Lp2>Lp1>Lp3.**

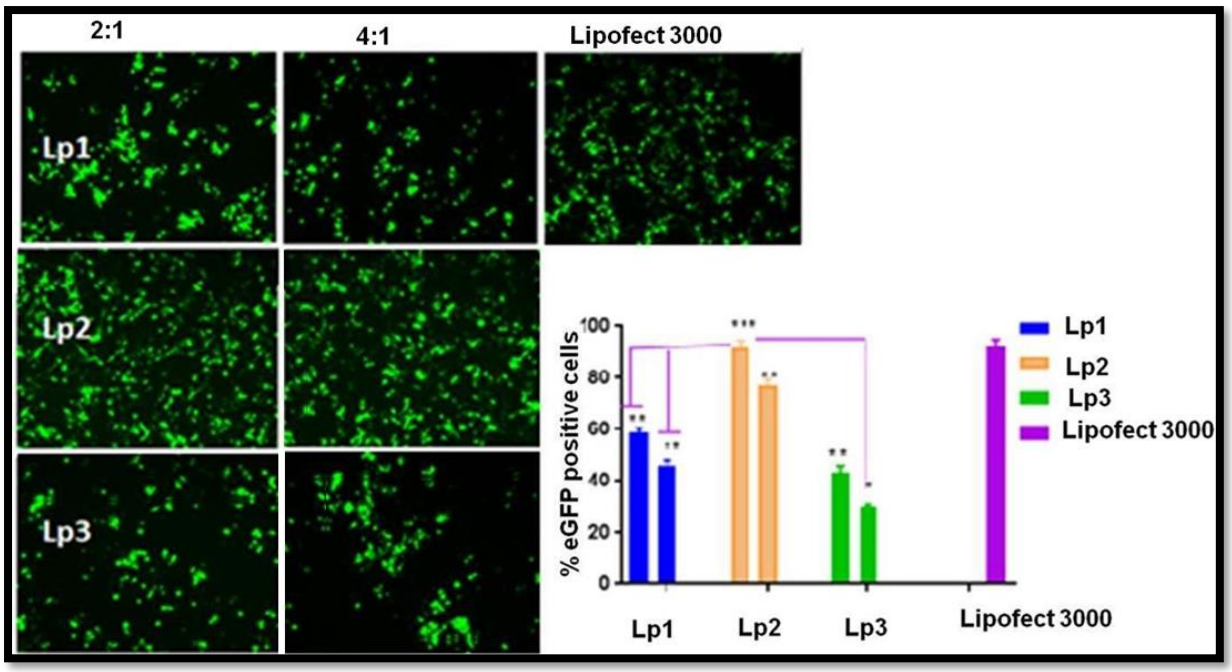

Figure 8. (A) Cellular expression of GFP. Inverted microscopic images of HEK-293 cells transfected with lipoplexes of lipids **Lp1-Lp3** prepared at high in vitro transfection lipid: DNA charge ratios of 2:1 and 4:1.The details of the experiments are as described in the text. Bars = 100µm. Standards shown are means ± SD of three independent experiments carryout in Triplicates. Statistical analysis was carry out by two-way ANOVA) (*P < 0.05; **P < 0.01; ***P < 0.001) **(B)** % positive GFP cells of eGFP plasmid transfection in HEK-293 cell lines using lipoplexes of **Lp1-Lp3** and eGFP at 2:1 and 4:1 N/P charge ratios. Lipofectmine 3000 (L3K) is taken as positive control.

6.2.10 Cellular uptake assay:

In order to demonstrate whether the major uptake occurs at this given charge ratio or not, lipoplexes of charge ratios 2:1 and 4:1 are prepared by complexing rhodamine-PE labeled liposomes of lipids **Lp1-Lp3** with eGFP and treated with HepG2 and HEK-293 cell lines. Cellular uptake of rhodamine-PE labelled lipoplexes was quantified using microplate fluorescent reader (**figure 9 A** and **B**). It was also observed under inverted fluorescent microscope (**Figure 10**).The observed cellular uptake examines demonstrate that maximum cellular uptake is obtained in HepG2 cell lines with all the three lipids **Lp1, Lp2** and **Lp3** at the given charge ratio compared to that of HEK-293 cell lines. Hence, these results in the

cellular uptake experiments (**Figures 9A** and **B**) support that the altering transfection profiles of lipids **Lp1-Lp2** could be predictable to the cellular uptake variations of lipids **Lp1-Lp3**. This accentuates the supposition that the degree of cellular uptake main key role in modulating the transfection efficiencies of the currently described tocopherol based cationic lipids. These assessments in the cellular uptake experiments (**Figures 9A and B**) show that the maximum uptake is observed for the lipoplexes of lipid **Lp2** amid the series of lipids studied at both the charge ratios and in both the cell lines studied. The findings from the fluorescent images (**Figure 10**) also demonstrate that maximum uptake is observed for the lipoplexes of **Lp2** than the lipoplexes of **Lp1** and **Lp3**. This might be due to the presence of ether-betahydroxy-triazole hybrid linker, and three hydroxyl groups in the head group of **Lp2.** This adumbrates possible supporting hydrogen bonding interactions between ether-betahydroxy-triazole hybrid linker; hydroxyl functionalities in the polar head group of the lipid **Lp2** and the biological membrane components. This could improve the cellular uptake of lipoplexes and thus showed up the highest transfection efficiency. Thus, the extent of cellular uptake appears to play a key role in modulating the transfection efficiencies of the presently give cationic lipids.

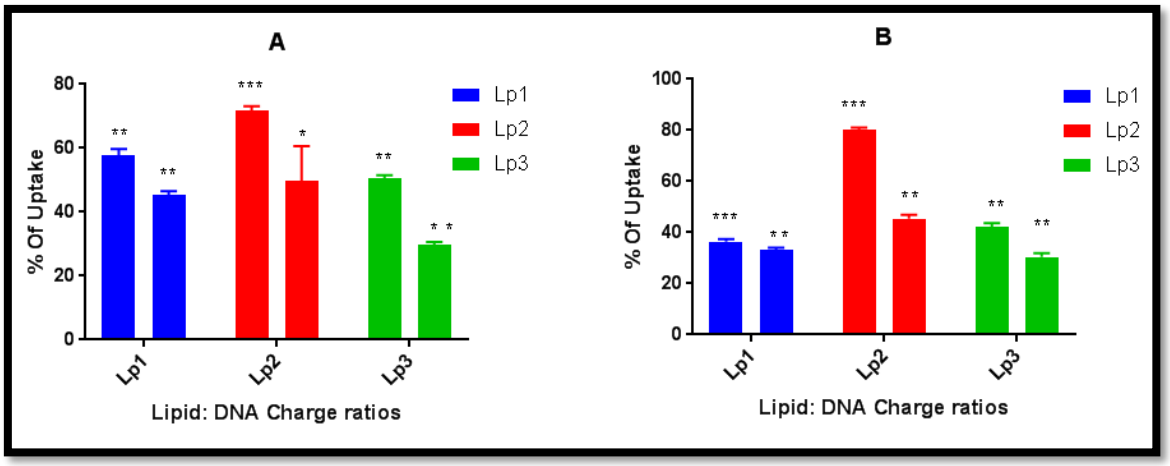

Figures. 9 (A-B) Cellular uptake of Rhodamine labeled lipoplexes. The fluorescence of lysates of (A)HepG2and (B) HEK-293 cells transfected with rhodamine labeled lipoplexes of

lipids **Lp1-Lp3** was measured by a microplate fluorescent reader (FLX 800, Bio-Tek instruments Inc, USA) using filter sets for red channels. The percentage uptake was calculated using the formula% uptake = 100x (fluorescence intensity of the fluorescence lipoplex treated cell lysate-background) / (fluorescence intensity of lipoplex added to the cells-background).The details of the experiments are as described in the text. Statistical analysis was carry out by two-way ANOVA) (*P < 0.05; **P < 0.01; ***P < 0.001) .

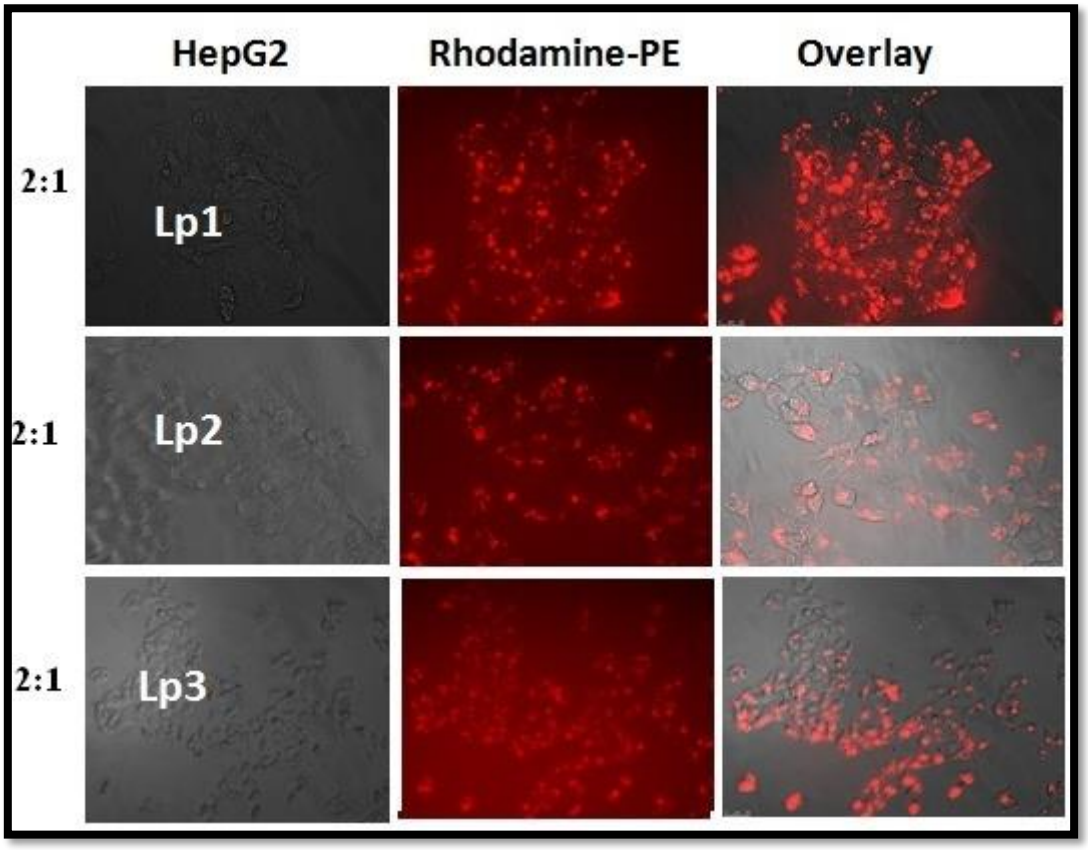

Figure. 10 Cellular uptake of Rhodamine labelled lipoplexes. Inverted fluorescent microscopic images of HepG2 cells transfected with lipoplexes of lipids **Lp1, Lp2** and **Lp3** prepared at the highest in vitro transfection lipid-DNA complex charge ratios of 2:1. Bright field images; fluorescent images; overlay images. The details of the experiments are as described in the text.

6.2. 11 Transfection biology in presence of serum

In general transfection activities of cationic liposomes are studied either in the absence of serum or in presence of only 10% (v/v) serum as reported in many earlier investigations[28-31]. However, the serum incompatibility/ serum stability still remains as the major setback

retarding clinical success of cationic lipid-mediated gene delivery system. Such common serum incompatability of cationic lipids is due to adsorption of negatively charged serum proteins onto the positively charged cationic liposome surfaces, which reduces their efficient interaction and internalization. Obviously, an opinion of gene transfer efficacies across a range of lipid-DNA charge ratios in multiple cultured cells in the presence of increasing concentrations of added serum is necessary for significant systemic potential of any *in vitro* efficient cationic transfection lipid. Towards this, serum-stability study was carried out for lipids **Lp1-Lp3** at lipid-DNA charge ratio 2:1 (at which all the three lipids showed their highest transfection capability in all 4 types of cells) in the presence of increasing concentrations of added serum (10-30%,v/v).The *in vitro* gene transfer efficacies of lipids **Lp1-Lp3** were found to be impervious in the presence of added serum (up to 30%) as shown in **Figure 11.** Lipid **Lp1** and **Lp2** were found to be the highest serum compatible at all the serum concentrations, while **Lp3** showed moderate transfection in the presence of added serum. Highly serum compatible transfection characteristics of lipids **Lp1** and **Lp2** up to 30% might be allied to large surface charge shielding of the lipid-DNA complexes induced by the ether-β hydroxy-triazole hybrid linker and hydroxyl functionalities in their polar head group region.

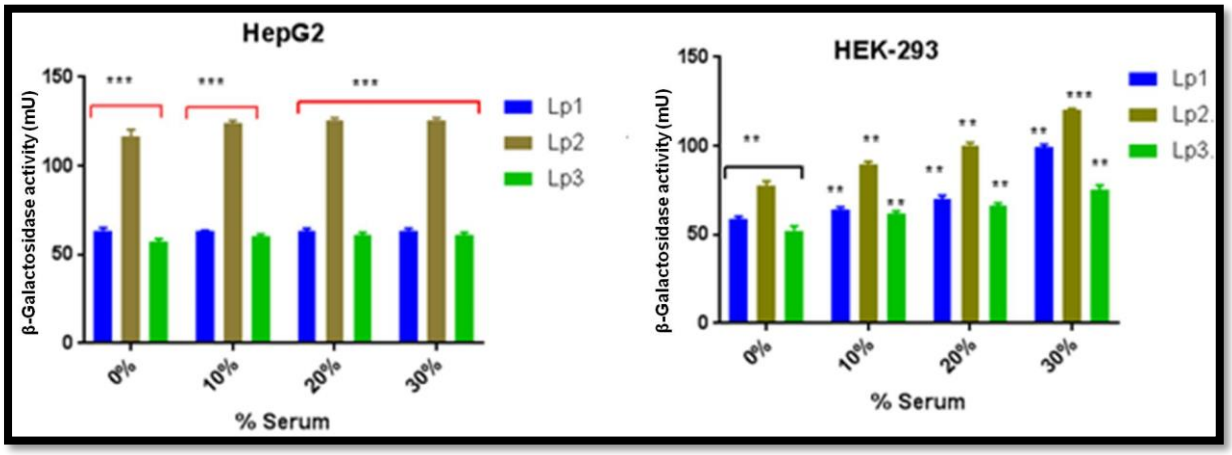

Figure.11 Transfection efficacies of the cationic lipids **Lp1−Lp3** in the presence of increasing concentrations of added serum. *In vitro* transfection efficiencies of lipid-DNA

complexes prepared using pCMV-β-gal-SPORT reporter gene at a lipid/DNA charge ratio of 2:1 were evaluated in the presence of enhancing concentrations of added serum in (A) HepG2 and (B) HEK-293 types of cells. The error bar indicates that the standard error. The difference in the data obtained is statistically significant in all charge ratios (*P< 0.05, **P< 0.01, ***P < 0.001).

6.2.12 Cell viability Assay

The cell viability assay (MTT assay) for liposomes of cationic lipids **Lp1-Lp3** in complexation with pDNA (pCMV-SPORT-β-galactosidase) were carried out in multiple cell lines such as NIH3T3, HEK-293, HepG2, and B16F10. Results from MTT assay showed that cationic lipids **Lp1-Lp3** exhibited less cytotoxicity i.e. about 85-100 % cell viability across lipid: DNA charge ratios (4:1-1:1) in all the cell lines studied. Cell viability is found to be moderate for lipids **Lp1** and **Lp2** even at higher charge ratio 8:1 where as for the lipid **Lp3** the cell viability is observed to be the least (69%) at this charge ratio (**Figure 12**). Thus, the cell viability data proves that enhancement in transfection efficacies of **Lp1, Lp2** and **Lp3** lipids cannot be correlated to their cytotoxic effects. Results were expressed as percent viability = [A540 (treated cells)-background/A540 (untreated cells)-background] x 100.

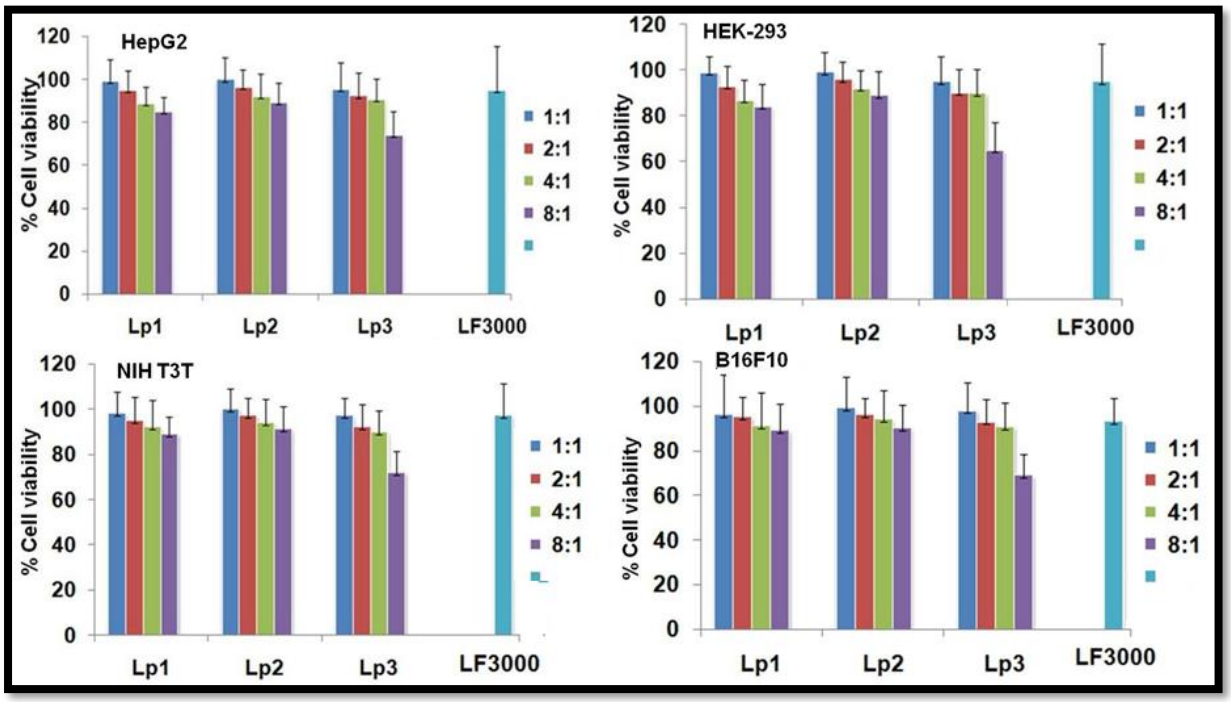

Figure 12. Representative percent of cell viabilities up on treatment with lipids **Lp1**-**Lp3** in HepG2 (A), B16F10 (B), NIH3T3 (C), and HEK-293 (D) cells using MTT assay. The absorbance obtained with reduced formazan with cell in the absence of cationic lipids was taken as 100. The toxicity assays were performed as depicted in the text. Data represent the mean SD (n = 3). The molar ratio of lipid/DOPE was 1: 1. *P < 0.05; **P < 0.01; ***P < 0.001. Data represent mean SD (n = 3).

6.3 Conclusions

In summary, the synthesized α-tocopherol based cationic amphiphile can efficiently deliver genes into multiple cultures cells. Among the three cationic lipids studied (**Lp1**, **Lp2** and **Lp3**) lipid **Lp2** with novel "ether-β-hydroxy-triazole" pH sensitive linker between tris (2-hydroxyethyl) ammonium head group and tocopherol anchoring group showed superior transfection activity. This novel linker has significantly affected the physico-chemical and biological properties of cationic lipids. Hence, the novel pH sensitive linker ether-β-hydroxy-triazole linker may be attractive in designing new lipids for gene delivery. It is also observed from the result that the present tocopherol based lipids are least cytotoxic and targeting to liver (HepG2 cell lines). Based on the results it is suggested that our lipid will be a promising non-viral gene delivery vector with superior transfection efficiency and least cytotoxicity. These findings collectively suggested that lipid**Lp2** could be used for liver specific gene delivery without destruction of liver cells.

6.4 Experimental Section

6.4.1 General procedure and chemicals reagents

Mass spectral data were acquired by using a commercial LCQ ion trap mass spectro-meter (ThermoFinnigan, SanJose, CA, U.S.) equipped with an ESI source.^{1}H NMR spectra were recorded on a Varian FT400 MHz NMR spectrometer. α-tocopherol was purchased from Sigma Co. eGFP plasmid, and rhodamine-PE were ample gifts from IICT (Indian Institute of Chemical Technology, Hyderabad, India). Lipofectamine-3000 was purchased from

Invitrogen Life Technologies, polyethylene glycol 8000, and o-nitrophenyl-β-D-galactopyranoside was purchased from Sigma (St. Louis, MO, U.S.). NP-40, antibiotics, and agarose were purchased from Hi-media, India. DOPE was purchased from Fluka (Switzerland). Unless otherwise stated, all the other reagents purchased from local commercial suppliers were of analytical grade and were used without further purification. The build up of the reaction was monitored by thin-layer chromatography using 0.25 mm silica gel plates. Column chromatography was executed with silica gel (Acme Synthetic Chemicals, India; finer than 200 and 60-120mesh). Elemental analyses were performed by High resolution mass spectrometry (HRMS) using QExactive equipment (Thermo Scientific). The purity of lipids were characterised by HPLC (Shimanzu LC Solution) and showed more than 95% purity. HepG2, NIH3T3, B16F10 and HEK-293 cells were procured from the National Centre for Cell Sciences (NCCS), Pune, India. Cell were grown at 37 ˚C either in Dulbecco's modified Eagle's medium (DMEM) with 10% FBS in humidified atmosphere containing 5% CO2 / 95 % air.

Synthesis of α-tocopherol glycidyl ether with epichlorohydrine (1A)

To a stirred mixture of (+/_)-α-tocopherol (5.42 g, 12.58 mmol), rac-epichlorohydrin (1.74 g, 18.87 mmol), and tetra-butylammonium hydrogensulfate (0.43 g, 1.13 mmol) at 0 °C, was added 50 % KOH solution (3.24 g, 57. 8 mmol) in water (6.5 mL). The reaction mixture was warmed to room temperature and stirred for 4 h. The product is extracted with Et_2O, the pooled organic layer is washed with water, dried with anhydrous Na_2SO_4, filtered, and concentrated under reduced pressure. The crude product was purified by silica gel column chromatography to give α-tocopheryl glycidyl ether **1A** (5.89 g, 12.10 mmol, 96 %) as a clear oil. The yield of compound was 86%. Rf = 0.69 (EtOAc/hexane).

^{1}HNMR (400 MHz, $CDCl_3$): δ = 0.84 (3 H), 0.85 (3 H), 0.87 (d, 6 H), 1.00–1.60 (m, 21 H), 1.23 (s, 3 H), 1.71–1.85 (m, 2 H), 2.08 (s, 3 H), 2.14 (s, 3 H), 2.18 (s, 3 H), 2.57 (t, 2 H), 2.70 (dd, 1 H), 2.87 (dd 1 H), 3.35 (dddd 1 H), 3.66 (ddd, 1 H), 3.90 (ddd, 1 H) ppm. **ESI-MS** *m/z*: Calculated 486 (for $C_{32}H_{54}O_3$); found 486 [M^+]

Synthesis of 2,2-{(2-hydroxy-3-[(-2,5,7,8-tetramethyl-2-(4,8,12-trimethyltridecyl) chroman-6-yl)oxy]propyl) azanedilyl} diethanaol (1B)

To a 100mLround bottom flask containing a stir bar was added 1.00 g of tocopheryl glycidyl ether (1mmol) in 2mLof methanol. To this mixture added a mixture of diethanolamine in methanol (0.5units, 1.1 mmol). The reaction mixture was refluxed under nitrogen atmosphere about 18h. After completion as indicated by TLC, the reaction mixture was extracted with ethyl acetate; the combined organic layers were washed with H_2O and brine, dried over anhydrous Na_2SO_4, and evaporated under reduced pressure. The residue was subjected to column chromatography on silica gel to give yellow colored α-tocopheryl trihydroxy ether. Rf = 0.5 (10% Methanol/Chloroform). The yield of final lipids was 78%.

^{1}H, NMR (400 MHz, $CDCl_3$):δ = 0.87 – 0.84 (m, 12H), 1.66 – 1.07 (m, 21H), 1.34 (m, 2H), 1.4 (m, 3H), 1.47 (m, 2H), 2.00 (s, 3H), 2.06 (s, 3H), 2.09 (s, 3H), 2.4 (m, 2H), 2.8 (m, 2H), 3.41 broad, 2OH), 3.48 (broad, 1OH), 3.8 (t, 4H), 4.2 (t, 4H), 4.2 (m, 3H). ESI Mass m/z: Calculated 591 (for $C_{36}H_{65}NO_5$); found 591[M^+].

Quarternization of α-tocopheryl trihydroxy ether with 2-chloro ethanol (Lipid Lp1)

To a mixture of α-tocopheryl trihydroxy ether (1 mmol) in excess 2-chloroethanol was added K_2CO_3 (1.1 mmol), and the reaction mixture was stirred at reflux temperature for a specified time as required to complete the reaction. After completion as indicated by TLC, the solvent was evaporated with the help of rota evaporator, and then the crude mixture was purified by column chromatography on silica gel (eluent: Methanol/Chloroform) to yield the pure yellow

colored final lipid**Lp1**. Rf = 3.5 (10% Methanol/ Chloroform). The yield of final compound was 88%.

^{1}HNMR (400 MHz, $CDCl_3$): δ = 0.87 – 0.84 (m, 12H), 1.66 – 1.07 (m, 24H), 1.34 (m, 2H), 1.4 (m, 3H), 1.47 (m, 2H), 2.00 (s, 3H), 2.06 (s, 3H), 2.09 (s, 3H), 2.4 (m, 2H), 3.4 (t, 6H), 3.93-4.01 (m, 2H), 3.8 (m, 1H), 3.1-3.2 (m, 2H), 3.6 (broad, 3OH), 3.5 (broad, 1secondary OH); **^{13}C NMR (101 MHz, $CDCl_3$)** δ 146.98, 146.89, 126.55, 124.58, 122.00, 116.60, 73.83, 70.15, 58.82, 56.11, 53.60, 39.02, 38.96, 38.35, 36.54, 36.43, 36.36, 36.26, 31.75, 31.67, 30.20, 28.68, 26.95, 23.78, 23.42, 22.81, 21.70, 21.61, 20.01, 19.64, 18.73, 18.66, 11.84, 10.97, 10.76. ESI Mass m/z: Calculated 636 (for C_{38} $H_{78}NO_6$); found 636[M^+], **HRMS-ESI**: Calculated 636.52; found 636.5225, HPLC Purity: 97%.

Synthesis of *N, N,* N-tris(2-hydroxyethyl)prop-2-yn-1-aminium (2A)

Proparzyl bromide (1.1eq, 1.1mmol) was added drop-wise to a solution of triethanolamine (1eq, 1mmol) in 9:1 propane in toluene at 4°C under argon atmosphere. After 1h, the reaction mixture was allowed slowly towarm to room temperature (within 1 h), then stirredfor 18 h andevaporatedthe solvent. The crude mixture was purified by column chromatography on silica gel (eluent: Methanol/Chloroform) to provide the pure yellow colour liquid (95%). Rf = 3.0 (10% Methanol/ Chloroform).

^{1}H, NMR (400 MHz, CD_3OD): δ = 2.5 (s, 1H), 3.9 (s, 2H), 3.5 (t, 6H), 3.98(t, 6H), 3.6 (3OH, broad). ESI Mass m/z: Calculated 188 (for C_9 $H_{18}NO_3$); found 188[M^+].

Synthesis of α-tocopheryl azidohydrin (2B)

To a mixture of epoxide (1 mmol) and $CeCl_3.7H_2O$ (0.5 mmol) in acetonitrile and water (9:1, 10 mL) was added NaN_3 (1.1 mmol), and the reaction mixture was stirred at acetonitrile reflux temperature for 12 h for the completion of the reaction. After completion as indicated by TLC, the reaction mixture was extracted with ethyl acetate; the combined organic layers

were washed with H_2O and brine, dried over anhydrous Na_2SO_4, and evaporated under reduced pressure. The residue was subjected to column chromatography on silica gel (eluent: hexane/ethyl acetate) to provide the pure tocopheryl azidohydrin**.** The yield of compound was 86%. Rf = 0.7 (EtOAc/hexane).

^{1}HNMR (400 MHz, $CDCl_3$): δ = 0.8-0.9 [m, 12H],], 2.1 [m, 9H tocopheryl], 2.08 [s, 3H Tocopheryl], 1.7 [m, 2H tocopheryl], 1.5 [m, 3H tocopheryl], 1.2 [m, 18H], 3.7 [m, 2H], 3.8 [m, 1H], 3.2 [m, 2H], 2.5 [m, 2H]. **ESI-MS** *m/z*: Calculated 529 (for C_{32} $H_{53}N_3$ O_3); found 529+Na = 552.

Synthesisof2-hydroxy-*N*-{(1-[2-hydroxy-3-((2,5,7,8-tetramethyl-2-(4,8,12-trimethyltridecyl)chroman-6-yl)oxy)propyl]-1*H*-1,2,3-triazol-4-yl)methyl}-*N*,*N*-bis(2-hydroxyethyl)ethanaminium chloride or bromide(2c and Lp2 lipid).

The α-tocopheryl azidohydrin (0.19 mg, 0.529 mmol), *N*, *N*, *N*-tris(2-hydroxyethyl)prop-2-yn1aminium (0.0674 mg, 0.188mmol) were suspended in solvent mixture THF/H_2O (7 mL, 1:1). To the mixture freshly prepared sodium ascorbate (0.014mg, 0.2 mmol) followed by $CuSO_4.5H_2O$ (0.06 mg, 0.1 mmol) were added. The reaction mixture was heated for 2 h under microwave irradiation (100 °C). The residue was precipitated by the addition of methanol (20 mL). The precipitate was filtered and washed with methanol. The residue was subjected to column chromatography on silica gel to give intermediate **2c** (64 mg, 88%). Rf = 1.8 (10% Methanol/Chloroform v/v). The intermediate **2c** is then subjected to chloride ion exchange chromatography to afford the titled lipid **Lp2** with 90 % yield.

^{1}HNMR (400 MHz, $CDCl_3$): δ = 0.87 – 0.84 (m, 12H), 1.66 – 1.07 (m, 21H), 1.34 (m, 2H), 1.4 (m, 3H), 1.47 (m, 2H), 2.00 (s, 3H), 2.06 (s, 3H), 2.09 (s, 3H), 2.4 (m, 2H), 2.58 (m, 2H), 3.2 (t, 6H), 3.4-3.6 (broad, 4OH), 3.8-3.7 (m, 9H), 4.6-4.3 (m, 1H); **^{13}C NMR (101 MHz,**

$CDCl_3$) δ 146.98, 146.89, 126.55, 124.58, 123.60, 122.00, 116.60, 73.83, 70.15, 61.34, 61.02, 58.82, 56.11, 53.60, 39.02, 38.96, 38.35, 36.54, 36.43, 36.36, 36.26, 31.75, 31.67, 30.20, 28.68, 26.95, 23.78, 23.42, 22.81, 21.70, 21.61, 20.01, 19.64, 18.73, 18.66, 11.84, 10.97, 10.76.**ESI Mass m/z**: Calculated 717 (for C_{41} $H_{73}N_4$ O_6); found 717 [M^+]. HRMS-ESI: Calculated 717.5446; found 717.5520, HPLC Purity: 96%.

Synthesis of *N, N, N*-triethylprop-2-yn-1aminium (3A)

Proparzyl bromide (1.1eq, 1.1mmol) was added drop wise to a solution of triethylamine (1eq,1 mmol) in toluene at 4 °C under argon atmosphere and stirred at this temperature for 1h, then the reaction mixture was allowed to warm slowly to room temperature (within 1 h), then stirred for 18 h and evaporated the solvent. The crude mixture was purified by column chromatography on silica gel (eluent: Methanol/Chloroform) to provide the pure yellow colour liquid (**3A**) (95%). Rf = 3.0 (10% Methanol/ Chloroform).

^{1}HNMR (400 MHz, $CDCl_3$): δ = 1.4 (t, 9H), 3.1 (q, 6H), 3.2 (s, 2H), 2.2 (s, 1H); **ESI-MS** *m/z*: Calculated 529 (for C_{32} $H_{53}N_3$ O_3); found: 529+Na = 552

Synthesis of N,N-diethyl-N-{(1-[(2,5,7,8-tetramethyl-2-(4,8,12 trimethyltridecyl) chroman-6-yloxy)-2-hydroxy-3-propyl]-1H-1,2,3-triazole-4-yl) methyl}ethanaminium bromide or chloride (3B and Lp3 lipid)

A mixture of $CuSO_4.5H_2O$ (0.0080 mg, 0.1 mmol), sodium ascorbate (0.019 mg, 0.39 mmol, 0.4 mL of freshly prepared solution in water), compound *N, N, N*,-triethylprop-2-ny-1-aminium (0.070 mg, 0.140 mmol) and α-tocopheryl azidohydrin (267 mg, 0.529 mmol) in THF/H_2O (7 mL, 1:1) was heated for 2h under microwave irradiation (100°C). The product was precipitated by the addition of methanol (20 mL). The precipitate was filtered and wished the residue with methanol. The residue was subjected to column chromatograph on silica gel to give intermediate **3B** (647 mg, 91%). Rf = 1.8 (10% Methanol/Chloroform).

The intermediate **3B** is then subjected to chloride ion exchange chromatography to afford the titled compound Lipid **Lp3** with 96% yield.

^{1}HNMR (400 MHz, $CDCl_3$): δ = 0.87 – 0.84 (m, 12H), 1.66 – 1.07 (m, 21H), 1.34 (m, 2H), 1.4 (m, 3H), 1.47 (m, 11H), 2.00 (s, 3H), 2.06 (s, 3H), 2.09 (s, 3H), 2.4 (m, 2H), 2.58 (m, 2H), 2.4 (m, 2H), 2.58 (m, 2H), 3.8 (s, 1H), 4.92 (m, 1H), 4.33 (s, 2H), 7.5 (s, 1H); **^{13}C NMR (101 MHz, $CDCl_3$)** δ 146.98, 146.89, 126.55, 124.58, 123.60, 122.00, 116.60, 73.83, 70.15, 61.34, 61.02, 58.82, 56.11, 53.60, 39.02, 38.96, 38.35, 36.54, 36.43, 36.36, 36.26, 31.75, 31.67, 30.20, 28.68, 26.95, 23.78, 23.42, 22.81, 21.70, 21.61, 20.01, 19.64, 18.73, 18.66, 11.84, 10.97, 10.76; **ESI Mass m/z**: Calculated 669 (for C_{41} $H_{73}N_4$ O_3); found 669 [M^+]. **HRMS-ESI**: Calculated 670.04214; found 670.04583, HPLC Purity: 96%.

6.4.2 Preparation of liposomes and plasmid DNA

The cationic lipid and the helper lipid DOPE (concentration of the each lipid and co-lipid is 1 mol, respectively) were dissolved in chloroform in an autoclaved dry glass vial. The solvent was removed with a thin flow of moisture free nitrogen gas, and further dried the thin film under high vacuum for 6 h. Then 1 ml of sterile deionized water was added to the vacuum-dried lipid film and the mixture was allowed to swell overnight. The vial was then vortexed for 2-3 min at room temperature till transparent solution appears and occasionally sonicated in a bath sonicator to produce multilamellar vesicles (MLVs). MLVs were then sonicated in an ice bath until clarity using a Branson 450 sonifier at 100% duty cycle and 25W output power. The resulting clear aqueous liposomes were used in forming lipid-DNA complexes. as described previously[32]. The purity of plasmid was checked by A_{260}/A_{280}ratio (around 1.9) and 1% agarose gel electrophoresis.

6.4.3 DNA binding assay

DNA-lipid complexes were formed by mixing 3μL of plasmid DNA (0.1 μg/μL in 10 mMHepes buffer, pH 7.4) with varying amounts of cationic lipids so that the final lipid:DNA charge ratios were maintained at 1:1 to 8:1 in a total volume of 30 μL. Complexes were incubated for 30 minutes at room temperature after which 15 μL of each lipoplex was loaded on a 1% agarose gel (pre-stained with ethidium bromide) and electrophoresed (80 V, 45 min.). The bands were visualized using a Bio-Rad Gel Doc XR+ imaging system (Bio-Rad, Hercules, CA, USA).

6.4.4 .Heparin Displacement Assay

Heparin helps to study the anionic dislocation of DNA within the lipoplexes. The lipid: DNA complexes were prepared as described in the above section (DNA binding assay) and incubated for 20 minutes. These lipids: DNA complexes were further incubated for 30 minutes with 0.1µg of sodium salt of heparin. The samples were electrophoresed in an agarose gel (1.5%) for Heparin displacement analysis and DNA bands were visualized as mentioned in the above section.

6.4.5 Zeta potential (ξ) and size measurements

The sizes and the surface charges (zeta potentials) of liposomes and lipoplexes with varying charge ratios (8:1 to 1:1) were measured by photon correlation spectroscopy and electrophoretic mobility on a Zetasizer 3000HSA (Malvern, U.K.). The sizes were measured in deionized water with a sample refractive index of 1.59 and a viscosity of 0.89 cP. The system was calibrated by using the200 nm $\pm$ 5 nm polystyrene polymers (Duke Scientific Corps., Palo Alto, CA). The diameters of liposomes and lipoplexes were calculated by using the automatic method in triplicate and represented as average values. . The sizes were measured in triplicate. The zeta potential was measured using the following parameters:

viscosity, 0.89 cP; dielectric constant, 79; temperature, 25°C; F (Ka), 1.50 (Smoluchowski); maximum voltage of the current, 80 V. The system was calibrated by using DTS0050 standard from Malvern. Measurements were done 10 times with the zero-field correction. The potentials were measured 10 times and represented as their average values as calculated by using the Smoluchowski approximation.

6.4. 6.Degradation studies of Lp1, Lp2 and Lp3

The stability of the **Lp1**, **Lp2** and **Lp3** lipids products under acidic environments were carry out at different pH (4.5, 5.5 and 7.4) values in 0.1 M acetate buffer. The percentage (%) of degradation was deduced from the integration of the peaks corresponding either to the starting material or to the lipids hydrolysis product, using HPLC (Shimadzu Lab Solutions). The microsorb® 100, RP-18e (10 µm), 125 x 4 mm column was used, eluted by a water/acetonitrile linear gradient (1 ml/min, 0–20 min, 20–100% CH_3CN), buffered with 0.01% HPLC-grade triethylamine. A stock solution of the lipids (10 mg/ml in 0.1 M triethylammonium acetate buffer, pH 7.5) was made and 0.1-ml aliquots were diluted in 1 ml of the desired buffer (pH 4.5 and 5.5), giving the initial time of the reaction. The pH of a sample was measured to ascertain that this buffer mixture did not noticeably affect the final pH. Final concentration of the lipid was in the range of 10^{-4} M. Measures at close intervals could be achieved by quenching aliquots of the reaction medium with excess triethylamine; other points were obtained through the use of the auto sampler timing of the HPLC equipment. All the experiments were carried out at room temperature.

6.4.7 Acid e base titration

The lipids **Lp**1, **Lp2** and **Lp3**, (0.050 mmol) were dissolved in 15 mL of 150 mM NaCl aqueous solution, and 1 N HCl was added to adjust pH to 2.0. Aliquots (40 µL for each) of 0.1 M NaOH solution were added, and the solution pH was measured with a pH meter (pHS-

25) after each addition. For comparison, NaCl (150 mM) and PEI (25 kDa) were used under the same experimental conditions.

6.4.8 Stability of the Lp1, Lp2 and Lp3 lipids complexes at different pH values

Liposome /DNA complexes were prepared as described above and subjected to different pH values (4.5, 5.5 & 7.4) by adjusting the pH of the buffer0.1 M sodium citrate buffer at 37 ˚C. Mean size increase was measured as a function of time. The hydrolysis of the pH-sensitive lipids induced a deshielding of the lipoplexes and aggregation of the neutral particles.

Statistical analysis:

The results were expressed as (mean standard deviation). Statistical importance between treatments was assessed by the ANOVA test followed by the Dennett multiple comparison test (*P<0.05, **P<0.01, ***P< 0.001).

6.4.8 Transfection Biology

Cells were seeded at a density of 10,000 (for B16F10) and 15,000 cells (for NIH3T3, HEK-293, and HepG2) per well in a 96-well plate 18-24 h before the transfection. Then 0.3 μg (0.91 nmol) of plasmid DNA was complexed with varying amounts of cationic lipids in plain DMEM medium (total volume made up to 100 μL) and incubated for 30 min. The charge ratios were changed from 1:1 to 8:1 over these ranges of the lipids. Just prior to transfection, cells plated in the 96-well plate were washed with PBS (2×100 μL) followed by the addition of lipid-DNA complexes. After 4 h of incubation, 100 μL of DMEM with 20% FBS was added to the cells. The medium was changed to 10% complete medium after 24 h, and the reporter gene activity was estimated after 48 h. The cells were washed twice with PBS (100 μL each) and lysed in 50 μL lysis buffer [0.25 M Tris-HCl (pH 8.0) and 0.5% NP40]. Care was taken to perform complete lysis. The β-galactosidase activity per well was estimated by adding 50 μL of 2X substrate solution [1.33 mg/mL ONPG, 0.2 M sodium phosphate (pH 7.3), and 2mM magnesium chloride] to the lysate in a 96-well plate. Absorbance of the

product ortho-nitrophenol at 405 nm was converted to β-galactosidase units by using a calibration curve constructed using pure commercial β-galactosidase enzyme. Each transfection experiment was repeated 3 times on 3 different days. The transfection values were noted average values from performed three replicate transfection plates assayed on three different days. The values of β-galactosidase units in replicate plates assayed on the same day varied by less than 20%. The day to day difference in transfection efficiency values for identically treated transfection plates was found to be small and was dependent on the cell density and condition of the cells.

6.4.9 Cellular Uptake Observed under Inverted Microscope

Cells were harvested at a density of 10 000 cells/well in a 24-well plate usually 18 h prior to the treatment. eGFP plasmid (0.3 μg of DNA diluted to 30 μL with serum free DMEM media) was complexed with rhodamine-PE labeled cationic liposomes (diluted to 50 μL with DMEM) using 2:1 lipid –DNA complexes charge ratio. The cells were washed with PBS (1×200 μL), then treated with lipoplexes and incubated at a humidified atmosphere containing 5% CO_2 at 37 °C. After 4 h of incubation, the cells were washed with PBS (3×200 μL) to remove the dye completely from the wells and the cells were observed under inverted microscope.

6.4.10 Cellular α5GFP Expression Study

For cellular α5GFP expression experiments in HEK-293 50, 000 cells were cultured in well of 24-well plate 18-24 h before the transfection. Then 0.9 μg of α5GFP plasmid DNA encoding green fluorescent protein was complexed with liposomes of lipids **Lp1-Lp3**at charge ratio (lipid-DNA complexes) 2:1 in plain DMEM medium (total volume made up to 100 μL) for 30 min. Just prior to transfection, cells plated in the 24-well plate were washed with PBS (2×100 μL) followed by addition of lipoplexes. The media 400 μL was added after

4 h incubation of the cells. After 24 h, the complete medium was removed from each well, and the total cells were washed with PBS (2× 200 μL). Finally 200 μL of PBS was added to each well and visualized under the inverted fluorescent microscope to observe the cells expressing the green fluorescent protein and after that the cells expressing EGFP was quantified using a FACS Calibur flow cytometer (Becton-Dickinson) equipped with an argon ion laser at 488 nm for excitation and detection at 530 nm. 10,000 cells were analyzed for each sample using the software, Cell Quest. Non transfected cells served as live cell controls for gate settings which in turn provided the cut off thresholds for quantification of fluorescent cell population.

6.4.11 Serum-stability of Lipoplexes

Cells were cultured at a density of 15, 000 cells HEK-293, and HepG2 per well in a 96-well plate 18-24 h before the transfection. Then 0.3 μg (0.91 nmol) of pDNA was complexed with lipids (**Lp1-Lp3**) in DMEM medium in the presence of increasing concentrations of added serum (10-30% v/v and total volume made up to 100 μL) for 30 min. The charge ratios of lipid-DNA complexes was maintained as 2:1 and 4:1, at which all the three lipids exhibited their highest transfection ability in two types of cells used for transfection HEK-293 and HepG2. The experimental procedure and determination of β-galactosidase activity per well are similar to that reported for the in vitro transfection experiments.

6.4.12 Cytotoxicity assay

The cytotoxicities of cationic lipids **Lp1-Lp3**in NIH3T3, B16F10, HEK-293 and HepG2 cells across the lipid: DNA charge ratios of 1:1-8:1 as used in the authentic transfection experiments were assessed by the help of MTT (3-(4, 5-dimethyathiazol-2-yl)-2, 5-diphenyltetrazolium Bromide) based reduction as reported previously. The cytotoxicity assay was performed in 96-well plates by maintaining the same ratio of number of cells to amount

of cationic lipid: DNA complexes, as used in the transfection experiments. Briefly, the cells were incubated with lipoplexes for 3 h followed by the addition of 100 μL of DMEM containing 20% FBS and 10 μL MTT (5mg/mL in PBS). After 3-4 h of incubation at 37 °C, the medium was removed and 100 μL of DMSO: Methanol (50:50, v/v) was added to the cells. The absorbance was measured at 550 nm and results were expressed as percent viability = [A_{540} (treated cells)-background/A_{540} (untreated cells)-background] x100.

6.5 References

1. D. Luo and W. M. Saltzman, *Nature biotechnology*, 2000, **18**, 33-37.
2. D. Oupicky, C. Konak, K. Ulbrich, M. A. Wolfert and L. W. Seymour, *Journal of controlled release : official journal of the Controlled Release Society*, 2000, **65**, 149-171.
3. J. Soto, M. Bessodes, B. Pitard, P. Mailhe, D. Scherman and G. Byk, *Bioorganic & medicinal chemistry letters*, 2000, **10**, 911-914.
4. B. Martin, M. Sainlos, A. Aissaoui, N. Oudrhiri, M. Hauchecorne, J. P. Vigneron, J. M. Lehn and P. Lehn, *Current pharmaceutical design*, 2005, **11**, 375-394.
5. S. Bhattacharya and A. Bajaj, *Chem Commun (Camb)*, 2009, DOI: 10.1039/b900666b, 4632-4656.
6. A. Mendez-Ardoy, N. Guilloteau, C. Di Giorgio, P. Vierling, F. Santoyo-Gonzalez, C. Ortiz Mellet and J. M. Garcia Fernandez, *The Journal of organic chemistry*, 2011, **76**, 5882-5894.
7. A. S. Malamas, M. Gujrati, C. M. Kummitha, R. Xu and Z. R. Lu, *Journal of controlled release : official journal of the Controlled Release Society*, 2013, **171**, 296-307.
8. K. Nishina, T. Unno, Y. Uno, T. Kubodera, T. Kanouchi, H. Mizusawa and T. Yokota, *Molecular therapy : the journal of the American Society of Gene Therapy*, 2008, **16**, 734-740.
9. R. Mukthavaram, S. Marepally, M. Y. Venkata, G. N. Vegi, R. Sistla and A. Chaudhuri, *Biomaterials*, 2009, **30**, 2369-2384.
10. B. Kedika and S. V. Patri, *Journal of medicinal chemistry*, 2011, **54**, 548-561.
11. B. Kedika and S. V. Patri, *Molecular pharmaceutics*, 2012, **9**, 1146-1162.
12. B. Kedika and S. V. Patri, *Bioconjugate chemistry*, 2011, **22**, 2581-2592.

13. A. Rigotti, *Molecular aspects of medicine*, 2007, **28**, 423-436.

14. J. M. Zingg, *Molecular aspects of medicine*, 2007, **28**, 400-422.

15. E. S. Stoyanov, I. V. Stoyanova and C. A. Reed, *Chemistry*, 2008, **14**, 7880-7891.

16. M. Gosangi, H. Rapaka, V. Ravula and S. V. Patri, *Bioconjugate chemistry*, 2017, **28**, 1965-1977.

17. C. H. Wu, C. H. Lan, K. L. Wu, Y. M. Wu, W. N. Jane, M. Hsiao and H. C. Wu, *International journal of oncology*, 2018, **52**, 389-401.

18. J. Wang, K. Liu, R. Xing and X. Yan, *Chemical Society reviews*, 2016, **45**, 5589-5604.

19. M. Fu, Q. Li, B. Sun, Y. Yang, L. Dai, T. Nylander and J. Li, *ACS nano*, 2017, **11**, 7349-7354.

20. Q. Zou, M. Abbas, L. Zhao, S. Li, G. Shen and X. Yan, *Journal of the American Chemical Society*, 2017, **139**, 1921-1927.

21. B. Singh, S. Maharjan, T. E. Park, T. Jiang, S. K. Kang, Y. J. Choi and C. S. Cho, *Macromolecular bioscience*, 2015, **15**, 622-635.

22. R. S. Singh, C. Goncalves, P. Sandrin, C. Pichon, P. Midoux and A. Chaudhuri, *Chemistry & biology*, 2004, **11**, 713-723.

23. M. G. Traber and H. Sies, *Annual review of nutrition*, 1996, **16**, 321-347.

24. M. G. Traber and H. Arai, *Annual review of nutrition*, 1999, **19**, 343-355.

25. S. Futaki, Y. Masui, I. Nakase, Y. Sugiura, T. Nakamura, K. Kogure and H. Harashima, *The journal of gene medicine*, 2005, **7**, 1450-1458.

26. V. Budker, V. Gurevich, J. E. Hagstrom, F. Bortzov and J. A. Wolff, *Nature biotechnology*, 1996, **14**, 760-764.

27. J. Y. Legendre and F. C. Szoka, Jr., *Pharmaceutical research*, 1992, **9**, 1235-1242.

28. R. Banerjee, P. K. Das, G. V. Srilakshmi, A. Chaudhuri and N. M. Rao, *Journal of medicinal chemistry*, 1999, **42**, 4292-4299.

29. R. S. Singh and A. Chaudhuri, *FEBS letters*, 2004, **556**, 86-90.

30. C. McGregor, C. Perrin, M. Monck, P. Camilleri and A. J. Kirby, *Journal of the American Chemical Society*, 2001, **123**, 6215-6220.

31. Y. Zhang and T. J. Anchordoquy, *Biochimica et biophysica acta*, 2004, **1663**, 143-157.

32. P. Dharmalingam, B. Marrapu, C. Voshavar, R. Nadella, V. K. Rangasami, R. V. Shaji, S. Abbas, R. B. N. Prasad, S. S. Kaki and S. Marepally, *Colloids and surfaces. B, Biointerfaces*, 2017, **152**, 133-142.